Synthesis and development of new bio-sourced Low Molecular Weight Organogelators

Dorian Rabaud

Thèse de doctorat de Sorbonne Université

Ecole doctorale 397 - Physique et Chimie des matériaux

Institut Parisien de Chimie Moléculaire (IPCM – UMR 8232) – Equipe Chimie des Polymères

Synthesis and development of new bio-sourced Low Molecular Weight Organogelators

Présentée par

Dorian RABAUD

Pour obtenir le grade de

Docteur de Sorbonne Université

Spécialité : Physique et Chimie des Matériaux

Dirigée par Laurent BOUTEILLER et Benjamin ISARE

Présentée et soutenue publiquement le 05 décembre 2022 devant un jury composé de :

M. Sylvain CAILLOL	DR – Université de Montpellier	Rapporteur
Mme. Christine GERARDIN	PR – Université de Lorraine	Rapporteur
Mme. Virginie MANSUY-MOURIES	PR – Sorbonne Université	Président du jury
M. Benoit MAGNY	Directeur R&D – COATEX	Examinateur
M. Laurent BOUTEILLER	DR – Sorbonne Université	Directeur de thèse
M. Benjamin ISARE	MC – Sorbonne Université	Co-encadrant de thèse

A ma maman Martine,

A mon épouse Clémence,

A notre fils Liam,

Et à notre fille Théa,

“And when I’m facing a wall, I do not quit.

...Cause if you mean it, you will make it.”

Motionless in White

Remerciements

Tout d'abord, je souhaite remercier Mme Christine GERARDIN et Mr Sylvain CAILLOL d'avoir accepté d'être les rapporteurs de cette thèse. Je remercie également Mme Virginie MANSUY-MOURIES et Mr Benoit MAGNY qui ont accepté d'être les examinateurs de ce travail.

Je remercie vivement Laurent BOUTEILLER qui a été directeur de cette thèse. Je te remercie pour tes conseils, pour ton écoute et tes explications chaque fois que j'en ai eu besoin. J'espère t'avoir rendu un peu de tout ce que tu as su m'apporter au cours de ces dernières années. Je remercie sincèrement Benjamin ISARE, co-encadrant de cette thèse. Avant d'être ton doctorant, j'ai été ton stagiaire et tu as su voir au-delà de mon parcours atypique. Tu m'as donné une chance lorsque personne ne m'en avait laissé et pour cela je ne te remercierai jamais assez. Notre café du matin et les bons moments passés ensemble vont me manquer. Pour finir, en partant, je te rends la place de la personne qui râle le plus de l'équipe !

Je souhaite remercier toutes les personnes extérieures au laboratoire avec qui j'ai pu collaborer et qui ont contribuées à l'avancement de ce projet. Merci à Guylaine DUCOURET avec qui nous avons réalisé l'étude rhéologique. Je te remercie pour ces échanges concernant les propriétés de mes gels. Merci à Pierre-Antoine ALBOUY pour les mesures de WAXS. Merci pour ta disponibilité et tes réponses (plus ou moins rapides) à mes nombreuses interrogations. Merci également à toutes les autres équipes de l'IPCM auxquelles j'ai emprunté grand nombre de réactifs que j'ai presque rendu sans qu'on me le demande.

Je remercie également Marie-Odile LAFON de la SATT Lutech pour son accompagnement dans le transfert de technologie et le dépôt de brevet, ainsi que Stéphane MASI de Novagraaf.

Je remercie également les stagiaires que j'ai encadré tout au long de cette thèse : Paul, Aurore et Lindsey. Encore merci à Paul qui a été le premier à faire un gel avec nos molécules !

Je remercie Claire TROUFFLARD et Régina MARUCHENKO pour les analyses RMN, pour avoir répondu à mes questions et pour m'avoir aidé sur certains spectres retors. Merci à Ludovic DUBREUCQ pour les analyses de masse que tu as faites. Merci à Gaelle PEMBOUONG pour tes formations et ton aide sur les analyses TGA, DSC, nano-DSC et SEC.

Je voulais également remercier de manière générale tous les membres de l'équipe Chimie des Polymères que j'ai rencontrés au cours de ces presque 4 années passées ici. Merci à Sandrine pour ta gentillesse, à Matthieu pour ton bonjour matinal, à Cécile pour nos nombreuses

conversations, à Fanny pour ta bienveillance, à Lydia pour ta bonne humeur, à François pour ta franchise et à Nicolas pour tes vannes douteuses.

Maintenant, je souhaite remercier mes collègues doctorants et post-doctorants avec qui j'ai partagé nombreux moments. Ainsi, merci à Danilo NUNES, portugais spécialiste de techniques dont je ne comprends pas grand-chose. Merci à Quentin SALLEMBIEN, ambassadeur Français du vin, de l'histoire et du dichroïsme circulaire. Merci à Ahmad HAMMOUD, libanais organicien jovial aux talents cachés. Merci à Laura LUIZ, ma *gavach* (montagnarde) guitariste qui m'a accueilli si chaleureusement. Merci à Océane FORT, toulousaine chanteuse à l'agenda de ministre et dernière rescapée de ce groupe. Je remercie également chaleureusement Khaled, Paméla, Mayte, Diana, Jana, David, Antonio, Pauline LB, Solène, Emma, Simon, Gwendoline, Valentin, Robin, Quentin F, Kévin et Mauricio.

Pour finir, je remercie ma famille et mes amis qui me sont chers. Merci à ma maman pour m'avoir toujours soutenu et surtout pour m'avoir laissé être qui je suis avec mon franc-parler et mon entêtement. Merci à Ben, mon meilleur ami et témoin de mariage avec qui j'ai tout partagé depuis plus de 15 ans. Merci à mon épouse Clémence pour ton amour, ton soutien et surtout pour me supporter dans la vie de tous les jours, ça ne doit pas être évident. Tout ça, c'est surtout grâce à toi. Et merci à mon fils Liam sans qui cette thèse n'aurait pas été ce qu'elle est. Tu ne m'as pas rendu cette dernière année facile mais rien ne vaut le bonheur de te tenir dans mes bras.

Abbreviations

2-EH	2-ethylhexylamine
Å	Angström
Ala	Alanine
APCI	Atmospheric Pressure Chemical Ionization
Asp	Aspartic acid
$(Boc)_2O$	Di-*tert*-butyl dicarbonate
γ	Strain
CAL B	Candida Antarctica Lipase B
CD	Circular dichroism spectroscopy
$CHCl_3$	Chloroform
Cl-TMDP	2-chloro-4,4,5,5-tetramethyl-1,3,2-dioxaphospholane
DCM	Dichloromethane
Δε	Molar extinction coefficient
DIPE	Diisopropyl ether
DMAP	4-Dimethylaminopyridine
DMF	*N*,*N*-dimethylformamide
DMSO	Dimethyl sulfoxide
DSC	Differential Scanning Calorimetry
EDC.HCl	(3-Dimethylamino-propyl)-ethyl-carbodiimide hydrochloride
ESI	ElectroSpray Ionization
Et_2O	Diethyl ether
EtOAc	Ethyl acetate
FDCA	Furan-2,5-dicarboxylic acid
FTIR	Fourier-Transform InfraRed spectroscopy
g	Gram
G'	Storage modulus
G''	Loss modulus
H_2SO_4	Sulfuric acid
HCl	Chlorhydric acid
HOBt	Hydroxybenzotriazole

HRMS	High Resolution Mass Spectrometry
HSQC	Heteronuclear Single Quantum Correlation spectroscopy
Hz	Hertz
L	Liter
λ	Longueur d'onde
Leu	Leucine
LMWG	Low Molecular Weight Gelator
M	Mole/liter
MeOH	Methanol
$MgSO_4$	Magnesium sulfate
mol	Mole
$NaHCO_3$	Sodium bicarbonate
NEt_3	Triethylamine
NMR	Nuclear Magnetic Resonance spectroscopy
OAc	Acetyl
Pa	Pascal
Phe	Phenylalanine
ppm	Parts-per-million
PTSA	*p*-Toluenesulfonic acid
rad	Radian
RT	Room Temperature
σ	Stress
$SOCl_2$	Thionyl Chloride
TA	Tannic acid
TFA	Trifluoroacetic acid
TGA	ThermoGravimetric Analysis
THF	Tetrahydrofurane
UV	Ultraviolet
VT-FTIR	Variable-Temperature Fourier-Transform InfraRed spectroscopy
WAXS	Wide Angle X-Ray Scattering
wt%	Mass percentage
ω	Frequency

Table of contents

General introduction

Gels are semi-solid materials, formed by a network that is present throughout the volume of a fluid. The transition from the liquid to the solid state of these materials is called gelation. Gels can be classified into two types: chemical and physical gels. Chemical gels are made up of polymer chains linked together by covalent bonds, while physical gels also called supramolecular gels are obtained by non-covalent interactions.

Nowadays, gels are ubiquitous soft solids that are widely used in everyday life. These are used in various industrial fields. In the field of cosmetics, gels usually serve as a base for the transport of active ingredients to the skin and can also be seen in products such as lipstick, sunscreen and anti-perspirant. In the food industry, they are widely used in particular in the production of gelatin and jelly. In the pharmaceutical industry, gels are commonly used for a great deal of applications such as drug delivery agents, materials responsive to specific molecules (glucose or antigens used as biosensors), diapers, contact lenses, medical electrodes, water gel explosives, breast implants. The materials industry also uses gels as additives in coatings, paints and adhesive materials.

Supramolecular chemistry is an expanding field of study, which has been recognized by the award of a Nobel Prize in 1987 to D. J. Cram, J.-M. Lehn and C. J. Pedersen.

Supramolecular gels are formed using Low Molecular Weight Gelators (LMWG), which self-assemble locally in a preferential direction. This leads to the formation of elongated structures, mainly fibers, that form an entangled network called Self-Assembled Fibrillar Network (SAFiN).[1–4] This particular mechanism of self-assembly is led by supramolecular interactions like hydrogen-bonding, π–π stacking, donor-acceptor interactions, metal coordination and van der Waals interactions. If the liquid to be gelled is water, they are called hydrogels. If the liquid is an organic solvent or an oil, they are called organogels.

Over the last decades, the use of organogels has expanded in various industrial fields. These materials are very interesting because cross-linking is reversible in the case of an organogel, which means that the gel can be formed several times if a certain amount of energy is applied to the system such as heating or shearing. However, a number of organogelators originate from the petrochemical industry, which still limits their field of application. Which is why developing new bio-sourced organogelators is a growing topic.

Among industrial bio-sourced organogelators, DBS (derived from sugars) and 12-HSA (derived from lipids) are the most known. There is a wide structural variety of organogelators that makes them such an interesting type of materials, allowing a wide range of properties and applications. The main difficulty is to synthesize an organogelator that gel a specific solvent or solution. Even knowing the "rules" for obtaining a gelling molecule such as having functional groups that provide strong and directional supramolecular interactions between molecules and solvophilic groups to balance the solubility, it is still not possible to predict gelation.

Due to the absence of predictive methodology, the discovery of new organogelators is still mainly by serendipity and their gelation abilities are usually probed by extensive trial and screening exercises.

In this project, we tried to develop new organogelators based on two bio-sourced building blocks: tannic acid (TA) and furan-2,5-dicarboxylic acid (FDCA). Tannic acid is a biomass-derived polyphenol containing 25 phenols that can provide hydrogen bonds for self-assembly of molecules and gel formation. FDCA is a biomass molecule containing a rigid core and two carboxylic acids that can be tuned to provide a good balance of solubility and self-association resulting in interesting gelling properties.

This thesis manuscript consists of three chapters.

The first chapter focuses on the bibliographical study of organogels and their supramolecular assemblies. The different families of bio-based organogelators and their applications are also presented.

The second chapter focuses on the use of tannic acid as a platform for new bio-based organogelators. First, tannic acid has been characterized by numerous techniques then, the syntheses of the different targeted molecules based on TA are presented as well as their thorough characterization with various techniques in order to determine precisely the functionalization rate.

The third and last chapter focuses on the use of FDCA as a platform for new bio-based organogelators. We demonstrate the influence of FDCA functionalization on the gelation properties of the synthesized molecules. Extensive characterization, from macroscopic to microscopic scale, is carried out in order to establish a correlation between the structure, the nature of the supramolecular assembly and the properties of the gels.

Experimental protocols and characterization methods and materials are presented in their respective chapters.

[1] P. Terech, R. G. Weiss, *Chem. Rev.* **1997**, *97*, 3133–3160.

[2] D. J. Abdallah, R. G. Weiss, *Advanced Materials* **2000**, *12*, 1237–1247.

[3] M. George, R. G. Weiss, *Acc. Chem. Res.* **2006**, *39*, 489–497.

[4] P. Dastidar, *Chem. Soc. Rev.* **2008**, *37*, 2699–2715.

Chapter I. State of the art on Low Molecular Weight Organogelators

I. Introduction

I.1. Gels

Many attempts to define what is a gel have been proposed since Jordan Lloyd's first sentence: "The colloidal condition, the 'gel', is one which it is easier to recognize than to define".[1]

A gel can be defined as an intermediate state between a liquid-like and a solid-like rheological behavior. It consists of a dispersed phase (polymers or colloids) and a dispersing medium (water or other liquids). They are semi-solid materials. Liquid-like properties are due to the fact that the main constituent is liquid. Solid-like behaviors are due to the network that prevents the system from flowing, and characterized by a finite modulus of elasticity and yield stress. As the gel is made up of liquid and solid, its mechanical properties are between ideal elasticity (Hookean) and ideal viscosity (Newtonian).[2]

Almdal et al.[3] proposed the following phenomenological definition of a gel:

1. A gel is a soft, solid or liquid-like material of two or more components, one of which is a liquid, present in substantial quantity.
2. Solid-like gels are characterized by the absence of an equilibrium modulus, by a storage modulus, G'(ω), which exhibits a pronounced plateau extending to times at least of the order of seconds, and by a loss modulus, G"(ω), which is considerably smaller than the storage modulus in the plateau region.

It is surely difficult to propose a final definition for a gel because it might be possible to find some exceptions.

Nowadays, gels are more and more present in our daily life. They can be used in the food industry, with the use of gelatin or formation of jelly, or in the cosmetic industry as in oils, balms and hair or shower gels for example. They are used in paints or adhesives materials. They can also be used in the pharmaceutical industry as drug delivery agents due to their high tunability or in medical devices.[4]

I.2. Classification of gels

When it comes to the classification of the different types of gels, several classifications have co-existed or still co-exist. In 1974, Flory [5] classified four different types of gels based on their structure:

1. Well-ordered lamellar structures, including gel mesophases, such as soap gels and inorganic gels formed from minerals and clays.
2. Covalent polymeric networks; completely disordered, such as vulcanized rubber or polyacrylamide gels in which network is formed by covalent crosslinks.
3. Polymer networks formed through physical aggregation; predominantly disordered, but with regions of local order, including gelatin, agar, carrageenan, methylcellulose gels where the junction zones are believed to be formed by the aggregation of helices or stiff chains.
4. Particulate, disordered structures which may include many gels of globular proteins where the network is formed by clusters of connected spheres.

In 1995, Keller [6] discussed more about the diversity of gel morphologies obtained by liquid-liquid phase separation intercepted by vitrification. He also showed two classes of gels arising from liquid to crystalline phase transformation:

1. Junctions, bundles or micelles, aggregated rigid chains which are connected by released chains.
2. The network elements are formed by fibrous crystals constituted by rigid or semi-flexible chains that do not fold on crystallization.

The most commonly used classification of gels is based on the nature of the bond involved in the cross-linking region, and the classification into chemical and physical gels has been widely accepted.

Chemical gels are made up of polymer chains linked together by covalent bonds (**Figure I.1**). The cross-linking nodes of the network are permanent and do not depend on external factors (temperature, pH, concentration, mechanical deformation, etc...).

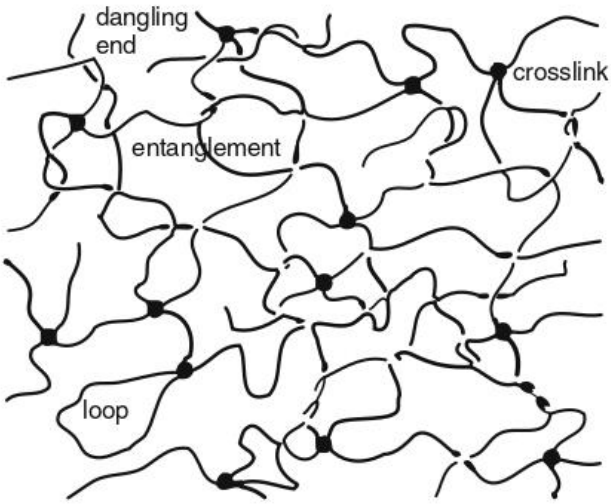

Figure I.1. Structure of a chemical gel [7]

On the other hand, physical gels also called supramolecular gels are obtained by non-covalent interactions like hydrogen-bonding, π–π stacking, donor–acceptor interactions, metal coordination and van der Waals interactions (**Figure I.2**).

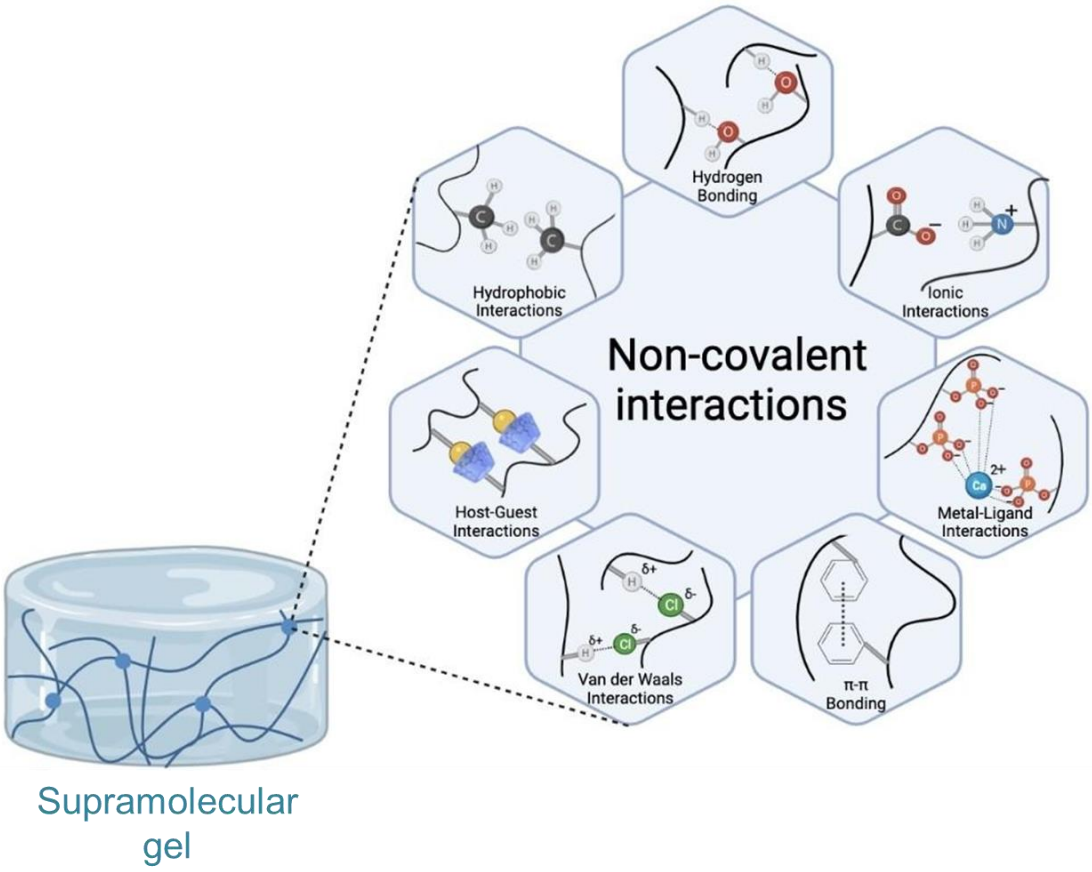

Figure I.2. Non-covalent interactions used to form supramolecular gels [8]

Supramolecular gels can be divided in two categories depending on the media gelled: hydrogels in water and organogels in organic media.

These supramolecular gels are formed using small molecules also called Low Molecular Weight Gelators (LMWG), which self-assemble in a preferential single direction. This leads to the formation of elongated structures, mainly fibers, that form an entangled network called Self-Assembled Fibrillar Network (SAFiN).[9–12] This particular mechanism of self-assembly is led by non-covalent interactions like hydrogen-bonding, π–π stacking, donor–acceptor interactions, metal coordination and van der Waals interactions.

In the following, we will focus on Low Molecular Weight Organogelators (also called Organogelators).

II. Organogelators

II.1. Definition of an organogelator

Low Molecular Weight Gelators (LMWGs) are small organic molecules, typically less than 3000 Da which, at low concentrations (≤ 2wt%) in solution, form a gel.[9] If the solvent is water, they are called hydrogelators. If the solvent is an organic solvent or an oil, they are called organogelators.

Organogels, as physical gels, mainly differ from other classes of gels. In fact, the cross-linking is reversible in the case of an organogel, meaning that the gel can be formed several times if a certain amount of energy is applied to the system like heating or shearing.

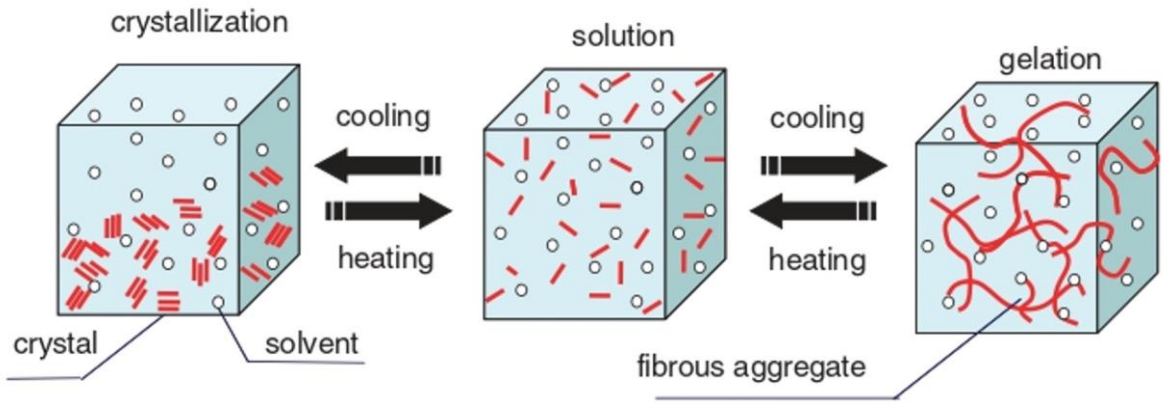

Figure I.3. Crystallization and gelation of low-molecular weight compounds [13]

Several phenomena can trigger gelation of the solvent, such as temperature variation [14,15], ultra-sonication, pH variation [16–18] or the addition of a molecule [19–22] enabling fiber formation and percolation. On **Figure I.3**, the crystallization and gelation of a low-molecular weight gelator are presented. When the crystals are heated in a suitable liquid, a homogeneous solution is formed. When this is cooled, crystallization occurs in response to the difference in solubility. However, in rare and interesting cases, gelation occurs rather than crystallization. When this gel is heated, it turns back into a homogeneous solution. Unlike supramolecular polymers in solution, the lateral dimension of the organogel fibers is large (10-100 nm) compared to the molecules and the organogels are not in thermodynamic equilibrium, but in a metastable state: the molecules are in an intermediate state between precipitation and crystallization, the latter being the most stable state. The viscosity of the gels formed limits the crystallization of the compounds. Consequently, their stability in time is limited.

Moreover, due to this metastable state, their preparation generally requires to heat the "organogelator + liquid" solution until dissolution of the organogelator, then let it cool down until formation of a gel. Lastly, the destructuring of gels by shearing is often irreversible: once broken, the gels do not reform. This last property also constitutes a limitation in the applications of these compounds.

To summarize, the characteristics of organogelators are listed as follows:

- They are characterized by good solubility under heat and induce gradual gelation of liquids.
- Gelling occurs at low organogelator concentration: < 50 g/L.
- The gels formed show a thermally reversible sol-gel phase transition.
- The forces leading to gelation are non-covalent interactions such as hydrogen bonds, van der Waals interactions or π-π stacking.

In the following, we will describe the different supramolecular interactions that can occur in the formation of an organogel.

II.2. Supramolecular interactions

Supramolecular compounds are formed by non-covalent interactions, called "physical bonds" or supramolecular interactions. These bonds vary in nature and intensity. Jean-Marie Lehn, Nobel Prize winner in 1987 defined supramolecular chemistry as “chemistry beyond the molecule”.[23]

II.2.1. van der Waals interactions

van der Waals interactions or forces, named after the Dutch physicist Johannes Diderik van der Waals, Nobel Prize winner in physics in 1910, arise from the polarization of an electron cloud by the proximity of the electrons of another atom, resulting in a weak electrostatic attraction. This deformation changes the charge distribution so that the sum of the energies of the electron clouds of the two atoms is less than the sum of the energies of the atoms alone. It is precisely this energy difference that determines the strength of the bond. The van der Waals forces are very weak (< 5 kJ/mol), resulting from interactions between permanent or induced dipoles.

These can be broken down into three distinct forces:

- Keesom forces (orientation force): interaction between two permanent dipoles
- Debye forces (induction force): interaction between a permanent dipole and an induced dipole. This is the ability of a polar molecule to induce a dipole in a polar or apolar molecule.
- London forces (dispersion force): interaction between two induced dipoles. They represent the main component of van der Waals interactions. London forces exist because the electron density of molecules is probabilistic: there is a high probability that at any moment it is not equally distributed throughout the molecule, which creates a dipole moment. Dipole moments will vary very rapidly over time. Thus, at each inhomogeneous distribution an induced dipole moment is created which can interact with the induced dipole moments of neighboring molecules and a force is then exerted between the molecules.

Although they are weak, these interactions are always present and influence certain phenomena. They are particularly important in the field of biology and life. They play an essential role in the formation of the three-dimensional structure of proteins [24] and are the main interactions between an antibody and an antigen.[25]

II.2.2. π-π interactions

The π-π interactions often referred to as π-stacking (0-50 kJ/mol) are present in aromatic or π-conjugated systems, mostly in the situation where one ring is relatively electron-rich and the other electron-poor. In general, there are three types of π-stacking, although there are a large

number of intermediate geometries: face-to-face, parallel-displaced and edge-to-face. These are shown on **Figure I.4**.

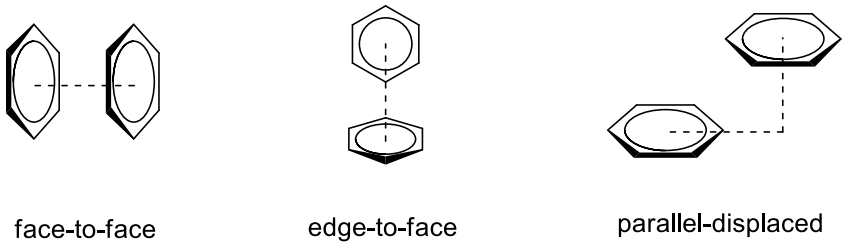

Figure I.4. Representation of the different types of π-π interactions [26]

The two most stable conformations are the parallel-displaced and edge-to-face, which are essentially of the same energy. In contrast, the face-to-face configuration maximizes the overlap of the π-system, which destabilizes the interaction. Parallel-displaced π-stacking is responsible for graphite's brittleness and lubricating properties.[27] These same interactions help stabilize the DNA double helix. Edge-to-face interactions are sometimes defined as weak forms of hydrogen bonds between the slightly electron-deficient hydrogen atom of one aromatic ring and the electron-rich electron cloud of another ring. Strictly speaking, they should not be considered π-stacking because there is no stacking of the π-electron surfaces.[27]

II.2.3. Hydrogen bonds

The hydrogen bond, due to its relatively strong and highly directional nature, is often described as the "master-key" anisotropic interaction.[28] Linus Pauling firstly described hydrogen bond in 1931.[29] He defined the hydrogen bond as a bond formed when the electronegativity of A relative to H in an A–H covalent bond is such that it can withdraw electrons and leave protons partially unshielded.[30]

Hydrogen bonds are omnipresent in nature, they determine the recognition of substrates by enzymes and are responsible for maintaining the double helix structure of DNA (**Figure I.5**). The IUPAC has established the hydrogen bond as "an attractive interaction between a hydrogen atom from a molecule or a molecular fragment A–H in which A is more electronegative than H, and an atom or a group of atoms in the same or a different molecule, in which there is evidence of bond formation".[31]

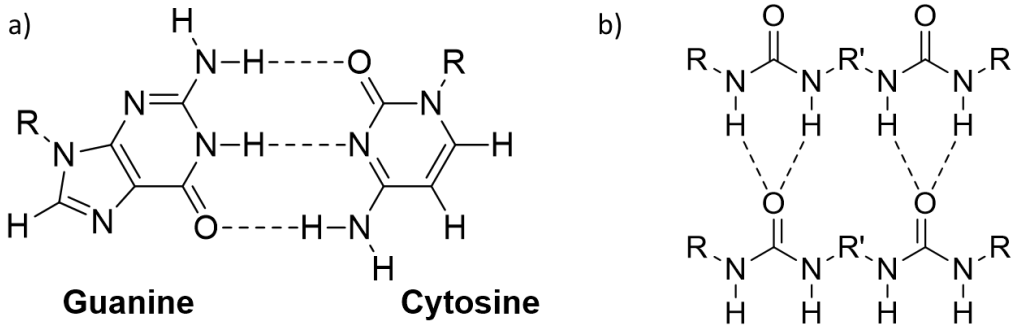

Figure I.5. Hydrogen bonding: a) example of DNA base pairing and b) bis-ureas

Hydrogen bonds can have different lengths, strengths, and geometries. A strong hydrogen bond may resemble a covalent bond in terms of the energy required to break the interaction, whereas the energy of a weak hydrogen bond will be closer to a van der Waals interaction.

Weak hydrogen bonds involving interactions of N–H, O–H, and C–H groups with double and triple bonds (C=C, C≡C), as well as aromatics, have also become important for understanding crystal stabilization, host-guest interactions and biomolecule conformations.[32]

III. Bio-based organogelators

Over the last decades, different families of bio-sourced compounds have been identified as having a tendency to create self-assembly in order to form gels. In the following, we will present these different families with selected examples of assembly processes. We will focus on systems with a single compound, although there are also two-component systems.[33]

III.1. Amino acids/peptides-based organogelators

One of the most important classes of organogelators is the one based on amino-acids or peptides.[34–39]

This family of compounds is incredibly large due to the rich variety of possible structures. The number of naturally occurring amino acids is large (24 amino acids) which allows a vast number of combinations. This family is also a great source of hydrogelators and amphiphilic gelling agents for gelling both aqueous and organic media.[38]

They can be associated with various non-covalent interactions like hydrogen bonding, π-π interactions, van der Waals forces and hydrophobic interactions as shown by Basu et al (**Figure I.6**).[40]

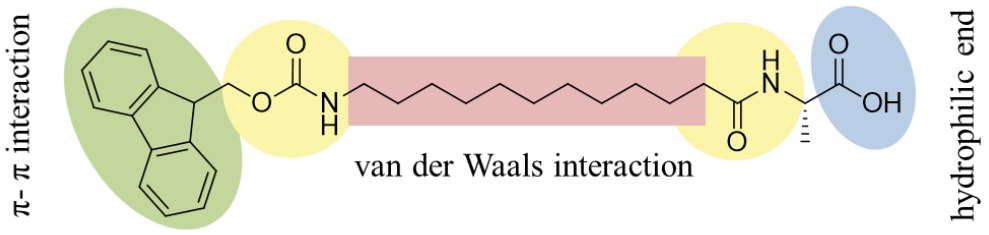

Figure I.6. Gelator molecule with various zones of interactions like π- π interactions (green), hydrogen-bonding sites (yellow), van der Waals interactions (red) and the polar head group (blue) [40]

Das et al. reported a family of dipeptide organogelators gelling aromatic organic solvents selectively in the presence of water. The authors demonstrated that structural variation controls fiber network morphology and dye uptake ability.[41]

With such a wide range of possibilities, Das et al. have also investigated the possibilities to obtain molecules that gel different media depending on the structure of the same precursor. In 2010, they investigated the tunability of a tryptophan precursor to provide, through simple synthetic modifications, a hydrogelator, an organogelator and an ionogelator (i.e. a gelator of ionic liquids) (**Figure I.7**).[42]

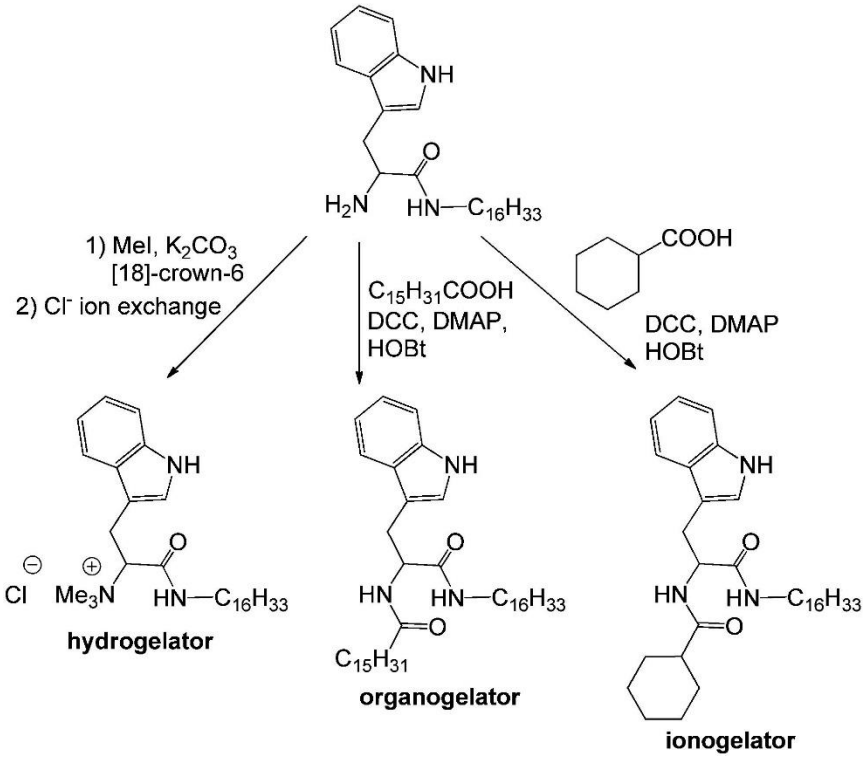

Figure I.7.Tuning the amphiphilicity of a non-gelator precursor to a hydrogelator, an organogelator and an ionogelator by simple chemical modifications [42]

Some amino acids are used more than others in the structure of organogelators. Indeed, phenylalanine is often used as a part of new organogelators. Brosse et al. described the synthesis route for phenylalanine-type organogelators, using an easy method of preparation with inexpensive starting materials. They investigated the relationship between chemical structure and gelation properties and demonstrated that the polar segment ruled the aggregation due to hydrogen bonds. The hydrophobic part seems to impact the flexibility and the interactions between fibers in the organogel network.[43]

The group of Haldar worked on phenylalanine-based peptides in order to obtain new organogelators. They studied the behavior of tripeptides with more or less sterically hindered groups and their capacity of self-assembly.[44]

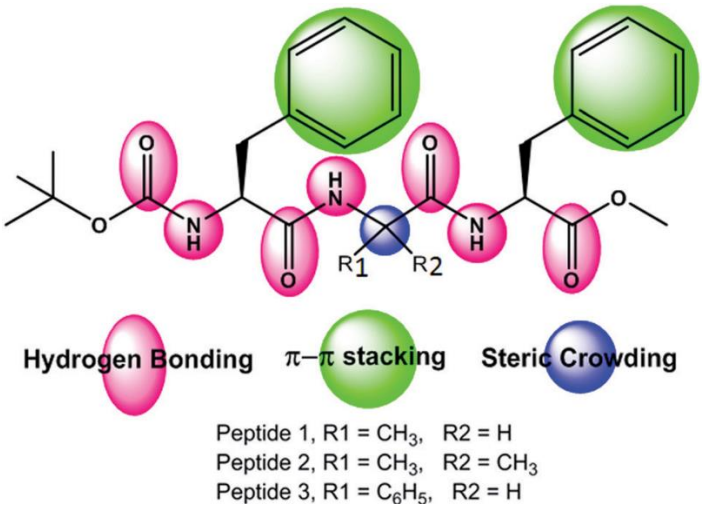

Figure I.8. Schematic representation of tripeptides [44]

They demonstrated that the most hindered sterically peptide are not able to self-assemble and thus not capable of forming supramolecular gels. On the opposite, peptides 1 and 3 (**Figure I.8**), with no side chain (R2), present a gelling behavior and are even called super-organogelators.

In another register, Hanabusa et al. studied the gelation properties of cyclodipeptides. They used different amino acids such as glycine, alanine, phenylalanine, leucine, valine as well as aspartic and glutamic acids, all of L configuration.[45] They focused on cyclodipeptides based on some expectations such as the number of hydrogen-bonding sites in each molecule (4) and the random alignment of cyclodipeptide consisting of differing amino acids in the aggregate preventing the crystallization and therefore stabilizing the gel state. They synthesized a family of compounds capable of making supramolecular gels in a wide variety of organic fluids, including edible oils, glyceryl esters, alcohols, and aromatic molecules.

III.2. Carbohydrates-based organogelators

Among the different families of organogelators, carbohydrate-based gelators have been an intense subject of study over the past decade.[46] Indeed, their structural diversity, rich stereochemistry, important occurrence , and their roles in biology and many disease-relevant processes make these molecules an infinite source of combination for supramolecular self-assembly. For the applications, as they are likely to be biocompatible, they may be used as advanced materials.[47,48]

Among this family of possible organogelators, one of them has shown particularly interesting results to the point of being used on an industrial scale: 1,3;2,4-dibenzylidene-D-sorbitol (DBS).

III.2.1. 1,3;2,4-Dibenzylidene-D-sorbitol (DBS) and its derivatives

1,3:2,4-Dibenzylidene-D-sorbitol (DBS) is a compound originally synthesized by Meunier in 1891 by condensation of two equivalents of benzaldehyde with sorbitol (**Figure I.9**). It is a chiral low molecular weight amphiphile gelator having a butterfly-shape conformation with hydrophilic hydroxyl groups and hydrophobic phenyl groups. It can self-assemble to form a three-dimensional network, at relatively low concentrations (< 5wt%) in a huge variety of organic liquids to produce organogels.[49–51]

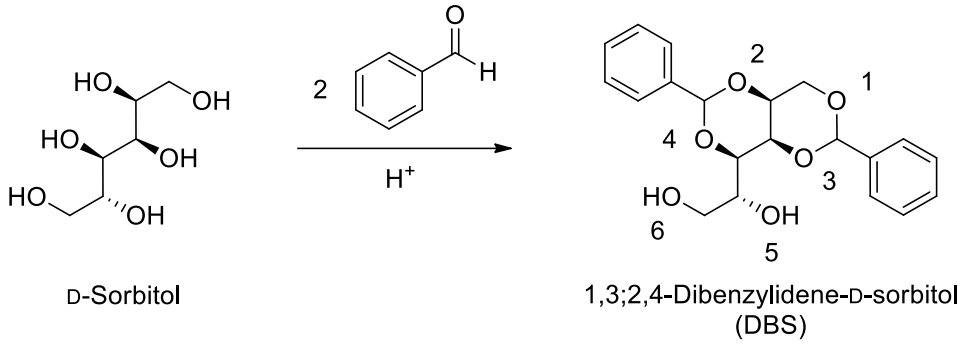

Figure I.9. Synthesis of 1,3;2,4-Dibenzylidene-D-sorbitol (DBS)

Afterwards, other chemically similar derivatives, such as 1,3:2,4-di(3,4-dimethylbenzylidene) sorbitol (DMDBS), 1,3:2,4-di-p-methylbenzylidene sorbitol (MDBS), and 1,2,3-trideoxy-4,6:5,7-bis-O-[(4-propylphenyl)-methylene]-nonitol (TBPMN) were produced.[52]

Although all scientists agree that hydrogen bonding and π-π stacking are permitting the self-assembly of DBS, some studies contradict each other as to determine which is really the driving force.

The group of Yamasaki have investigated thoroughly the self-assembly of DBS. They demonstrated that although the 5-OH group is capable of forming hydrogen bonds, these do not favor the self-assembly. Nevertheless, they suggested that the 6-OH group has a paramount role in DBS gelation due to intermolecular hydrogen bonding to acetal oxygen. Based on their results, Yamasaki et al. reported the first qualitative assembly model for DBS, which shows the side-by-side positioning of phenyl groups forming helical fibers (**Figure I.10**).[53]

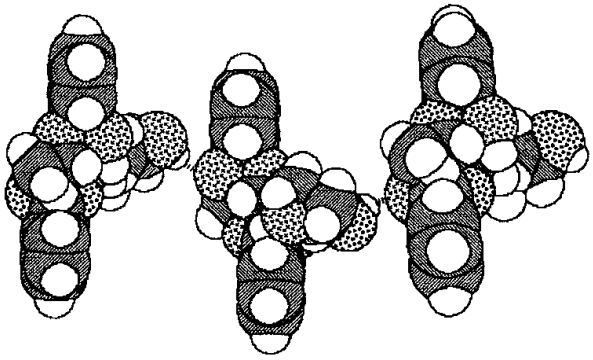

Figure I.10. Structural model of D-DBS aggregates in the gel state [53]

Watase et al. investigated the ground state dimerization of DBS molecules, this time in alcoholic solvents including ethylene glycol and glycerol which are hydrogen bond competitors. It was concluded that the self-assembly of DBS was also mediated by π-π stacking to form a molecular fiber.[54]

Due to their interesting self-assembly behavior, the rheological properties and microstructures of the gels prepared from these DBS derivatives have been thoroughly studied in a variety of polar and non-polar organic liquids and soft polymers.[55–58] It has been found that the self-assembly of the gels were meaningfully influenced by the liquid used. Yamasaki et al. have shown that solvent polarity has a significant effect on the microstructure of the DBS gels. The self-assembly behavior of the gels was impacted by the DBS concentrations but also by the chemical structures of the matrix media.[55]

Liu et al. studied the solvent effects on the DBS-based gel formation and the resulting rheological properties of the gels. The researchers showed that the polarity of the solvent had an influence on the diameters of the nanofibrils as well as on the gel dissolution temperatures (**Figure I.11**).[56]

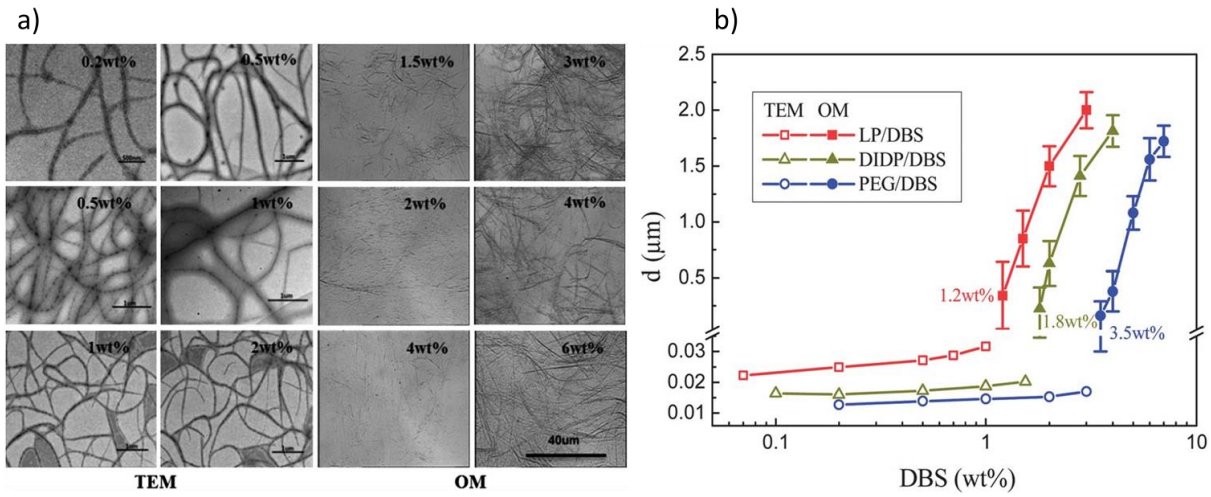

Figure I.11. a) Fibril morphology of solvent–DBS gel with different DBS concentrations: LP–DBS (top), DIDP–DBS (middle) and PEG–DBS (bottom). LP stands for liquid paraffin, DIDP for diisodecyl phthalate and PEG for poly(ethylene glycol). The left two columns are TEM images, the right two columns are OM images; b) The dependence of DBS fibrils and the fibril cluster diameter on DBS [56]

Despite the number of studies on individual compounds, comparisons of the self-assembly behaviors among the different dibenzylidene sorbitol derivatives are seldom reported.

III.2.2. Other Carbohydrates-based organogelators

Several classes of effective carbohydrates-based gelators have been reported by Wang's group.[59–72] The sugar starting materials are shown in **Figure I.12**.

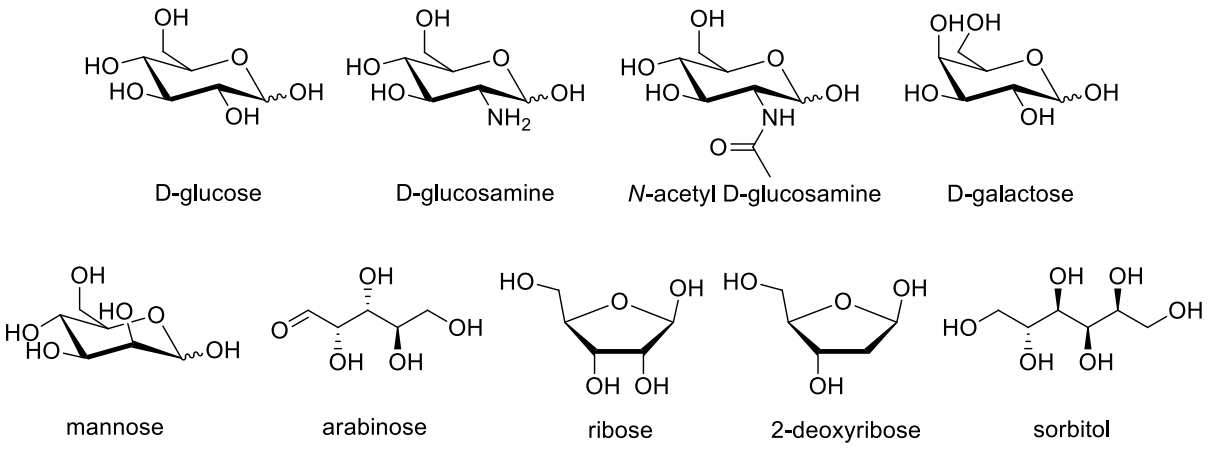

Figure I.12. Structures of the sugar starting materials often used for designing LMWGs

Studies have revealed that amphiphilic sugar derivatives having vicinal diol functionality undergo 1D self-assembly in nonpolar solvents through zigzag H-bonding, leading to fibrillar structures resulting in gelation.[47,73,74]

Starting from the D-glucose, Cheuk et al. designed a variety of LMWGs through the selective functionalization of 4, 6-benzylidene acetal protected α-methyl D-glucose derivatives.[62] They showed that short-chain esters with terminal alkyne functional groups could gel several solvents, including hexane and water. Their study has led to an understanding of the relationship between glucose structure and gelation, which paved the way for the design of new esters that were more effective gelators.

Peters and Davis studied self-assembling properties of nucleosides/nucleotides. Their molecular structure includes a ribose sugar with purines or pyrimidines that can induce self-assembly via several mechanisms, such as π-π stacking, electrostatic interactions and hydrogen bonding.[75] They prepared their gelators by modifying the ribose sugar or nucleobase moiety to introduce lipophilic linkers that provide hydrophobicity in order to favor gelation. The gelators have been found to form gels in a wide variety of solvents ranging from water all the way to non-polar solvents like hexane.

Ramos et al. combined galactosyl moieties with squaramide groups and long aliphatic chains to synthesized galactose-based LMWGs.[76] They showed that the amphiphilic derivative (**Figure I.13a**) performed very well in ethyl acetate, acetonitrile, ethanol and 1:1 aqueous ethanol mixture at low concentration. After the removal of the acetyl groups, the amphiphilic derivative (**Figure I.13b**) showed a supergelator behavior in a 1:1 aqueous ethanol solution with a minimum gelation concentration of 0.1wt%.

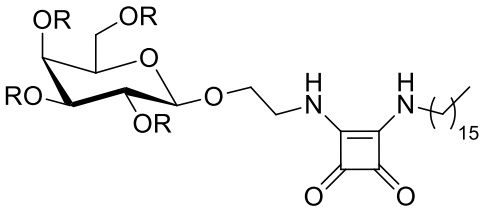

a) R = Ac; b) R = H

Figure I.13. Structure of novel glycosyl squaramide supramolecular gelators [76]

III.3. Fatty acids-based organogelators

III.3.1. 12-Hydroxystearic acid (12-HSA)

12-Hydroxystearic acid (12-HSA) has been studied extensively due to its low cost, simple structure and superior gelation capacity.[77–81] The unique self-assembly behavior of 12-HSA is due to its chemical structure. This molecule is composed of a carboxylic acid at the end of the chain as well as a secondary hydroxyl group at position 12 of a stearic acid (C18) which allows a greater possibility of interaction compared to the standard stearic acid molecule.[79] In addition, this hydroxyl function introduces chirality which is important for morphology and supramolecular assembly (**Figure I.14**).

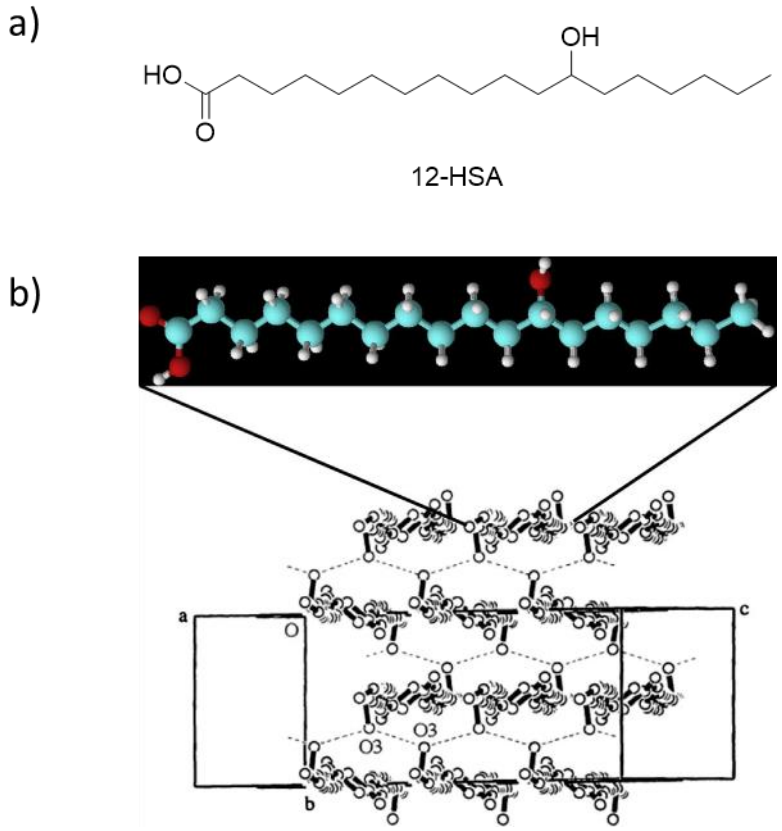

Figure I.14. a) Chemical structure of the 12-hydroxystearic acid (12-HSA), b) Crystal conformation of DL 12-hydroxystearic acid (a, b, and c are the unit cell axis) [82]

For the self-assembly, the main interaction is hydrogen bonding and to a lesser extent van der Waals interactions, London dispersion forces to be precise.[80] In optically pure R- or L-12-HSA, the hydroxyl groups are linked via unidirectional hydrogen bonds resulting in helical aggregates.[81]

The solvent-gelator interplay has an influence on the gelation behavior of 12-HSA. As solvent-gelator interactions increase and compete with gelator-gelator interactions, the probability of forming shorter and thus thicker fibers increases.[83] Due to the solvent-gelator interplay, it is also expected that more polar solvents, especially hydrogen-bonding rich solvents are more likely to dissolve 12-HSA preventing gelation or crystallization.

12-HSA-based gels have shown interest in various fields. The macroscopic scale properties of the materials are dependent on the unique structure of 12-HSA. Chemical modifications to the carboxylic acid or secondary alcohol allow these properties to be tailored to the specific needs of the material.

In conclusion, soft materials can be designed based on the unique character of 12-HSA gels.

III.3.2. Other fatty acids-based organogelators

Apart from 12-HSA, which is a star gelling agent, there are other fatty acids-based organogelators. Tri-, di- or monoglycerides (TAG, DAG, MAG) organogelators (**Figure I.15**) are, extensively, used as a mixture of glycerol esterified with different fatty acids, in order to control the gelation process.[84–87] The particularity of this category of organogelators is their ability to self-assemble into an inverse bilayer. These nanostructures are organized into lamellar and planar microstructures, which then organize into a three-dimensional network.[84]

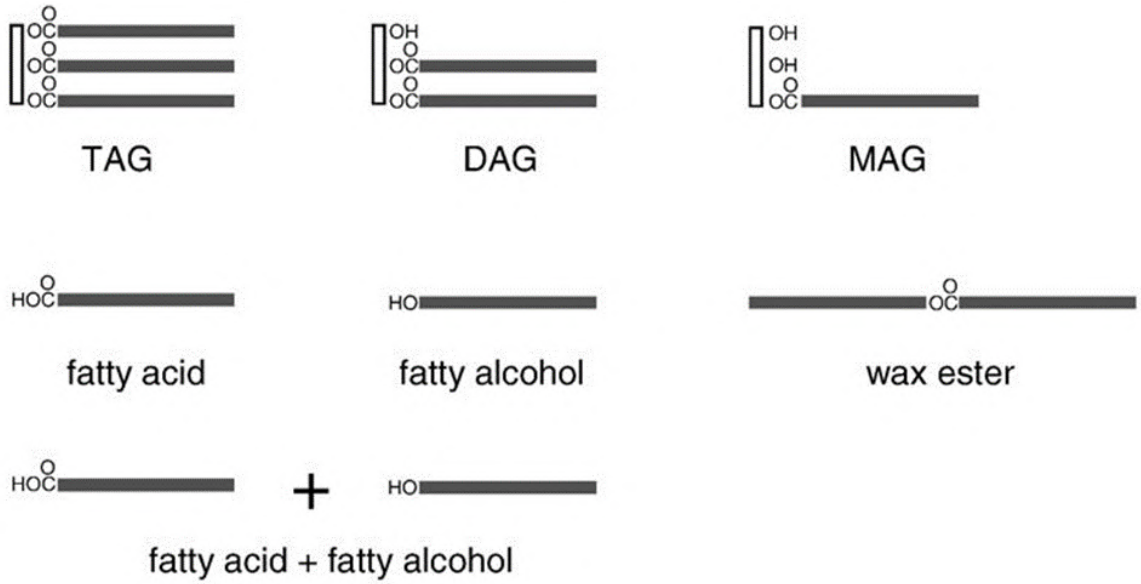

Figure I.15. Schematic representation of various fatty acid-based organogelators [87]

Gandolfo et al. investigated palmitic, stearic, arachidic and behenic acid, and established oil structuring ability in sunflower oil above ~ 2wt% at 5 °C.[88]

Daniel and Rajasekharan studied an even wider range of fatty acids, showing that the amount needed to structure the oil does not decrease much more with chain lengths above 31. They also showed that long-chain saturated fatty alcohols, wax esters, and dicarboxylic acids had the ability to gel plant oils and hydrocarbons.[89]

Wright and Marangoni confirmed the gelation of rapeseed oil with at least 0.5wt% of ricinelaidic acid, the *trans*-unsaturated analogue of 12-HSA.[90]

III.4. Cholesterol-based organogelators

Although several steroids have found excellent applications in many areas of supramolecular chemistry[91], cholesterol has emerged as the most versatile unit on which to base the systematic design of functional LMOGs.[92]

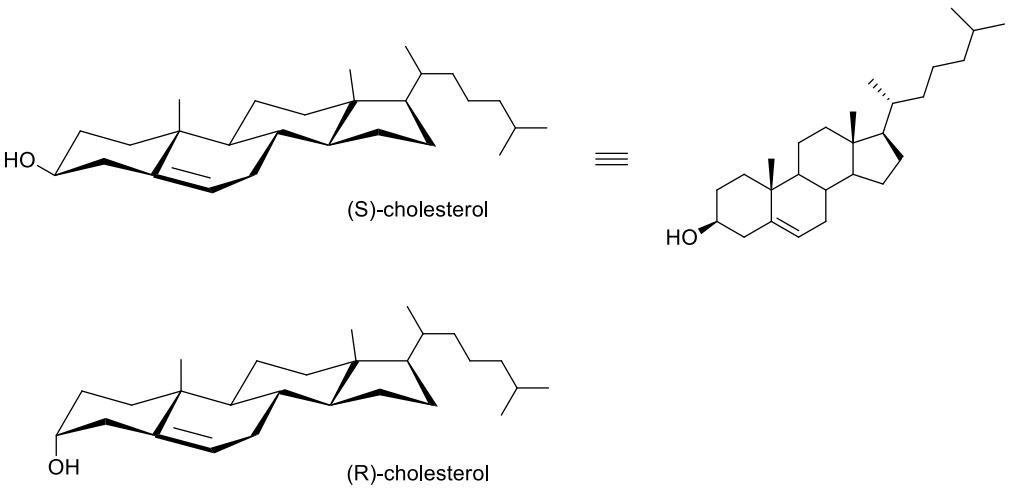

Figure I.16. Molecular structures of the cholesterol (α- and β- epimers)

The first LMOG based on cholesterol has been discovered by serendipity in 1987 by Terech and Weiss.[9]

Cholesterol contains four rings fused together, three six-membered and one five-membered (**Figure I.16**). The cyclohexane rings are *trans* fused, which means that they are locked in the chair conformation. As a result, the cholesterol skeleton is rigid, flat, and straight. Despite its amphiphilic structure, with a hydroxyl group and a long hydrocarbon skeleton, cholesterol is

not a gelator molecule in itself. Indeed, only molecules derived from cholesterol have been reported to exhibit gelling properties.

However, Weiss and coworkers showed that a molecular system comprising an aromatic (A) moiety connected to a steroidal (S) group through a functionalized link (L) could exhibit effective and perhaps predictable gelation ability (**Figure I.17**).[93]

Figure I.17. ALS architecture of cholesterol-based LMOGs

The use of the ALS structure as design principle for new organogelators allows access to a very large family of cholesterol-based systems. Over the past decades, numerous ALS-type gelators, varying the A and L components, have been synthesized and studied. The steroidal group (S) is often restricted to either cholesterol or cholestanol (hydrogenated cholesterol).

In cholesterol-based gelators, aromatic-aromatic and cholesterol-cholesterol interactions work cooperatively as driving forces in the self-assembly and gelation processes. It is probable that the additional self-association between the aromatic groups promotes the growth of unidirectional aggregates at the detriment of the large three-dimensional structures that are usually observed with amphiphilic cholesterols.[94] Structure-property studies have shown that the determining factor for this type of gelator is the aromatic group. The aromatic group is not only essential for the gelling process but also allows the organization of the self-assembled structure and therefore defines the properties of the resulting gels (**Figure I.18**).[95] In addition, the presence of the π-delocalized aromatic unit confers electronic and optical properties to the gels.

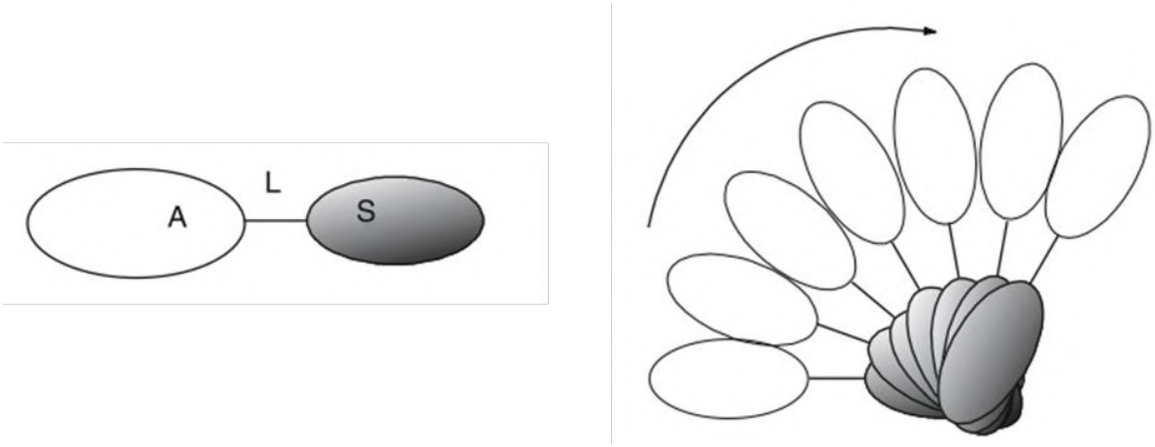

Figure I.18. Unidirectional self-assembly of LMOG molecules driven by cholesterol-cholesterol interactions forms a helical array as self-assembled unit fiber [95]

IV. Applications

Owing to their inherent semi-solid property, organogels manifest various unique characteristics, such as surface lubricity, and anti-drying capacity, arousing particular interests in diverse practical applications (**Figure I.19**).

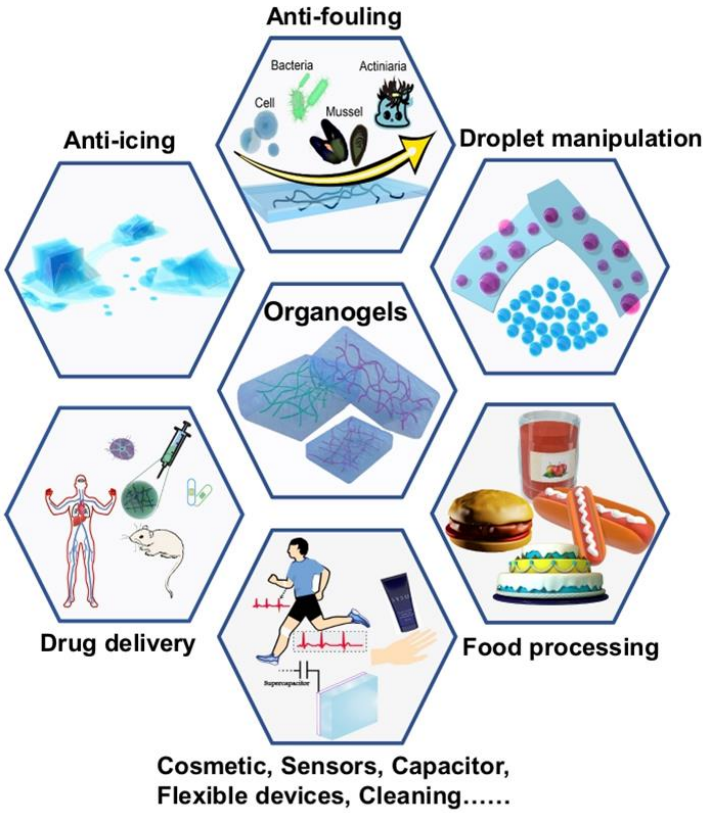

Figure I.19. Schematic illustration of organogels and their applications [96]

IV.1. Biomedical field

A wide variety of systems have been developed using organogelators for biomedical application, especially as drug delivery systems.

Some research on drug delivery systems designed with 12-HSA supramolecular gels has been investigated.[97] As many drugs are poorly or not at all soluble in water, this low solubility prevents good bioaccessibility and therefore bioavailability. In order to do this, a technology using gelled lipid nanoparticles (GLN) has been used to overcome the problem of solubility.

Siqueira-Moura et al. prepared stable dispersions of soybean oil GLN with excellent chloroaluminum phthalocyanine (ClAlPc) encapsulation efficiency.[98] In the first step, 12-HSA is used to form an organogel then, a water-soluble stabilizing agent is introduced to form an aqueous dispersion (**Figure I.20**).

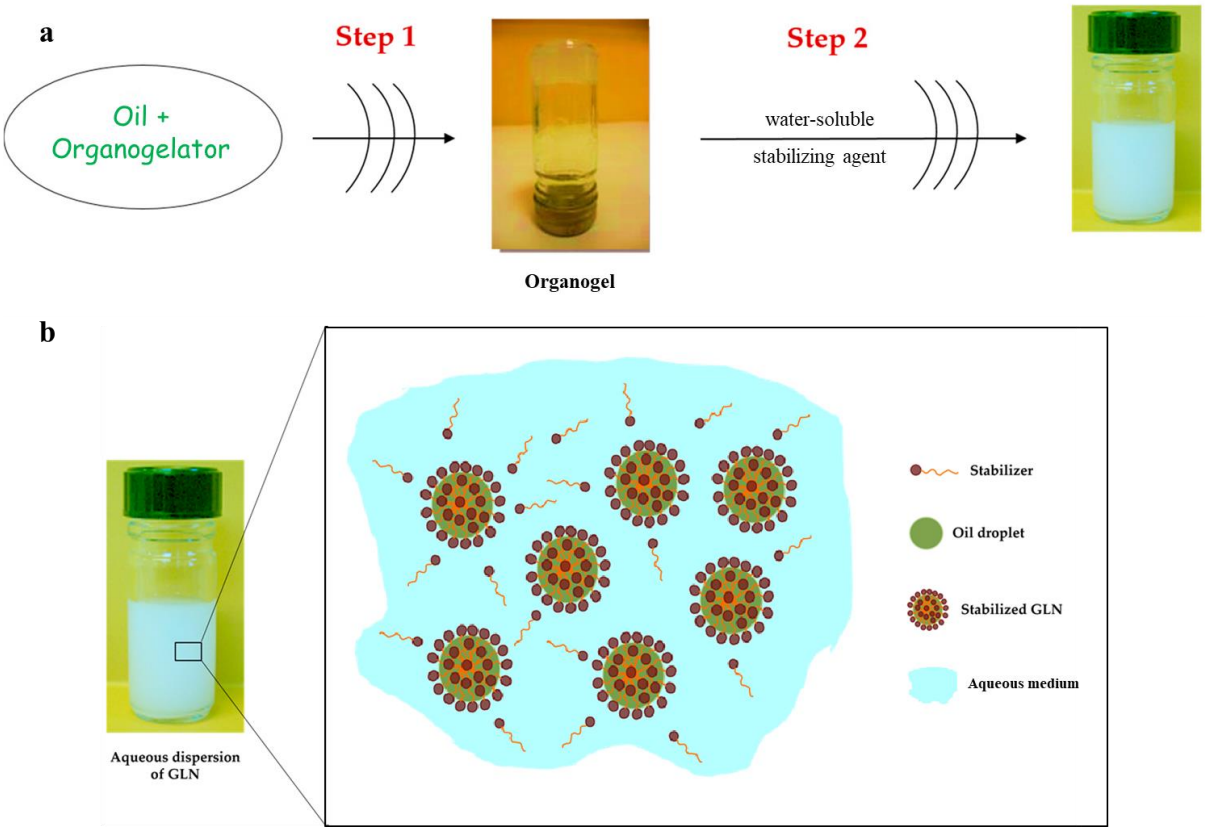

Figure I.20. a) Schematic representation of gelled lipid nanoparticle (GLN) colloidal dispersion preparation process. b) schematic representation of GLN dispersion [98]

Polyethyleneimine (PEI) is used to stabilize the nanoparticles composed of gelled oil (250-350 nm). The phthalocyanine interacted weakly with the gelation process, leading to good

encapsulation and potential use of the resulting particles in photodynamic therapy (PDT) procedures.

In another area, GLN nanoparticles have also been studied for other applications, particularly in cosmetics. It has been shown that organogel dispersions can improve the sun protection factor (SPF) value, increasing the ability to absorb UV radiation.

Carbohydrate-based materials have also been studied for biomedical applications. A few gluconamide-based amphiphiles have been reported as antibacterial agents that can prevent biofilm formation.[99] The gelation tests revealed that one of the compounds formed gels in toluene, dichlorobenzene, benzene and xylene with critical gelation concentration of 0.8wt%, respectively.

IV.2. Cosmetics

Gelled lipid nanoparticles have also been studied for other applications, particularly in cosmetics. It has been shown that organogel dispersions can improve the sun protection factor (SPF) value, increasing the ability to absorb UV radiation.

Kirilov et al. obtained gelled particles containing a sunscreen model molecule with 12-HSA by hot emulsification (T>Tgel), with a surfactant (acetylated glycol stearate) and polymers (sodium hyaluronate and polyvinyl alcohol) as stabilizing agents.[100] According to the UVB absorption evaluation, gelled particles improved the photoprotective ability and the photostability of immobilized UVB blocker. They also showed a highwater resistance (~83%) even after 40 min of immersion.

DBS and 12-HSA were also used to formulate lipsticks, then were compared to lipsticks made without any LMOG. LMOG formulations exhibited higher UVA protection factor (UVA-PF) and in vitro SPF, particularly in the 12-HSA-based lipstick.[101]

DBS has long been used in cosmetic formulation because of its ability to gel the cosmetic source materials, thereby imparting the product with the desired thickness, adhesion, strength, and consistency. Roehl patented the first DBS-mediated gelation of glycols with acidic aluminum anti-perspirant salts.[102] DBS was used to give a clear solid antiperspirant composition, with suitable stick hardness and adhesion. Since then, many improvements have been done in order to avoid the destabilization of the formula.

IV.3. Food additives

One of the most recent ways to reduce the content of saturated fatty acids is to use oleogels in the formulations. Oleogels are structured oils prepared by oleogelation of a liquid oil using organogelators such as vegetable waxes, mono- and diglycerides, alcohols or esters of fatty acids, phospholipids and phytosterols.[103]

As a typical example, Si et al. reported an organogel gelling with 3% or 6% monoglycerides and soybean oil.[104] The organogels formed with crystallization at ambient temperature, and displayed similar properties to those of confectionery filling fats. The organogels formed with monoglycerides and high oleic sunflower oil were also investigated to replace the commercial margarine in muffins.[105]

Many confectionery and bakery products use creams made up of saturated and unsaturated fats. In order to avoid the degradation of the product due to the melt of fat leading to a non-appealing product, LMOGs can be used for preventing/slowing the oil mobility and migration in product.[106]

Despite the promising results and the wide range of oleogelation techniques and organogelators, there are yet no commercially available oleogel containing food products but the research on oleogels is in expansion.[107]

IV.4. Other applications

Organogels can also be used as lubricant additives. Wang et al. synthesized a methionine-based organogelator called HMTA and successfully applied it as an additive to several types of blank lubricant oils. HMTA self-assembles to fibrous structures and traps lubricant oils to form gel lubricants. The prepared gel lubricants show thermo-reversible properties and 3 to 5 times improved lubricating performance.[108]

Among the large number of LMOG, those capable of gelling one solvent preferentially over the other in a given two-phase mixture are named phase-selective organogelators (PSOG). This interesting ability has opened the way for environmental applications in water purification. In this field, the ideal PSOG must be efficient to gel the oil phase from water at room temperature, be synthesized with less waste and without toxic agents, with good recovery of the oil from the gel, and be reusable.

Organogels are also used as adhesives,[109] stimuli-responsive materials,[110] sensors,[111] anti-icing,[112] coatings,[113] etc.

V. Conclusion

In this chapter, we have presented what are organogels and the main families of bio-based organogelators. As described, their gelling properties come from the balance between the solubility and self-assembly strength of these molecules. We see that many bio-based organogelators have been reported but only very few are really used commercially (DBS and HSA).

VI. References

[1] J. D. Lloyd, in *Colloid Chemistry*, Chemical Catalogue Co., New York, **1926**, pp. 767–782.

[2] M. Tokita, K. Nishinari, *Gels: Structures, Properties, and Functions*, Springer, Berlin, Heidelberg, **2009**.

[3] K. Almdal, J. Dyre, S. Hvidt, O. Kramer, *Polymer Gels and Networks* **1993**, *1*, 5–17.

[4] E. R. Draper, D. J. Adams, *Chem* **2017**, *3*, 390–410.

[5] P. J. Flory, *Faraday Discuss. Chem. Soc.* **1974**, *57*, 7–18.

[6] A. Keller, *Faraday Discuss.* **1995**, *101*, 1–49.

[7] V. G. Rostiashvili, T. A. Vilgis, in *Encyclopedia of Polymeric Nanomaterials* (Eds.: S. Kobayashi, K. Müllen), Springer, Berlin, Heidelberg, **2014**, pp. 1–18.

[8] J. Omar, D. Ponsford, C. A. Dreiss, T.-C. Lee, X. J. Loh, *Chemistry – An Asian Journal* **2022**, *17*, e202200081.

[9] P. Terech, R. G. Weiss, *Chem. Rev.* **1997**, *97*, 3133–3160.

[10] D. J. Abdallah, R. G. Weiss, *Advanced Materials* **2000**, *12*, 1237–1247.

[11] M. George, R. G. Weiss, *Acc. Chem. Res.* **2006**, *39*, 489–497.

[12] P. Dastidar, *Chem. Soc. Rev.* **2008**, *37*, 2699–2715.

[13] K. Hanabusa, M. Suzuki, *Polym J* **2014**, *46*, 776–782.

[14] D. J. Overstreet, D. Dutta, S. E. Stabenfeldt, B. L. Vernon, *Journal of Polymer Science Part B: Polymer Physics* **2012**, *50*, 881–903.

[15] S. Bhattacharjee, B. Maiti, S. Bhattacharya, *Nanoscale* **2016**, *8*, 11224–11233.

[16] S.-L. Zhou, S. Matsumoto, H.-D. Tian, H. Yamane, A. Ojida, S. Kiyonaka, I. Hamachi, *Chemistry – A European Journal* **2005**, *11*, 1130–1136.

[17] D. J. Adams, L. M. Mullen, M. Berta, L. Chen, W. J. Frith, *Soft Matter* **2010**, *6*, 1971–1980.

[18] S. Sutton, N. L. Campbell, A. I. Cooper, M. Kirkland, W. J. Frith, D. J. Adams, *Langmuir* **2009**, *25*, 10285–10291.

[19] N. Zanna, S. Focaroli, A. Merlettini, L. Gentilucci, G. Teti, M. Falconi, C. Tomasini, *ACS Omega* **2017**, *2*, 2374–2381.

[20] Y. J. Zheng, X. J. Loh, *Polymers for Advanced Technologies* **2016**, *27*, 1664–1679.

[21] P. Chakraborty, E. Gazit, *ChemNanoMat* **2018**, *4*, 730–740.

[22] N. Zanna, A. Merlettini, C. Tomasini, *Org. Chem. Front.* **2016**, *3*, 1699–1704.

[23] J.-M. Lehn, *Angewandte Chemie International Edition in English* **1990**, *29*, 1304–1319.

[24] J. N. Israelachvili, *Intermolecular and Surface Forces: With Applications to Colloidal and Biological Systems*, Academic Press, **2015**.

[25] S. Sheriff, in *Encyclopedia of Immunology (Second Edition)* (Ed.: P.J. Delves), Elsevier, Oxford, **1998**, pp. 159–163.

[26] T. Chen, M. Li, J. Liu, *Crystal Growth & Design* **2018**, *18*, 2765–2783.

[27] J. C. Ma, D. A. Dougherty, *Chem. Rev.* **1997**, *97*, 1303–1324.

[28] G. A. Jeffrey, *An Introduction to Hydrogen Bonding*, Oxford University Press, **1997**.

[29] Linus. Pauling, *J. Am. Chem. Soc.* **1931**, *53*, 1367–1400.

[30] L. Pauling, *The Nature of the Chemical Bond, and the Structure of Molecules and Crystals: An Introduction to Modern Structural Chemistry*, Cornell University Press, Ithaca, NY, **1940**.

[31] A. D. MacNaught, A. Wilkinson, *Compendium of Chemical Terminology: IUPAC Recommendations*, Blackwell Science, Oxford, **1997**.

[32] T. Steiner, G. Koellner, *J Mol Biol* **2001**, *305*, 535–557.

[33] A. R. Hirst, D. K. Smith, *Chemistry – A European Journal* **2005**, *11*, 5496–5508.

[34] A.-C. Couffin-Hoarau, A. Motulsky, P. Delmas, J.-C. Leroux, *Pharm Res* **2004**, *21*, 454–457.

[35] A. Motulsky, M. Lafleur, A.-C. Couffin-Hoarau, D. Hoarau, F. Boury, J.-P. Benoit, J.-C. Leroux, *Biomaterials* **2005**, *26*, 6242–6253.

[36] G. Bastiat, F. Plourde, A. Motulsky, A. Furtos, Y. Dumont, R. Quirion, G. Fuhrmann, J.-C. Leroux, *Biomaterials* **2010**, *31*, 6031–6038.

[37] K. Tao, A. Levin, L. Adler-Abramovich, E. Gazit, *Chem. Soc. Rev.* **2016**, *45*, 3935–3953.

[38] C. K. Rouse, A. D. Martin, C. J. Easton, P. Thordarson, *Sci Rep* **2017**, *7*, 43668.

[39] M. Chetia, S. Debnath, S. Chowdhury, S. Chatterjee, *RSC Adv.* **2020**, *10*, 5220–5233.

[40] K. Basu, N. Nandi, B. Mondal, A. Dehsorkhi, I. W. Hamley, A. Banerjee, *Interface Focus* **2017**, *7*, 20160128.

[41] S. Debnath, A. Shome, S. Dutta, P. K. Das, *Chemistry – A European Journal* **2008**, *14*, 6870–6881.

[42] S. Dutta, D. Das, A. Dasgupta, P. K. Das, *Chemistry – A European Journal* **2010**, *16*, 1493–1505.

[43] N. Brosse, D. Barth, B. Jamart-Grégoire, *Tetrahedron Letters* **2004**, *45*, 9521–9524.

[44] D. Podder, S. R. Chowdhury, S. K. Nandi, D. Haldar, *New J. Chem.* **2019**, *43*, 3743–3749.

[45] K. Hanabusa, M. Matsumoto, M. Kimura, A. Kakehi, H. Shirai, *Journal of Colloid and Interface Science* **2000**, *224*, 231–244.

[46] J. Morris, J. Bietsch, K. Bashaw, G. Wang, *Gels* **2021**, *7*, 24.

[47] S. Datta, S. Bhattacharya, *Chem. Soc. Rev.* **2015**, *44*, 5596–5637.

[48] K. Soundarajan, R. Periyasamy, T. M. Das, *RSC Adv.* **2016**, *6*, 81838–81846.

[49] D. J. Cornwell, O. J. Daubney, D. K. Smith, *J. Am. Chem. Soc.* **2015**, *137*, 15486–15492.

[50] H. Oh, N. Yaraghi, S. R. Raghavan, *Langmuir* **2015**, *31*, 5259–5264.

[51] K. K. Diehn, H. Oh, R. Hashemipour, R. G. Weiss, S. R. Raghavan, *Soft Matter* **2014**, *10*, 2632–2640.

[52] W.-C. Lai, Y.-C. Lee, *RSC Adv.* **2016**, *6*, 98042–98051.

[53] S. Yamasaki, Y. Ohashi, H. Tsutsumi, K. Tsujii, *BCSJ* **1995**, *68*, 146–151.

[54] M. Watase, Y. Nakatani, H. Itagaki, *J. Phys. Chem. B* **1999**, *103*, 2366–2373.

[55] S. Yamasaki, H. Tsutsumi, *BCSJ* **1995**, *68*, 123–127.

[56] S. Liu, W. Yu, C. Zhou, *Soft Matter* **2012**, *9*, 864–874.

[57] W.-C. Lai, S.-J. Tseng, P.-H. Huang, *J Nanopart Res* **2015**, *17*, 456.

[58] W. Chen, Y. Yang, C. H. Lee, A. Q. Shen, *Langmuir* **2008**, *24*, 10432–10436.

[59] G. Wang, S. Cheuk, K. Williams, V. Sharma, L. Dakessian, Z. Thorton, *Carbohydrate Research* **2006**, *341*, 705–716.

[60] X. Nie, G. Wang, *J. Org. Chem.* **2006**, *71*, 4734–4741.

[61] G. Wang, H. Yang, S. Cheuk, S. Coleman, *Beilstein J. Org. Chem.* **2011**, *7*, 234–242.

[62] S. Cheuk, E. D. Stevens, G. Wang, *Carbohydrate Research* **2009**, *344*, 417–425.

[63] N. Goyal, S. Cheuk, G. Wang, *Tetrahedron* **2010**, *66*, 5962–5971.

[64] G. Wang, S. Cheuk, H. Yang, N. Goyal, P. V. N. Reddy, B. Hopkinson, *Langmuir* **2009**, *25*, 8696–8705.

[65] N. Goyal, H. P. R. Mangunuru, B. Parikh, S. Shrestha, G. Wang, *Beilstein J. Org. Chem.* **2014**, *10*, 3111–3121.

[66] H. P. R. Mangunuru, H. Yang, G. Wang, *Chem. Commun.* **2013**, *49*, 4489–4491.

[67] G. Wang, N. Goyal, H. P. R. Mangunuru, H. Yang, S. Cheuk, P. V. N. Reddy, *J. Org. Chem.* **2015**, *80*, 733–743.

[68] H. P. R. Mangunuru, J. R. Yerabolu, G. Wang, *Tetrahedron Letters* **2015**, *56*, 3361–3364.

[69] H. P. R. Mangunuru, J. R. Yerabolu, D. Liu, G. Wang, *Tetrahedron Letters* **2015**, *56*, 82–85.

[70] G. Wang, A. Chen, H. P. R. Mangunuru, J. R. Yerabolu, *RSC Adv.* **2017**, *7*, 40887–40895.

[71] I. S. Okafor, G. Wang, *Carbohydrate Research* **2017**, *451*, 81–94.

[72] A. Chen, S. B. Adhikari, K. Mays, G. Wang, *Langmuir* **2017**, *33*, 8076–8089.

[73] S. Bhattacharya, S. N. G. Acharya, *Chem. Mater.* **1999**, *11*, 3504–3511.

[74] S. Bhattacharya, S. N. G. Acharya, *Langmuir* **2000**, *16*, 87–97.

[75] G. M. Peters, J. T. Davis, *Chem. Soc. Rev.* **2016**, *45*, 3188–3206.

[76] J. Ramos, S. Arufe, H. Martin, D. Rooney, R. B. P. Elmes, A. Erxleben, R. Moreira, T. Velasco-Torrijos, *Soft Matter* **2020**, *16*, 7916–7926.

[77] M. Burkhardt, S. Kinzel, M. Gradzielski, *J Colloid Interface Sci* **2009**, *331*, 514–521.

[78] J. Gao, S. Wu, M. A. Rogers, *J. Mater. Chem.* **2012**, *22*, 12651–12658.

[79] A.-L. Fameau, M. A. Rogers, *Current Opinion in Colloid & Interface Science* **2020**, *45*, 68–82.

[80] Y. Lan, M. A. Rogers, *CrystEngComm* **2015**, *17*, 8031–8038.

[81] V. A. Mallia, R. G. Weiss, *J. Phys. Org. Chem.* **2014**, *27*, 310–315.

[82] M. A. Rogers, in *Edible Oleogels*, Elsevier, **2018**, pp. 85–102.

[83] S. Wu, J. Gao, T. J. Emge, M. A. Rogers, *Soft Matter* **2013**, *9*, 5942–5950.

[84] S. Da Pieve, S. Calligaris, E. Co, M. C. Nicoli, A. G. Marangoni, *Food Biophysics* **2010**, *5*, 211–217.

[85] N. K. Ojijo, I. Neeman, S. Eger, E. Shimoni, *J. Sci. Food Agric.* **2004**, *84*, 1585–1593.

[86] A. López-Martínez, J. A. Morales-Rueda, E. Dibildox-Alvarado, M. A. Charó-Alonso, A. G. Marangoni, J. F. Toro-Vazquez, *Food Research International* **2014**, *64*, 946–957.

[87] M. Pernetti, K. F. van Malssen, E. Flöter, A. Bot, *Current Opinion in Colloid & Interface Science* **2007**, *12*, 221–231.

[88] F. G. Gandolfo, A. Bot, E. Flöter, *J Amer Oil Chem Soc* **2004**, *81*, 1–6.

[89] J. Daniel, R. Rajasekharan, *J Amer Oil Chem Soc* **2003**, *80*, 417–421.

[90] A. J. Wright, A. G. Marangoni, *J Am Oil Chem Soc* **2006**, *83*, 497–503.

[91] E. Virtanen, E. Kolehmainen, *European Journal of Organic Chemistry* **2004**, *2004*, 3385–3399.

[92] T. D. James, H. Kawabata, R. Ludwig, K. Murata, S. Shinkai, *Tetrahedron* **1995**, *51*, 555–566.

[93] Y. Chyuan. Lin, R. G. Weiss, *Macromolecules* **1987**, *20*, 414–417.

[94] K. Urata, N. Takaishi, *European Journal of Lipid Science and Technology* **2001**, *103*, 29–39.

[95] M. Žinic, F. Vögtle, F. Fages, in *Low Molecular Mass Gelator*, Springer, Berlin, Heidelberg, **2005**, pp. 39–76.

[96] L. Zeng, X. Lin, P. Li, F.-Q. Liu, H. Guo, W.-H. Li, *Progress in Organic Coatings* **2021**, *159*, 106417.

[97] N. E. Hughes, A. G. Marangoni, A. J. Wright, M. A. Rogers, J. W. E. Rush, *Trends in Food Science & Technology* **2009**, *20*, 470–480.

[98] M. P. Siqueira-Moura, S. Franceschi-Messant, M. Blanzat, M. I. Ré, E. Perez, I. Rico-Lattes, A. Lattes, A. C. Tedesco, *Journal of Colloid and Interface Science* **2013**, *401*, 155–160.

[99] Y. Siva Prasad, S. Manikandan, K. Lalitha, M. Sandeep, R. Vara Prasad, R. Arun Kumar, C. S. Srinandan, C. Uma Maheswari, V. Sridharan, S. Nagarajan, *Nano Select* **2020**, *1*, 510–524.

[100] P. Kirilov, S. Rum, E. Gilbert, L. Roussel, D. Salmon, R. Abdayem, C. Serre, C. Villa, M. Haftek, F. Falson, F. Pirot, *International Journal of Cosmetic Science* **2014**, *36*, 336–346.

[101] C. L. Esposito, P. Kirilov, *Gels* **2021**, *7*, 97.

[102] E. L. Roehl, H. B. Tan, *Antiperspirant and Deodorant Sticks*, **1979**, US Patent 4154816.

[103] E. J. Pérez-Monterroza, C. J. Márquez-Cardozo, H. J. Ciro-Velásquez, *LWT - Food Science and Technology* **2014**, *59*, 673–679.

[104] H. Si, L.-Z. Cheong, J. Huang, X. Wang, H. Zhang, *Journal of the American Oil Chemists' Society* **2016**, *93*, 1075–1084.

[105] A. S. Giacomozzi, M. E. Carrín, C. A. Palla, *Journal of Food Science* **2018**, *83*, 1505–1515.

[106] T. A. Stortz, A. K. Zetzl, S. Barbut, A. Cattaruzza, A. G. Marangoni, *Lipid Technology* **2012**, *24*, 151–154.

[107] A. Pușcaș, V. Mureșan, C. Socaciu, S. Muste, *Foods* **2020**, *9*, 0.

[108] K. Wang, W. Zhang, N. Liu, D. Hu, F. Yu, Y.-P. He, *Langmuir* **2022**, *38*, 11492–11501.

[109] Z. Zhang, L. Wang, H. Yu, F. Zhang, L. Tang, Y. Feng, W. Feng, *ACS Appl. Mater. Interfaces* **2020**, *12*, 15657–15666.

[110] C. Gao, L. Wang, Y. Lin, J. Li, Y. Liu, X. Li, S. Feng, Y. Zheng, *Advanced Functional Materials* **2018**, *28*, 1803072.

[111] H. Xia, G. Liu, C. Zhao, X. Meng, F. Li, F. Wang, L. Duan, H. Chen, *RSC Adv.* **2017**, *7*, 17264–17270.

[112] Y. Yu, B. Jin, M. I. Jamil, D. Cheng, Q. Zhang, X. Zhan, F. Chen, *ACS Appl. Mater. Interfaces* **2019**, *11*, 12838–12845.

[113] H. Y. Lai, A. de Leon, K. Pangilinan, R. Advincula, *Progress in Organic Coatings* **2018**, *115*, 122–129.

Chapter II. Tannic acid: a new platform for bio-sourced supramolecular materials?

I. Introduction

Tannic acid (Acidum tannicum) is a polyphenol from the tannin family, more precisely from the class of hydrolysable tannins. Tannins are phenolic compounds that occur naturally in plants. They are considered the fourth component of biomass after cellulose, hemicellulose and lignin.[1] Hydrolysable tannins are esters of a variable number of phenolic acids, gallic acid and its dimers, linked to a monosaccharide, usually glucose. The structure of tannic acid consists of gallic units linked to a glucose. The chemical formula for commercial tannic acid is given as $C_{76}H_{52}O_{46}$, which corresponds to decagalloyl glucose. But in reality, it is a mixture of polygalloyl glucose with a number of gallic units ranging from two to twelve, depending on the plant from which the tannic acid was extracted.[2] It should also be noted that within the tannic acid structure itself, there are several positional isomers. Indeed, the galloyl units are linked by an ester function called depside bond which can be in meta or para position with a different proportion of one or the other according to the tannic acid samples (**Figure II.1**). The chemistry of tannic acid is complicated due to its natural origin and consists of a mixture of complex substances. Furthermore, there are few studies on chemical modification of hydrolysable tannins. The main reason is the fragility of the depside bond, bond between two galloyl units which can lead to a degradation of the molecule.[3]

Among these studies, tannic acid has been used notably to create new epoxy composites.[4–6] This can explain the fact that they did not characterize the structure of the new materials obtained except by FTIR spectroscopy to confirm that the functionalization occurred.

Kim et al.[7] have epoxidized the phenols of tannic acid and they described the difficulties to functionalize all the 25 phenol groups with epoxy groups.

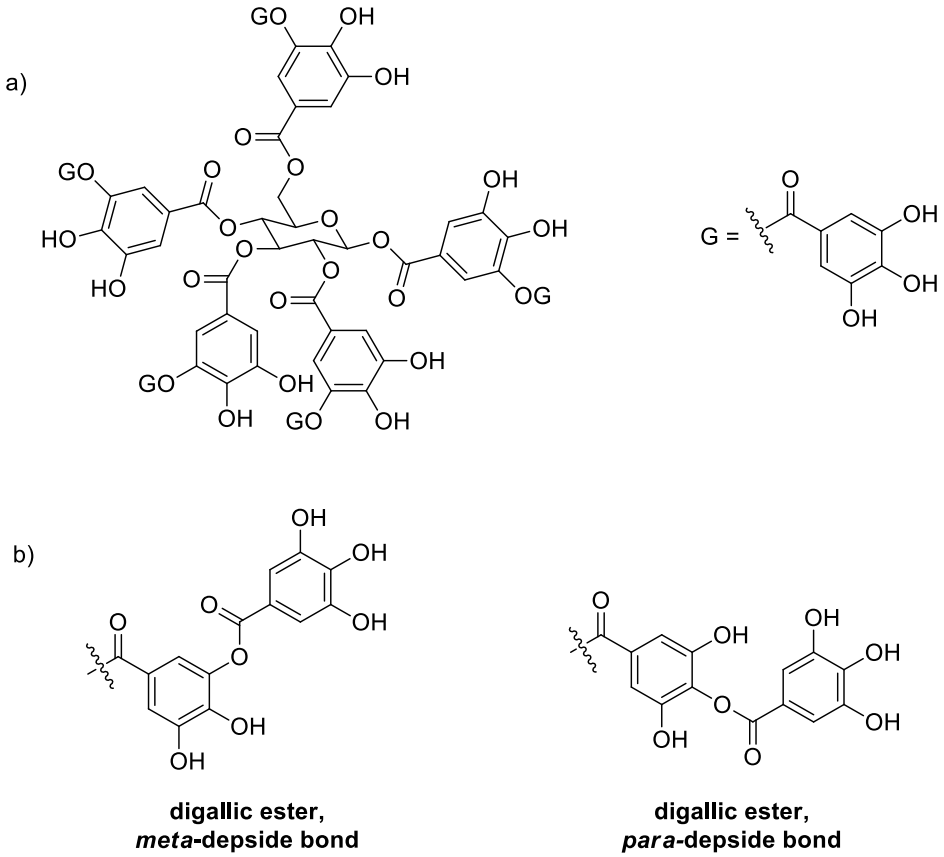

Figure II.1. a) Nominal structure of tannic acid, b) structural isomerism of depside bond (*meta* or *para*)

Sayed et al.[8] esterified the phenolic groups of tannic acid with castor oil to synthesize new biodegradable nonionic surfactants with different functionalization rate depending on the equivalents of castor oil used. During this study, the structure of one derivative with four phenols esterified was characterized. The ^{1}H NMR analysis does not allow the number of esterified phenols to be determined precisely.

Also, Zaborniak et al.[9] synthesized new star-like macromolecules derived from tannic acid by esterifying precisely twenty phenolic groups with 2-bromoisobutyryl bromide. However, the ^{1}H NMR showed that the protons from the glucose core are not properly defined and the number of phenolics esterified cannot be quantify precisely.

As presented before, the characterization of those products is not an easy task. In the present work, we decided to functionalize the phenolic groups of tannic acid into acetyl, ester and ether functions, and thoroughly characterize their structures by different analysis such as ^{1}H NMR, ^{13}C NMR, ^{31}P NMR, FTIR spectroscopy, mass spectrometry and total phenolic content determination.

II. Results and discussion

Intensive characterization of commercially available tannic was achieved first to be used as reference for the determination of the functionalization rate of the other derivatives.

II.1. Tannic acid

II.1.1. ^{1}H and ^{13}C NMR analyses

The TA commercially available starting material was analyzed by ^{1}H and ^{13}C NMR **(Figure II.2)**.

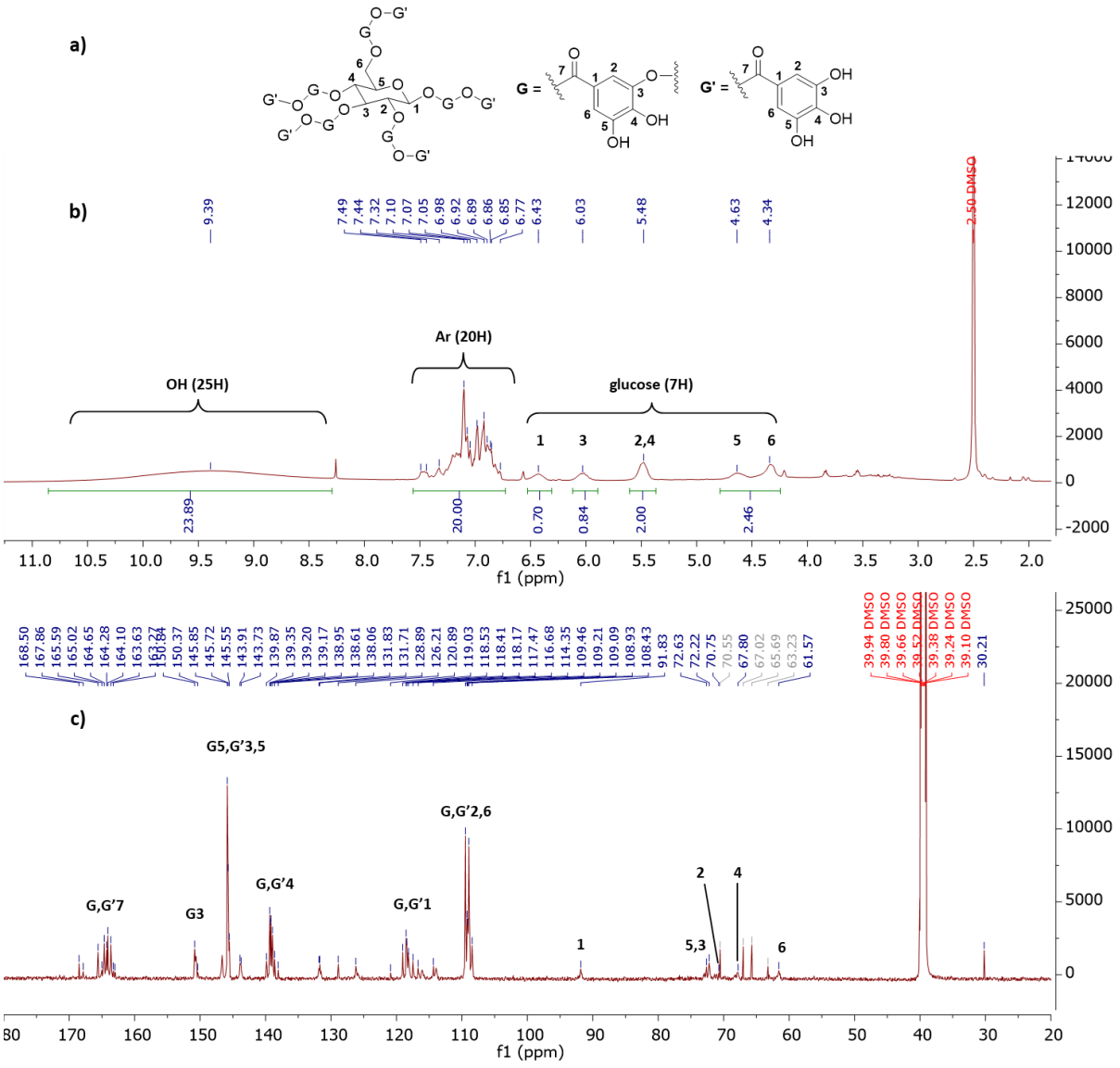

Figure II.2. a) Tannic acid nominal representation; b) ^{1}H NMR spectrum of our commercial

tannic acid in DMSO-D_6; c) ^{13}C NMR spectrum of our commercial tannic acid in DMSO-D_6. Assignments according to Lavoie et al.[10]

The different signals on the ^{13}C NMR spectrum of commercial TA were assigned based on the study published by Lavoie et al.[10]. The chemical shifts of pentagalloyl glucose in ^{1}H and ^{13}C NMR were clearly identified for the two anomers of the glucose. The ^{1}H NMR spectrum of our commercial TA was in agreement with the nominal structure of tannic acid with 10 galloyl units and a glucose beta anomer.

By ^{13}C NMR, the regions for the glucose core and for the galloyl unit's chemical shifts were identified referencing to the study of Lavoie et al.[10] An HSQC NMR analysis was performed (see **Figure II.34**) to correlate the proton signals to the carbons for the glucose core and assigned the peaks as follows: 91.83 ppm (C1), 72.63 ppm (C5), 72.22 ppm (C3), 70.75 ppm (C2), 67.80 ppm (4) and 61.57 ppm (C6). The other intense peaks in the same area should correspond to some impurities of our tannic acid.

For the galloyl units, the chemical shifts were in agreement with Lavoie et al.[10] and assigned as follows : 168.5-163 ppm (G7 and G'7), 151-150 ppm (G3), 146-143.5 ppm (G5, G'5 and G'3), 140-138 ppm (G4 and G'4), 119.1-114.3 ppm (G1 and G'1) and 109.6-108.2 ppm (G6 and G'6). We represented the tannic acid molecule with only *meta*-depside bond even if we show later that we have 30% of *para*-depside bond, only for the sake of clarity and ease of reading.

II.1.2. ^{31}P NMR analysis

A sample of TA was submitted to quantitative ^{31}P NMR after phosphitylation in situ with Cl-TMDP. On **Figure II.3**, the different types of phenolics that can be phosphitylated were presented and analyzed by ^{31}P NMR spectroscopy.

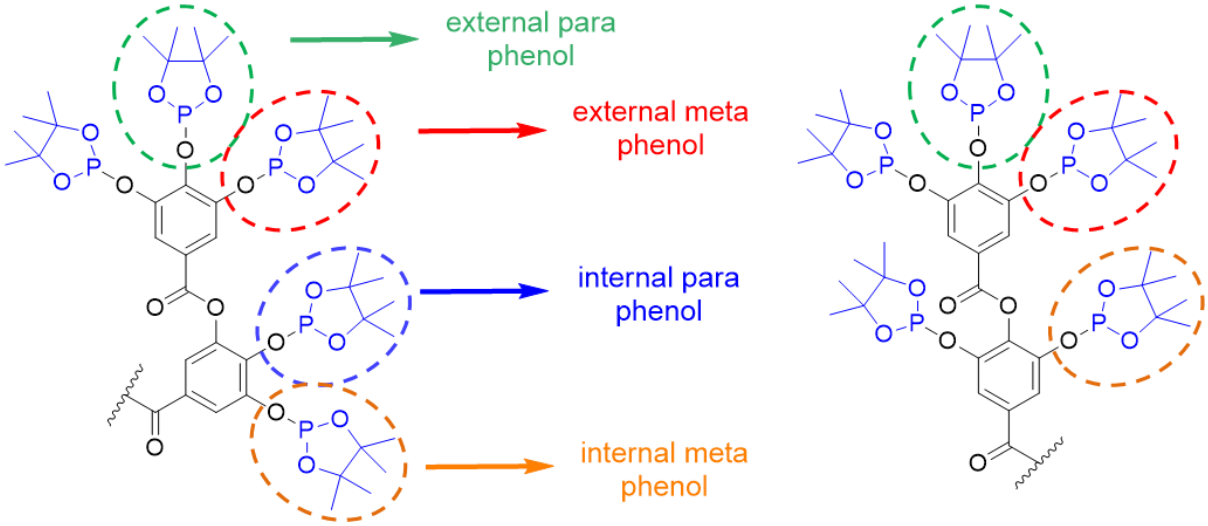

Figure II.3. Representation of different phosphitylated phenol positions (*para* and *meta*; internal and external) in TA; Left) representation of digallic unit with *meta* depside bond; Right) representation of digallic unit with *para* depside bond

The spectrum in **Figure II.4** show weak signals in the acid region (132-135 ppm) indicating that the sample contains free acids, corresponding to free gallic acid (10 mol% or 1 wt%). All of the signals have been assigned according to Melone et al.[11]. Two regions were identified and attributed respectively to signals for *para* and *meta* phenolics, ranging from 142.5 to 140.5 ppm and from 140.5 to 137.8 ppm respectively. These regions can again be subdivided into two regions for the internal phenolics and the external phenolics which lead to four distinct types of signals.

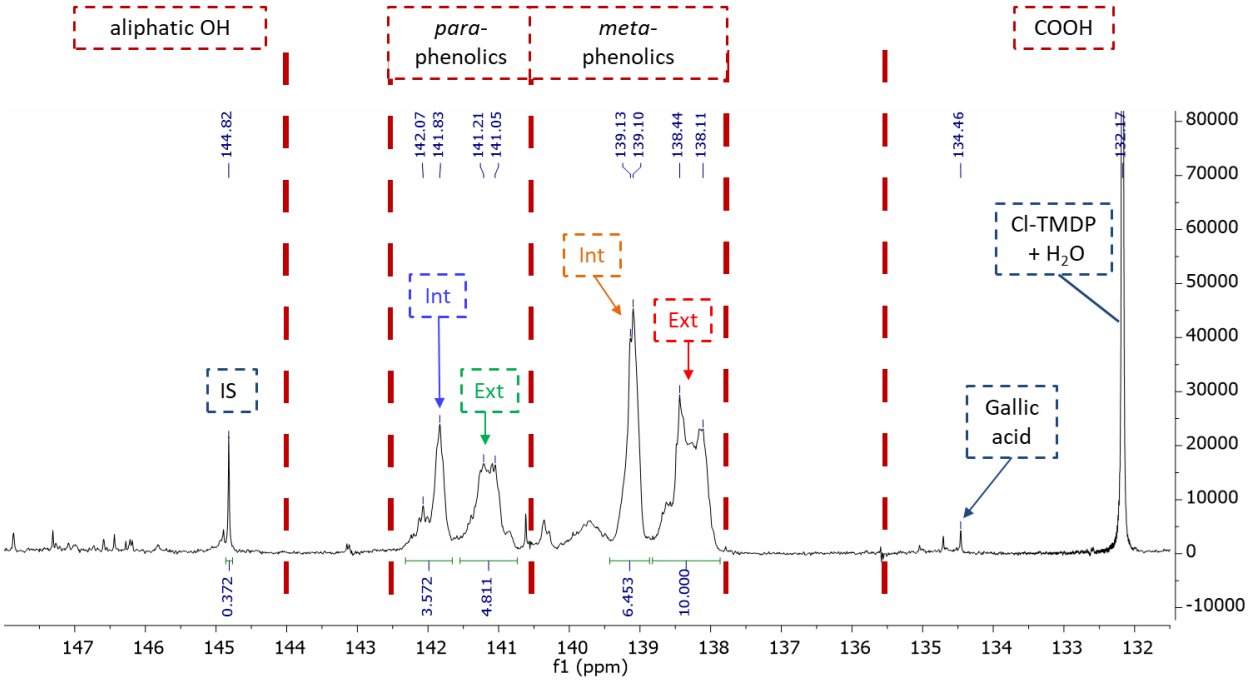

Figure II.4. ^{31}P NMR spectrum of tannic acid, $CDCl_3$/Pyr, 151MHz, 4096 scans, D1=15sec, IS = cholesterol

The *para*-phenolics show two peaks, the signal at 141.2 ppm was assigned to the external phenols and the signal at 141.9 ppm to the internal phenolics.[11] The *meta*-phenols are grouped into two broad peaks centered at 139.1 and 138.3 ppm, respectively. The ratio between the integrals of the internal and the external *para*-phenolics provides quantitative information about the regiochemistry of the depside bond. In a fully *meta*-depside bond tannic acid, we would expect five internal and five external *para*-phenol groups per molecule. In contrast, when *para*-depside bonds are present, the internal *para*-phenolics are absent (**Figure II.3**).

In the analysis of our batch of TA, the integrations showed a 3.5:5 ratio between the internal and external *para*-phenolics meaning that there is on average 1.5 *para*-depside bond per tannic acid molecule.

This is also confirmed by the integration of the *meta*-phenolics. We determined the presence of 16.5 (15 + 1.5) phenol groups which is in accordance with the average 1.5 *para*-depside bonding pattern per tannic acid molecule. This result proved that we have 30% of *para*-depside bond inside our tannic acid.

II.1.3. ATR-FTIR spectroscopy

Our batch of TA has been also analyzed by ATR-FTIR spectroscopy. The spectrum is displayed on **Figure II.5**.

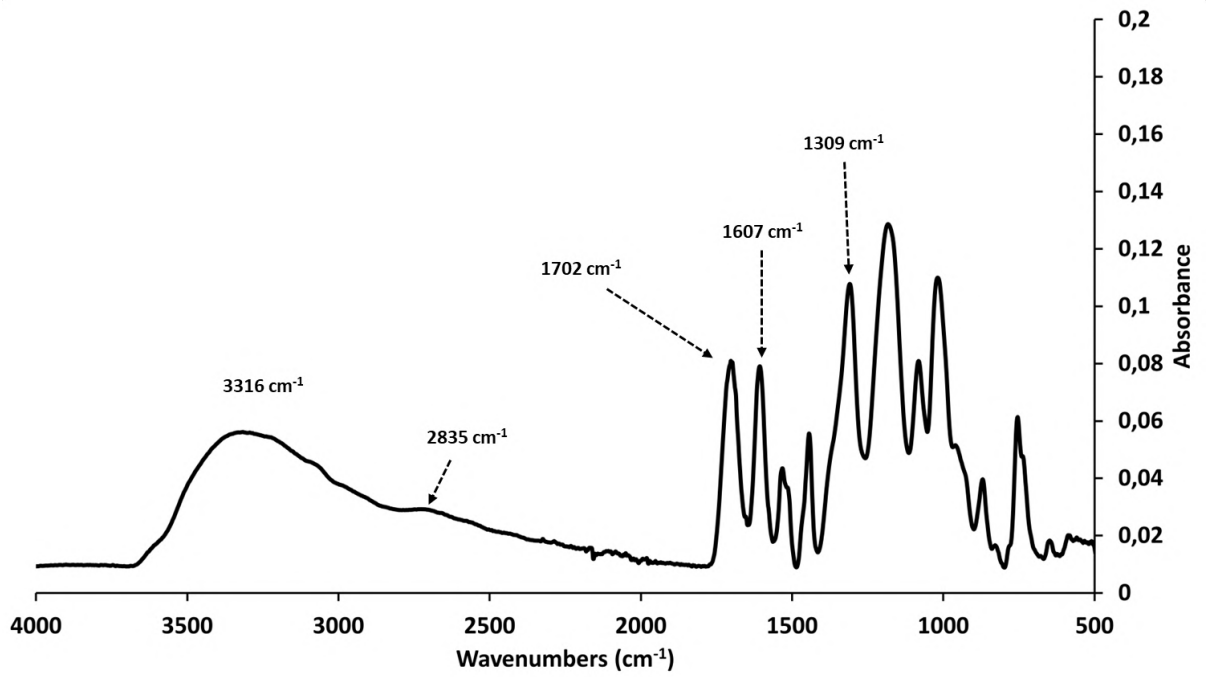

Figure II.5. FTIR analysis of commercially available TA, ATR, absorbance mode

The spectrum shows a wide and strong band absorption centered at 3316 cm^{-1} (3600-3000 cm^{-1}). This band was assigned to the hydroxyl groups υ(OH). At 2835 cm^{-1}, a band corresponding to the aliphatic υ(C–H) was observed and attributed to the glucose core.[12] The characteristic signal of carbonyl groups υ(C=O) was observed at 1702 cm^{-1}. We observed a signal at 1607 cm^{-1} which we attributed to the aromatic υ(C=C). The spectrum displayed an intense absorption band at 1309 cm^{-1} which is related to the coupled vibrations of the ring υ(C–C) with the contribution from the δ(C–H) and δ(C–OH) vibrations.[13] The deformation vibrations of the C-H bonds in the benzene rings also gave weak absorption bands between the ranges of 900-550 cm^{-1}, with a strong one at 754 cm^{-1}.

II.1.4. Mass spectrometry

TA is a polyphenol with several gallic units. Even if its structure is not precisely defined, mass spectrometry allows us to analyze the distribution of the number of gallic units. Electrospray (ESI) is the most commonly used ionization technique.[14,15]

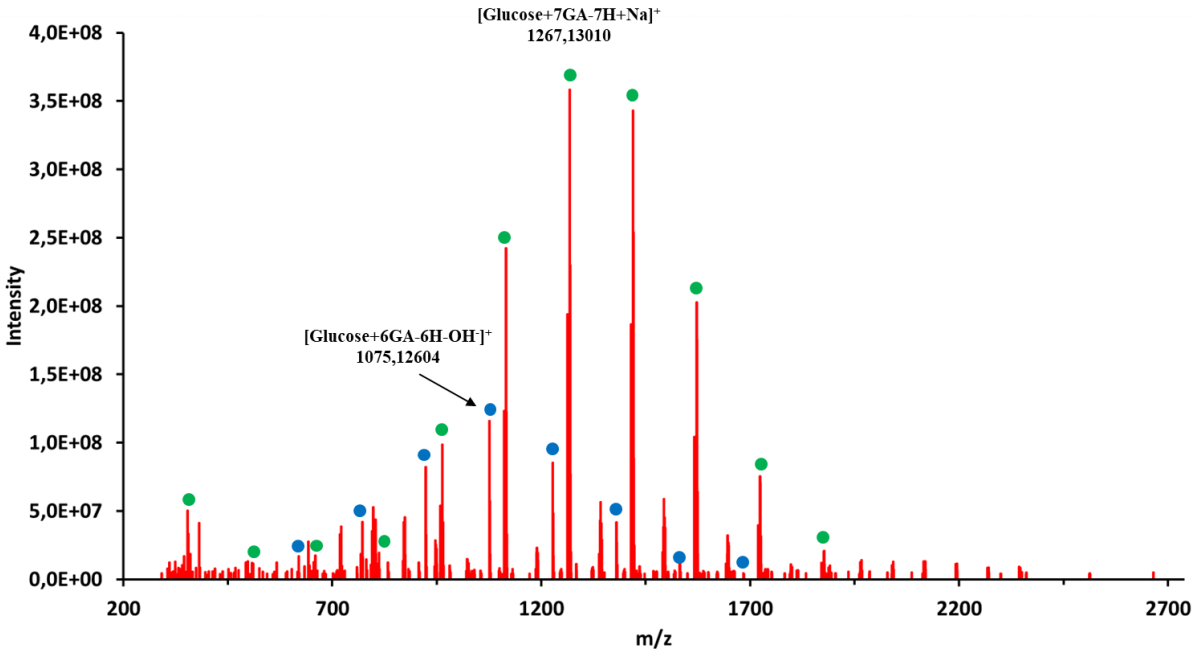

Figure II.6. Positive ion ESI mass spectrum of TA in 0.1% formic acid/methanol solution (v/v); GA stands for gallic acid unit. The colored circles correspond to different ionization (green: $+Na^+$, blue: $-OH^-$). See Table II.9 for tabulated data

Figure II.6 shows the positive ion ESI mass spectrum of tannic acid in 0.1% formic acid/methanol solution (v/v). We used the same conditions as Fu et al.[14] and observed the same strong peaks, corresponding to the sodium adduct ions of TA with 5 to 10 galloyl groups (green circle), although with different relative intensities.

Also, we identified a second distribution marked with a blue circle on the spectrum. These peaks correspond to adduct ions of TA after abstraction of a OH^-. The peaks are reported on **Table II.9**.

II.1.5. Determination of total phenolic content

The principle of this method is the formation of blue complex compounds due to the reaction between the phenolic compounds and the Folin-Ciocalteu reactant, which can be quantified by UV spectrometry. The total phenolic content can be determined after oxidation of phenolics

and comparison to a calibration curve with gallic acid. We therefore built a gallic acid calibration curve according to Singleton et al.[16] (see **Figure II.38**) and analyzed with the same method TA solutions at different concentrations.

We used three solutions with molar concentrations between 3mM and 9mM, the number of free phenols determined were between 28 and 31 with an average of 29.6 phenols instead of 25 theoretically.

As the environment of the internal phenols in TA and in gallic acid are not identical, we tested other possible analogues of the internal phenols of TA: 3,4- and 3,5-dihydroxybenzoic acids. The results are displayed in **Table II.1**.

Table II.1. Total phenolic content of model phenols

Molecules	Free phenols (experimental)	Free phenols (theoretical)
3,4-dihydroxybenzoic acid	**2.52**	**2**
3,5-dihydroxybenzoic acid	**1.45**	**2**

The results showed a large difference of absorbance between the two dihydroxybenzoic acid molecules after oxidation. This proved the impact of the phenols environment on the results. We can see that the 3,5-dihydroxybenzoic acid absorbed 25% less than theoretical and the 3,4-dihydroxybenzoic acid absorbed 25% more than theoretical. This can be explained by the oxidation process. Indeed, for this method to work, the phenols need to be oxidized and the Folin-Ciocalteu reactant needs to be reduced. Studies on oxidation processes of catechol and resorcinol, simpler analogues of 3,4- and 3,5-dihydroxybenzoic acid showed that the energy required to oxidize 3,5-dihydroxybenzoic acid is 15 times higher than for the oxidation of 3,4-dihydroxybenzoic acid.[17,18] In addition, the intermediate radicals formed can react with each other or with another molecule, which requires less energy than the oxidation. This could explain the difference in terms of absorbance between both molecules.

The values in **Table II.1** are relative to the gallic acid molecule which presents the same oxidation problem as for the 3,5-dihydroxybenzoic acid meaning that only two out of the three phenols of gallic acid are easily oxidized. Therefore, the gallic acid calibration curve induces

an overestimation of the phenol content for 3,4-dihydroxybenzoic acid, explaining the value higher than 2.

According to our NMR data, TA is composed of 5 x galloyl units, 3.5 x (3,4-dihydroxybenzoyl units) and 1.5 x (3,5-dihydroxybenzoyl units). Adding up the individual response for each unit (3, 2.52 and 1.45, respectively) yields an expected total phenolic content of 26. This value is closer to the experimentally determined value of 29.6 but the agreement is still not perfect. It means that this approach is only semi-quantitative.

After characterizing the tannic acid batch, we used the same characterization techniques for the functionalized molecules.

II.2. Fully acetylated derivative

II.2.1. ^{1}H NMR analysis

The solubility in organic solvents increased with the increase of the functionalization rate. The NMR analyses were run using CD_2Cl_2 and acetone-D_6 as deuterated solvents. On the ^{1}H NMR spectra, we observed a signal ranging from 8.2 to 7.6 ppm attributed to the aromatic protons. By comparing with the tannic acid spectrum (**Figure II.7**), we can see a shift by almost one ppm that is probably the direct effect of the acetylation.

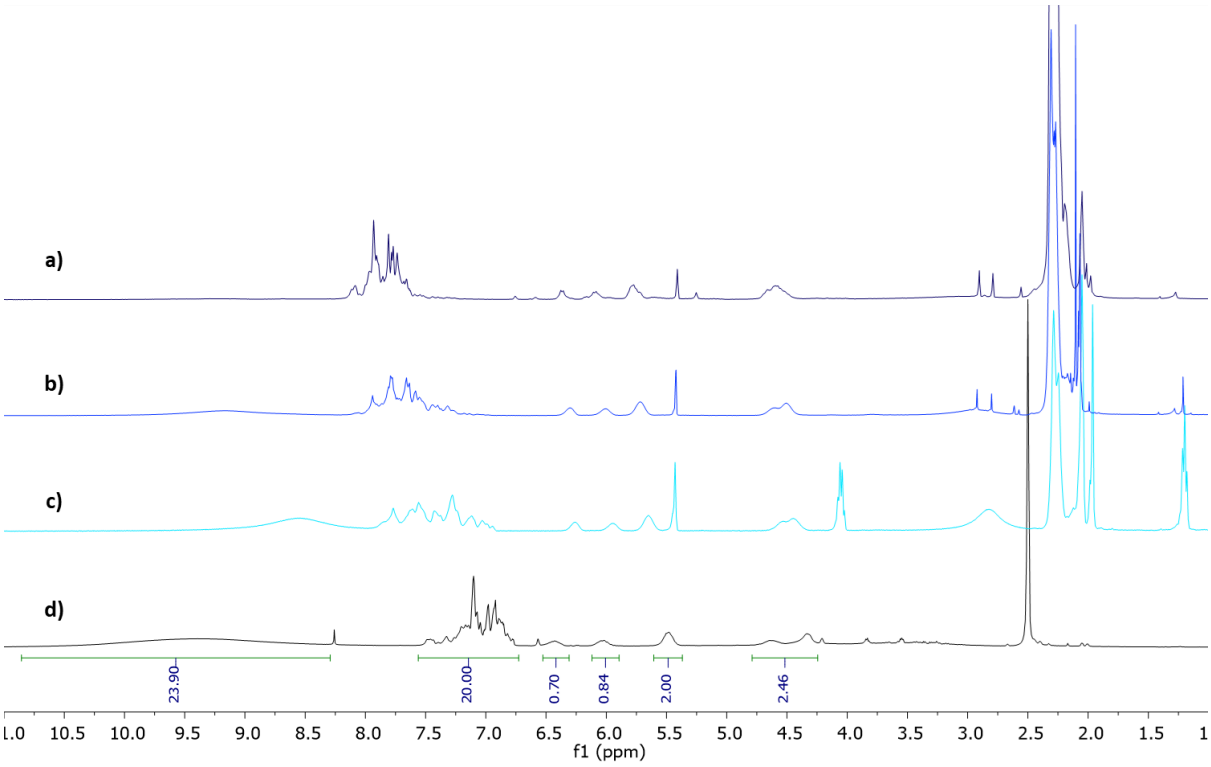

Figure II.7. Comparison of ^{1}H NMR spectra between TA and acetylated products; a) $TA(OAc)_{25}$ in CD_2Cl_2/acetone-D_6 (dark blue line); b) $TA(OAc)_{15}$ in CD_2Cl_2/acetone-D_6 (blue line); c) $TA(OAc)_8$ in CD_2Cl_2/acetone-D_6 (light blue line); d) tannic acid in DMSO-D_6 (black line)

The glucose core signals were similar to the tannic acid analysis. They were identified (**Figure II.7a**) with three signals from 6.41 to 5.57 ppm and two signals between 4.7-4.4 ppm. The latter signals shifted closer to each other than for TA. The acetyl groups appear as a strong signal around 2.3 ppm integrating for 85 protons (75 protons theoretical expected). A ^{1}H NMR of acetic acid (side product of the acetylation reaction) in the same solvent mixture (CD_2Cl_2

/acetone D_6) showed a signal for the CH_3 of the acetic acid at 1.99 ppm therefore it does not interfere with the integration of our products. In the fully acetylated product, less than 1% of acetic acid remained (calculated with ^{1}H NMR integration).

II.2.2. ^{13}C NMR analysis

In comparison with the spectrum of tannic acid, displayed in **Figure II.8**, we identified some new signals.

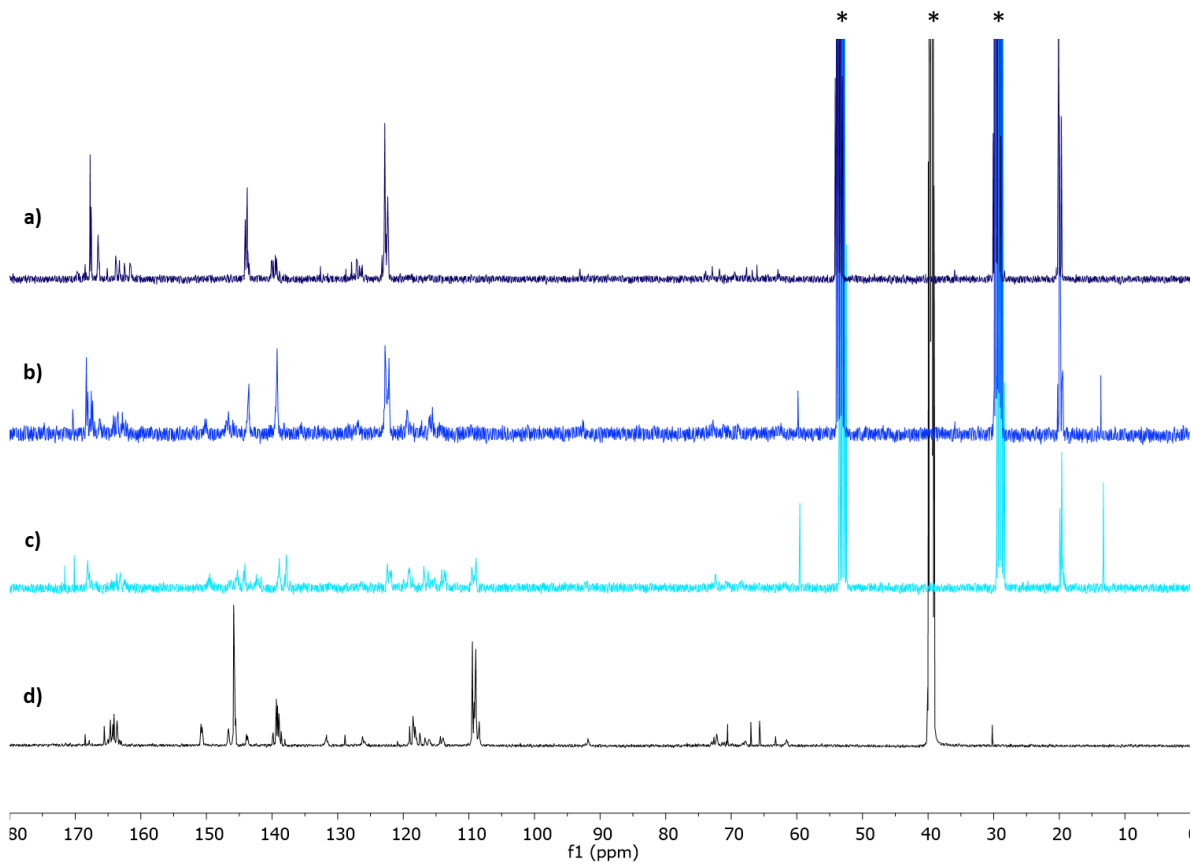

Figure II.8. Comparison of ^{13}C NMR spectra between TA and acetylated products; a) $TA(OAc)_{25}$ in CD_2Cl_2/acetone-D_6 (dark blue line); b) $TA(OAc)_{15}$ in CD_2Cl_2/acetone-D_6 (blue line); c) $TA(OAc)_8$ in CD_2Cl_2/acetone-D_6 (light blue line); d) tannic acid in DMSO-D_6 (black line). * represent the residual signals from the deuterated solvents CD_2Cl_2, DMSO-D_6 and acetone-D_6

The strong signal around 168 ppm was easily attributed to the C=O from the acetyl groups and the intense peaks around 20 ppm attributed to the CH_3 from the acetyl groups.

For the carbons of the galloyl units, we observed a shift of the signals from 110 to 122 ppm. This can be the result of the acetylation process. Indeed, these carbons are close to the new

electron withdrawing acetyl groups. The peaks of the glucose core are still visible with the signal from the anomeric position at 93 ppm and the other carbon signals between 73 and 62 ppm.

II.2.3. ATR-FTIR spectroscopy

FTIR spectroscopy analysis were carried out in order to see if the difference in terms of intensity can help us determine the functionalization rate.

In **Figure II.9a**, the signal corresponding to the υ(O–H) band was still visible, implying that a tiny fraction of OH groups were still not functionalized. This was also observed by Xia et al. on some esterified tannic acid derivatives.[19] It is also possible that we observed the OH band from the carboxylic acid acetic acid side product.

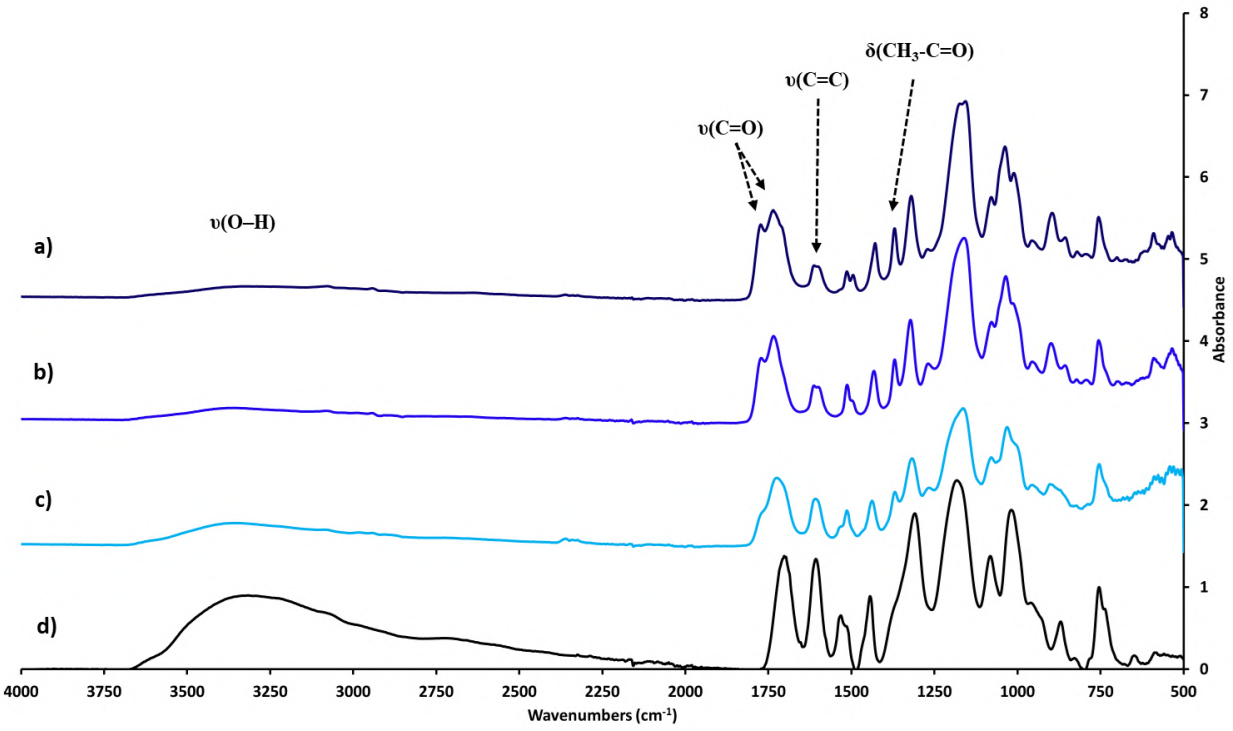

Figure II.9. Comparison of ATR FTIR spectra between TA and acetylated products in absorbance mode; a) $TA(OAc)_{25}$ (dark blue line); b) $TA(OAc)_{15}$ (blue line); c) $TA(OAc)_{8}$ (light blue line); d) tannic acid (black line)

Two bands at 1773 and 1735 cm^{-1} were respectively attributed to the υ(C=O) from the acetyl groups and from the inner structure of tannic acid respectively. The signals for the υ(C=O) from the inner structure of tannic acid shifted by comparison with tannic acid (1702 cm^{-1}). This shift can be attributed to the acetylation of the phenolics.

At 1513 cm^{-1}, the band was attributed to υ(C–C ar) of the initial structure. The band at 1370 cm^{-1} correspond to the carbon-hydrogen δ(C-H) bending in acetyl group , which is in accordance with the literature.[20]

II.2.4. Mass spectrometry

Unlike TA, the fully acetylated derivative is not soluble in methanol. We therefore had to use a methanol/dichloromethane mixture (50/50) in order to solubilize the molecule, while keeping a good proportion of methanol in order to facilitate the ionization of the sample. The analysis has been conducted with the same ESI/FT-ICR conditions as for TA. The spectrum obtained is displayed in **Figure II.10**.

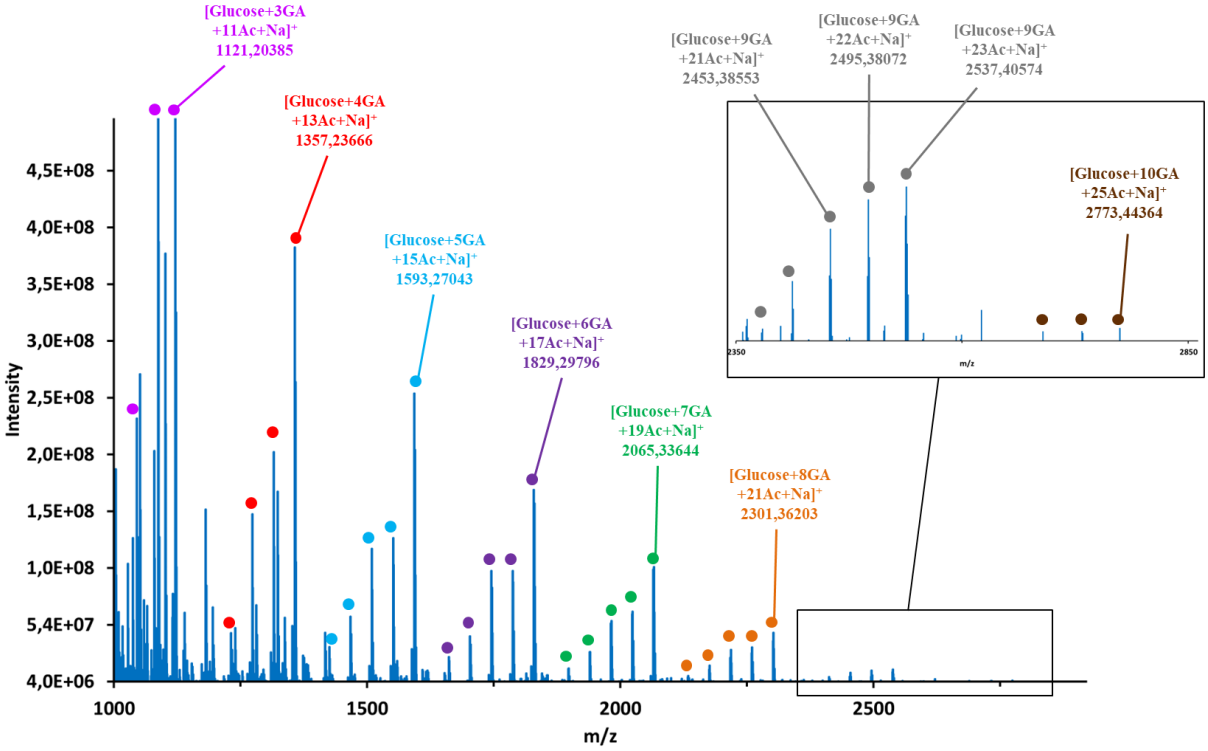

Figure II.10. Positive ion ESI mass spectrum of $TA(OAc)_{25}$ in methanol/dichloromethane solution (v/v); GA stands for gallic acid unit and Ac for acetyl groups. The colored circles correspond to the number of GA in the molecule (pink: 3GA; red: 4GA; blue: 5GA; purple: 6GA; green: 7GA; orange: 8GA; grey: 9GA; brown: 10GA). The mass difference between two circles of the same color corresponds to 42 g/mol, i.e. 1 Ac unit. See Table II.10 for tabulated data

We identified several distributions marked with colored circles on the spectrum. These correspond to the sodium adduct ions of acetylated TA with 3 to 10 galloyl groups. The peaks

are reported on **Table II.10**. For each color, the largest peak corresponds to the fully acetylated molecule confirming the efficiency of the reaction.

II.3. Partially acetylated derivatives

II.3.1. ^{1}H NMR analyses

Signals corresponding to ethyl acetate and acetone (solvent used for purification) remained despite all our attempts to remove these traces from the sample, we did not succeed. It is likely that the phenols interact with the solvent by hydrogen bonding.

On the ^{1}H NMR spectrum of TA(OAc)$_{15}$ (**Figure II.7b**), we observed a signal centered at 9.16 ppm attributed to the non-functionalized OH groups. Partial acetylation of tannic acid was confirmed by the presence of the peak at 2.3 ppm. The aromatic protons were observed around 8-7.2 ppm, showing a slight shift compared to the fully acetylated molecule. This is an effect of the partial acetylation. The glucose core signals were similar to the fully acetylated molecule.

In terms of integration, a variation between the expectation and the experiment was observed. For TA(OAc)$_{8}$, we observed 8-9 protons for the free OH phenolics and 23 protons for the acetyl groups. This implied that the acetylation rate is around 8 but, some of the phenolics were not visible. Indeed, we would expect 17 protons instead of 8-9. For TA(OAc)$_{15}$, we observed 7 protons for the phenolics and 51 protons for the acetyl groups. In this case, the acetylation rate is around 17-18 instead of 15 but the integration of the phenol and acetyl showed the same rate.

II.3.2. ^{13}C NMR analyses

On the ^{13}C NMR spectrum of TA(OAc)$_{15}$ (see **Figure II.8b**), the signals were weaker compared to the fully acetylated product and the almost disappearance of glucose peaks. Perhaps the balance between the hydrophilic and hydrophobic parts of the molecule combined with the mixture of deuterated solvents used for the analyses prevented us from seeing the inner core of these molecules. For TA(OAc)$_{8}$, we recovered the peaks of the galloyl units between 150 and 105 ppm but, the signals from the glucose core were weak.

II.3.3. ^{31}P NMR analyses

The partially acetylated tannic acid derivatives have been analyzed with the same phosphitylation conditions as tannic acid. As explained with tannic acid, we can identify two regions of signals attributable to *para*-phenolics and *meta*-phenolics. The spectra displayed on **Figure II.11** still show two peaks in the *para*-phenolics area, meaning that both internal and external phenolic groups in *para*-position are not fully acetylated.

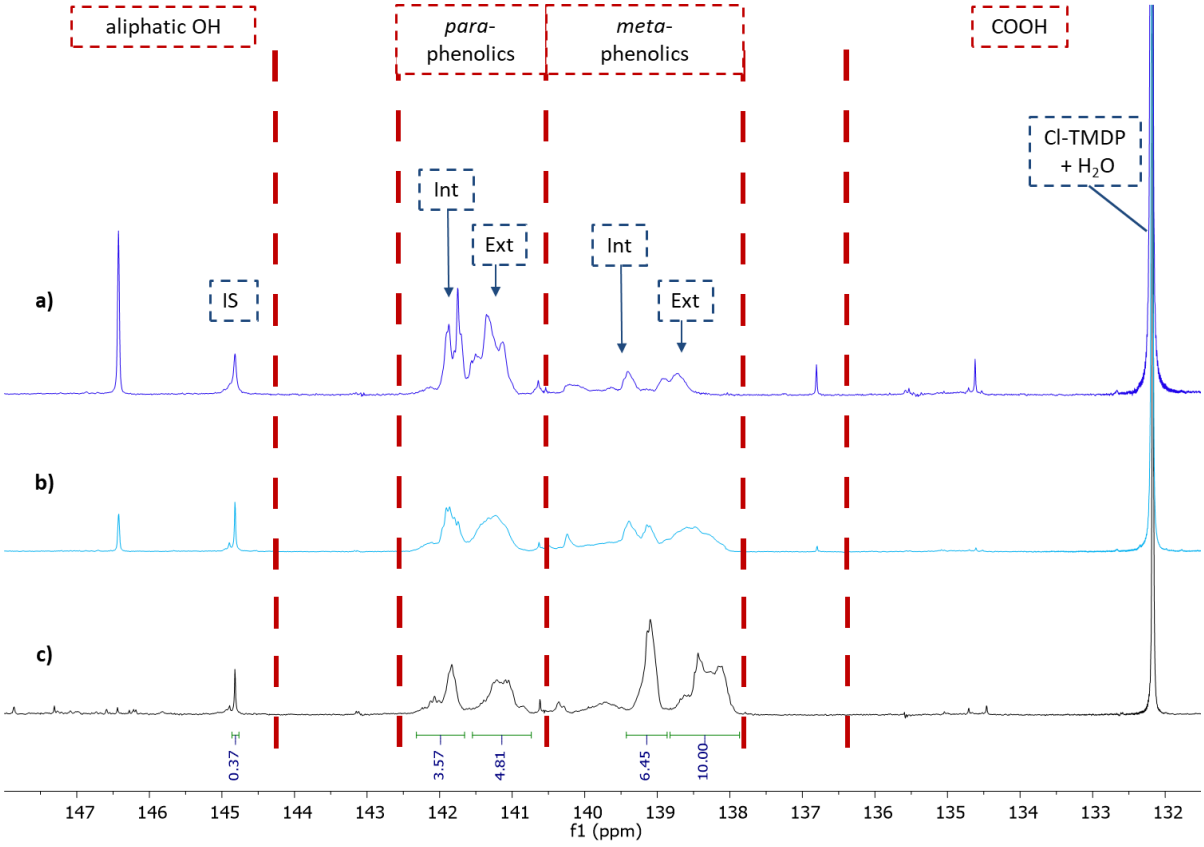

Figure II.11. Comparison of ^{31}P NMR spectra between TA and acetylated products; a) ^{31}P NMR spectrum of TA(OAc)$_{15}$ (blue line); b) ^{31}P NMR spectrum of TA(OAc)$_8$ (light blue line); c) ^{31}P NMR spectrum of tannic acid (black line). The spectra have been normalized on the internal standard (IS) signal

In the tannic acid molecule, we have 8.5 *para*-phenolics (3.5 internal and 5 external). In TA(OAc)$_8$, we still have 8.5 *para*-phenolics with the same ratio of 3.5:5 (internal : external). This implies that the acetylation occurs only on the *meta*-position. This is confirmed by the integration in the *meta*-phenolics area. We determined the presence of 7 phenolic groups instead of 16.5 for the starting tannic acid molecule implying that we functionalized an average of 9.5 phenolic OH groups, all in *meta*-position.

For $TA(OAc)_{15}$, in the *meta*-phenolics area, we determined the presence of 1,5 phenolics, meaning that mainly the phenolics in *meta*-position have been acetylated, the same as the previous molecule.

Therefore, in the *para*-phenolics area, we do not have 8,5 phenolics but 6,5 meaning that 2 phenolic groups have been functionalized. In this area, the ratio is now 2,5:4 (internal : external) *para*-phenolics meaning that one internal and one external phenolic group in *para*-position have been acetylated. The steric hindrance must be the explanation, meaning that the phenolics in *para*-position are more available than the remaining phenolics in *meta*-position and therefore more easily acetylated.

II.3.4. ATR-FTIR spectroscopy

For the partially acetylated derivatives, we observed the same phenomenon for υ(C=O), the bands shifting with the increase of acetylated phenolics.

For $TA(OAc)_8$, we observed an intense band at 1724 cm^{-1} with a small shoulder. For $TA(OAc)_{15}$, we observed two bands at 1771 and 1734 cm^{-1} respectively (**Figure II.9**). These bands were attributed to the C=O from the acetyl groups and from the ester depside bond of tannic acid. These observations were in agreement with the functionalization rate used.

II.3.5. Mass Spectrometry

The same conditions as for the fully acetylated derivative have been used. The spectrum for $TA(OAc)_{15}$ is displayed in **Figure II.12 (Top)**. The peaks are reported on **Table II.11**.

The same distributions as for $TA(OAc)_{25}$ have been observed, with 3 to 10 galloyl groups. No signal corresponding to a functionalization higher than 15 was detected and the target molecule $TA(OAc)_{15}$ was observed at *m/z* 2353,32519.

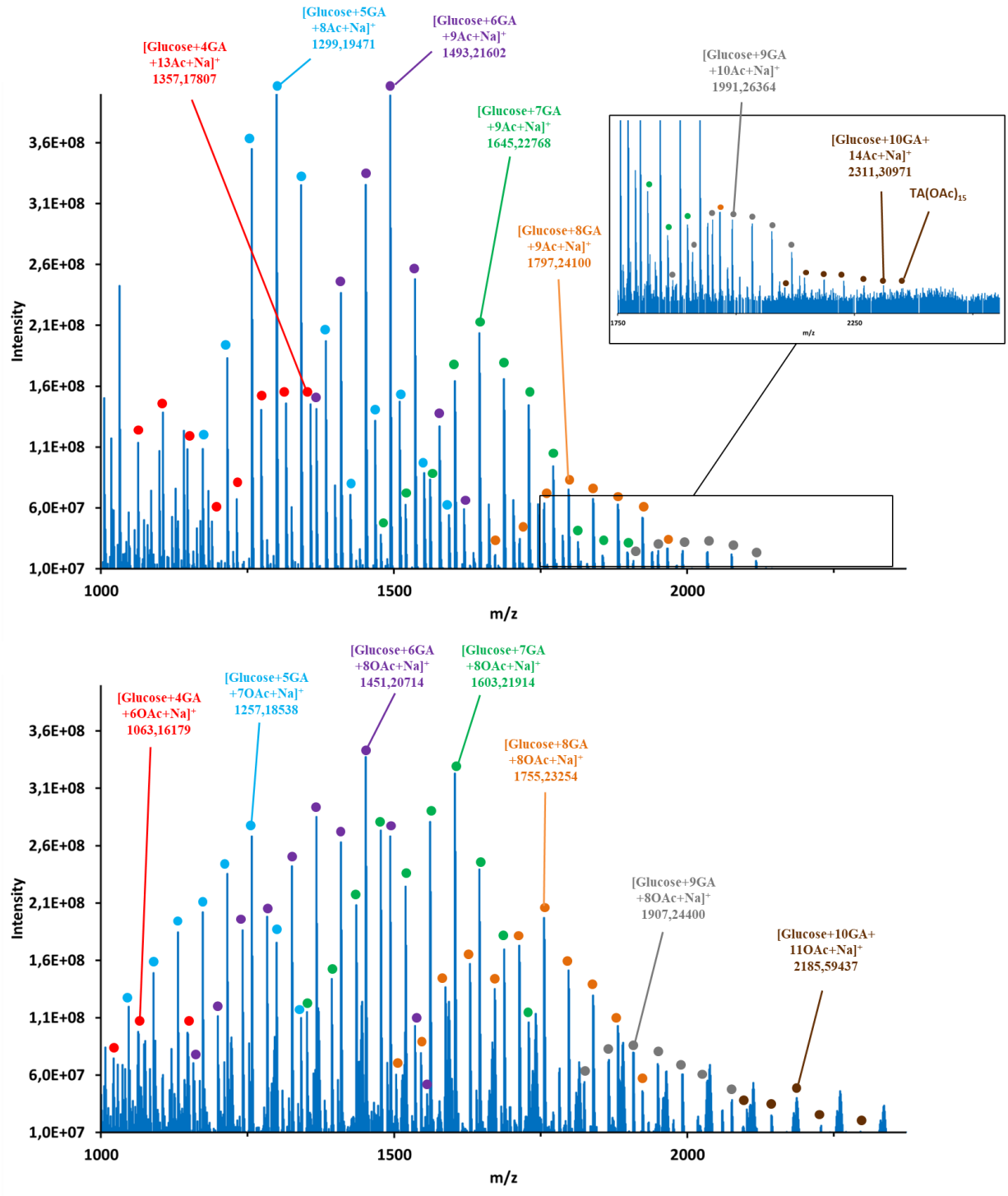

Figure II.12. Top) Positive ion ESI mass spectrum of $TA(OAc)_{15}$ in methanol/dichloromethane solution (v/v); Bottom) Positive ion ESI mass spectrum of $TA(OAc)_8$ in methanol/dichloromethane solution (v/v); GA stands for gallic acid unit and Ac for acetyl groups. The colored circles correspond to the number of GA in the molecule (red: 4GA; blue: 5GA; purple: 6GA; green: 7GA; orange: 8GA; grey: 9GA; brown: 10GA). The mass difference

between two circles of the same color corresponds to 42 g/mol, i.e. 1 Ac unit. See Table II.11 for tabulated data.

For $TA(OAc)_8$, the spectrum is displayed in **Figure II.12 (Bottom)**. The same distributions as previous molecules were observed. Some signals correspond to a functionalization higher than 8, but the average functionalization is indeed lower than for $TA(OAc)_{15}$.

II.3.6. Determination of total phenolic content

As explained for tannic acid analysis, a calibration curve was determined with gallic acid. However, the synthesized molecules are organosoluble and the calibration curve of gallic acid was done in water, we decided to compare the absorbances of methyl gallate solutions in acetone with gallic acid to check if both conditions were reliable. Solutions of methyl gallate at different molar concentrations were analyzed and an average of 3.16 phenols was obtained instead of 3 phenols theoretical. We could conclude that the solvent used, acetone in the case of methyl gallate and water in the case of gallic acid, does not have a significant impact on the final result.[21]

Calibration with gallic acid was used also for the organosoluble compounds. The functionalized tannic acid molecules were solubilized in acetone and analyzed. We have done the same procedure three times to obtain an average absorbance for each molecule. The results are shown in **Table II.2**.

Table II.2. Determination of free phenols remaining by Folin-Ciocalteu's method in partially acetylated molecules

Molecules	Solvent	Free phenols (experimental)	Free phenols (theoretical)
TA	water	**29.6**	**25**
$TA(OAc)_{15}$	acetone	**8.9**	**10**
$TA(OAc)_8$	acetone	**21**	**17**

We observed that the method was reliable for the acetylated molecules. Indeed, the results obtained by ^1H NMR and ^{31}P NMR were consistent (see **Figure II.40**).

II.4. Fully esterified derivative

II.4.1. ^{1}H NMR analysis

The ^{1}H NMR spectra showed (**Figure II.13)** some differences compared to the starting material. The aromatics and the glucose core were as visible as the fully acetylated product with the same shift attributed to the mixture of solvents used.

For the specific protons from the stearoyl moieties, we observed 4 different signals: **1)** from 2.80 to 2.36 ppm is the CH_2-C=O, **2)** from 1.82 to 1.62 ppm is the CH_2 in β-position, **3)** from 1.49 to 1.04 ppm is the $(CH_2)_{15}$ signal and **4)** at 0.95 to 0.80 ppm is the CH_3 signal from the end of the ester chains. However, traces of stearic acid remaining in our final product (~ 10 % mol) can be seen at 2.35-2.16 ppm and 1.62-1.50 ppm.

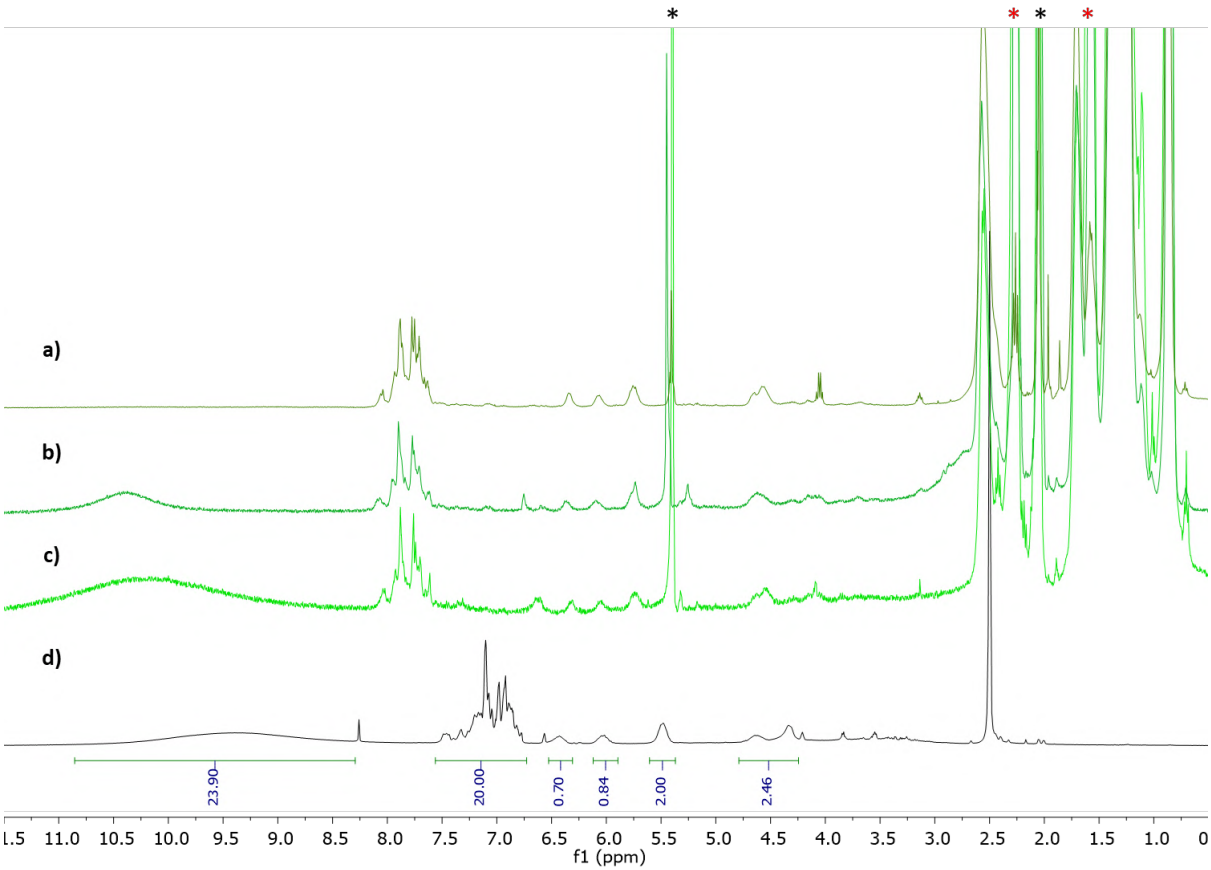

Figure II.13. Comparison of ^{1}H NMR spectra between TA and esterified products; a) ^{1}H NMR spectrum of TA(stearoyloxy)$_{25}$ in CD_2Cl_2/acetone-D_6 (dark green line); b) ^{1}H NMR spectrum of TA(stearoyloxy)$_{15}$ in CD_2Cl_2/acetone-D_6 (green line); c) ^{1}H NMR spectrum of TA(stearoyloxy)$_{9}$ in CD_2Cl_2/acetone-D_6 (light green line); d) ^{1}H NMR spectrum of tannic acid

in DMSO-D_6 (black line). * represent the signals from the remaining stearic acid and * the signals from the deuterated solvents CD_2Cl_2 and acetone-D_6

The integration of C**H₂**-C=O signals led to a rate of 31.5 when the integration of CH_2 in β-position led to a rate of 25. These results are in accordance with the analysis of the fully acetylated molecule. However, despite the fact that 25 is in accordance with the expectation, the signal from CH_2 in β-position is less precise than the one from CH_2-C=O.

II.4.2. ^{13}C NMR analysis

The analysis of this molecule was not easy. Firstly, we can see on **Figure II.14** that the signals of the galloyl units (140-110 ppm) from the inner structure were less or not visible by ^{13}C NMR.

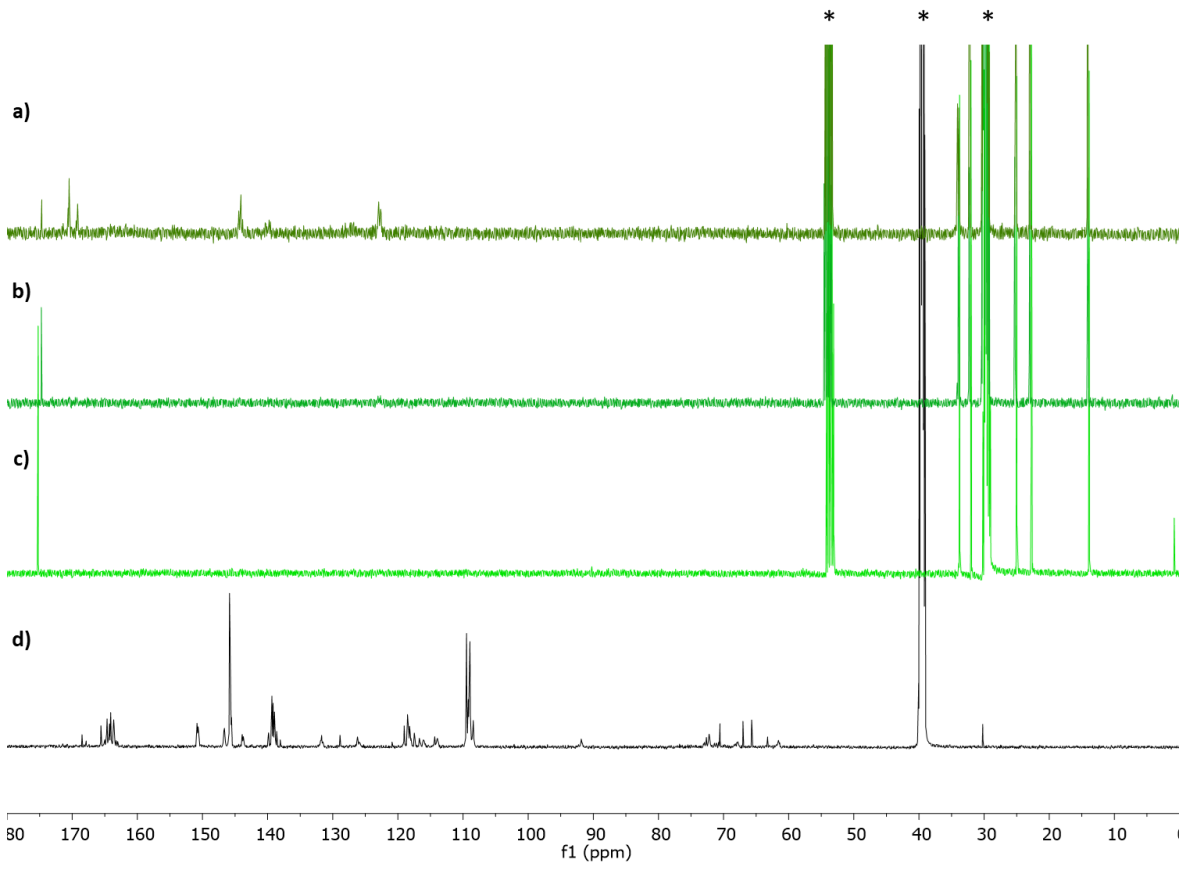

Figure II.14. Comparison of ^{13}C NMR spectra between TA and esterified products; a) ^{13}C NMR spectrum of TA(stearoyloxy)$_{25}$ in CD_2Cl_2/acetone-D_6 (dark green line); b) ^{13}C NMR spectrum of TA(stearoyloxy)$_{15}$ in CD_2Cl_2/acetone-D_6 (green line); c) ^{13}C NMR spectrum of TA(stearoyloxy)$_9$ in CD_2Cl_2/acetone-D_6 (light green line); d) ^{13}C NMR spectrum of tannic acid in DMSO-D_6 (black line); * represent the signals from the deuterated solvents CD_2Cl_2, DMSO-D_6 and acetone-D_6

For the carbonyl region, we observed several signals from 175 to 169 ppm, with a new peak at 174.67 attributed to the C=O from the stearoyl moieties. Few peaks from the aromatics between 145 and 120 ppm were still visible but barely.

From 34 to 22 ppm, we observed intense peaks attributed to the different CH_2 groups in the stearoyl chains and the CH_3 groups were visible around 14 ppm.

II.4.3. ATR-FTIR spectroscopy

As for the tannic acid, we decided to analyze the functionalized molecules by FTIR spectroscopy in order to see if the difference in terms of intensity can help us determine the functionalization rate.

Like the fully acetylated molecule, the υ(O–H) band was not visible on the spectra of the fully esterified molecule (**Figure II.15**).

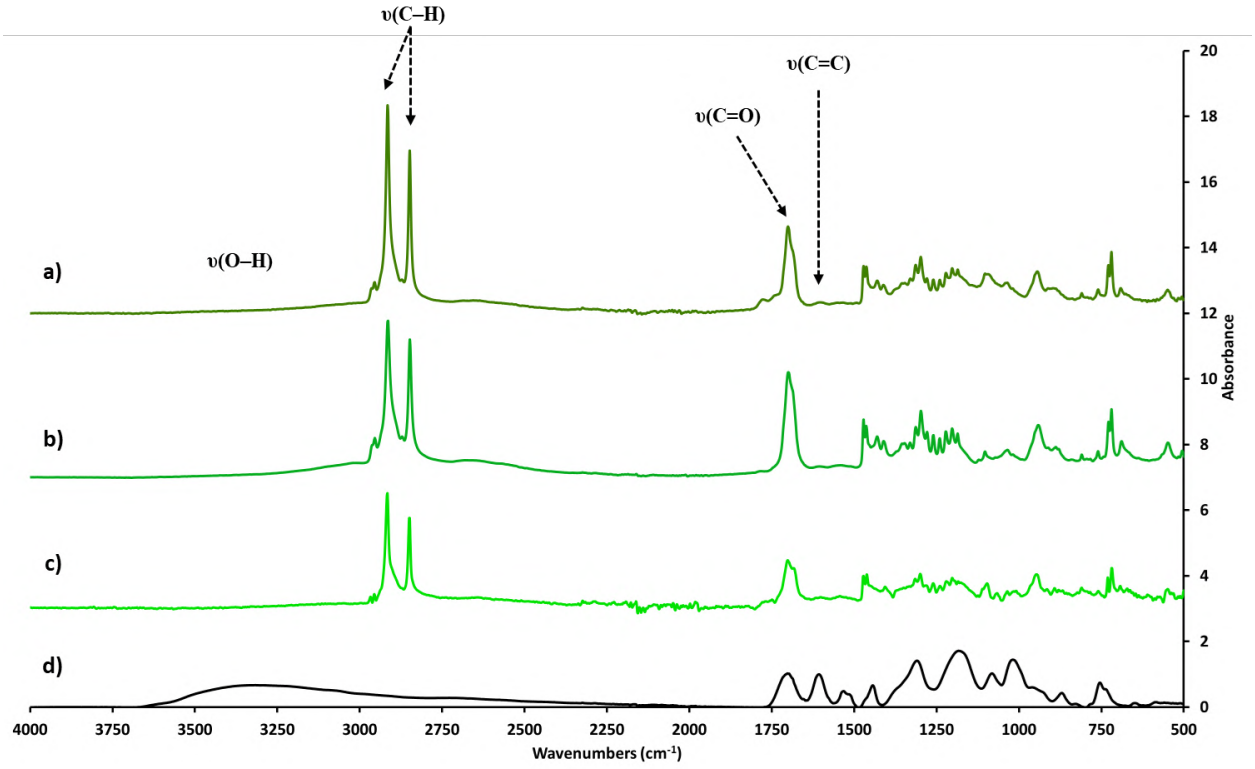

Figure II.15. Comparison of ATR FTIR spectra between TA and esterified products in absorbance mode; a) FTIR spectrum of TA(stearoyloxy)$_{25}$ (dark green line); b) FTIR spectrum of TA(stearoyloxy)$_{15}$ (green line); c) FTIR spectrum of TA(stearoyloxy)$_9$ (light green line); d) FTIR spectrum of tannic acid (black line); Spectra have been normalized on the C=C band

If the molecule is fully functionalized, no phenol groups should remain and no signal should be observed. However, we should see a signal corresponding to the COOH (3300-2500 cm^{-1}) of the stearic acid remaining that was observed on the ^{1}H NMR spectrum.

For the υ(C–H), we observed strong bands around 2920 cm^{-1} and 2850 cm^{-1} from the alkyl chains of the esters.

For the carbonyl groups, we observed a large band around 1702 cm^{-1} corresponding to the overlapping of the bands from the depside esters and from the new fatty ester functions.

II.4.4. Mass spectrometry

Neither electrospray ionization nor APCI (Atmospheric Pressure Chemical Ionization) was successful on the fully esterified tannic acid derivative, therefore no mass spectrometry data is available.

II.5. Partially esterified derivatives

II.5.1. ^{1}H NMR analyses

For both partially esterified molecules, the protons for the aromatics and the glucose were still observed but with a weaker resolution compared to tannic acid or TA(stearoyloxy)$_{25}$ in the same conditions (**Figure II.13**). The specific protons from the stearoyl moieties were present at the same chemical shifts. It is clear that some stearic acid remains in the final product, same as for the fully esterified product.

Unfortunately, the ^{1}H NMR spectra of the partially functionalized molecules present integrations not allowing to determine the rate of phenolic functionalized into ester groups contrarily to the fully esterified molecule. For TA(stearoyloxy)$_{15}$, we have 13 protons remaining for the phenolics showing a functionalization rate of 12 compared to theoretical 15. But the alkyl chains integration are similar to the fully esterified due to the presence of stearoyl acid coming from the synthesis.

In the case of TA(stearoyloxy)$_{9}$, the OH signal was weak and undefined. But with an integration of 20 protons for the aromatics, the stearoyl chains showed a functionalization rate of 19.

II.5.2. ^{13}C NMR analyses

The only signals observed were the ones from the ester chains for the partially esterified molecules. At 175 ppm, the signal of the carbonyl from the stearoyl chains was identified. From 33.6 to 22.6 ppm, these peaks to the CH_2 groups in the stearoyl chains and the CH_3 groups were attributed around 13.7 ppm. The rest of the structure was not visible neither for TA(stearoyloxy)$_{15}$ or for TA(stearoyloxy)$_9$ (see **Figure II.14**). For TA(stearoyloxy)$_9$, another NMR analysis at 600MHz instead of 400MHz , with a relaxation delay of 30 sec instead of 4, a concentration of 120 mg/mL and around 2600 scans has been conducted. Nevertheless, the result remained the same with only the carbonyl from the stearoyloxy visible.

II.5.3. ^{31}P NMR analyses

The esterified molecules have been analyzed with the same phosphitylation conditions as the acetylated derivatives. These spectra displayed very small signals characteristic for *para*- and *meta*-phenolic groups compared to the acetylated molecules (**Figure II.16**).

For TA(stearoyloxy)$_{15}$, the spectrum showed an integration of 0.5 phenolics in the *para*-phenolics region and 2.5 phenolics in the *meta*-phenolics region for a total of three phenolic groups which is less than the ten theoretical OH groups remaining free. In the case of TA(stearoyloxy)$_9$, the spectrum showed an integration of 2,5 phenolics in the *para*-phenolics region and 0,5 phenolics in the *meta*-phenolics region for a total of three phenolic groups which is not coherent with the previous analysis.

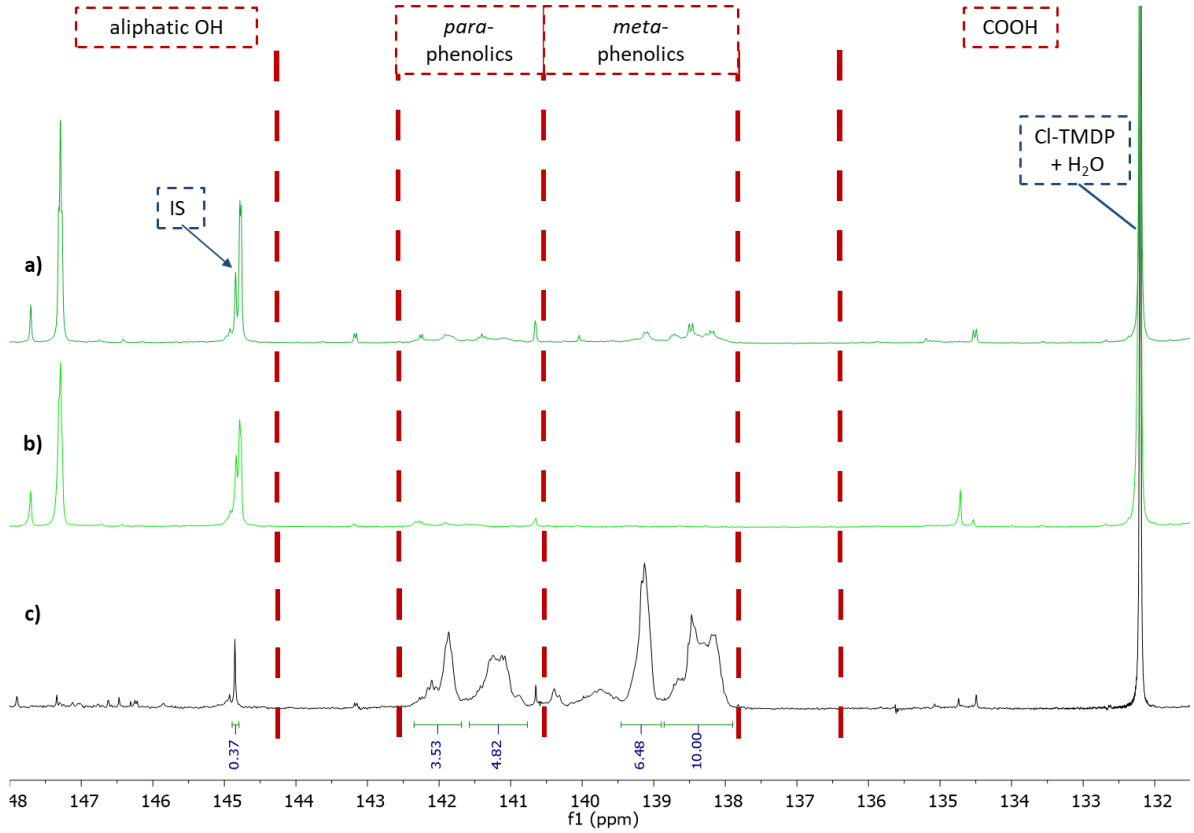

Figure II.16. Comparison of ^{31}P NMR spectra between TA and esterified products; a) ^{31}P NMR spectrum of TA(stearoyloxy)$_{15}$ (green line); b) ^{31}P NMR spectrum of TA(stearoyloxy)$_{9}$ (light green line); c) ^{31}P NMR spectrum of tannic acid (black line). The spectra have been normalized on the internal standard (IS) signal

After obtaining inconsistent results, we supposed that the phosphitylation process was uncomplete. At 132.2 ppm, the signal from the reaction product of water with Cl-TMDP was observed implying that there is enough reagent for the phosphitylation.

The steric hindrance of the stearoyloxy groups could prevent the phosphitylation process or from seeing the phosphitylated groups. This implies that the free phenolic groups remaining are not properly analyzed by NMR. Maybe that the spatial configuration and the steric hindrance of the molecule prevents the analysis to give better results. The second possible explanation is the consequence of the esterification with the increase of the van der Waals interactions.

II.5.4. ATR-FTIR spectroscopy

Contrarily to the spectrum of tannic acid, the spectra of the esterified derivatives (functionalization rate 9 or 15) displayed on **Figure II.15**, do not show the strong band in the ranges of 3600-3000 cm^{-1} assigned to the hydroxyl groups. Two hypotheses can be done: firstly,

the OH groups were esterified and by extension not seen; secondly, the esterified molecule is in a conformation that prevents from seeing the OH groups, regarding the fact that the band at 2835 cm^{-1} corresponding to the υ(C–H) from the glucose core was not visible neither.

A large signal for the υ(C=O) around 1700 cm^{-1} was observed and was attributed to the υ(C=O) of the stearoyloxy groups and to the internal ester depside bonds respectively. The stearoyloxy signal intensity has also increased as the functionalization rate was higher.

Furthermore, two strong signals were observed at 2915 cm^{-1} and 2850 cm^{-1} respectively, assigned to the υ(C–H) of the ester chains. The bands for TA(stearoyloxy)$_{15}$ were more intense than the ones for TA(stearoyloxy)$_9$ which implies an higher functionalization rate.

II.5.5. Determination of total phenolic content

We used the same calibration curve (gallic acid) and the same methodology as for the partially acetylated molecules. The results are presented in **Table II.3**.

Table II.3. Determination of free phenols remaining by Folin-Ciocalteu's method on partially esterified molecules

Molecules	Solvent	Free phenols (experimental)	Free phenols (theoretical)
TA	water	**29.6**	**25**
TA(stearoyloxy)$_{15}$	acetone	**8.1**	**10**
TA(stearoyloxy)$_9$	acetone	**0.04**	**16**

For TA(stearoyloxy)$_{15}$, the theoretical free phenol were in agreement with the experimental results obtained with the Folin-Ciocalteu method. Surprisingly, the results obtained were close to 0 for TA(stearoyloxy)$_9$ even after many attempts.

In conclusion, the Folin-Ciocalteu method on partially esterified molecules did not allow us to determine precisely the number of free phenols and was not adapted for these molecules.

II.6. Fully etherified derivative

II.6.1. ^{1}H NMR analyses

The spectrum for TA(dodecyloxy)$_{25}$ is displayed in **Figure II.17**. The aromatic protons were less shifted than the acetylated or esterified molecules. This confirms that the shift is correlated to the chemical modifications of the molecules and not only to the analysis solvent used for the analysis. The signals from the glucose core were not well-defined, especially the ones around 4.5 ppm and the phenol groups were not visible.

For the specific protons from the ether chains, we observed 4 different signals: **1)** from 4.3 to 3.9 ppm is the -OCH$_2$, **2)** from 1.85 to 1.65 ppm is the CH$_2$ in β-position, **3)** from 1.64 to 0.99 ppm is the (CH$_2$)$_n$ signal and **4)** at 0.98 to 0.80 ppm is the CH$_3$ signal from the end of the ether chains.

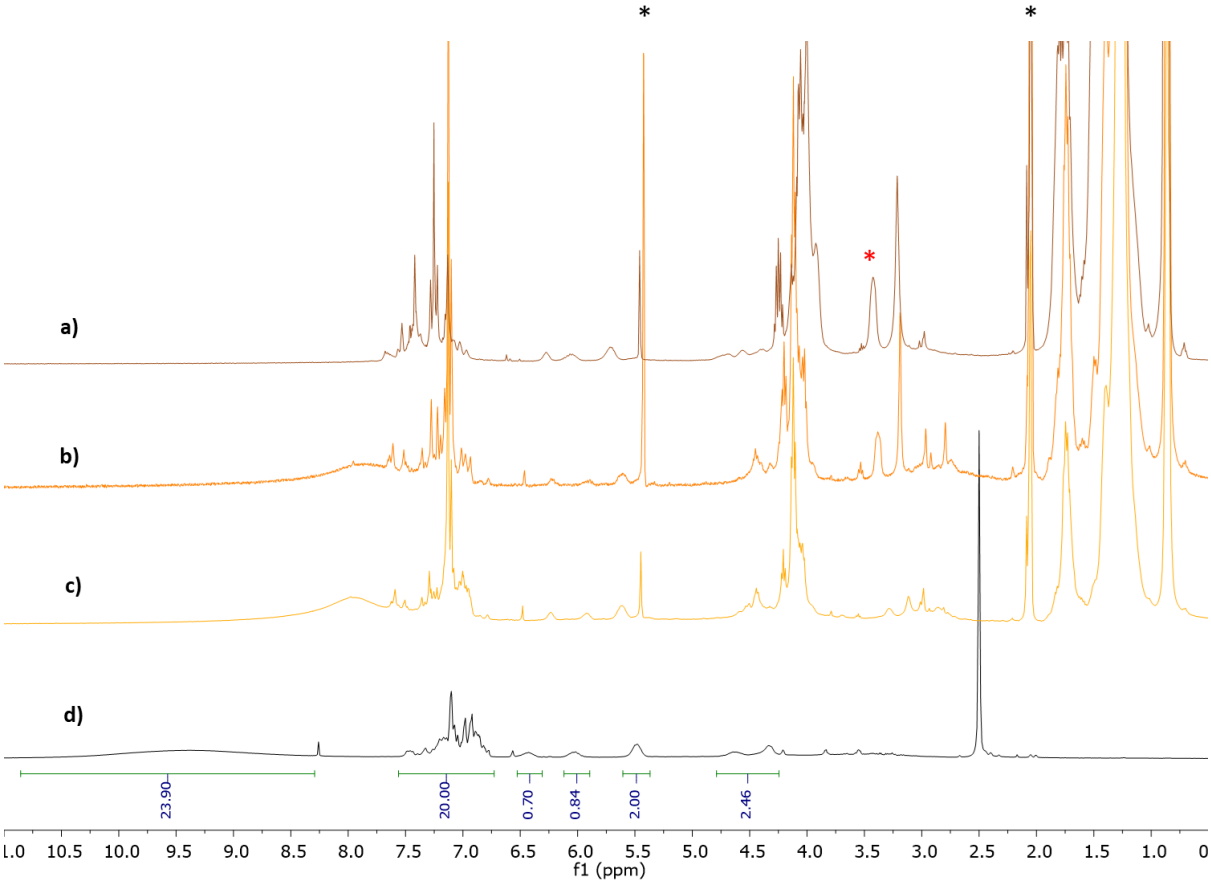

Figure II.17. Comparison of ^{1}H NMR spectra between TA and etherified products; a) ^{1}H NMR spectrum of TA(dodecyloxy)$_{25}$ in CD_2Cl_2/acetone-D_6 (dark orange line); b) ^{1}H NMR spectrum of TA(dodecyloxy)$_{15}$ in CD_2Cl_2/acetone-D_6 (orange line); c) ^{1}H NMR spectrum of

TA(dodecyloxy)$_5$ in CD_2Cl_2/acetone-D_6 (light orange line); d) ^{1}H NMR spectrum of tannic acid in DMSO-D_6 (black line). * represent the signals from the remaining bromododecane and * the signals from the deuterated solvents CD_2Cl_2 and acetone-D_6

The integration of the chains peaks compared to the peaks from the initial tannic acid structure were accurate with the functionalization rate. The rate was around 27 by integrating the signal of the -OCH_2, 25 by integrating the signal of the CH_2 in β-position and 31 with the CH_3 signal. This last result tends to prove that we still have some 1-bromododecane remaining despite the purification process. For the hexyloxy product, the rate was around 22-23 (**Figure II.35**).

These results showed that even for the fully functionalized molecules, in some case, the determination of the functionalization rate is not totally accurate but will be used for the partially functionalized ones.

II.6.2. ^{13}C NMR analyses

The spectrum of TA(dodecyloxy)$_{25}$ is displayed on **Figure II.18**.

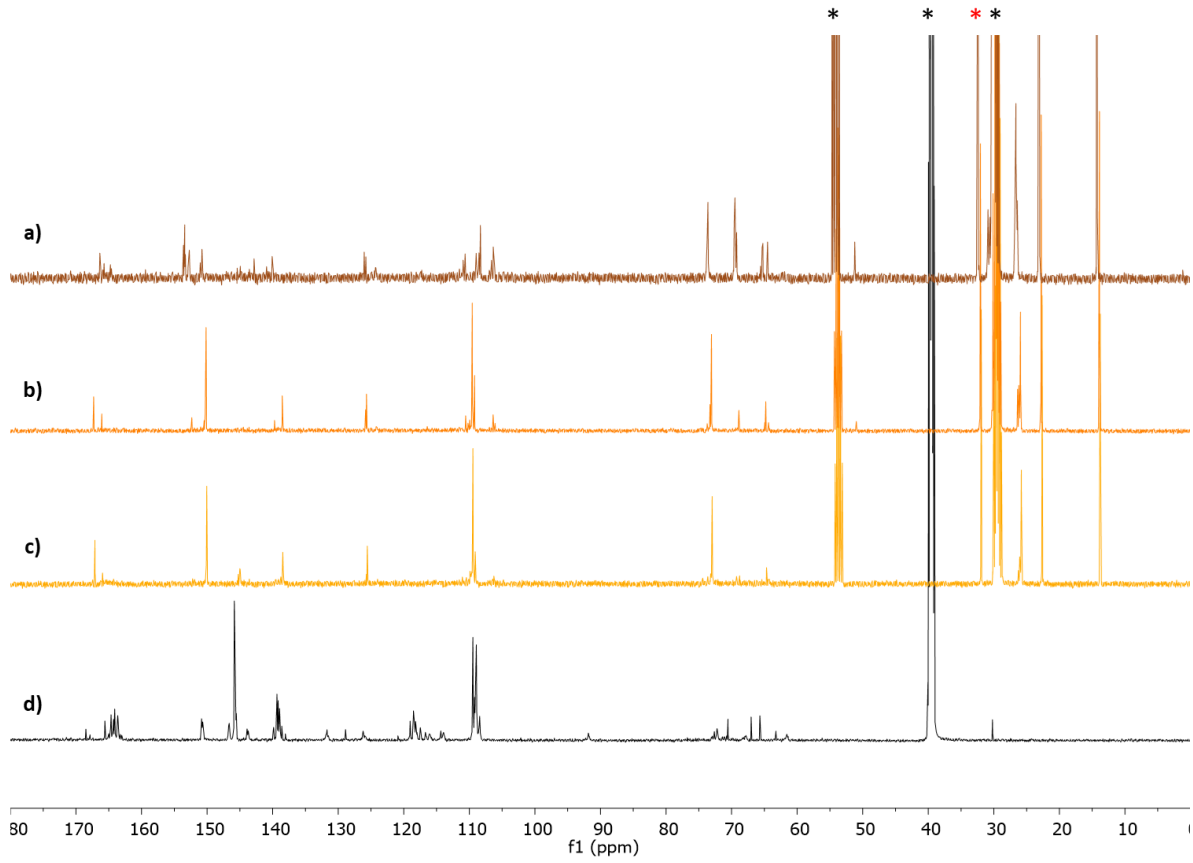

Figure II.18. Comparison of ^{13}C NMR spectra between TA and dodecyloxy products; a) ^{13}C NMR spectrum of TA(dodecyloxy)$_{25}$ in CD_2Cl_2/acetone-D_6 (dark orange line); b) ^{13}C NMR

spectrum of TA(dodecyloxy)$_{10}$ in CD_2Cl_2/acetone-D_6 (orange line); c) ^{13}C NMR spectrum of TA(dodecyloxy)$_5$ in CD_2Cl_2/acetone-D_6 (light orange line); c) ^{13}C NMR spectrum of tannic acid in DMSO-D_6 (black line). * represent the signals from the remaining bromododecane and * represent the signals from the deuterated solvents CD_2Cl_2, DMSO-D_6 and acetone-D_6

The carbonyl signals from the depside ester groups of TA core were visible around 165 ppm, which is approximately the same shifts as commercial tannic acid. The aromatics were identified between 154 and 106 ppm. For these, the different carbons of the aromatics were identified, unlike the fully esterified molecule where the signals were not clearly visible in this area. The signals attributed to the carbons of the glucose core are visible, which was also not the case previously. Indeed, we observed some signals around 75-65 ppm. These can be attributed to the glucose carbons and also to the carbons of the ether functions. This may be due to the spatial arrangement of the chains, as the core should be more accessible with alkyl functionalized phenols instead of carbonyl functionalized due to the increase of steric hindrance.

Also, the peaks from the tannic acid structure were visible with more intense peaks for the hexyloxy than for the dodecyloxy chains (**Figure II.36**).

II.6.3. ATR-FTIR spectroscopy

The υ(O–H) band was not visible on the spectra of fully etherified molecules similarly as the fully esterified molecule (**Figure II.19**).

For the υ(C–H), we observed the same strong bands around 2920 cm^{-1} and 2850 cm^{-1}. The intensity of the bands from the dodecyloxy product compared to the hexyloxy was much higher due to the increase of the chain length (**Figure II.37**).

We observed a large band for the υ(C=O) around 1725 cm^{-1} for the fully etherified molecules. This demonstrates that the etherification has the same effect on the carbonyls no matter the length of the ether chains. However, the full hexyloxy molecule shows two bands. This could be the demonstration that not all the carbonyls are equivalent and this has been demonstrated by changing the electronic environment. Either the increase in chain length makes the analysis more difficult and does not allow this phenomenon to be seen, or the increase in chain length leads to a greater effect on the electronic environment of the carbonyls and the signals overlap.

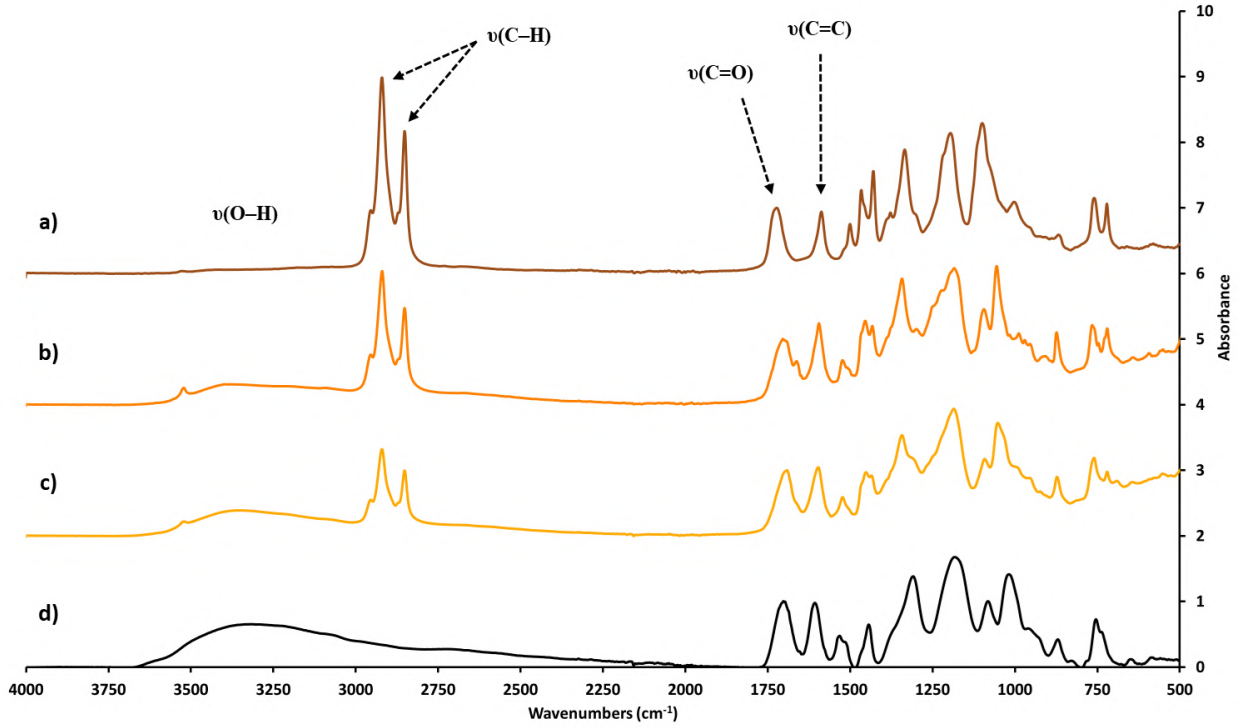

Figure II.19. Comparison of ATR FTIR spectra between TA and dodecyloxy products in absorbance mode; a) FTIR spectrum of TA(dodecyloxy)$_{25}$ (dark orange line); b) FTIR spectrum of TA(dodecyloxy)$_{10}$ (orange line); c) FTIR spectrum of TA(dodecyloxy)$_5$ (light orange line); d) FTIR spectrum of tannic acid (black line). Spectra have been normalized on the C=O band

II.6.4. Mass Spectrometry

Neither electrospray ionization nor APCI (Atmospheric Pressure Chemical Ionization) was successful on the fully etherified tannic acid derivative, therefore no mass spectrometry data is available.

II.7. Partially etherified derivatives

II.7.1. ^{1}H NMR analyses

For etherified molecules, we observed that the glucose core was much less defined than for other molecules. On the other hand, the integration of the ether chains compared to the esters is much better. The spectrum for TA(dodecyloxy)$_5$ is shown in **Figure II.17** and showed that for 20 aromatic protons, the phenol protons integrate for 11 which corresponding to a higher functionalization rate of about 14 instead of 5. The same result was obtained for

TA(dodecyloxy)$_{10}$. On this one, the integrations show a functionalization rate of about 15 instead of 10. For the ether chains, the integration also shows a twofold integration.

For the hexyloxy molecules, the same result was obtained but with integration closer to the expectation. For TA(hexyloxy)$_{10}$, a functionalization rate around 12-13 and for TA(hexyloxy)$_5$ a functionalization rate around 6-7 were obtained (**Figure II.35**).

II.7.2. ^{13}C NMR analyses

The spectrum of TA(dodecyloxy)$_5$ is displayed on **Figure II.18**. The glucose core could not be observed, the same as for the esterified derivatives. The carbonyl signals from the starting material structure were visible around 167 ppm, then few signals from the aromatics were identified between 151 and 108 ppm. We observed some signals around 70-65 ppm that can be attributed to the -OCH$_2$ from the etherification process. Then, the carbons from the CH$_2$ of the ether chains from 32 to 22 ppm and the CH$_3$ around 13 ppm.

In the case of the hexyloxy molecules, we could observe more signals (**Figure II.36**). The inner structure was clearly more visible demonstrating that the length chain has an effect on the analysis.

Increasing the mass concentration, increasing the relaxation time or increasing the number of scans did not improve the results.

II.7.3. ^{31}P NMR analysis

The spectrum is displayed on **Figure II.20**.

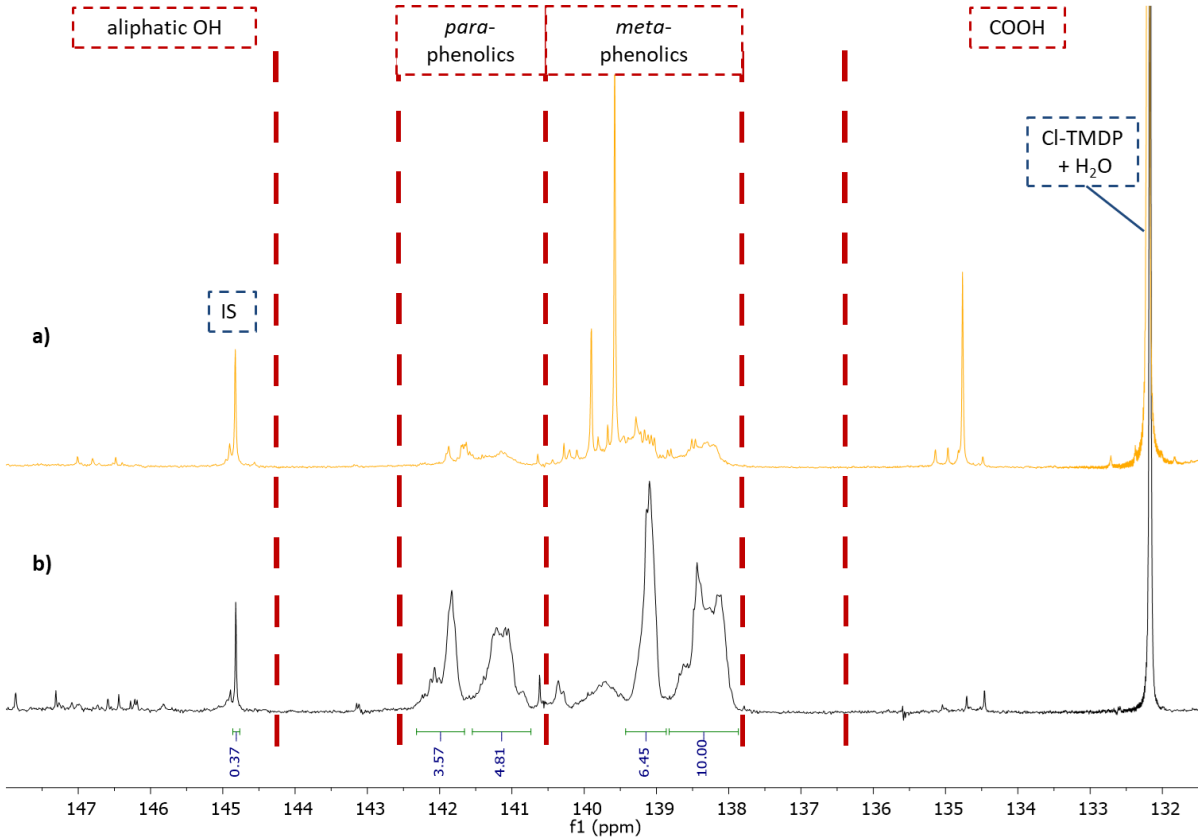

Figure II.20. Comparison of ^{31}P NMR spectra between TA and TA(dodecyloxy)$_5$; a) ^{31}P NMR spectrum of TA(dodecyloxy)$_5$ (light orange line); b) ^{31}P NMR spectrum of tannic acid (black line)

Unfortunately, the spectrum of TA(dodecyloxy)$_5$ is very similar to the ones from the esterified molecules described previously. Very small signals for *para*- and *meta*-phenolic groups were observed.

Indeed, the spectrum showed an integration of 1 in the *para*-phenolic region and 2,5 in the *meta*-phenolic region for a total of 3,5 phenolic groups which is way less than the twenty theoretical OH groups remaining free. The phosphitylation characterization method was not suitable for functionalized TA derivatives probably due to the steric hindrance.

II.7.4. ATR-FTIR spectroscopy

We observed the same behavior no matter the length of the ether chains. The spectra of TA(dodecyloxy)$_{10}$ and TA(dodecyloxy)$_5$ are displayed on **Figure II.19**. The spectra for the partially etherified hexyloxy molecules are displayed on **Figure II.37**.

The band of the υ(O-H), centered at 3380 cm^{-1} was observed with a slight decrease in terms of intensity as the functionalization rate increased. Two strong signals were observed at 2920 cm^{-1} and 2851 cm^{-1} and were assigned to the υ(C-H) of the ether chains. The intensity of the υ(C-H) increase with the increase of grafted alky chains. The characteristic signal of the υ(C=O) carbonyl groups from the inner esters was observed around 1690 cm^{-1} with a slight shift depending on the functionalization rate. This implies that the etherification process has an impact on the υ(C=O) environment within the tannic acid molecule itself.

Nevertheless, characterizing the tannic acid derivatives by FTIR allowed us to confirm that the molecules were more functionalized as the number of equivalents used in the first place was higher.

II.7.5. Determination of total phenolic content

Calibration curve with gallic acid and the same methodology as for the previous partially functionalized molecules were used. The results are shown in **Table II.4**.

Table II.4. Determination of free phenols remaining by Folin-Ciocalteu's method on partially etherified molecules

Molecules	Solvent	Free phenols (experimental)	Free phenols (theoretical)
TA	water	**29.6**	**25**
$TA(hexyloxy)_{10}$	acetone	**10.8**	**15**
$TA(hexyloxy)_5$	acetone	**17**	**20**
$TA(dodecyloxy)_{10}$	acetone	**5.8**	**15**
$TA(dodecyloxy)_5$	acetone	**8.8**	**20**

For the TA(hexyloxy) derivatives, results were reasonably accurate, especially for the less etherified molecule (20 phenol theoretical for 17 with the dosage).

However, the results for TA(dodecyloxy) were twice as low as expected. The length of the chains and the increase in van der Waals interactions could explain this unexpected result.

Overall, the Folin-Ciocalteu method gave us accurate results for most of the molecules, with a good accuracy for the acetylated ones. Nevertheless, for molecules with long ester or ether chains, the results were less precise.

III. Conclusion

In this extensive study, we functionalized tannic acid with three different groups allowing the solubilization of the synthesized molecules in organic solvent. We have characterized these molecules by several analytical methods, showing that each group brings additional difficulties, more or less important, to the characterization.

We were able to synthesize the fully functionalized derivatives, which was demonstrated by characterization techniques. However, we have some derivatives that are not completely pure.

Concerning the partially functionalized derivatives, the results are variable. We have shown through the different NMR and mass spectrometry that we have synthesized acetylated derivatives with the desired functionalization rate. For the esterified and etherified derivatives, the purification and characterization were more complex.

Through this study, we have shown that it is possible to obtain an average functionalization rate on tannic acid.

In conclusion, the functionalization performed and the analyses proved that the number of reagent equivalents has a direct effect on the functionalization rate. Nevertheless, despite the numerous analyses, we could not demonstrate precisely that one equivalent functionalized one phenol and that the functionalization was proportional. However, the results allowed us to determine that the more the number of equivalents, the more the number of free phenols decreased.

IV. Additional results

IV.1. Synthetic methodology

In order to better understand the reactivity of the phenolic functions of tannic acid, it was decided to use a model platform constituting a fragment of tannic acid: methyl gallate. Methyl gallate is the methyl ester of gallic acid which constitutes tannic acid. The objective of this methodology is to achieve the functionalization of the phenols, totally and selectively, before applying the procedure to tannic acid. Methyl gallate is a more soluble molecule in organic solvents than gallic acid and tannic acid.

IV.1.1. Total functionalization of methyl gallate

IV.1.1.1. Acetylation

Acetylation is a reaction that has already been described for systems with phenols and which will make tannic acid more soluble in organic medium despite the short chain.[22]

In order to acetylate the phenols, acetic anhydride in the presence of H_2SO_4 is used at room temperature for 4h (**Figure II.21**).

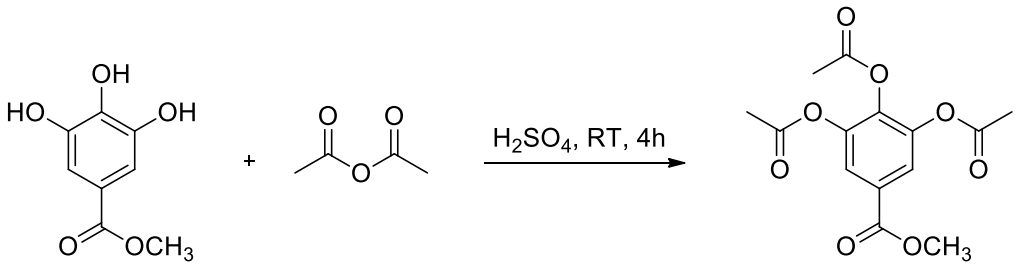

Figure II.21. Full acetylation of methyl gallate with acetic anhydride

The yield of this reaction is 90% and the fully acetylated product has been obtained, as proved by ^{1}H NMR (**Figure II.31**).

IV.1.1.2. Esterification

For esterification, fatty acids have been used as natural and inexpensive molecules capable of forming ester functions.

Therefore, stearic acid, an 18-carbon compound, has been chosen to make it react with methyl gallate in the presence of an APTS catalyst (0.01%) in ethyl acetate using a Dean-Stark set-up. This method allows the removal of water molecules as they are formed in order to shift the equilibrium and obtain a complete reaction. After NMR analysis of the product, it was found that no reaction had taken place. The reaction was reproduced with an amount of APTS of 1 wt%, i.e. 100 times the normal amount, but the final result remained unchanged.

Synthesizing the product in bulk has also been tried. The reaction was heated to 250°C in order to melt our fatty acid and allow the evaporation of the water molecules formed during the reaction. After analysis of the final product, no signals from the desired molecule have been observed. This led to the conclusion that the phenols in the methyl gallate are not sufficiently reactive to react with a fatty acid such as stearic acid.

In order to increase the reactivity, stearic acid anhydride has been synthesized and made it react with methyl gallate. In a first step, the fatty acid anhydride is synthesized from stearic acid in the presence of DCC (DiCyclohexylCarbodiimide) which is a coupling agent in dichloromethane for 2h at 0°C then 2h at RT. The anhydride was obtained in 47% yield. In the second step, the anhydride was placed in the presence of methyl gallate with H_2SO_4 as catalyst and MEK (MethylEthylKetone) as solvent (**Figure II.22**).

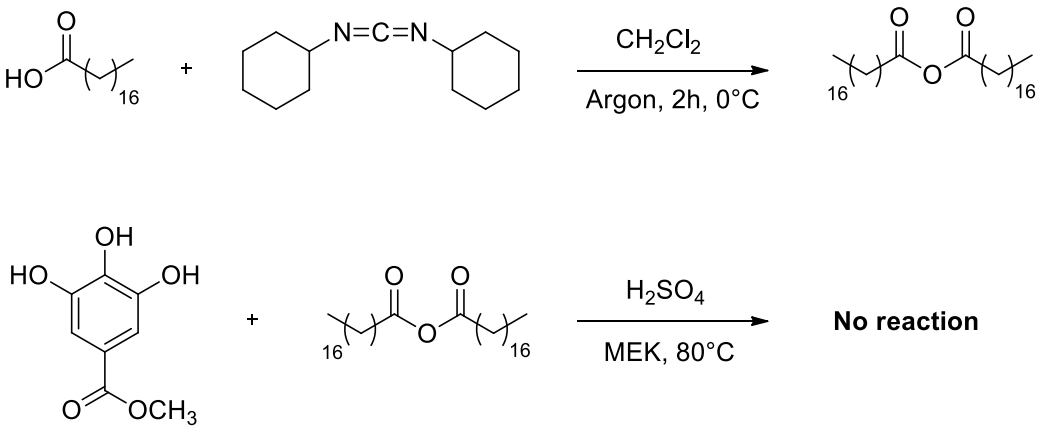

Figure II.22. 2-steps reaction of methyl gallate esterification with stearic acid anhydride

After analysis of the product by ^{1}H NMR, it was concluded that the reaction did not work. As the acid and anhydride did not react with the phenols, using stearoyl chloride has been decided. It was first synthesized then made it react on methyl gallate in a second step (**Figure II.23**).

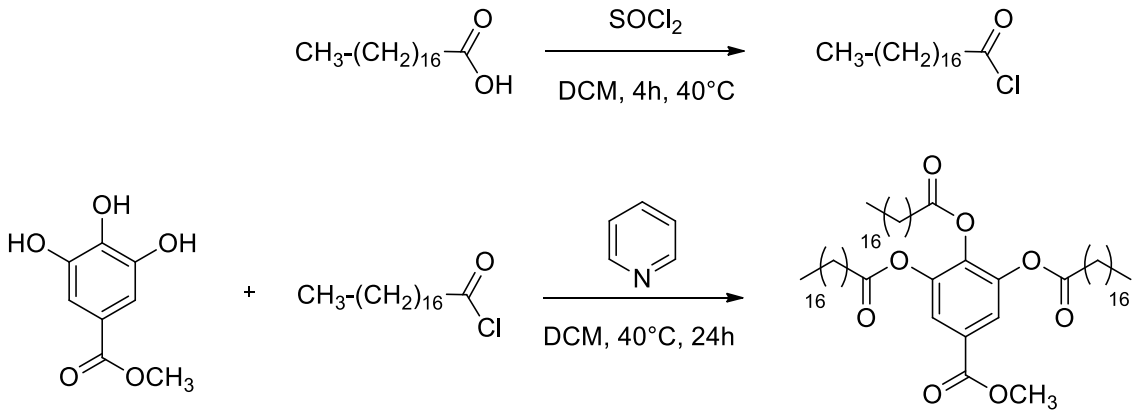

Figure II.23. 2-steps reaction of methyl gallate esterification with stearoyl chloride

The ^{1}H NMR (**Figure II.32**) showed that the signals from CH_2-C=O and CH_2 in β-position are more unshielded than on the stearic acid NMR. For the CH_2-C=O, the signals are at 2.52 ppm for the final product against 2.35 ppm for stearic acid and for CH_2 in β-position, 1.72 ppm for the product against 1.63 ppm for stearic acid.

Concerning the ^{13}C NMR, two different signals can be observed for the carbonyls, corresponding to the *meta* and *para* positions. The shifts are 170.61 ppm for the *meta* C=O and 169.39 for the *para* C=O which confirms that the positions are not equivalent.

The product has been obtained with a yield of 89%.

IV.1.1.3. Etherification

Thereafter, the phenolic functions were functionalized by forming ethers rather than esters to see if the solubility in organic solvent was also obtained.

Bromododecane as bromoalkane was used and the reaction was carried out in the presence of potassium carbonate as base and DMF as solvent (**Figure II.24**).

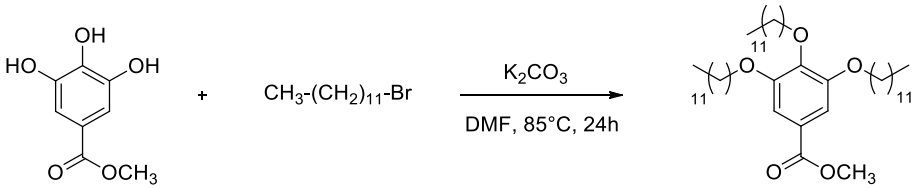

Figure II.24. Etherification of methyl gallate with bromododecane

After purification, the yield obtained was 15%. On the ^{1}H NMR spectrum, a quadruplet at 4 ppm corresponding to the -OCH_2 of the ether was observed proving that the etherification

success. For the reactions on tannic acid, sodium iodide would be added which can increase the reactivity and lead to better yields.

IV.1.2. Partial functionalization of methyl gallate

In the previous section, it has been shown that full functionalization of the phenols was possible, with varying degrees of success. Therefore, the next step was to achieve the selective functionalization of methyl gallate, i.e. functionalizing only one OH.

For this part, esterification process has been the main topic. In order to do this, two methods have been used: the reaction under stoichiometric conditions and the protection/deprotection of two phenolic functions.

IV.1.2.1. Stoichiometric conditions

For the reaction under stoichiometric conditions, one equivalent of stearoyl chloride for one equivalent of methyl gallate was used. The reaction crude has been analyzed by NMR, in order to determine if one or more products were formed during the synthesis before the purification step.

The ^{1}H NMR presented different signals for the aromatic protons, proving that we had a mixture of several products. The crude product has been purified by precipitation in ethanol. The NMR spectrum after purification is displayed on **Figure II.25**.

After purification, only one product is observed: tristearoyloxymethyl gallate.

From this analysis, several things can be deduced. First of all, the reaction under stoichiometric conditions does not allow us to obtain a single product but a mixture. After purification, only the tri-esterified product re-precipitated which means that the other products were not hydrophobic enough.

The major finding is the formation of this tri-esterified product. Even though the yield of the reaction is very low (4-5%), obtaining this product raises questions. With only one equivalent of stearoyl chloride, tri-esterified product should not be formed. The most likely hypothesis is that once one of the phenols is functionalized, the aromatic ring is more reactive than a non-functionalized molecule and the reaction tends to be favored on a ring that is already esterified. In the bibliography carried out, no study or allusion to such a phenomenon was reported. If the

explanation were correct and extrapolated to the tannic acid molecule, it would mean that one could have both fully functionalized and fully free gallic units on the same molecule.

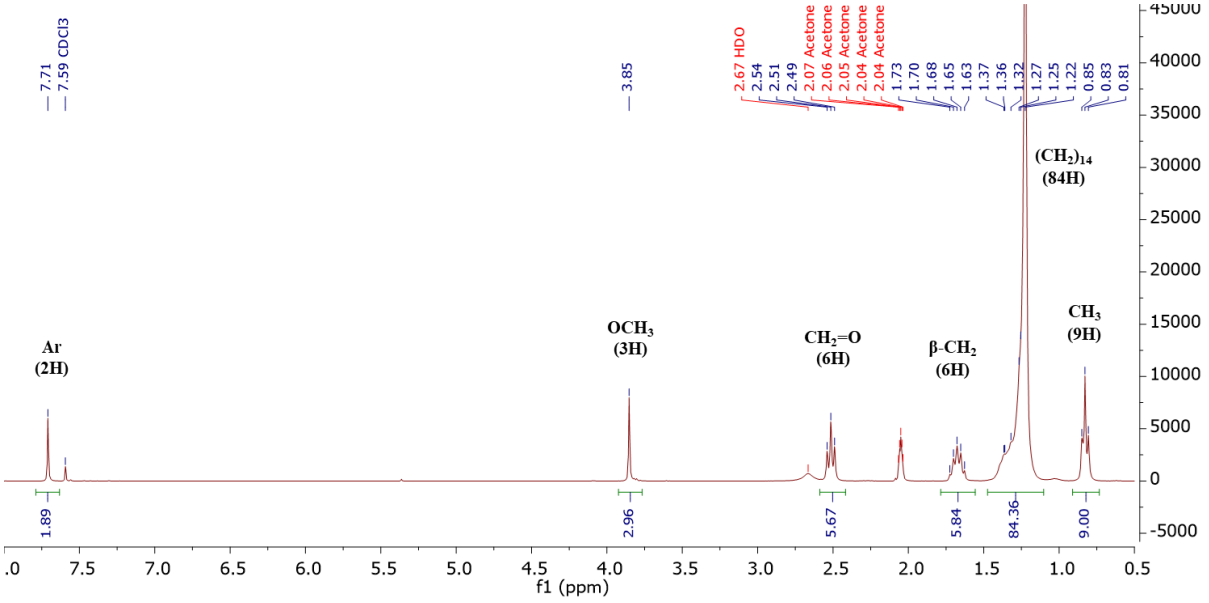

Figure II.25. ^{1}H NMR spectrum of monoesterified methylgallate after purification in $CDCl_3$/acetone-D_6

IV.1.2.2. Protection/deprotection of phenols

For this method, the first step was the protection of two phenolic functions before functionalizing the free phenol and then deprotecting to obtain a mono-esterified molecule. The scheme of this 3-step reaction is shown in **Figure II.26**.

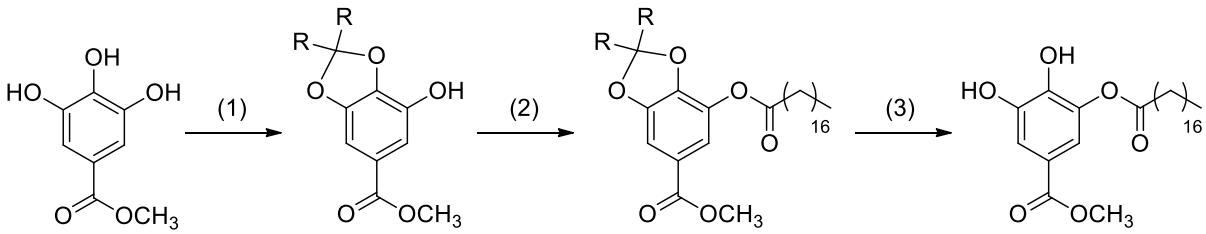

Figure II.26. Partial functionalization by a 3-steps (protection/functionalization/deprotections) reaction of methylgallate phenols

Several tests for the protection steps were carried out. The results are listed in **Table II.5**.

Table II.5. Conditions used for the protection of methyl gallate phenols

Chemicals	eq	Base or acid	Solvent	Temperature (°C)	Reaction time	Yield
Acetone/PCl_3	1.2/0.4	/	Toluene	RT	24h	No reaction
2,2-Diméthoxypropane	2x1.5	/	Toluene	110	24h	10% conversion
Benzaldehyde	1.3	APTS	Toluene	110	48h	Low conversion
Benzaldehyde (Dean-Stark)	2.3	APTS	Toluene	140	48h	Low conversion
Benzaldehyde (Dean-Stark)	2.3	H_2SO_4	Cyclohexane	110	48h	Low conversion
Dichlorodiphenylmethane	1.4	Pyridine	Acetone	RT	24h	No reaction
Dichlorodiphenylmethane	excess	/	/	170	10 min	99%

The protection of diols in the presence of acetone or 2,2-dimethoxypropane has been widely reported.[23] On our molecule, the reaction in presence of acetone gave no results. Concerning 2,2-dimethoxypropane, the conversion rate obtained was about 10% at best. This low conversion rate led us to consider an alternative method of protection.

Then, the methodology of catechol protection has been carried out, generally protected with benzaldehyde. First, APTS as a catalyst has been used in toluene at reflux for 48h. After purification, ^{1}H NMR spectrum showed a mixture of product, indicating a low conversion rate and a significant amount of benzaldehyde remaining. This proved that a small amount of benzaldehyde reacted.

In order to improve the conversion rate, Dean-Stark apparatus has been used to trap the water released during the reaction, as well as a large excess of benzaldehyde. After carrying out the same purification method, the conversion rate was no greater than before. The excess benzaldehyde was still present in the final product a change of catalyst has been decided, using

H_2SO_4 instead of APTS and to change the solvent using cyclohexane. Unfortunately, same results were obtained.

Subsequently, protection of the phenols has been conducted with dichlorodiphenylmethane. After a first attempt without results, dichlorodiphenylmethane was used as reagent and as solvent on the second attempt. After purification, the product was obtained in close to 100% yield. This method will be used afterwards to protect the phenols from tannic acid.

Then, the second step consists in functionalizing the free phenol function with stearoyl chloride using the same method as before. After purification, the product could be recovered in 72% yield. The ^{1}H NMR spectrum is displayed in **Figure II.27**.

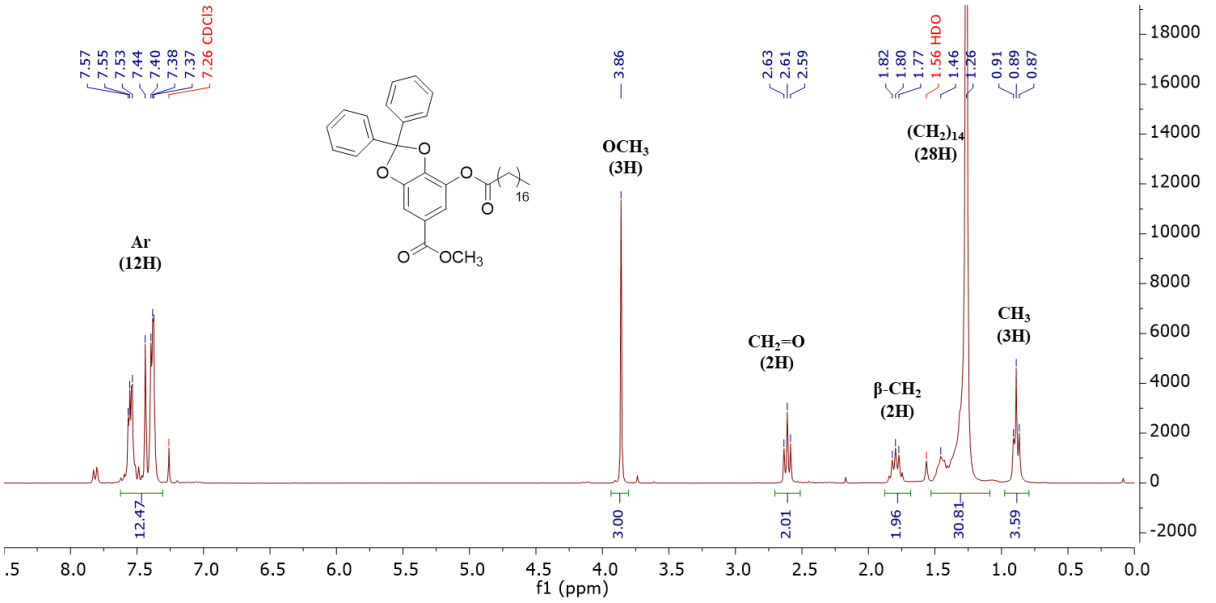

Figure II.27. ^{1}H NMR spectrum of diprotected stearoyloxymethyl gallate

This last step is the most delicate because the objective is to deprotect the protecting group without breaking the ester function that we want to preserve. In order to do this, several deprotection methods have been tried. These are listed in **Table II.6**.

The main method was the hydrolysis in acidic medium. According to the publication followed, the deprotection takes place in acetic acid and water.[24] Therefore, proportions of acetic acid as well as the reaction time in order to find the optimal conditions have been varied.

Table II.6. Deprotection reactions of the ketal group

Chemicals	Ratio	Temperature (°C)	Reaction time	Observations
Acetic acid/ H_2O	2:1	110	1h	No reaction
Acetic acid/ H_2O	2:1	110	24h	**Partial deprotection of both groups**
Acetic acid/ H_2O	2:1	110	48h	**Total deprotection**
Acetic acid/ H_2O	4:1	110	4h	**Partial deprotection of both groups**

In acetic acid/water proportions 2:1, we let the reaction take place for 1h, 24h and 48h. After 1h, nothing has been deprotected yet. After 24h, both the protective group and the ester were deprotected in similar proportions. After 48h, the deprotection was complete and the initial methyl gallate was recovered. What can be concluded from these conditions is that the deprotection of the ketal seems to start at a reaction time similar to that of the hydrolysis of the ester.

The proportion of acetic acid was increased in order to fasten the reaction time. The ^{1}H NMR showed a partial deprotection of the two groups, the ketal and the ester, in similar proportions. Therefore, same result as with a 2:1 ratio after 24h has been obtained. Although the reaction is faster, one deprotection is not more favored than the other.

After many unsuccessful attempts, it has been decided to try to find the right conditions directly on the protected tannic acid. The other procedure for removing the ketal is catalytic hydrogenation [25] so this will be the considered method after the tannic acid protection.

IV.1.3. Regioselective functionalization of tannic acid

In order to functionalize regioselectively, the phenol protection method used on methyl gallate has been adapted to tannic acid. The reaction is shown in **Figure II.28**.

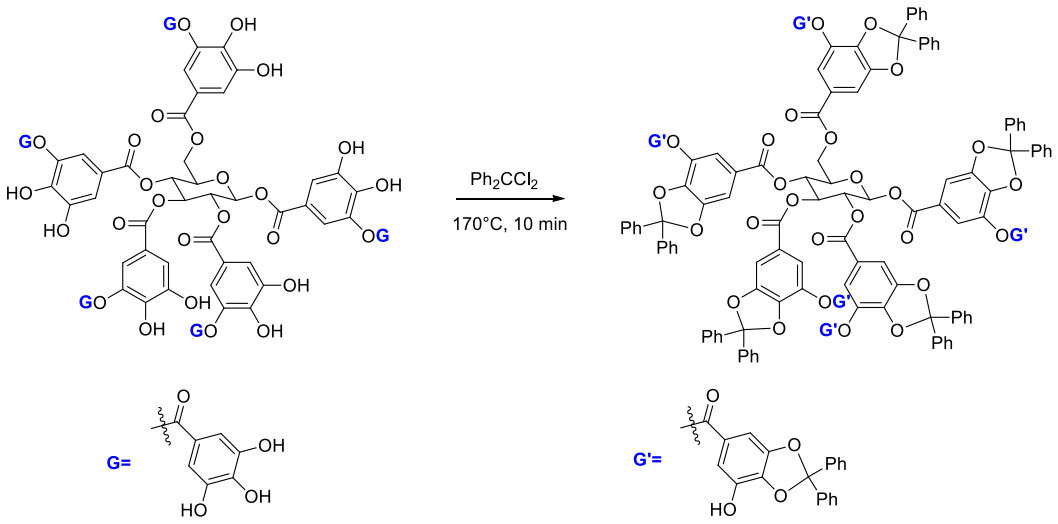

Figure II.28. Protection of tannic acid phenols by dichlorodiphenylmethane

Dichlorodiphenylmethane was used as solvent and the reaction was heated to 170°C for 10 min. After purification, the NMR spectra (^{1}H and ^{13}C) showed only signals from dichlorodiphenylmethane. Despite working on methyl gallate, this reaction did not work on tannic acid.

Furthermore, fragments of tannic acid have been recovered in the aqueous phase of the washings meaning that the ester bond in the tannic acid structure were broken and that the reaction is destructive. Then, protection of the phenols using acetone or 2,2-dimethoxypropane has been conducted but the reaction failed as for methyl gallate.

After failing to selectively functionalize tannic acid, it has been decided to functionalize statistically tannic acid as is already a mixture of isomers.

IV.2. Gelation tests of tannic acid derivatives

The main goal of this thesis was to synthesize new organogelators from bio-sourced building blocks. However, **Table II.7** and **Table II.8** show that none of the tested molecules form a gel in any liquid tested.

Table II.7. Gelation tests of tannic acid derivatives at 2%wt [a]

	Acetylated derivatives				Etherified derivatives					
Solvents	**$TA(OAc)_8$**	**$TA(OAc)_{10}$**	**$TA(OAc)_{15}$**	**$TA(OAc)_{25}$**	**$TA(hexyloxy)_3$**	**$TA(octyloxy)_3$**	**$TA(decyloxy)_3$**	**$TA(octyloxy)_8$**	**$TA(decyloxy)_8$**	**$TA(dodecyloxy)_5$**
water	I	I	I	I	I	I	I	I	I	I
ethanolamine	S	S	S	S	S	S	S	S	P	S
N-methylformamide	S	S	S	S	S	S	S	S	S	S
methanol	S	S	S	I	S	S	S	S	S	S
propylene glycol	S	S	S	S	S	S	S	P	I	I
propylene carbonate	S	S	S	S	S	S	S	S	S	S
DMSO	S	S	S	S	S	S	S	S	S	S
N,N-dimethylformamide	S	S	S	S	S	S	S	S	S	S
acetonitrile	S	S	S	S	I	I	I	P	P	I
benzyl alcohol	S	S	S	S	S	S	S	S	S	S
1-butanol	S	S	S	I	S	S	S	S	S	S
N,N-diethylacetamide	S	S	S	S	S	S	S	S	S	S
diacetone alcohol	S	S	S	S	S	S	S	S	S	S
cyclohexanone	S	S	S	S	S	S	S	S	S	S
1,4-dioxane	S	S	S	S	S	S	S	S	S	S
MEK	S	S	S	S	S	S	S	S	S	S
chlorobenzene	I	I	I	P	I	I	I	S	S	S
Toluene	I	I	I	I	I	I	I	S	S	S
1-chloropentane	I	I	I	I	I	I	I	I	S	S
cyclohexane	I	I	I	I	I	I	I	I	S	S
t-butylacetate	I	I	I	I	I	I	S	S	S	S
n-hexadecane	I	I	I	I	I	I	I	I	I	I

[a] P: precipitate; S: soluble; I: insoluble.

Table II.8. Gelation tests of partially acetylated derivatives at 5%wt [a]

Solvents	$TA(OAc)_{10}$	$TA(OAc)_{15}$
water	I	I
ethanolamine	S	S
N-methylformamide	S	S
methanol	S	S
propylene glycol	S	I
propylene carbonate	S	S
DMSO	S	S
N,N-dimethylformamide	S	S
acetonitrile	S	S
benzyl alcohol	S	S
1-butanol	S	I
N,N-diethylacetamide	S	S
diacetone alcohol	S	S
cyclohexanone	S	S
1,4-dioxane	S	S
MEK	S	S

[a] S: soluble; I: insoluble.

V. References

[1] P. J. Hernes, J. I. Hedges, *Anal. Chem.* **2000**, *72*, 5115–5124.

[2] P. Arapitsas, S. Menichetti, F. F. Vincieri, A. Romani, *J. Agric. Food Chem.* **2007**, *55*, 48–55.

[3] Ann. E. Hagerman, *Tannin Handbook*, Miami University, Oxford, **2002**.

[4] X. Feng, J. Fan, A. Li, G. Li, *ACS Sustainable Chem. Eng.* **2020**, *8*, 874–883.

[5] M. Qi, Y.-J. Xu, W.-H. Rao, X. Luo, L. Chen, Y.-Z. Wang, *RSC Adv.* **2018**, *8*, 26948–26958.

[6] A. S. Singh, S. Halder, A. Kumar, P. Chen, *Materials Chemistry and Physics* **2020**, *243*, 122112.

[7] Y.-O. Kim, J. Cho, H. Yeo, B. W. Lee, B. J. Moon, Y.-M. Ha, Y. R. Jo, Y. C. Jung, *ACS Sustainable Chem. Eng.* **2019**, *7*, 3858–3865.

[8] G. H. Sayed, F. M. Ghuiba, M. I. Abdou, E. A. A. Badr, S. M. Tawfik, N. A. M. Negm, *Colloids and Surfaces A: Physicochemical and Engineering Aspects* **2012**, *393*, 96–104.

[9] I. Zaborniak, P. Chmielarz, K. Wolski, G. Grzes´, A. A. Isse, A. Gennaro, S. Zapotoczny, A. Sobkowiak, *Macromol. Chem. Phys.* **2019**, 1900073.

[10] S. Lavoie, M. Ouellet, P.-Y. Fleury, C. Gauthier, J. Legault, A. Pichette, *Magnetic Resonance in Chemistry* **2016**, *54*, 168–174.

[11] F. Melone, R. Saladino, C. Crestini, *J. Agric. Food Chem.* **2013**, *61*, 9316–9324.

[12] T. Wahyono, D. A. Astuti, I. K. Gede Wiryawan, I. Sugoro, A. Jayanegara, *IOP Conf. Ser.: Mater. Sci. Eng.* **2019**, *546*, 042045.

[13] C. Garrido, G. Diaz-Fleming, M. M. Campos-Vallette, *Spectrochimica Acta Part A: Molecular and Biomolecular Spectroscopy* **2016**, *163*, 68–72.

[14] L. Fu, X. Sun, Y. Gao, R. Chen, *J. Am. Soc. Mass Spectrom.* **2019**, *30*, 1545–1549.

[15] A. R. S. Ross, M. G. Ikonomou, K. J. Orians, *Analytica Chimica Acta* **2000**, *411*, 91–102.

[16] V. L. Singleton, R. Orthofer, R. M. Lamuela-Raventós, in *Methods in Enzymology*, Academic Press, **1999**, pp. 152–178.

[17] N. Schweigert, A. J. B. Zehnder, R. I. L. Eggen, *Environmental Microbiology* **2001**, *3*, 81–91.

[18] K. Ngamchuea, B. Tharat, P. Hirunsit, S. Suthirakun, *RSC Adv.* **2020**, *10*, 28454–28463.

[19] Z. Xia, W. Kiratitanavit, P. Facendola, S. Thota, S. Yu, J. Kumar, R. Mosurkal, R. Nagarajan, *Polymer Degradation and Stability* **2018**, *153*, 227–243.

[20] R. Asadpour, N. B. Sapari, M. H. Isa, S. Kakooei, K. U. Orji, *Fibers Polym* **2015**, *16*, 1830–1835.

[21] K. I. Berker, F. A. Ozdemir Olgun, D. Ozyurt, B. Demirata, R. Apak, *J. Agric. Food Chem.* **2013**, *61*, 4783–4791.

[22] A. Arbenz, L. Avérous, *Green Chem.* **2015**, *17*, 2626–2646.

[23] In *Greene's Protective Groups in Organic Synthesis*, John Wiley & Sons, Ltd, **2014**, pp. 472–553.

[24] S. Takaoka, N. Takaoka, Y. Minoshima, J.-M. Huang, M. Kubo, K. Harada, H. Hioki, Y. Fukuyama, *Tetrahedron* **2009**, *65*, 8354–8361.

[25] D. Ferreira, D. Slade, *Nat. Prod. Rep.* **2002**, *19*, 517–541.

[26] A. Granata, D. S. Argyropoulos, *J. Agric. Food Chem.* **1995**, *43*, 1538–1544.

[27] Z.-H. Jiang, D. S. Argyropoulos, A. Granata, *Magnetic Resonance in Chemistry* **1995**, *33*, 375–382.

[28] L. Zoia, E.-L. Tolppa, L. Pirovano, A. Salanti, M. Orlandi, *Archaeometry* **2012**, *54*, 1076–1099.

[29] F. Melone, R. Saladino, H. Lange, C. Crestini, *J Agric Food Chem* **2013**, *61*, 9307–9315.

VI. Experimental part

VI.1. Materials and methods

VI.1.1. Reagents

Tannic acid (TA) was purchased from Fischer Chemicals as an extra pure grade. Methyl gallate (MG), acetic anhydride, 1-bromohexane, pyridine, sodium iodide and potassium carbonate were purchased from Sigma Aldrich. Triethylamine (NEt_3), thionyl chloride ($SOCl_2$) and 1-bromododecane were purchased from Acros Organics. Stearoyl chloride was synthesized from stearic acid (TCI Chemicals) and thionyl chloride. Deionized water was used for preparing aqueous solutions. All the chemicals were used as received if not mentioned elsewhere.

VI.1.2. Characterization

VI.1.2.1. ^{1}H and ^{13}C NMR

Proton nuclear magnetic resonance (^{1}H NMR) and carbon nuclear magnetic resonance (^{13}C NMR) analyses were recorded on a Bruker Avance 400 spectrometer. DMSO-D_6 (99.80% D, Eurisotop), acetone-D_6 (99.80% D, Eurisotop) and CD_2Cl_2 (99.80% D, Eurisotop) were used as solvents. Calibration was done using the chemical shift of the solvent residual resonance. The external reference used was trimethylsilane. Shifts were given in ppm.

VI.1.2.2. ^{31}P NMR

VI.1.2.2.a. Preparation of solutions

For our samples, a solvent mixture of pyridine and $CDCl_3$ (1.6:1 v/v) with 50mg of Cr (III) acetylacetonate as relaxation agent was prepared under anhydrous conditions (Cr solution). The internal standard (IS) solution was prepared using cholesterol at a concentration of 38.67 mg/mL (0.1M) in a pyridine and $CDCl_3$ (1.6:1 v/v) solvent mixture.

VI.1.2.2.b. Phosphitylation procedure

Ten to fifteen milligrams of modified tannic acid were accurately weighed in a volumetric flask and suspended in 300 μL of the “Cr solution”. One hundred microliters of the internal standard

solution were added followed by 100 μL of 2-chloro-4,4,5,5-tetramethyl-1,3,2-dioxaphospholane (Cl-TMDP). The flask was tightly closed, and the mixture was stirred at 20°C for 90 min, rendering the initially heterogeneous mixture homogeneous.

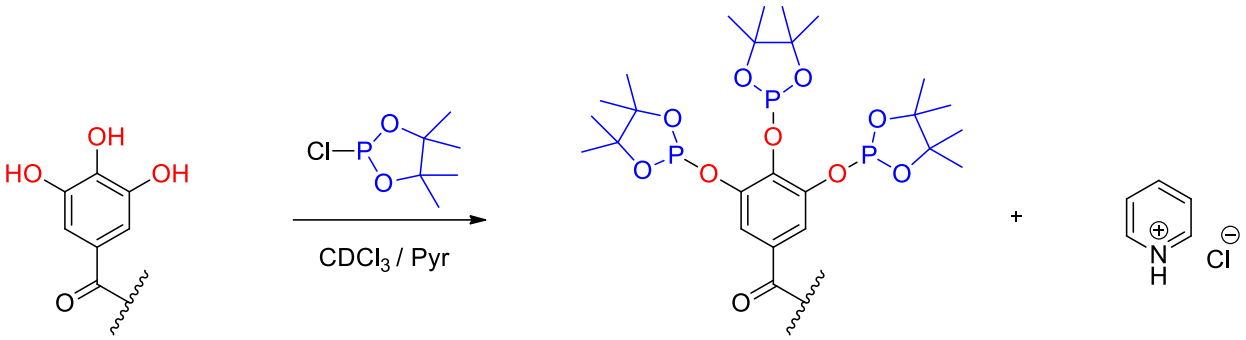

Figure II.29. Phosphitylation reaction on phenolics

VI.1.2.2.c. NMR Spectroscopy

The ^{31}P NMR spectra were recorded on a Bruker 400 MHz spectrometer. The probe temperature was set to 20°C. To eliminate NOE effects, the inverse gated decoupling technique was used. Typical spectral parameters for quantitative studies were as follows: 90° pulse width, sweep width of 6600 Hz. The spectra were accumulated with a delay of 15 s between successive pulses. All chemical shifts reported are relative to the reaction product of water with Cl-TMDP, which has been observed to give a sharp signal in pyridine/$CDCl_3$ at 132.2 ppm.[26–29]

VI.1.2.3. ATR-FTIR spectroscopy

The spectra of the samples were recorded using ATR-FTIR spectrometer (Spectrum Two Spectrometer, Perkin Elmer) equipped with a single bounce diamond crystal and a $LiTaO_3$ (lithium tantalate) detector. The FTIR spectra of samples were determined to be in the MIR range of 400–4000 cm^{-1} with a resolution of 4 cm^{-1}. Each spectrum was collected from 50 scans in the absorbance mode.

VI.1.2.4. Mass Spectrometry

Analysis of tannic acid was performed on SolariX XR 7T FT-ICR mass spectrometer (Bruker, R = 2 000 000) mass spectrometer with electrospray ionization source (ESI) in positive-ion mode. Mass spectra were gained using either a SolariX XR 7T FT-ICR mass spectrometer (Bruker, R = 2 000 000) mass spectrometer with ESI source or a LTQ Orbitrap XL mass

spectrometer (Thermo Fisher Scientific, R = 100 000) equipped with atmospheric pressure chemical ionization source (APCI).

VI.1.2.5. Determination of total phenolic content

Total phenolic content of the modified tannic acid molecules was evaluated with Folin-Ciocalteu method [16] with minor modifications. Samples containing polyphenols are oxidized by the Folin-Ciocalteu reagent thereby producing blue colored complex. The phenolic concentration of extracts was evaluated from a gallic acid calibration curve. The reaction mixture was prepared by mixing 200 µL of aqueous gallic acid solutions at different concentrations (100, 200, 300, 400, 500 and 600 µg/mL), 1 mL of 10% Folin-Ciocalteu's reagent dissolved in water and 18.8 mL of 7.5% Na_2CO_3 solution. After incubation at 25°C for 30 min under stirring, the quantitative phenolic estimation was performed at 765 nm against reagent blank by UV-vis Spectrophotometer (JASCO V-670). Blank was concomitantly prepared, containing 200 µL of water, 1 mL of 10% Folin-Ciocalteu's reagent dissolved in water and 18.8 mL of 7.5% Na_2CO_3 solution. The calibration curve was constructed by putting the value of absorbance vs. concentration. A similar procedure with minor modifications was adopted for the extract as above described in the preparation of the calibration curve. The samples have been solubilized in acetone instead of water because the molecules are hydrophobic. All determinations were performed in triplicate. Total phenolic content was expressed number of phenols as gallic acid equivalent.

VI.1.2.6.Gelation tests

Gelation was tested by introducing the desired amount of gelator and 1 mL of liquid in a screw-cap vial, heating until dissolution, if possible and leaving the vial to cool on the bench. If the gelator solubilized at high temperature and reprecipitated at room temperature, it was reported as precipitate. If the gelator remained insoluble at high temperature, it was reported as insoluble.

VI.1.2.7. Thermogravimetric analysis (TGA)

A TGA Q50 (TA Instruments) was used to characterize the thermal properties of commercial tannic acid and derivatives. The sample was heated at a rate of 20°C/min from room temperature to 600°C under argon.

VI.2. Synthesis of model compounds

VI.2.1. Methyl gallate - acetylated (MG(OAc)$_3$)

Methyl gallate (1 g, 5.45 mmol, 16.35 mmol hydroxyl group) was added in 30 mL (large excess) of acetic anhydride in a 100 mL round-bottom flask. The slurry was stirred and the flask put in an ice bath. The triethylamine (5mL, 37 mmol) was added dropwise then the mixture was stirred at room temperature over 4h. Next, 10 mL of ethanol was added to quench the reaction. The mixture was diluted with 60 mL of water then the product was extracted with ethyl acetate (3x50 mL). The organic phase was washed with brine (50 mL). The organic phase was dried over $MgSO_4$ and evaporated under vacuum to give a solid which was recrystallized in ethyl acetate/heptane (5/5).

VI.2.2. Methyl gallate - esterified (MG(stearoyloxy)$_3$)

Methyl gallate (1 g, 5.45 mmol, 16.35 mmol hydroxyl group) and pyridine (1.6 mL) were dissolved in 30 mL of dry dichloromethane in a 100 mL three-necked round-bottom flask. To this solution, 5.9 g (19.5 mmol) of stearoyl chloride, diluted with some dry dichloromethane, was added dropwise with stirring at room temperature for 30 min. The temperature was raised and maintained under reflux for 24h. The mixture was cooled to room temperature and filtered to remove the pyridinium salt, which was washed three times with dichloromethane. The reaction mixture was placed in a separation funnel and washed with water (50 mL), HCl 2M (40 mL), a sodium bicarbonate solution until a neutral pH (2x40 mL) and brine (2x50mL). The organic phase was dried over anhydrous magnesium sulfate, and the excess dichloromethane was evaporated off. A small amount of dichloromethane was added then the mixture was added dropwise to 200 mL of ethanol under stirring. A white precipitate appeared then the solution was filtered and the white solid obtained was dried under vacuum.

VI.2.3. Methyl gallate - etherified (MG(dodecyloxy)$_3$)

Methyl gallate (1 g, 5.45 mmol, 16.35 mmol hydroxyl group) was added in 30 mL of DMF in a 100 mL round-bottom flask. The mixture was stirred then, the dry potassium carbonate (7 g, 50.65 mmol) and the bromododecane (4.2 mL, 17.5 mmol) were added. The temperature was raised and maintained at 85°C for 48h. The mixture was cooled to room temperature and 150 mL of water was added. A brown precipitate appeared then the solution was filtered and the solid was recrystallized with ethanol. The solid obtained was dried under vacuum at 60°C.

VI.3. Synthesis of tannic acid derivatives

VI.3.1. Acetylated tannic acid molecules

Tannic acid (1 eq) was added in acetic anhydride (8 eq, 15 eq or large excess) in a 100 mL round-bottom flask. The slurry was stirred as a catalytic amount of sulfuric acid (50 µL) was added. The temperature rose rapidly from RT to 75°C in about 1 min then the mixture was allowed to cool to room temperature over 20 min. Next, 50 mL of water was added to the flask to hydrolyze any excess acetic anhydride and the mixture was stirred overnight. A white crystalline product was isolated by filtration and further washed with aliquots of water (3x20 mL). The solid was solubilized in hot ethyl acetate then placed in a separation funnel and washed with HCl 2M (3x40 mL), brine (3x40 mL) and water (2x40 mL). The organic phase was dried over anhydrous magnesium sulfate, the excess ethyl acetate was evaporated off and the white solid obtained was dried under vacuum at 50°C for 24h.

VI.3.2. Esterified tannic acid molecules

Tannic acid (1 g, 0.5878 mmol, 14.7 mmol hydroxyl group) and pyridine (0.8 mL for 15 eq or 0.5 mL for 9 eq) were dissolved in 30 mL of dry dichloromethane in a 100 mL three-necked round-bottom flask. To this solution, 2.671 g (15 eq) or 1.603 g (9 eq) of stearoyl chloride, diluted with 10 mL of dry dichloromethane, was added dropwise with stirring at room temperature for 30 min. The temperature was raised and maintained under reflux for 24h. The mixture was cooled to room temperature and filtered to remove the pyridinium salt, which was washed three times with dichloromethane. The reaction mixture was placed in a separation funnel and washed with water (50 mL), HCl 2M (40 mL), a sodium bicarbonate solution until a neutral pH (2x40 mL) and brine (2x50mL). The organic phase was dried over anhydrous magnesium sulfate, and the excess dichloromethane was evaporated off. A small amount of dichloromethane was added then the mixture was added dropwise to 200 mL of ethanol under stirring. A white precipitate appeared then the solution was filtered and the white solid obtained was dried under vacuum.

VI.3.3. Etherified tannic acid molecules

Tannic acid (1 g, 0.5878 mmol, 14.7 mmol hydroxyl group), dried potassium carbonate (1 eq for each phenolic function to functionalize), sodium iodide (5mg, 0.4% wt) and the corresponding bromoalkane (1 eq for each phenolic function to functionalize) were added in 20

mL of *N*,*N*-dimethylformamide in a 100 mL round-bottom flask. The temperature was raised and maintained at 85°C for 24h. The mixture was cooled down to room temperature and 150 mL of water was added. With a solution of HCl 2M, the pH was adjusted to 4. A brown precipitate appeared then the solution was filtered and the solid was washed with water (4 x 50 mL). The solid was dried under vacuum at 100°C for 10 days.

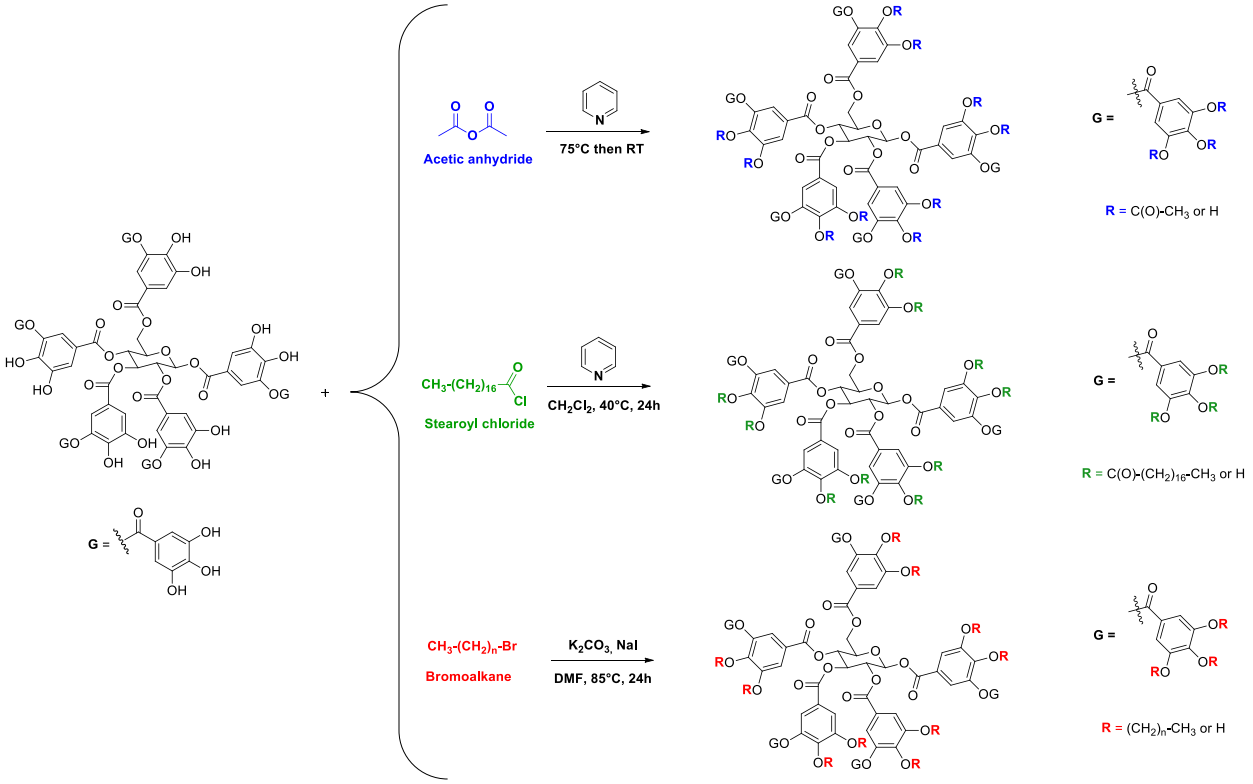

Figure II.30. Proposed reactions of tannic acid derivatives

VI.4. Experimental data

VI.4.1. Methyl gallate derivatives

Triacetoxymethyl gallate (MG(acetoxy)$_3$): 90%; white solid; **^{1}H NMR** (300 MHz, $CDCl_3$), δ (ppm): 7.80 (s, 2H, Ar-**H**), 3.90 (s, 3H, OC**H$_3$**), 2.29 (d, *J* = 2.0 Hz, 9H, C**H$_3$**). **^{13}C NMR** (75 MHz, $CDCl_3$), δ (ppm): 167.69, 166.53, 165.02, 143.54, 138.72, 128.42, 122.33, 52.68, 20.69, 20.28.

Tristearoyloxymethyl gallate (MG(stearoyloxy)$_3$): 89%; white solid; **^{1}H NMR** (300 MHz, $CDCl_3$), δ (ppm): 7.78 (s, 2H, Ar-**H**), 3.90 (s, 3H, OC**H$_3$**), 2.52 (t, *J* = 7.5 Hz, 6H, C(O)-C**H$_2$**), 1.72 (p, *J* = 7.4 Hz, 6H, C(O)-CH_2-C**H$_2$**), 1.26 (m, 84H, (C**H$_2$**)$_{14}$), 0.96-0.80 (m, 9H, C**H$_3$**). **^{13}C**

NMR (75 MHz, $CDCl_3$), δ (ppm): 170.61, 169.39, 165.17, 143.67, 138.85, 128.24, 122.24, 52.65, 34.18, 33.92, 32.08, 29.87, 29.82, 29.79, 29.67, 29.63, 29.52, 29.44, 29.34, 29.28, 25.12, 25.01, 22.84, 14.26.

Tridodecyloxymethyl gallate (MG(dodecyloxy)$_3$): 15%; white solid; **^{1}H NMR** (400 MHz, CD_2Cl_2), δ (ppm): 7.24 (s, 2H, Ar-**H**), 4.00 (q, *J* = 5.9 Hz, 6H, OC**H$_2$**), 3.85 (s, 3H, OC**H$_3$**), 1.76 (dp, *J* = 37.2, 6.9 Hz, 6H, OCH_2-C**H$_2$**), 1.53-1.20 (m, 54H, (C**H$_2$**)$_9$), 0.88 (t, *J* = 6.6 Hz, 9H, C**H$_3$**).

VI.4.2. Acetylated tannic acid molecules

Octaacetoxytannic acid (TA(OAc)$_8$): 72%; white solid; **^{1}H NMR** (400 MHz, CD_2Cl_2/acetone-D_6), δ (ppm): 8.56 (s, 17H, O**H**), 7.96-6.86 (m, 20H, Ar-**H**), 6.38-5.53 (m, 4H, C**H** glucose), 4.49 (m, 3H, C**H** glucose + OC**H$_2$**), 2.27 (d, 23H, C**H$_3$**). **^{13}C NMR** (101 MHz, CD_2Cl_2/acetone-D_6), δ (ppm): 171.60 (**C**=O), 168.10 (**C**=O), 168.04 (**C**=O), 163.73 (**C**=O), 163.13 (**C**=O), 163.10 (**C**=O), 162.51 (**C**=O), 149.72, 149.51, 149.32, 145.29, 145.28, 144.32, 144.15, 142.41, 139.07, 138.90, 137.85, 137.70, 122.43, 121.80, 121.80, 119.30, 119.02, 118.95, 116.87, 116.22, 114.13, 113.76, 113.53, 109.57, 109.56, 108.90, 72.37, 19.64 (**C**H_3), 19.55 (**C**H_3), 19.49 (**C**H_3), 19.28 (**C**H_3).

Decaacetoxytannic acid (TA(OAc)$_{10}$): 64%; white solid; **^{1}H NMR** (400 MHz, CD_2Cl_2/acetone-D_6), δ (ppm):): 8.57 (s, 15H, O**H**), 7.98-6.89 (m, 20H, Ar-**H**), 6.38-5.55 (m, 4H, C**H** glucose), 4.47 (m, 3H, C**H** glucose + OC**H$_2$**), 2.26 (m, 30H, C**H$_3$**).

Pentadecaacetoxytannic acid (TA(OAc)$_{15}$): 77%; white solid; **^{1}H NMR** (400 MHz, CD_2Cl_2/acetone-D_6), δ (ppm): 9.21 (s, 10H, O**H**), 8.18-7.14 (m, 20H, Ar-**H**), 6.42-5.59 (m, 4H, C**H** glucose), 4.52 (m, 3H, C**H** glucose + OC**H$_2$**), 2.28 (m, 51H, C**H$_3$**). **^{13}C NMR** (101 MHz, CD_2Cl_2/acetone-D_6), δ (ppm): 172.30 (**C**=O), 168.89 (**C**=O), 168.70 (**C**=O), 168.12 (**C**=O), 167.90 (**C**=O), 167.63 (**C**=O), 166.87 (**C**=O), 164.04 (**C**=O), 163.36 (**C**=O), 147.19 144.07, 140.02, 139.78, 139.71, 123.54, 123.33, 123.18, 123.07, 122.71, 120.83, 120.43, 119.97, 116.11, 20.55 (**C**H_3), 20.53 (**C**H_3), 20.50 (**C**H_3), 20.40 (**C**H_3), 20.19 (**C**H_3), 20.02 (**C**H_3).

Pentacosaacetoxytannic acid (TA(OAc)$_{25}$): 87%; white solid; **^{1}H NMR** (400 MHz, CD_2Cl_2/acetone-D_6), δ (ppm): 8.15-7.58 (m, 20H, Ar-**H**), 6.41-5.57 (m, 4H, C**H** glucose), 4.68-4.40 (m, 3H, C**H** glucose + OC**H$_2$**), 2.40-2.10 (m, 85H, C**H$_3$**). **^{13}C NMR** (101 MHz, CD_2Cl_2 /acetone-D_6), δ (ppm): 168.50 (**C**=O), 167.78 (**C**=O), 167.74 (**C**=O), 167.72 (**C**=O), 167.58 (**C**=O), 167.51 (**C**=O), 166.63 (**C**=O), 166.53 (**C**=O), 166.43 (**C**=O), 166.37 (**C**=O), 163.84

(**C**=O), 163.69 (**C**=O), 163.27 (**C**=O), 162.52 (**C**=O), 161.69 (**C**=O), 144.09, 143.86, 143.79, 143.71, 143.53, 140.12, 140.04, 139.82, 139.64, 139.50, 139.32, 132.63, 128.74, 127.88, 127.13, 126.96, 126.68, 126.26, 123.24, 122.81, 122.64, 122.37, 122.28, 93.07, 72.89, 71.79, 69.50, 67.67, 66.83, 66.10, 62.89, 54.16, 53.89, 53.62, 53.35, 53.07, 35.96, 30.13, 30.08, 29.88, 29.69, 29.50, 29.31, 29.11, 28.92, 20.22, 20.11, 20.08, 20.06, 19.70, 19.66 (**C**H_3).

VI.4.3. Esterified tannic acid molecules

Nonastearoyloxytannic acid (TA(stearoyloxy)$_9$): 25%; white solid; **^{1}H NMR** (400 MHz, CD_2Cl_2/acetone-D_6), δ (ppm): 11.65-9.01 (s, O**H**), 8.06-7.62 (m, 20H, Ar-**H**), 6.64-5.75 (m, 4H, C**H** glucose), 4.63-4.56 (m, 3H, C**H** glucose + OC**H$_2$**), 2.64-2.23 (m, C(O)-C**H$_2$**), 1.82-1.53 (m, C(O)-CH_2-C**H$_2$**), 1.50-1.06 (m, (C**H$_2$**)$_{15}$), 0.89-0.86 (t, C**H$_3$**). **^{13}C NMR** (101 MHz, CD_2Cl_2/acetone-D_6), δ (ppm): 175.22 (**C**=O), 33.76 (**C**H_2), 32.01 (**C**H_2), 29.74 (**C**H_2), 29.71 (**C**H_2), 29.45 (**C**H_2), 29.23 (**C**H_2), 24.98 (**C**H_2), 22.74 (**C**H_2), 13.87 (**C**H_3).

Pentadecastearoyloxytannic acid (TA(stearoyloxy)$_{15}$): 37%; white solid; **^{1}H NMR** (400 MHz, CD_2Cl_2/acetone-D_6), δ (ppm): 11.30-9.55 (s, O**H**), 8.23-7.36 (m, 20H, Ar-**H**), 6.43-5.64 (m, 4H, C**H** glucose), 4.77-4.43 (m, 3H, C**H** glucose + OC**H$_2$**), 2.68-2.16 (m, C(O)-C**H$_2$**), 1.82-1.50 (m, C(O)-CH_2-C**H$_2$**), 1.48-1.04 (m, (C**H$_2$**)$_{15}$), 0.88-0.83 (m, C**H$_3$**). **^{13}C NMR** (101 MHz, CD_2Cl_2/acetone-D_6), δ (ppm): 174.74 (**C**=O), 34.15 (**C**H_2), 33.97 (**C**H_2), 32.34 (**C**H_2), 32.30 (**C**H_2), 30.10 (**C**H_2), 30.06 (**C**H_2), 30.03 (**C**H_2), 29.88 (**C**H_2), 29.72 (**C**H_2), 29.52 (**C**H_2), 25.30 (**C**H_2), 23.05 (**C**H_2), 23.01 (**C**H_2), 14.17 (**C**H_3), 14.12 (**C**H_3).

Pentacosastearoyloxytannic acid (TA(stearoyloxy)$_{25}$): 50%; white solid; **^{1}H NMR** (400 MHz, CD_2Cl_2/acetone-D_6), δ (ppm): 8.15-7.55 (m, 20H, Ar-**H**), 6.47-5.61 (m, 4H, C**H** glucose), 4.78-4.41 (m, 3H, C**H** glucose + OC**H$_2$**), 2.80-2.16 (m, C(O)-C**H$_2$**), 1.82-1.50 (m, C(O)-CH_2-C**H$_2$**), 1.49-1.04 (m, (C**H$_2$**)$_{15}$), 0.95-0.80 (t, C**H$_3$**). **^{13}C NMR** (101 MHz, CD_2Cl_2/acetone-D_6), δ (ppm): 174.67 (**C**=O), 170.63 (**C**=O), 170.48 (**C**=O), 170.40 (**C**=O), 169.40 (**C**=O), 169.18 (**C**=O), 169.14 (**C**=O), 144.43, 144.09, 122.95, 122.66, 34.12 (**C**H_2), 34.08 (**C**H_2), 33.89 (**C**H_2), 32.25 (**C**H_2), 30.06 (**C**H_2), 29.99 (**C**H_2), 29.90 (**C**H_2), 29.70 (**C**H_2), 29.64 (**C**H_2), 29.46 (**C**H_2), 25.23 (**C**H_2), 25.20 (**C**H_2), 25.11 (**C**H_2), 22.97 (**C**H_2), 14.11 (**C**H_3), 14.07 (**C**H_3).

VI.4.4. Etherified tannic acid molecules

Tri(hexyloxy)tannic acid (TA(hexyloxy)$_3$): 77%; brown solid; **^{1}H NMR** (400 MHz, CD_2Cl_2/acetone-D_6), δ (ppm): 8.26-6.74 (m, 20H, Ar-**H**), 6.32-5.52 (m, 4H, C**H** glucose), 4.45

(m, 3H, C**H** + OC**H₂** glucose), 4.11 (m, OC**H₂**), 1.79 (m, C**H₂**-CH_2-O), 1.35 (m, (C**H₂)₃**), 0.86 (m, C**H₃**).

Penta(hexyloxy)tannic acid (TA(hexyloxy)₅): 80%; brown solid; **^{1}H NMR** (400 MHz, CD_2Cl_2/acetone-D_6), δ (ppm): 8.26-6.74 (m, 20H, Ar-**H**), 6.32-5.52 (m, 4H, C**H** glucose), 4.45 (m, 3H, C**H** + OC**H₂** glucose), 4.11 (m, OC**H₂**), 1.79 (m, C**H₂**-CH_2-O), 1.35 (m, (C**H₂)₃**), 0.86 (m, C**H₃**). **^{13}C NMR** (101 MHz, CD_2Cl_2/acetone-D_6), δ (ppm): 166.81 (**C**=O), 165.64 (**C**=O), 165.15 (**C**=O), 163.93 (**C**=O), 158.57, 158.47, 151.35, 149.59, 149.53, 149.53, 147.37, 144.62, 144.48, 143.09, 139.06, 138.57, 135.92, 125.14, 124.43, 123.53, 112.28, 111.14, 110.62, 109.07, 108.71, 74.08, 72.66, 64.36, 31.26, 31.23, 31.20, 31.09, 29.77, 29.65, 29.58, 28.31, 25.07, 25.03, 24.98, 22.21, 22.16, 13.32, 13.30.

Deca(hexyloxy)tannic acid (TA(hexyloxy)₁₀): 83%; brown solid; **^{1}H NMR** (400 MHz, CD_2Cl_2/acetone-D_6), δ (ppm): 8.29-6.86 (m, 20H, Ar-**H**), 6.35-5.57 (m, 4H, C**H** glucose), 4.39 (m, 3H, C**H** + OC**H₂** glucose), 4.13 (m, OC**H₂**), 1.76 (m, C**H₂**-CH_2-O), 1.36 (m, (C**H₂)₃**), 0.83 (m, C**H₃**). **^{13}C NMR** (101 MHz, CD_2Cl_2/acetone-D_6), δ (ppm): 167.14 (**C**=O), 167.11 (**C**=O), 166.36 (**C**=O), 165.84 (**C**=O), 164.02 (**C**=O), 154.26, 152.15, 152.12, 150.79, 150.30, 150.13, 150.10, 150.01, 149.97, 144.26, 143.42, 139.55, 139.50, 139.18, 138.38, 138.32, 125.55, 125.48, 125.43, 125.40, 125.31, 123.99, 116.19, 115.83, 115.41, 110.37, 110.00, 109.74, 109.35, 109.28, 108.99, 108.29, 106.46, 106.15, 105.85, 74.24, 73.44, 73.24, 73.16, 73.04, 72.89, 72.80, 69.58, 68.80, 68.65, 64.89, 64.71, 64.55, 64.16, 31.60, 31.56, 31.51, 31.48, 31.37, 31.07, 30.18, 30.02, 29.98, 29.93, 29.80, 29.23, 28.59, 28.56, 25.76, 25.69, 25.61, 25.47, 25.34, 25.29, 22.49, 22.44, 22.41, 22.33, 22.24, 13.57.

Pentacosa(hexyloxy)tannic acid (TA(hexyloxy)₂₅): 85%; brown solid; **^{1}H NMR** (400 MHz, CD_2Cl_2/acetone-D_6), δ (ppm): 7.79-6.92 (m, 20H, Ar-**H**), 6.46-5.55 (m, 4H, C**H** glucose), 4.77-4.47 (m, 3H, C**H** + OC**H₂** glucose), 4.05 (m, OC**H₂**), 1.78 (m, C**H₂**-CH_2-O), 1.39 (m, (C**H₂)₃**), 0.90 (m, C**H₃**). **^{13}C NMR** (101 MHz, CD_2Cl_2/acetone-D_6), δ (ppm): 167.54 (**C**=O), 166.76 (**C**=O), 164.47 (**C**=O), 164.41 (**C**=O), 153.23, 153.11, 153.01, 152.43, 152.21, 150.49, 150.19, 145.13, 144.51, 143.18, 142.47, 140.39, 139.66, 125.48, 125.37, 125.16, 123.93, 117.82, 117.29, 112.42, 110.96, 110.49, 108.56, 108.24, 106.73, 106.44, 73.67, 73.52, 73.46, 73.44, 73.39, 73.35, 73.31, 69.26, 69.13, 69.04, 68.90, 31.89, 31.87, 31.82, 31.77, 31.71, 31.66, 30.45, 30.41, 29.47, 29.45, 26.06, 25.98, 25.94, 25.91, 25.88, 25.80, 25.73, 25.70, 25.66, 22.79, 22.73, 22.70, 22.64, 13.89, 13.86, 13.83.

Tri(octyloxy)tannic acid (TA(octyloxy)$_3$): 75%; brown solid; **^{1}H NMR** (400 MHz, CD_2Cl_2-d_2/Acetone-d_6), δ (ppm): 8.32-6.83 (m, 20H, Ar-**H**), 6.29-5.51 (m, 4H, C**H** glucose), 4.42 (m, 3H, C**H** + OC**H$_2$** glucose), 4.10 (m, 6H, OC**H$_2$**), 1.74 (m, 6H, C**H$_2$**-CH_2-O), 1.29 (m, 30H, (C**H$_2$**)$_5$), 0.86 (m, 9H, C**H$_3$**).

Octa(octyloxy)tannic acid (TA(octyloxy)$_8$): 78%; brown solid; **^{1}H NMR** (400 MHz, CD_2Cl_2-d_2/Acetone-d_6), δ (ppm): 8.42-6.73 (m, 20H, Ar-**H**), 6.33-5.52 (m, 4H, C**H** glucose), 4.40 (m, 3H, C**H** + OC**H$_2$** glucose), 4.12 (m, 16H, OC**H$_2$**), 1.76 (m, 16H, C**H$_2$**-CH_2-O), 1.34 (m, 80H, (C**H$_2$**)$_5$), 0.87 (m, 24H, C**H$_3$**).

Tri(decyloxy)tannic acid (TA(decyloxy)$_3$): 77%; brown solid; **^{1}H NMR** (400 MHz, CD_2Cl_2-d_2/Acetone-d_6), δ (ppm): 8.37-6.72 (m, 20H, Ar-**H**), 6.29-5.52 (m, 4H, C**H** glucose), 4.44 (m, 3H, C**H** + OC**H$_2$** glucose), 4.13 (m, 6H, OC**H$_2$**), 1.76 (m, 6H, C**H$_2$**-CH_2-O), 1.30 (m, 42H, (C**H$_2$**)$_7$), 0.89 (m, 9H, C**H$_3$**).

Octa(decyloxy)tannic acid (TA(decyloxy)$_8$): 82%; brown solid; **^{1}H NMR** (400 MHz, CD_2Cl_2-d_2/Acetone-d_6), δ (ppm): 7.76-6.72 (m, 20H, Ar-**H**), 6.29-5.53 (m, 4H, C**H** glucose), 4.42 (m, 3H, C**H** + OC**H$_2$** glucose), 4.11 (m, 16H, OC**H$_2$**), 1.76 (m, 16H, C**H$_2$**-CH_2-O), 1.28 (m, 112H, (C**H$_2$**)$_7$), 0.86 (m, 24H, C**H$_3$**).

Penta(dodecyloxy)tannic acid (TA(dodecyloxy)$_5$): 78%; brown solid; **^{1}H NMR** (400 MHz, CD_2Cl_2/acetone-D_6), δ (ppm): 7.97 (s, 13H, O**H**), 7.42-6.85 (m, 20H, Ar-**H**), 6.31-5.52 (m, 4H, C**H** glucose), 4.44 (m, 3H, C**H** + OC**H$_2$** glucose), 4.10 (m, OC**H$_2$**), 1.74 (m, C**H$_2$**-CH_2-O), 1.29 (m, (C**H$_2$**)$_3$), 0.86 (t, J = 6.5 Hz, C**H$_3$**). **^{13}C NMR** (101 MHz, CD_2Cl_2/acetone-D_6), δ (ppm): 167.11 (**C**=O), 165.96 (**C**=O), 150.09, 150.05, 145.01, 138.45, 138.39, 125.57, 109.90, 109.46, 109.11, 72.97, 64.67, 31.92, 29.98, 29.96, 29.67, 29.64, 29.48, 29.35, 28.76, 26.25, 26.06, 25.95, 25.81, 22.64, 13.76.

Deca(dodecyloxy)tannic acid (TA(dodecyloxy)$_{10}$): 80%; brown solid; **^{1}H NMR** (400 MHz, CD_2Cl_2/acetone-D_6), δ (ppm): 7.70-6.87 (m, 20H, Ar-**H**), 6.32-5.54 (m, 4H, C**H** glucose), 4.45 (m, 3H, C**H** + OC**H$_2$** glucose), 4.12 (m, OC**H$_2$**), 1.77 (m, C**H$_2$**-CH_2-O), 1.27 (m, (C**H$_2$**)$_3$), 0.86 (t, J = 6.6 Hz, C**H$_3$**). **^{13}C NMR** (101 MHz, CD_2Cl_2/acetone-D_6), δ (ppm): 167.34 (**C**=O), 167.11 (**C**=O), 166.07 (**C**=O), 152.33, 150.45, 150.29, 150.20, 150.15, 139.72, 138.54, 138.48, 125.82, 125.70, 125.62, 110.57, 109.95, 109.56, 109.21, 106.38, 106.07, 73.72, 73.30, 73.18, 73.07, 68.89, 64.94, 64.78, 64.36, 50.97, 32.07, 32.05, 30.29, 30.24, 30.09, 29.86, 29.81, 29.77, 29.62, 29.49, 29.43, 28.90, 28.87, 26.38, 26.19, 26.08, 25.94, 22.79, 22.77, 22.65, 13.91, 13.89.

Pentacosa(dodecyloxy)tannic acid (TA(dodecyloxy)$_{25}$): 84%; brown solid; **^{1}H NMR** (400 MHz, CD_2Cl_2/acetone-D_6), δ (ppm): 7.72-6.90 (m, 20H, Ar-**H**), 6.35-5.61 (m, 4H, C**H** glucose), 4.56 (m, 3H, C**H** + OC**H$_2$** glucose), 4.35-3.79 (m, 53H, OC**H$_2$**), 1.78 (m, 50H, C**H$_2$**-CH_2-O), 1.27 (m, (C**H$_2$)$_3$**), 0.88 (m, C**H$_3$**). **^{13}C NMR** (101 MHz, CD_2Cl_2/acetone-D_6), δ (ppm): 166.36 (**C**=O), 165.72 (**C**=O), 164.75 (**C**=O), 153.61, 153.42, 152.72, 150.79, 142.84, 140.08, 126.04, 125.78, 110.95, 110.64, 108.96, 108.53, 108.32, 106.62, 106.36, 73.73, 73.61, 69.61, 69.48, 69.23, 65.58, 65.34, 65.22, 64.51, 51.21, 32.46, 32.43, 30.89, 30.60, 30.30, 30.27, 30.21, 30.19, 30.17, 30.14, 30.11, 29.96, 29.93, 29.89, 29.21, 26.77, 26.72, 26.66, 26.63, 26.46, 26.43, 23.14, 23.02, 14.26, 14.24.

VII. Annexes

VII.1. NMR spectra

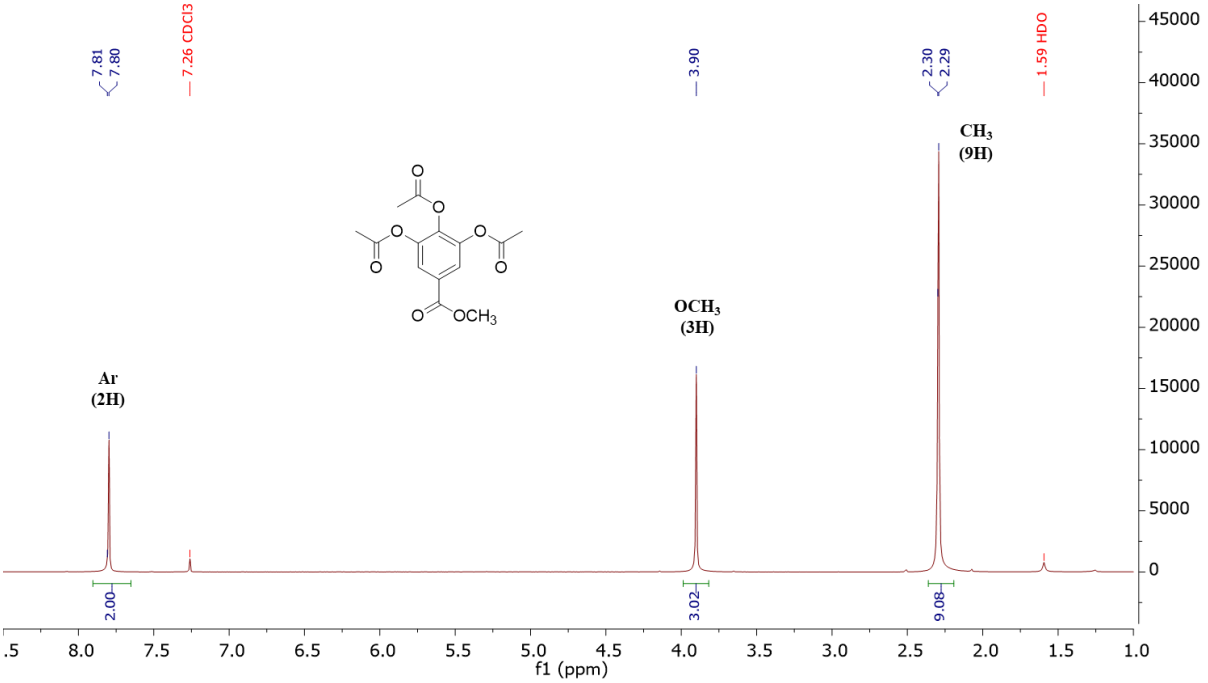

Figure II.31. ^{1}H NMR spectrum of triacetoxymethyl gallate in $CDCl_3$

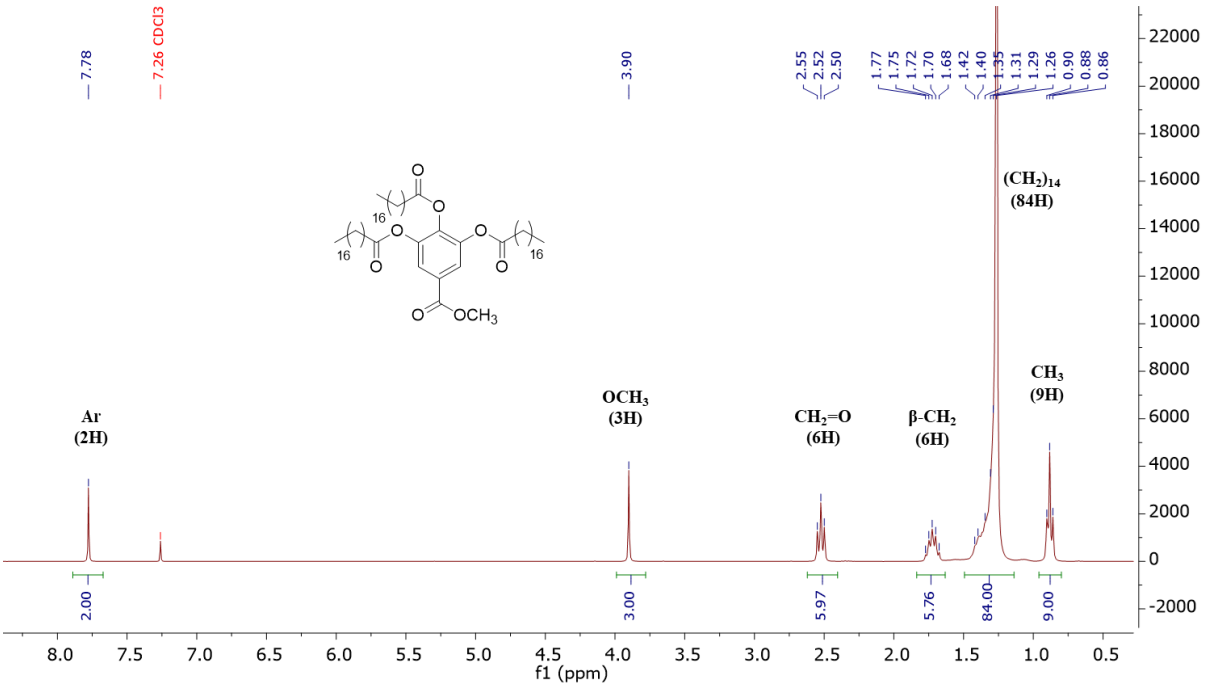

Figure II.32. ^{1}H NMR spectrum of tristearoyloxymethyl gallate in $CDCl_3$

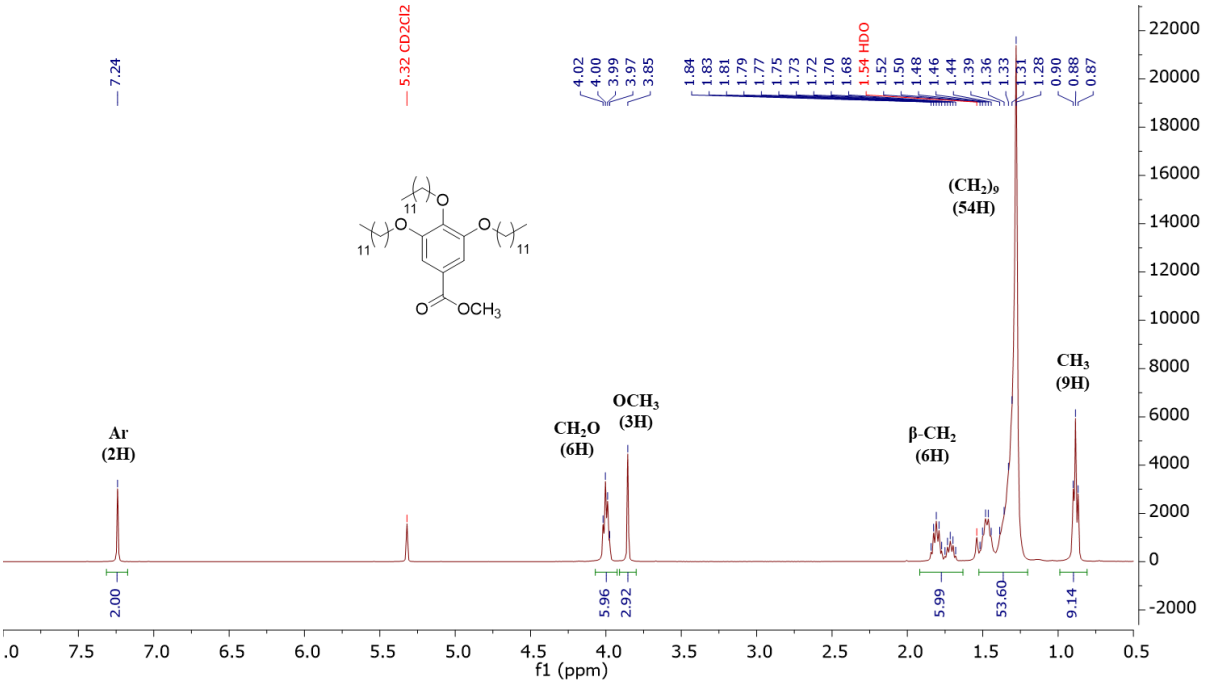

Figure II.33. ^{1}H NMR spectrum of tridodecyloxymethyl gallate in CD_2Cl_2

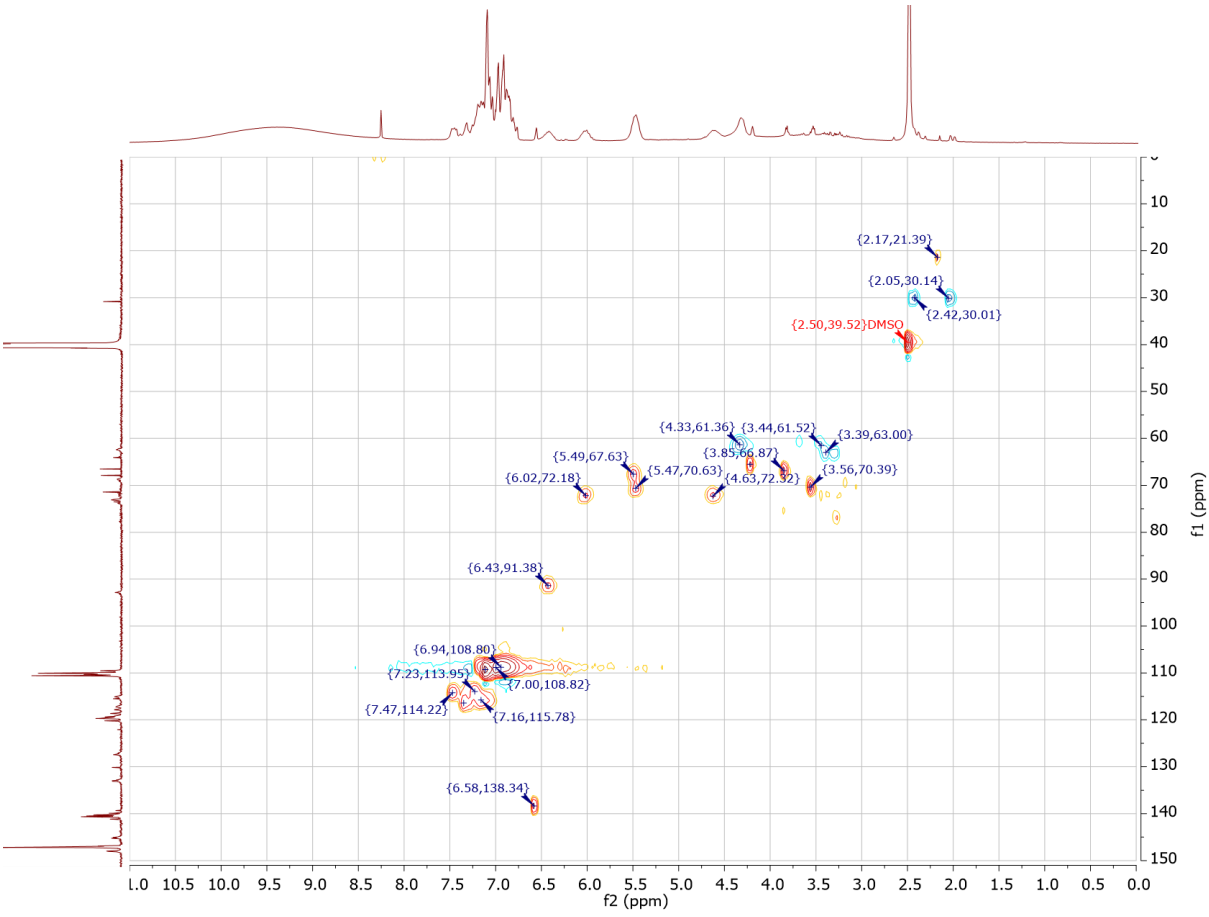

Figure II.34. HSQC ^{13}C-^{1}H spectrum of tannic acid in DMSO-D_6

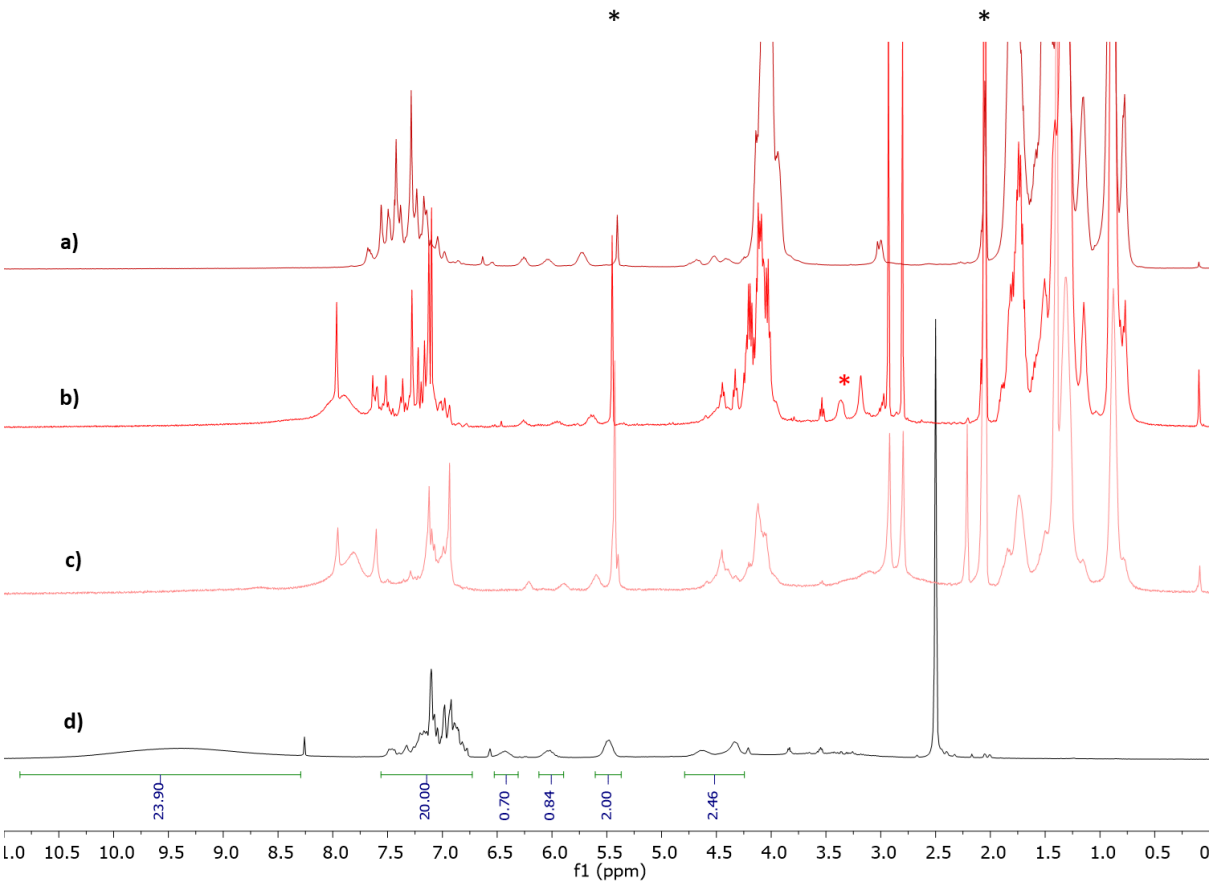

Figure II.35. Comparison of ^{1}H NMR spectra between TA and hexyloxy products; a) ^{1}H NMR spectrum of $TA(hexyloxy)_{25}$ in CD_2Cl_2/acetone-D_6 (dark red line); b) ^{1}H NMR spectrum of $TA(hexyloxy)_{15}$ in CD_2Cl_2/acetone-D_6 (red line); c) ^{1}H NMR spectrum of $TA(hexyloxy)_{5}$ in CD_2Cl_2/acetone-D_6 (light red line); d) ^{1}H NMR spectrum of tannic acid in DMSO-D_6 (black line). * represent the signals from the remaining bromohexane and * the signals from the deuterated solvents CD_2Cl_2 and acetone-D_6

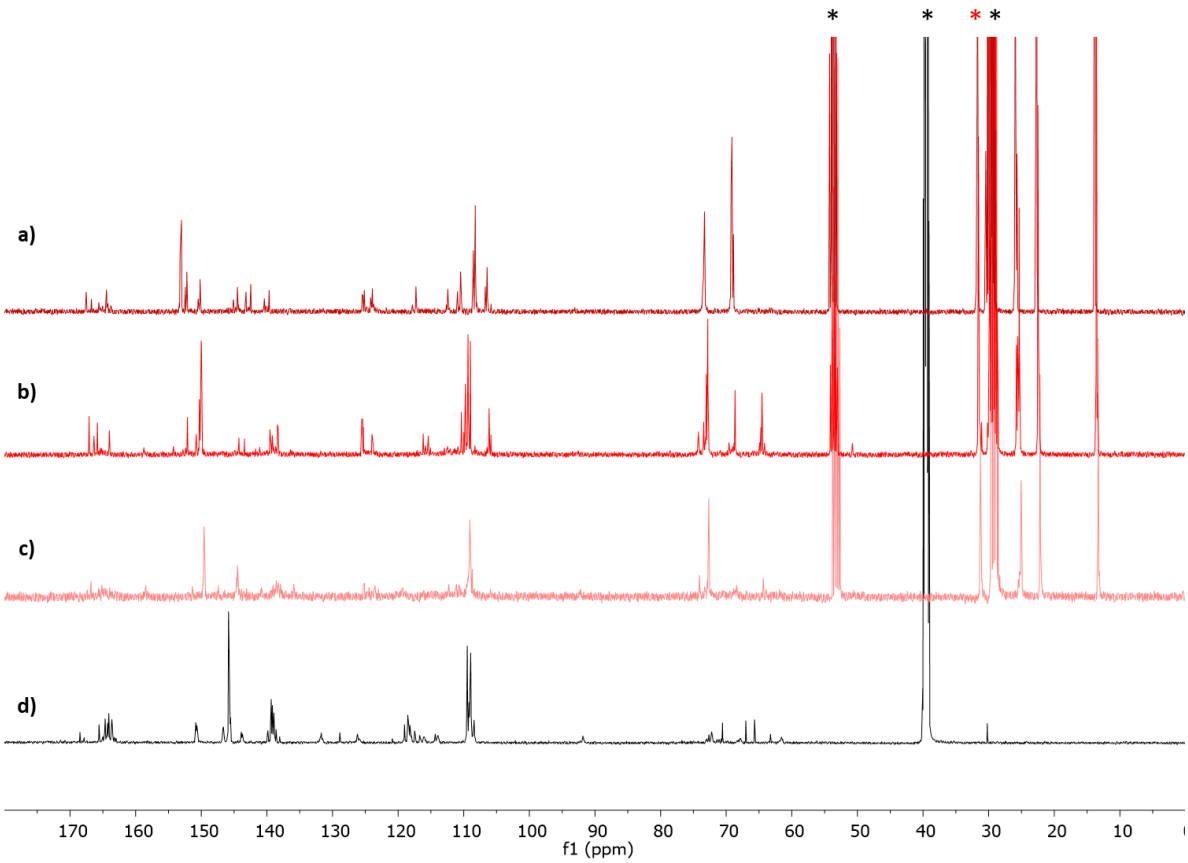

Figure II.36. Comparison of ^{13}C NMR spectra between TA and hexyloxy products; a) ^{13}C NMR spectrum of TA(hexyloxy)$_{25}$ in CD_2Cl_2/acetone-D_6 (dark red line); b) ^{13}C NMR spectrum of TA(hexyloxy)$_{10}$ in CD_2Cl_2/acetone-D_6 (red line); c) ^{13}C NMR spectrum of TA(hexyloxy)$_5$ in CD_2Cl_2/acetone-D_6 (light red line); c) ^{13}C NMR spectrum of tannic acid in DMSO-D_6 (black line). * represent the signals from the remaining bromohexane and * represent the signals from the deuterated solvents CD_2Cl_2, DMSO-D_6 and acetone-D_6

VII.2. FTIR spectroscopy

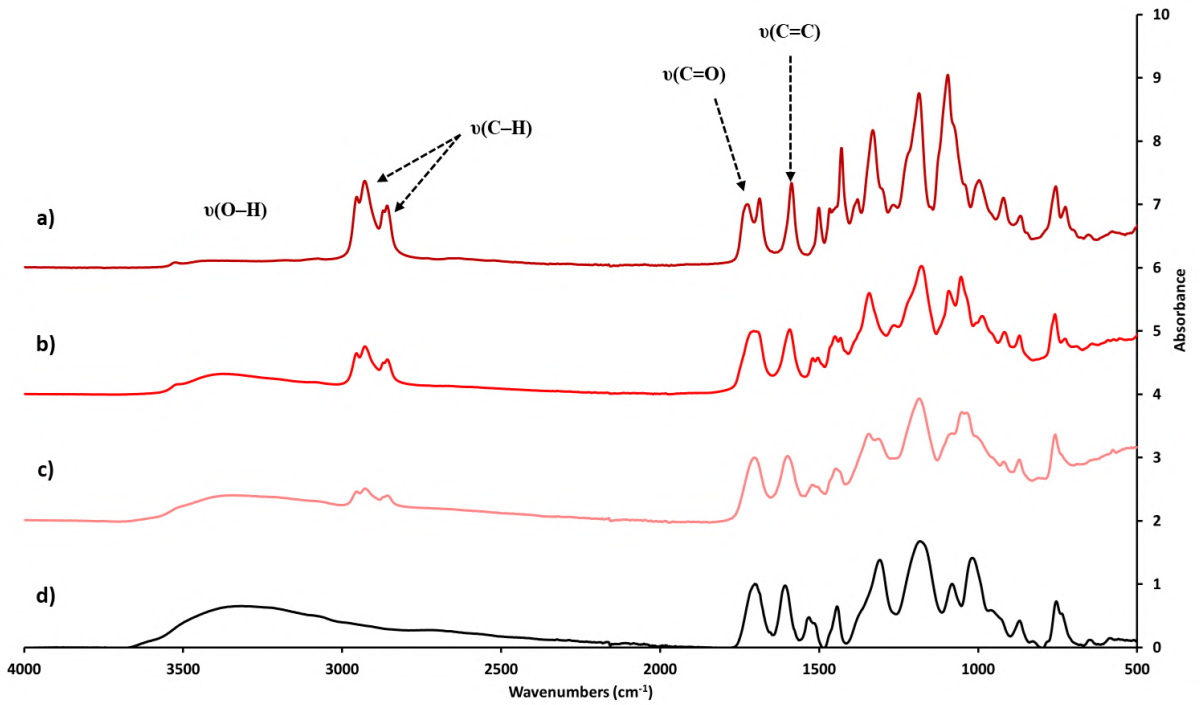

Figure II.37. Comparison of ATR FTIR spectra between TA and hexyloxy products in absorbance mode; a) FTIR spectrum of TA(hexyloxy)$_{25}$ (dark red line); b) FTIR spectrum of TA(hexyloxy)$_{10}$ (red line); c) FTIR spectrum of TA(hexyloxy)$_{5}$ (light red line); d) FTIR spectrum of tannic acid (black line). Spectra have been normalized on the C=O band

VII.3. Total phenolic content

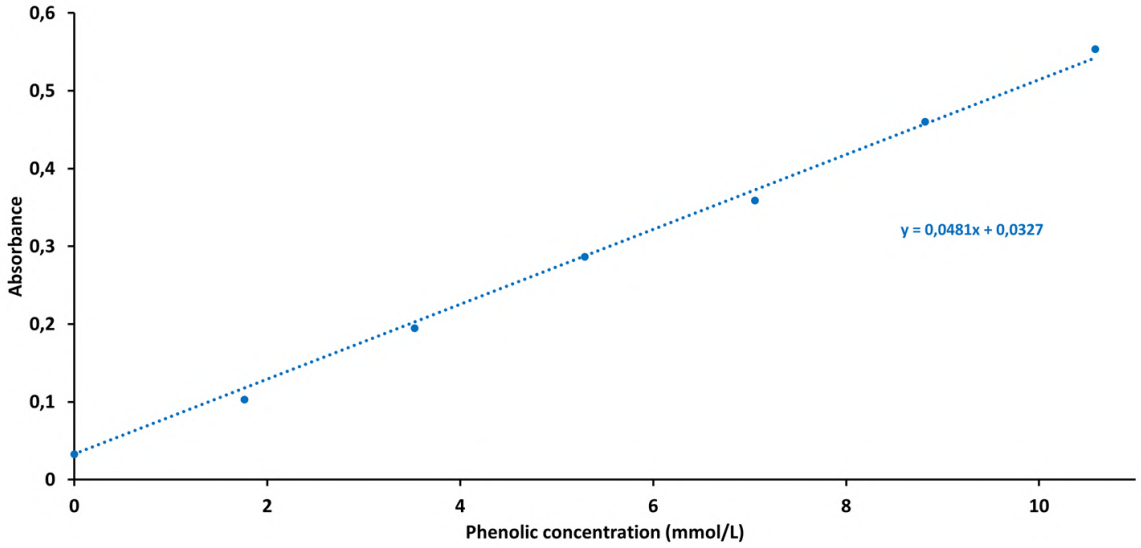

Figure II.38. Calibration curve of gallic acid

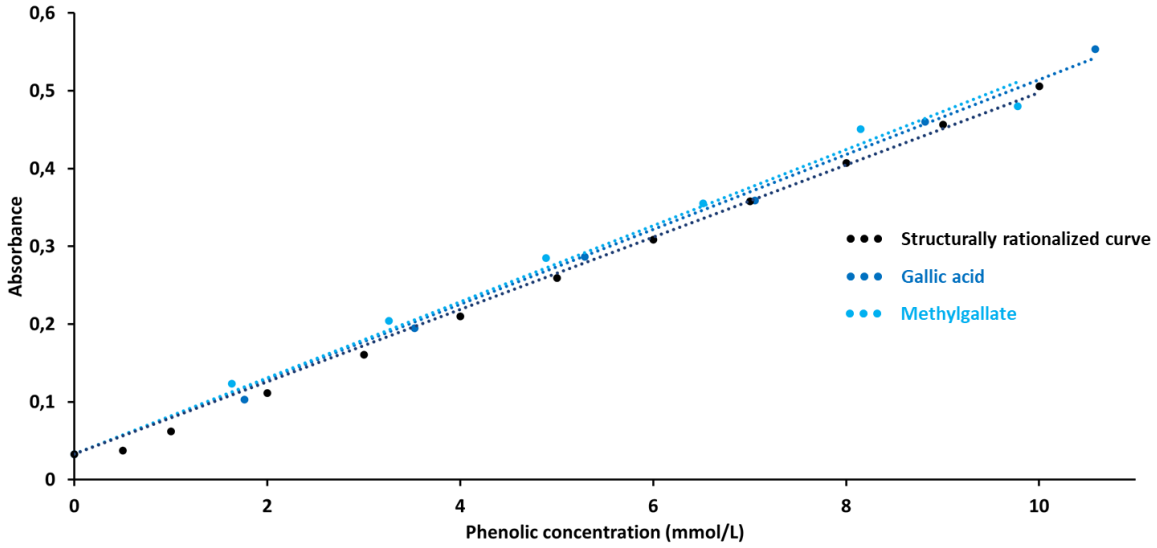

Figure II.39. Comparison between the structurally rationalized curve, gallic acid and methyl gallate

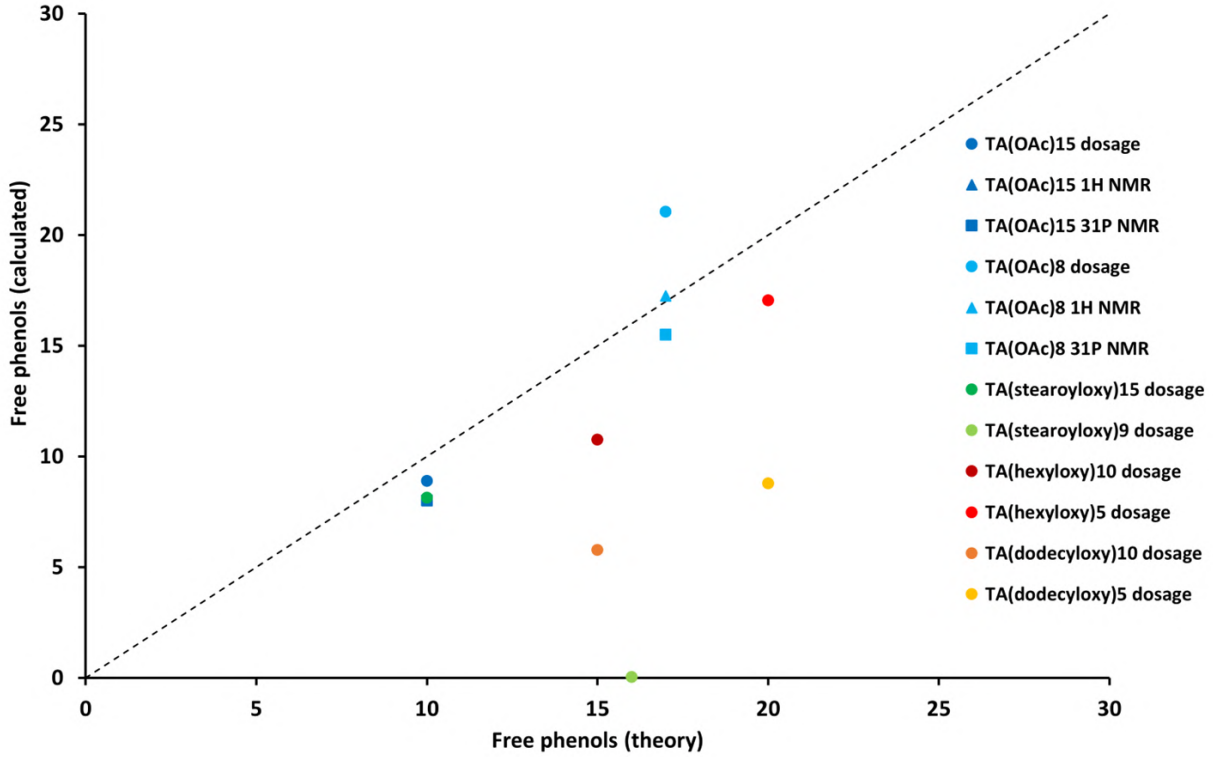

Figure II.40. Results of Folin-Ciocalteu method on tannic acid derivatives

VII.4. Mass spectrometry

Table II.9. Attribution to distributions of tannic acid mass spectrum

Mass of the ion obtained (m/z)	Exact mass of the ion (m/z)	Relative error (ppm)	Ion chemical formula	Gallic units	Distribution (circle color)
1876,17629	1876,17655	0,14	$C_{83}H_{56}O_{50}Na^+$	11	**Green**
1723,1621	1723,16219	0,05	$C_{76}H_{52}O_{46}Na^+$	10	**Green**
1571,15603	1571,15124	3,05	$C_{69}H_{48}O_{42}Na^+$	9	**Green**
1419,14046	1419,14028	0,13	$C_{62}H_{44}O_{38}Na^+$	8	**Green**
1267,1301	1267,12932	0,62	$C_{55}H_{40}O_{34}Na^+$	7	**Green**
1115,11937	1115,11836	0,91	$C_{48}H_{36}O_{30}Na^+$	6	**Green**
963,1077	963,1074	0,31	$C_{41}H_{32}O_{26}Na^+$	5	**Green**
811,09617	811,09644	-0,33	$C_{34}H_{28}O_{22}Na^+$	4	**Green**
659,08556	659,08549	0,11	$C_{27}H_{24}O_{18}Na^+$	3	**Green**
507,07453	507,07453	0,00	$C_{20}H_{20}O_{14}Na^+$	2	**Green**
355,06382	355,06357	0,70	$C_{13}H_{16}O_{10}Na^+$	1	**Green**
1683,17076	1683,16969	0,63	$C_{76}H_{51}O_{45}^+$	10	**Blue**
1531,1601	1531,15873	0,89	$C_{69}H_{47}O_{41}+$	9	**Blue**
1379,14869	1379,14777	0,67	$C_{62}H_{43}O_{37}^+$	8	**Blue**
1227,13799	1227,13681	0,96	$C_{55}H_{39}O_{33}^+$	7	**Blue**
1075,12604	1075,12585	0,18	$C_{48}H_{35}O_{29}^+$	6	**Blue**
923,1147	923,11489	-0,21	$C_{41}H_{31}O_{25}^+$	5	**Blue**
771,10389	771,10393	-0,05	$C_{34}H_{27}O_{21}^+$	4	**Blue**
619,09302	619,09298	0,06	$C_{27}H_{23}O_{17}^+$	3	**Blue**

Table II.10. Attribution to distributions of $TA(OAc)_{25}$ mass spectrum

Mass of the ion obtained (m/z)	Exact mass of the ion (m/z)	Relative error (ppm)	Ion chemical formula	Gallic units	Number of Ac	Distribution (circle color)
2773,44364	2773,42631	-6,25	$C_{126}H_{102}NaO_{71}^+$	10	25	**Brown**
2731,41386	2731,41575	0,69	$C_{124}H_{100}NaO_{70}^+$	10	24	**Brown**
2689,40845	2689,40518	-1,22	$C_{122}H_{98}NaO_{69}^+$	10	23	**Brown**
2537,40574	2537,39422	-4,54	$C_{115}H_{94}NaO_{65}^+$	9	23	**Grey**
2495,38072	2495,38366	1,18	$C_{113}H_{92}NaO_{64}^+$	9	22	**Grey**
2453,38553	2453,37310	-5,07	$C_{111}H_{90}NaO_{63}^+$	9	21	**Grey**
2411,37558	2411,36253	-5,41	$C_{109}H_{88}NaO_{62}^+$	9	20	**Grey**
2369,36216	2369,35197	-4,30	$C_{107}H_{86}NaO_{61}^+$	9	19	**Grey**
2301,36203	2301,36214	0,05	$C_{104}H_{86}NaO_{59}^+$	8	21	**Orange**
2259,36266	2259,35157	-4,91	$C_{102}H_{84}NaO_{58}^+$	8	20	**Orange**
2217,34538	2217,34101	-1,97	$C_{100}H_{82}NaO_{57}^+$	8	19	**Orange**
2175,33314	2175,33044	-1,24	$C_{98}H_{80}NaO_{56}^+$	8	18	**Orange**
2133,32409	2133,31988	-1,97	$C_{96}H_{78}NaO_{55}^+$	8	17	**Orange**
2065,33644	2065,33005	-3,09	$C_{93}H_{78}NaO_{53}^+$	7	19	**Green**
2023,32846	2023,31948	-4,44	$C_{91}H_{76}NaO_{52}^+$	7	18	**Green**
1981,31794	1981,30892	-4,55	$C_{89}H_{74}NaO_{51}^+$	7	17	**Green**
1939,30740	1939,29835	-4,67	$C_{87}H_{72}NaO_{50}^+$	7	16	**Green**
1897,29445	1897,28779	-3,51	$C_{85}H_{70}NaO_{49}^+$	7	15	**Green**
1855,28470	1855,27723	-4,03	$C_{83}H_{68}NaO_{48}^+$	7	14	**Green**
1829,30659	1829,29796	-4,72	$C_{82}H_{70}NaO_{47}^+$	6	17	**Purple**
1787,29303	1787,28740	-3,15	$C_{80}H_{68}NaO_{46}^+$	6	16	**Purple**
1745,27700	1745,27683	-0,10	$C_{78}H_{66}NaO_{45}^+$	6	15	**Purple**
1703,27154	1703,26627	-3,09	$C_{76}H_{64}NaO_{44}^+$	6	14	**Purple**
1661,25926	1661,25570	-2,14	$C_{74}H_{62}NaO_{43}^+$	6	13	**Purple**
1593,27043	1593,26587	-2,86	$C_{71}H_{62}NaO_{41}^+$	5	15	**Blue**
1551,26037	1551,25531	-3,26	$C_{69}H_{60}NaO_{40}^+$	5	14	**Blue**

1509,24830	1509,24474	-2,36	$C_{67}H_{58}NaO_{39}^{+}$	5	13	**Blue**
1467,23614	1467,23418	-1,34	$C_{65}H_{56}NaO_{38}^{+}$	5	12	**Blue**
1425,22441	1425,22361	-0,56	$C_{63}H_{54}NaO_{37}^{+}$	5	11	**Blue**
1357,23666	1357,23378	-2,12	$C_{60}H_{54}NaO_{35}^{+}$	4	13	**Red**
1315,22534	1315,22322	-1,61	$C_{58}H_{52}NaO_{34}^{+}$	4	12	**Red**
1273,21382	1273,21266	-0,91	$C_{56}H_{50}NaO_{33}^{+}$	4	11	**Red**
1231,20433	1231,20209	-1,82	$C_{54}H_{48}NaO_{32}^{+}$	4	10	**Red**
1121,20385	1121,20170	-1,92	$C_{49}H_{46}NaO_{29}^{+}$	4	11	**Pink**
1079,19296	1079,19113	-1,70	$C_{47}H_{44}NaO_{28}^{+}$	4	10	**Pink**
1037,18139	1037,18057	-0,79	$C_{45}H_{42}NaO_{27}^{+}$	4	9	**Pink**

Table II.11. Attribution to distributions of $TA(OAc)_{15}$ mass spectrum

Mass of the ion obtained (m/z)	Exact mass of the ion (m/z)	Relative error (ppm)	Ion chemical formula	Gallic units	Number of Ac	Distribution (circle color)
2353,32519	2353,32067	-1,92	$C_{106}H_{82}NaO_{61}^+$	10	15	**Brown**
2311,30971	2311,31010	0,17	$C_{104}H_{80}NaO_{60}^+$	10	14	**Brown**
2269,30700	2269,29954	-3,29	$C_{102}H_{78}NaO_{59}^+$	10	13	**Brown**
2227,28920	2227,28897	-0,10	$C_{100}H_{76}NaO_{58}^+$	10	12	**Brown**
2185,28583	2185,27841	-3,40	$C_{98}H_{74}NaO_{57}^+$	10	11	**Brown**
2143,27724	2143,26784	-4,39	$C_{96}H_{72}NaO_{56}^+$	10	10	**Brown**
2101,2633	2101,25728	-2,86	$C_{94}H_{70}NaO_{55}^+$	10	9	**Brown**
2117,29424	2117,28858	-2,67	$C_{95}H_{74}NaO_{55}^+$	9	13	**Grey**
2075,28332	2075,27801	-2,56	$C_{93}H_{72}NaO_{54}^+$	9	12	**Grey**
2033,27463	2033,26745	-3,53	$C_{91}H_{70}NaO_{53}^+$	9	11	**Grey**
1991,26364	1991,25688	-3,39	$C_{89}H_{68}NaO_{52}^+$	9	10	**Grey**
1949,25102	1949,24632	-2,41	$C_{87}H_{66}NaO_{51}^+$	9	9	**Grey**
1907,2387	1907,23575	-1,55	$C_{85}H_{64}NaO_{50}^+$	9	8	**Grey**
1865,22806	1865,22519	-1,54	$C_{83}H_{62}NaO_{49}^+$	9	7	**Grey**
1965,28471	1965,27762	-3,61	$C_{88}H_{70}NaO_{51}^+$	8	13	**Orange**
1923,27152	1923,26705	-2,32	$C_{86}H_{68}NaO_{50}^+$	8	12	**Orange**
1881,25812	1881,25649	-0,87	$C_{84}H_{66}NaO_{49}^+$	8	11	**Orange**
1839,24970	1839,24593	-2,05	$C_{82}H_{64}NaO_{48}^+$	8	10	**Orange**
1797,24100	1797,23536	-3,14	$C_{80}H_{62}NaO_{47}^+$	8	9	**Orange**
1755,22844	1755,22480	-2,07	$C_{78}H_{60}NaO_{46}^+$	8	8	**Orange**
1713,21552	1713,21423	-0,75	$C_{76}H_{58}NaO_{45}^+$	8	7	**Orange**
1671,20807	1671,20367	-2,63	$C_{74}H_{56}NaO_{44}^+$	8	6	**Orange**
1897,23488	1897,28779	27,89	$C_{85}H_{70}NaO_{49}^+$	7	15	**Green**
1855,28566	1855,27723	-4,54	$C_{83}H_{68}NaO_{48}^+$	7	14	**Green**
1813,27163	1813,26666	-2,74	$C_{81}H_{66}NaO_{47}^+$	7	13	**Green**
1771,26025	1771,25610	-2,34	$C_{79}H_{64}NaO_{46}^+$	7	12	**Green**

1729,24906	1729,24553	-2,04	$C_{77}H_{62}NaO_{45}^{+}$	7	11	**Green**
1687,23893	1687,23497	-2,35	$C_{75}H_{60}NaO_{44}^{+}$	7	10	**Green**
1645,22768	1645,22440	-1,99	$C_{73}H_{58}NaO_{43}^{+}$	7	9	**Green**
1603,21647	1603,21384	-1,64	$C_{71}H_{56}NaO_{42}^{+}$	7	8	**Green**
1561,20425	1561,20327	-0,63	$C_{69}H_{54}NaO_{41}^{+}$	7	7	**Green**
1519,19519	1519,19271	-1,63	$C_{67}H_{52}NaO_{40}^{+}$	7	6	**Green**
1477,18453	1477,18214	-1,62	$C_{65}H_{50}NaO_{39}^{+}$	7	5	**Green**
1619,24877	1619,24514	-2,24	$C_{72}H_{60}NaO_{42}^{+}$	6	12	**Purple**
1577,23534	1577,23457	-0,49	$C_{70}H_{58}NaO_{41}^{+}$	6	11	**Purple**
1535,22793	1535,22401	-2,55	$C_{68}H_{56}NaO_{40}^{+}$	6	10	**Purple**
1493,21602	1493,21344	-1,73	$C_{66}H_{54}NaO_{39}^{+}$	6	9	**Purple**
1451,20465	1451,20288	-1,22	$C_{64}H_{52}NaO_{38}^{+}$	6	8	**Purple**
1409,19509	1409,19231	-1,97	$C_{62}H_{50}NaO_{37}^{+}$	6	7	**Purple**
1367,18416	1367,18175	-1,76	$C_{60}H_{48}NaO_{36}^{+}$	6	6	**Purple**
1593,2106	1593,26587	34,69	$C_{71}H_{62}NaO_{41}^{+}$	5	15	**Blue**
1551,20158	1551,25531	34,64	$C_{69}H_{60}NaO_{40}^{+}$	5	14	**Blue**
1509,19016	1509,24474	36,16	$C_{67}H_{58}NaO_{39}^{+}$	5	13	**Blue**
1467,23776	1467,23418	-2,44	$C_{65}H_{56}NaO_{38}^{+}$	5	12	**Blue**
1425,22527	1425,22361	-1,16	$C_{63}H_{54}NaO_{37}^{+}$	5	11	**Blue**
1383,21467	1383,21305	-1,17	$C_{61}H_{52}NaO_{36}^{+}$	5	10	**Blue**
1341,20439	1341,20248	-1,42	$C_{59}H_{50}NaO_{35}^{+}$	5	9	**Blue**
1299,19471	1299,19192	-2,15	$C_{57}H_{48}NaO_{34}^{+}$	5	8	**Blue**
1257,18315	1257,18136	-1,42	$C_{55}H_{46}NaO_{33}^{+}$	5	7	**Blue**
1215,17266	1215,17079	-1,54	$C_{53}H_{44}NaO_{32}^{+}$	5	6	**Blue**
1173,16197	1173,16023	-1,48	$C_{51}H_{42}NaO_{31}^{+}$	5	5	**Blue**
1357,17807	1357,23378	41,05	$C_{60}H_{54}NaO_{35}^{+}$	4	13	**Red**
1315,16718	1315,22322	42,61	$C_{58}H_{52}NaO_{34}^{+}$	4	12	**Red**
1273,15628	1273,21266	44,28	$C_{56}H_{50}NaO_{33}^{+}$	4	11	**Red**
1231,20359	1231,20209	-1,22	$C_{54}H_{48}NaO_{32}^{+}$	4	10	**Red**
1189,1939	1189,19153	-1,99	$C_{52}H_{46}NaO_{32}^{+}$	4	9	**Red**

1147,18226	1147,18096	-1,13	$C_{50}H_{44}NaO_{31}^{+}$	4	8	**Red**
1105,17176	1105,17040	-1,23	$C_{48}H_{42}NaO_{30}^{+}$	4	7	**Red**
1063,16044	1063,15983	-0,57	$C_{46}H_{40}NaO_{29}^{+}$	4	6	**Red**
1021,15095	1021,14927	-1,65	$C_{44}H_{38}NaO_{28}^{+}$	4	5	**Red**

VII.5. TGA analyses

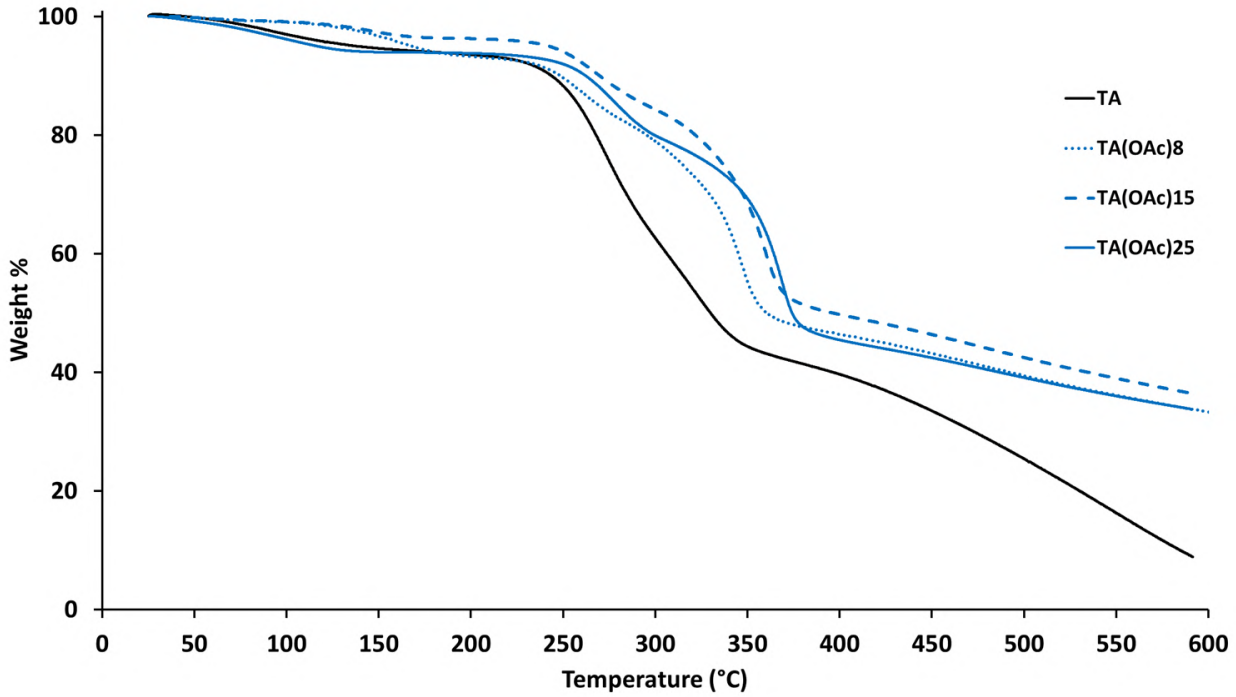

Figure II.41. TGA curves of acetylated tannic acid derivatives, 20°C/min ramp

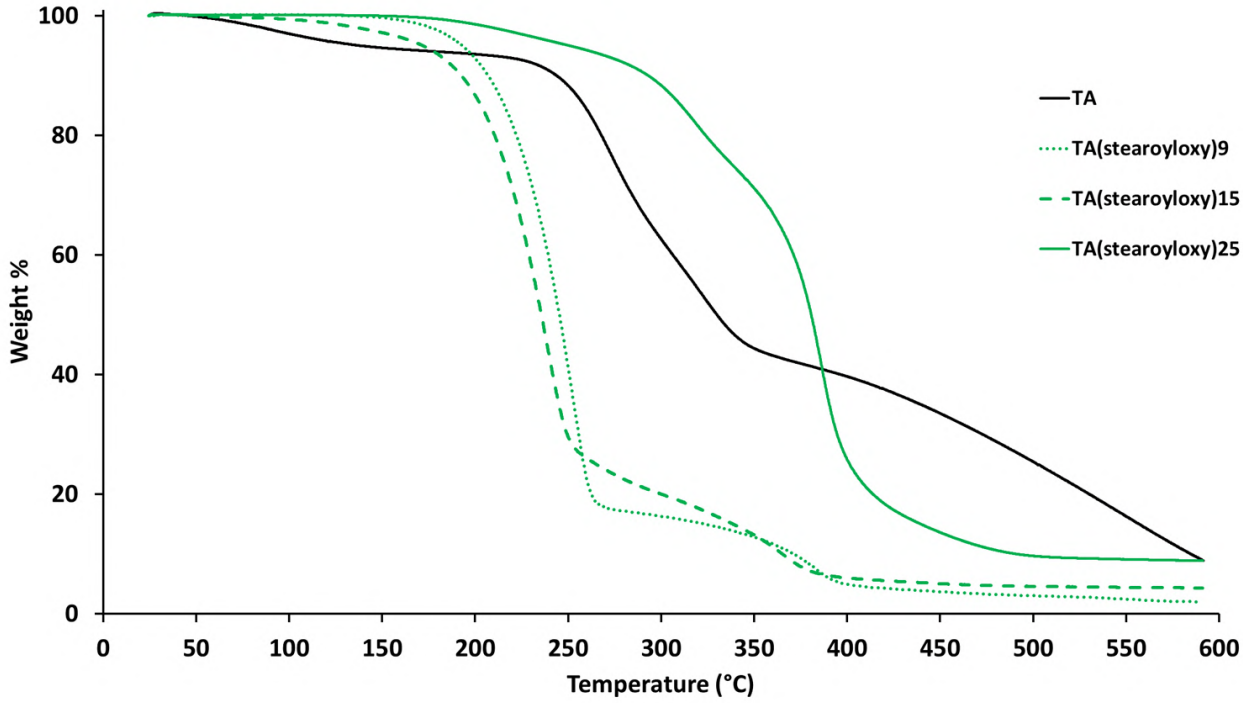

Figure II.42. TGA curves of esterified tannic acid derivatives, 20°C/min ramp

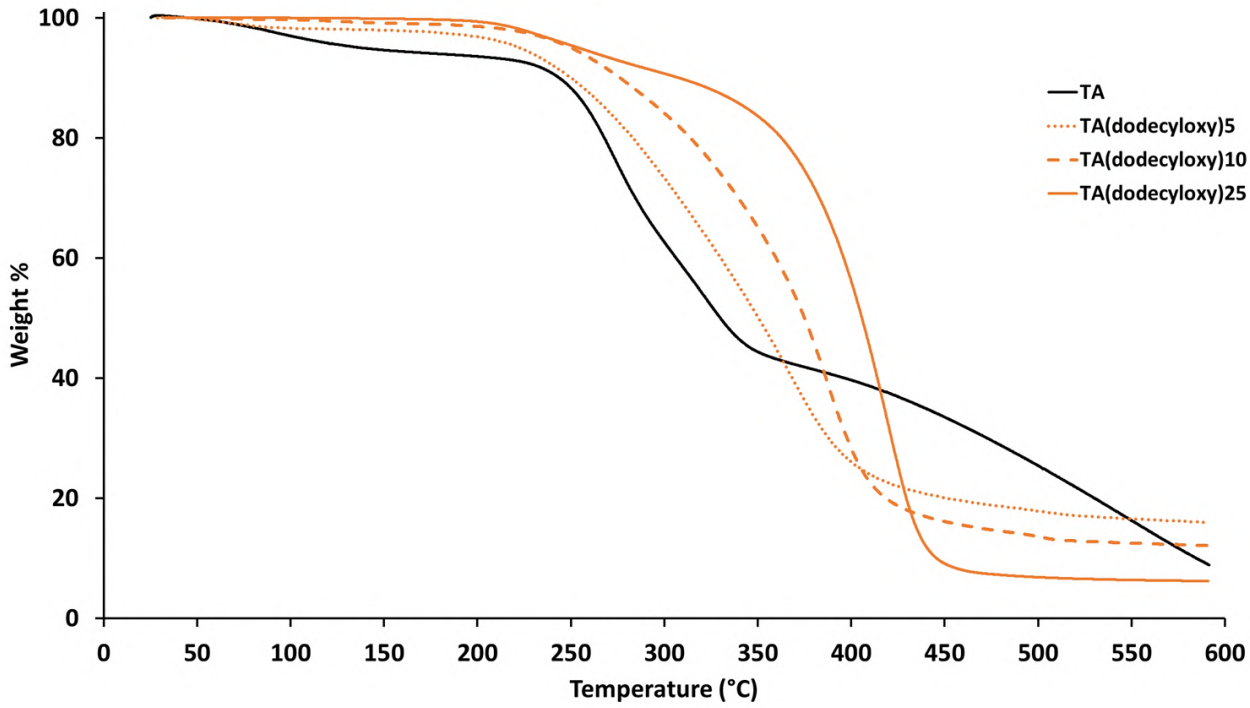

Figure II.43. TGA curves of dodecyloxy tannic acid derivatives, 20°C/min ramp

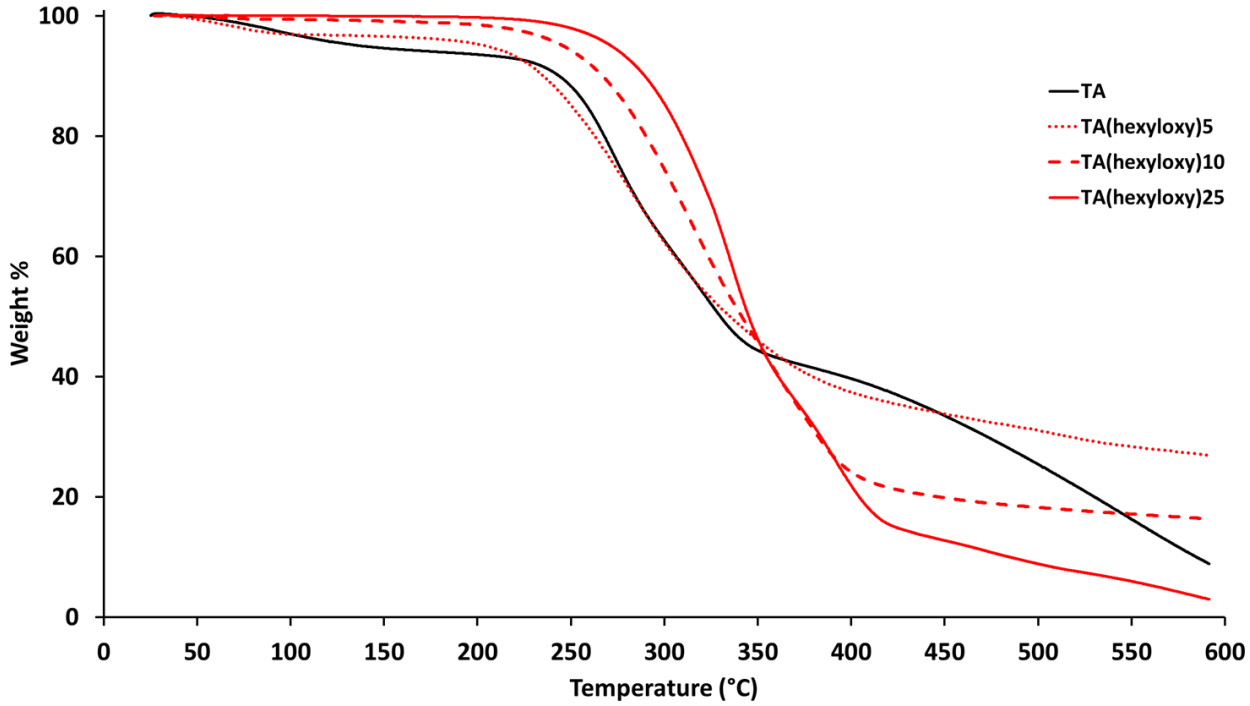

Figure II.44. TGA curves of hexyloxy tannic acid derivatives, 20°C/min ramp

Chapter III. Supramolecular gels based on furan-2,5-dicarboxylic acid

I. Introduction

With the increasing demand over the last decades to replace products from the petrochemical industry, the use of more sustainable processes as well as the production of new molecules from biomass has become one of the most important topics in chemical research worldwide. In 2004, the US Department of Energy (DOE) listed 12 molecules having the potential to replace petrochemical building blocks.[1] Amongst them, furan-2,5-dicarboxylic acid (FDCA) has been identified as a key bio-based platform because of its potential as a source of a wide variety of chemicals and materials.

For the past decade, the studies involving FDCA have mainly been concentrated on two topics: the improvement of its production [2] and its use in the synthesis of bio-based polymers [3–7], notably the replacement of terephthalic acid (TPA). FDCA is composed of a furan ring with two carboxylic acid groups, which can be chemically modified to form numerous materials. Furanic–aliphatic polyesters are one of the most studied furan polymer families [3], with poly(ethylene 2,5-furandicarboxylate) (PEF) being a possible substitute for poly(ethylene terephthalate) (PET).[8]

Some FDCA-based molecules such as 2,5-diamidofurans have also been exploited in the context of supramolecular chemistry for their ability to form hydrogen bonds.[9–11] In particular, Camiolo et al. have demonstrated the possibility to form extended chains of hydrogen bonds in the crystal state (**Figure III.1**).[9]

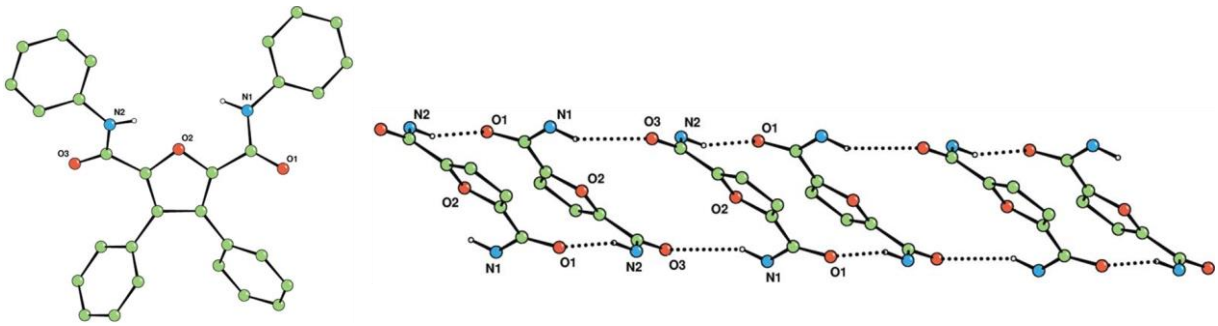

Figure III.1. Left) X-ray crystal structure of 3,4-diphenylfuran-2,5-dicarboxylic acid bis-*N*-phenylamide (acetonitrile and certain hydrogen atoms omitted for clarity); Right) Hydrogen bond chains formed along a-axis (certain atoms have been omitted for clarity). Reproduced with permission from Ref. [9]

Such linear chains of hydrogen bonds are particularly useful in the context of Low Molecular Weight Gelators (LMWGs). These gelators are small organic molecules that self-assemble into anisotropic structures, mostly fibers which entangle and form a network, thus turning a liquid into a gel.[12–16] The presence of such strong directional interaction is a desirable feature to design an organogelator because it favors the formation of highly anisotropic fibers.[17]

Only few bio-sourced organogelators are on the market, the best-known being (1,3:2,4) dibenzylidene sorbitol (DBS) and 12-hydroxystearic acid (12-HSA).[18,19] Therefore, in this study, we decided to investigate FDCA as platform to synthesize new bio-based organogelators. Their gelling properties were tested in a range of liquids with different polarities.

II. Results and discussion

II.1. Diamides and di(amido-esters)

First, a range of diamides molecules have been synthesized FDCA ester **1** and alkyl or aromatic amines. The method used in this section has been adapted from Ravasco et al.[20], and the resulting molecules are shown in **Figure III.2.**

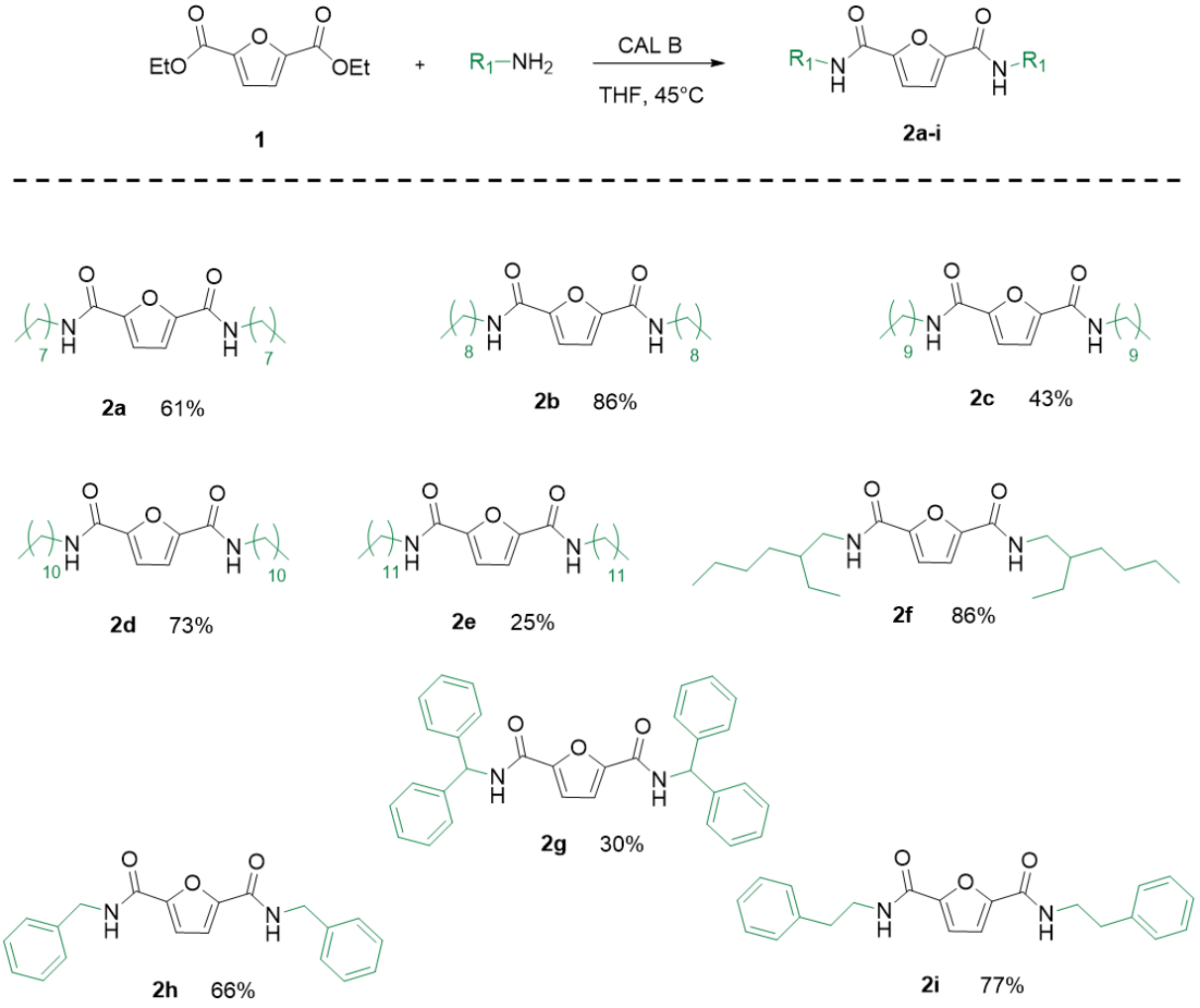

Figure III.2. Synthesis of alkyl and aromatic diamides

The yields obtained range from good to very good, except for **2e** and **2g**. The former was synthesized with a more dilute concentration which led to the synthesis of both the monoamide and the diamide. For the latter molecule, the low yield is probably due to steric hindrance.

Gelation tests were performed in a range of liquids with different polarities, even if the main goal was to gel apolar liquids such as vegetable oils or n-hexadecane.

Table III.1. Gelation tests of alkyl and aromatic diamides at 1wt% [a]

Compound	propylene carbonate	diacetone alcohol	benzyl acetate	1,4-dioxane	*m*-xylene	*R*(+)-limonene	rapeseed oil	n-hexadecane
2a	P	S	S	S	S	P	I	I
2b	I	S	P	S	P	P	I	I
2c	I	S	P	S	P	P	I	I
2d	I	P	P	S	P	P	I	I
2e	I	P	P	P	P	P	I	I
2f	S	S	S	S	S	S	S	I
2g	I	I	I	S	I	I	I	I
2h	S	S	S	S	I	I	I	I
2i	S	S	S	S	P	I	I	I

[a] P: precipitate; S: soluble; I: insoluble.

As displayed in **Table III.1**, no gel was obtained and most diamides remained insoluble or precipitated in apolar liquids. In order to increase the solubility of the molecules while retaining the amide functions for self-assembly, amines were replaced by esterified amino acids (**Figure III.3**).

The corresponding ammonium salt (chloride or tosylate salt) was reacted in a second step with furan-2,5-dicarbonyl dichloride (FDCDCl) to obtain a di(amido-ester) with the desired alkyl chain. Four amino acids have been selected: alanine (Ala), phenylalanine (Phe), leucine (Leu) and aspartic acid (Asp) to tune weak intermolecular interactions and solubility.

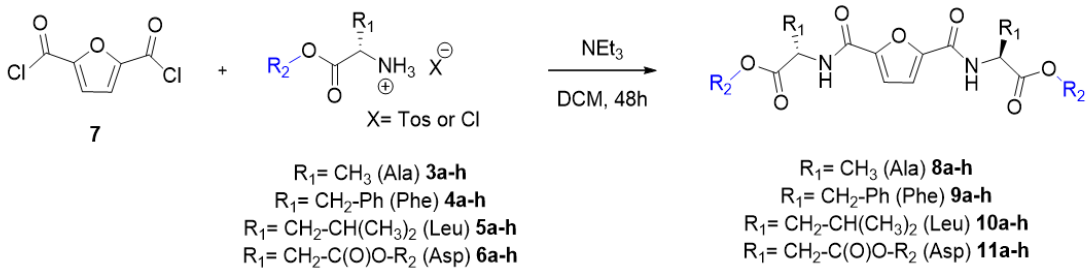

	(*S*)-Ala		(*S*)-Phe		(*S*)-Leu		(*S*)-Asp	
R_2	Entry	Yield	Entry	Yield	Entry	Yield	Entry	Yield
Ethyl (C2)	**8a**	84%	**9a**	62%	**10a**	85%	**11a**	82%
Hexyl (C6)	ns		**9b**	81%	ns		**11b**	86%
Octyl (C8)	**8c**	84%	**9c**	80%	**10c**	89%	ns	
Dodecyl (C12)	**8d**	75%	**9d**	77%	**10d**	88%	**11d**	75%
Tridecyl (C13)	**8e**	80%	**9e**	78%	**10e**	73%	**11e**	74%
Pentadecyl (C15)	**8f**	63%	**9f**	65%	**10f**	65%	ns	
Hexadecyl (C16)	**8g**	71%	**9g**	70%	**10g**	88%	**11g**	47%
Octadecyl (C18)	**8h**	88%	**9h**	90%	**10h**	77%	**11h**	64%

Figure III.3. Results of the reaction between FDCDCl and ester ammonium salts. ns: not synthesized

The yields are quite good going from 47% to 90%. All of the molecules have been characterized by ^{1}H and ^{13}C NMR (chemical shifts in the experimental section) and gelation tests have been carried out (**Table III.2)**.

The results show that the insertion of amino ester units indeed improve the solubility of the molecules in apolar liquids. Unfortunately, none of the synthesized molecules have formed a gel or even a viscous solution in any liquid. In almost all cases, solutions have been obtained which indicates that intermolecular interactions are not strong enough to trigger self-assembly and form a gel. In order to promote the assembly, the number of hydrogen bonding groups has been increased by replacing the ester functions by amide functions.

Table III.2. Gelation tests of di(amido-esters) at 1wt% [a]

Compound	propylene carbonate	diacetone alcohol	benzyl acetate	1,4-dioxane	*m*-xylene	*R*(+)-limonene	rapeseed oil	n-hexadecane
8a	S	S	S	S	S	S	I	I
8c	S	S	S	S	S	S	S	S
8d	S	S	S	S	S	S	S	S
8e	S	S	S	S	S	S	S	S
8f	P	S	S	S	S	S	S	S
8g	P	S	S	S	S	S	S	S
8h	P	S	S	S	S	S	S	P
9a	S	S	S	S	S	S	S	I
9b	S	S	S	S	S	S	S	P
9c	S	S	S	S	S	S	S	S
9d	S	S	S	S	S	S	S	S
9e	S	S	S	S	S	S	S	S
9f	S	S	S	S	S	S	S	S
9g	P	S	S	S	S	S	S	S
9h	P	S	S	S	S	S	S	S
10a	S	S	S	S	S	S	S	P
10c	S	S	S	S	S	S	S	S
10d	S	S	S	S	S	S	S	S
10e	S	S	S	S	S	S	S	S
10f	P	S	S	S	S	S	S	S
10g	P	S	S	S	S	S	S	S
10h	P	S	S	S	S	S	S	S
11a	S	S	S	S	S	S	S	I
11b	S	S	S	S	S	S	S	S
11d	P	S	S	S	S	S	S	S
11e	P	S	S	S	S	S	S	S
11g	P	P	S	S	S	S	P	P
11h	P	P	P	S	P	P	P	P

[a] P: precipitate; S: soluble; I: insoluble.

II.2. Di(amido-amides)

The synthesis of the di(amido-amides) involved a longer synthesis than for the di(amido-esters) because of the necessity for the protection and deprotection of the amine function of the amino acid. First step is the protection of the amine, followed by the reaction between an alkyl amine and the carboxylic acid of the protected amino acid. The third step is the deprotection of the boc-protected amino-amide. Finally, the last step is similar to that of the di(amido-esters), i.e., reacting FDCDCl with the synthesized amino-amide to obtain the di(amido-amides) (**Figure III.4**).

7

R_1= CH_3 (Ala) **12a-d**
R_1= CH_2-Ph (Phe) **13a-f**
R_1= CH_2-$CH(CH_3)_2$ (Leu) **14a-f**
R_1= CH_2-C(O)NH-R_2 (Asp) **15a-b**

R_1= CH_3 (Ala) **16a-d**
R_1= CH_2-Ph (Phe) **17a-f**
R_1= CH_2-$CH(CH_3)_2$ (Leu) **18a-f**
R_1= CH_2-C(O)NH-R_2 (Asp) **19a-b**

	(*S*)-Ala		(*S*)-Phe		(*S*)-Leu		(*S*)-Asp	
R_2	Entry	Yield	Entry	Yield	Entry	Yield	Entry	Yield
Hexyl (C6)	**16a**	80%	**17a**	37%	**18a**	52%	**19a**	27%
2-ethylhexyl (2-EH)	ns		**17b**	21%	**18b**	46%	**19b**	18%
Decyl (C10)	ns		ns		**18c**	36%	ns	
Dodecyl (C12)	**16d**	17%	**17d**	39%	**18d**	57%	ns	
Tetradecyl (C14)	ns		ns		**18e**	46%	ns	
Octadecyl (C18)	ns		**17f**	61%	**18f**	67%	ns	

Figure III.4. Results of the reaction between FDCDCl and amino-amides. ns: not synthesized

Yields at this stage have been highly variable. These results can be explained by the small quantities involved and the possible hydrolysis of FDCDCl during the reaction. For the aspartic acid-based molecules, the fact that hexaamides instead of tetraamides have been synthesized increased the difficulty to purify them.

The products have been characterized by NMR (^{1}H and ^{13}C) in order to ensure their purity, and to verify that epimers have not been formed. Then, gelation tests have been carried out (**Table III.3**).

Table III.3. Gelation tests of di(amido-amides) at 1wt% [a]

Compounds	propylene carbonate	diacetone alcohol	benzyl acetate	1,4-dioxane	*m*-xylene	*R*(+)-limonene	rapeseed oil	cyclohexane	n-hexadecane	methyl-cyclohexane	petroleum ether
16a	I	I	I	I	I	I	I	/	I	I	/
16d	I	I	I	I	I	I	I	/	I	I	/
17a	I	I	I	I	I	I	I	/	I	I	/
17b	I	I	I	I	I	I	I	/	I	I	/
17d	I	P	I	P	V	V	I	/	I	V	/
17f	I	S	V	S	S	S	I	G	I	V	I
18a	P	S	S	S	P	I	I	/	I	/	/
18b	P	S	S	S	P	S	I	/	I	/	/
18c	G	S	V	S	V	S	G	G	V	G	I
18d	V	S	G	S	V	S	G	G	G	G	G
18e	OG	P	G	P	V	S	V	P	G	P	I
18f	P	P	V	P	V	S	V	P	G	P	I
19a	OG	G	OG	G	S	S	I	I	I	I	I
19b	I	S	P	S	G	G	G	G	I	PG	I

[a] G: gel; OG: opaque gel; PG: partial gel; V: viscous; P: precipitate; S: soluble; I: insoluble; /: not tested.

In contrast to diamides and di(amido-esters), di(amido-amides) displayed an interesting gelling behavior. Indeed, some molecules based on phenylalanine, leucine or aspartic acid form gels or viscous solutions in apolar liquids. In general, the C6 alkyl chain is too short, which means that the molecules remain insoluble in apolar solvents.

Except for alanine, increasing the length of the chain improved the solubility of the compound when heated, which led to the formation of gels (2-EH for Asp, C10 for Leu and C18 for Phe). On the other hand, it can be seen that too great an increase in the length of the alkyl chain unbalances the polarity of the molecule and reduces its ability to self-assemble.

Besides the influence of the length of the alkyl chain which is a key factor in tuning the solubility of the molecules in organic solvents, the lateral chain of the amino acids also has to be taken into account.

When comparing the molecules with dodecyl chain, **16d** (alanine) does not show results indicating supramolecular assembly, **17d** (phenylalanine) increases the viscosity of some liquids and **18d** (leucine) displays promising gelling properties. The compound **18d** seems to be the most promising as it formed gels in all the apolar liquids of the list. It should also be noted that with the range of molecules synthesized, any liquid of the list can be gelled, which shows the versatility of this gelator family.

II.3. Specificity of the furan group in the gel formation

After understanding the effect of the amino acid and alkyl chain length, we investigated the impact of the furanic cycle on the supramolecular self-assembly. Therefore, three analogues of compound **18d** have been synthesized by varying the core of the molecule (**Figure III.5**). Terephthalic and isophthalic acids were selected as the closest possible analogues to reveal if any particular behavior can be attributed to the furanic cycle. Furoic acid was chosen as the final analogue to determine whether disubstitution of the furanic cycle is necessary to obtain gelation.

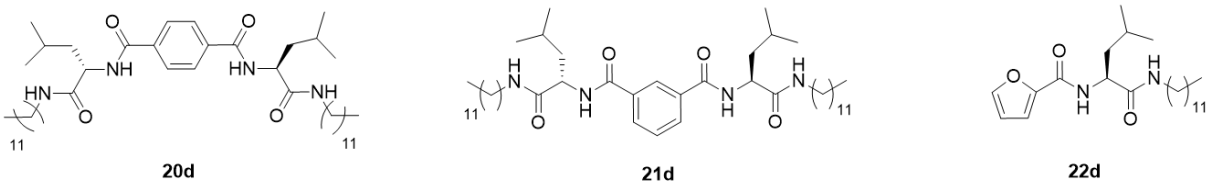

Figure III.5. Synthesized analogues of di(amido-amide) **18d**

The synthesis as well as the gelation tests were carried out according to the same procedures as for the di(amido-amides). On **Table III.4**, the results of the gelation tests of the analogues have been compared.

Table III.4. Gelation properties of di(amido-amide) **18d** and synthesized analogues at 1wt% [a]

Compounds	propylene carbonate	diacetone alcohol	benzyl acetate	1,4-dioxane	*m*-xylene	*R*(+)-limonene	rapeseed oil	cyclohexane	n-hexadecane	methyl-cyclohexane	petroleum ether
20d	I	G	S	P	S	S	I	I	I	I	I
21d	I	S	S	S	S	S	I	V	I	S	V
22d	S	S	S	S	S	S	S	S	S	S	S
18d	V	S	G	S	V	S	G	G	G	G	G

[a] G: gel; V: viscous; P: precipitate; S: soluble; I: insoluble.

First of all, the compound **22d** did not display any gelling properties. This could be explained by the number of hydrogen bond donor/acceptor groups which is twice less important than for gelator **18d**.

In apolar solvents, compound **20d** based on terephthalic acid remained mostly insoluble probably because its straight conformation stabilizes too much the crystal state. With compound **21d** based on isophthalic acid, the solubility is improved, possibly due to its bent chemical structure. For example, poly(butylene isophthalate) (PBI) is known to exhibits less stable crystals than poly(butylene terephthalate).[21]

However, in contrast to furan-based **18d**, this improved solubility results only in the formation of a few viscous solutions, but no gels. Therefore, among these analogues, the furanic core brings the best balance between solubility and supramolecular interactions.

II.4. Supramolecular assembly characterization

Among the range of gelators described above, **18d** was selected to probe the gel properties and the self-assembly mechanism by complementary techniques and over a large range of concentrations, going from the gel state to the monomeric state.

II.4.1. Rheology

The strength of the gels has been quantified by rheology, at different concentrations (0.8 to 2wt%) in a vegetable oil (rapeseed oil). The storage (G') and loss (G") moduli in the linear domain at each concentration are shown on **Figure III.6**.

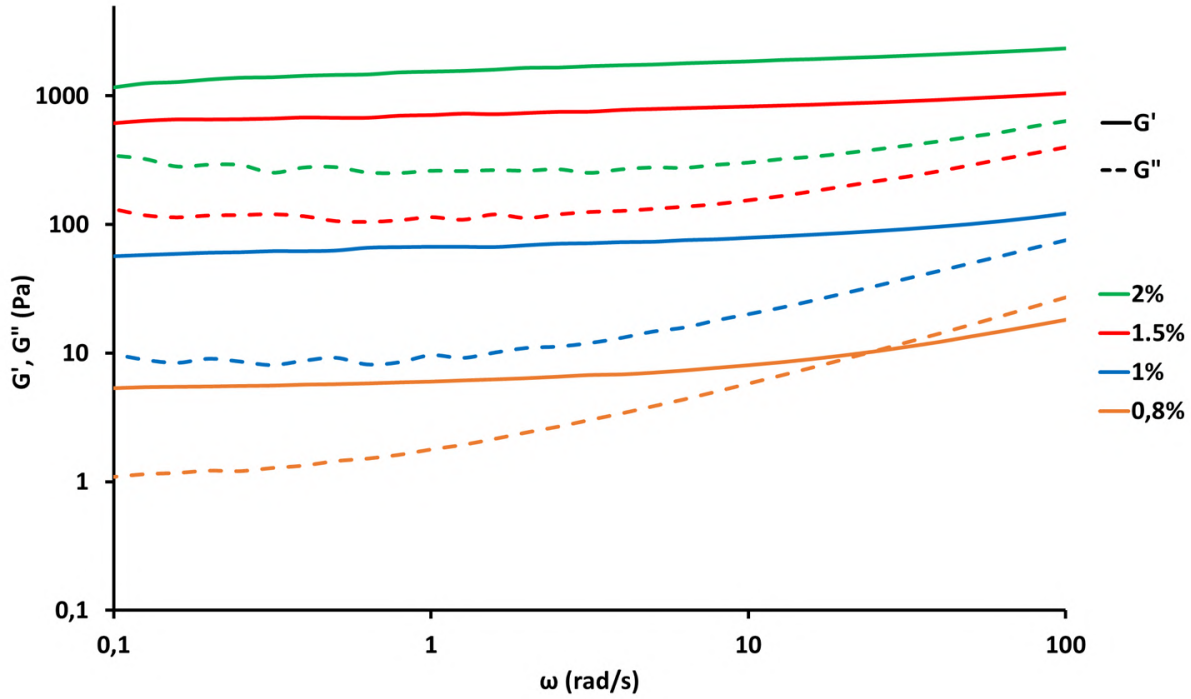

Figure III.6. Storage (G′) and loss (G″) moduli as a function of oscillation frequency (ω) for solutions of gelator **18d** in rapeseed oil at different mass percentages (γ = 0.08%, 25°C)

At concentrations above 1wt% an elastic behavior is observed with G' > G" over the whole frequency range, while at 0.8wt%, a viscoelastic solution is obtained (G" > G' at high frequency). The critical gel concentration is therefore close to 1wt%. As expected, both moduli increase with the concentration of the solutions.

Then, a total oscillating strain sweep has been performed (**Figure III.7**) in order to evaluate the yield stress which increases from 1.2 Pa at 1wt% to 4.5 Pa at 2wt% (**Figure III.51-53**).

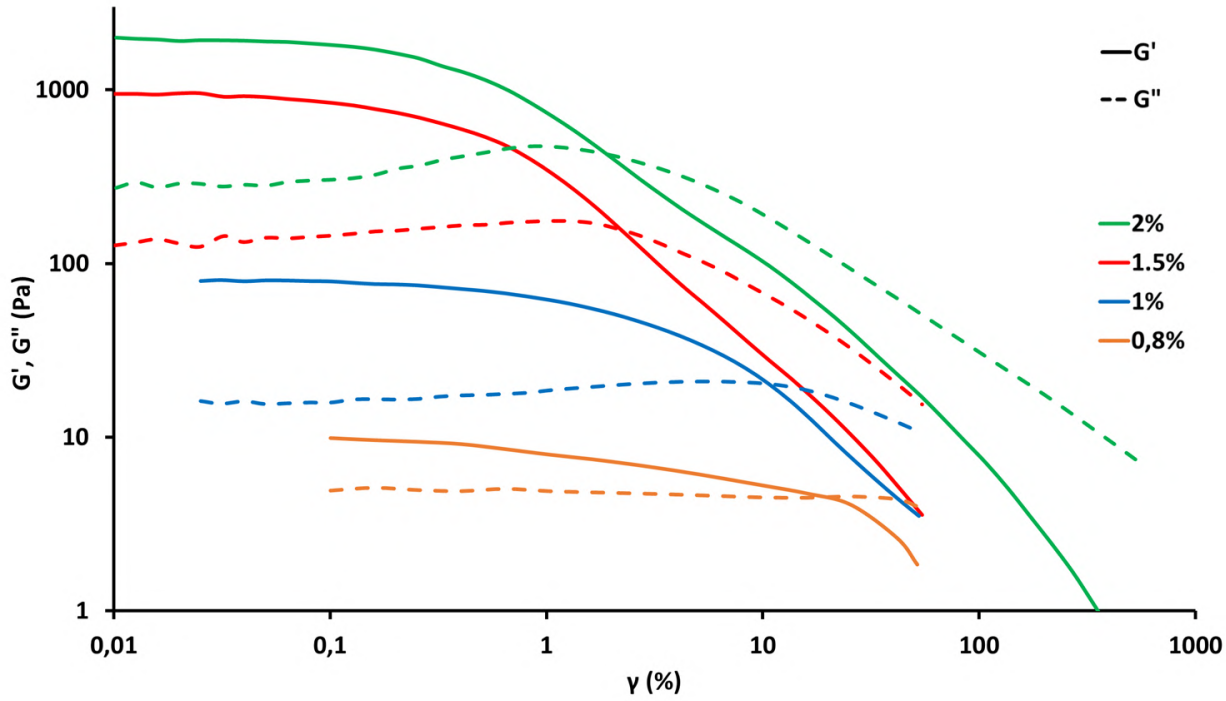

Figure III.7. Evolution of the storage (G′) and loss (G″) moduli as a function of strain (γ) (ω = 1Hz)

II.4.2. FTIR spectroscopy

Then, the involvement of hydrogen bonding in the supramolecular assembly has been characterized by FTIR spectroscopy. For this study, methylcyclohexane has been used as liquid because of its suitable transparency.

First, a gel of **18d** at 1wt% (14.8mM) in methylcyclohexane has been studied. The spectrum in the NH stretching region is displayed in **Figure III.8** (see **Figure III.42** for C=O region). Two bands are observed in the NH stretching region: they correspond to the NH from the amide closest to the furan ring (3370 cm^{-1}) and to the NH from the aliphatic amide (3250 cm^{-1}) (see **Figure III.45** for the assignment). Interestingly, both NH groups are hydrogen bonded but the larger shift of the latter indicates a much stronger hydrogen bond.

Increasing the temperature reveals a broadening of the hydrogen bonded NH bands and the appearance at 90°C of a very small band at 3450 cm^{-1} which corresponds to free NH groups.

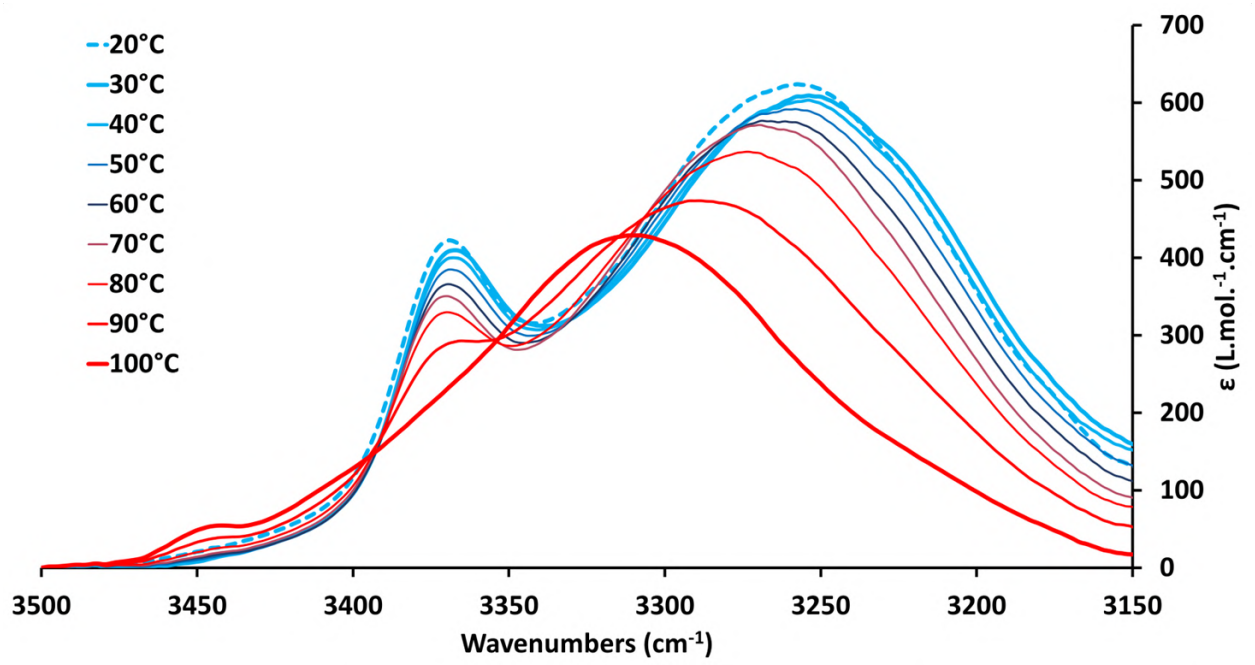

Figure III.8. VT-FTIR spectra of gelator **18d** in methylcyclohexane; 1wt% (14.8mM), heating process, 1°C/min ramp; NH bands.

Therefore, at 100°C, although the solution is fluid, most molecules are still hydrogen bonded, but the broadness of the band indicates that these hydrogen bonds are poorly ordered.

It can be seen that the intensity of the peak at 3250 cm^{-1} decreases significantly above 70°C (**Figure III.43**). This change corresponds to a reorganization in the assembly, from ordered to disordered hydrogen bonds.

The influence of concentration is shown on **Figure III.9**. The same evolution is observed when the concentration is decreased as when the temperature is increased: even at 1mM (i.e. much lower than the gelation concentration) no free NH band is observed but a broad hydrogen bonded NH band is present. Therefore, the gelator is not in the monomeric state at this concentration but is hydrogen bonded into ill-defined aggregates.

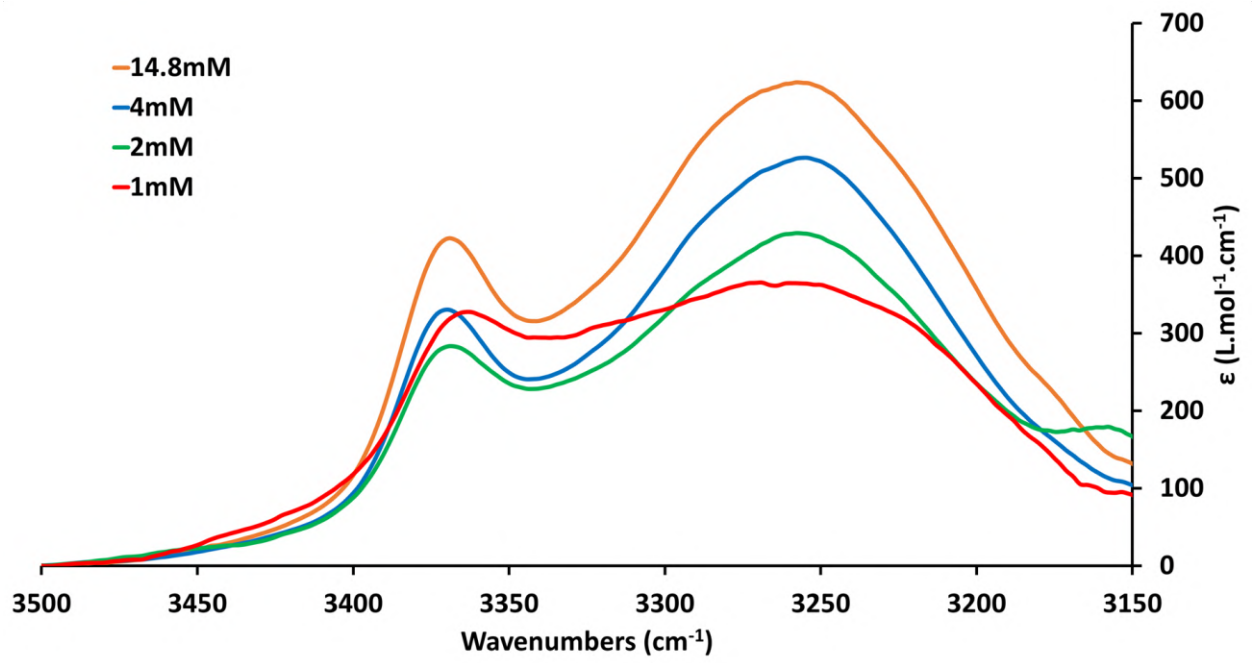

Figure III.9. FTIR spectra of gelator **18d** solutions at 20°C in methylcyclohexane at various concentrations: 14.8mM (orange line), 4mM (blue line), 2mM (red line) and 1mM (green line)

II.4.3. Circular dichroism spectroscopy

It was not possible to measure FTIR spectra at concentrations below 1mM, therefore CD spectroscopy was used to extend the concentration range (**Figure III.10).**

At 1mM in methylcyclohexane and at 20°C, an intense signature was observed which decreases when the temperature increases. This signal therefore corresponds to the supramolecular chirality of the assembly. This indicates that the molecules are still self-assembled and not in a monomeric state at 1mM and 20°C, in agreement with the FTIR spectroscopy results.

Then, the supramolecular assembly has been investigated at lower concentration. A strong decrease in intensity is observed at 0.5mM (**Figure III.10**).

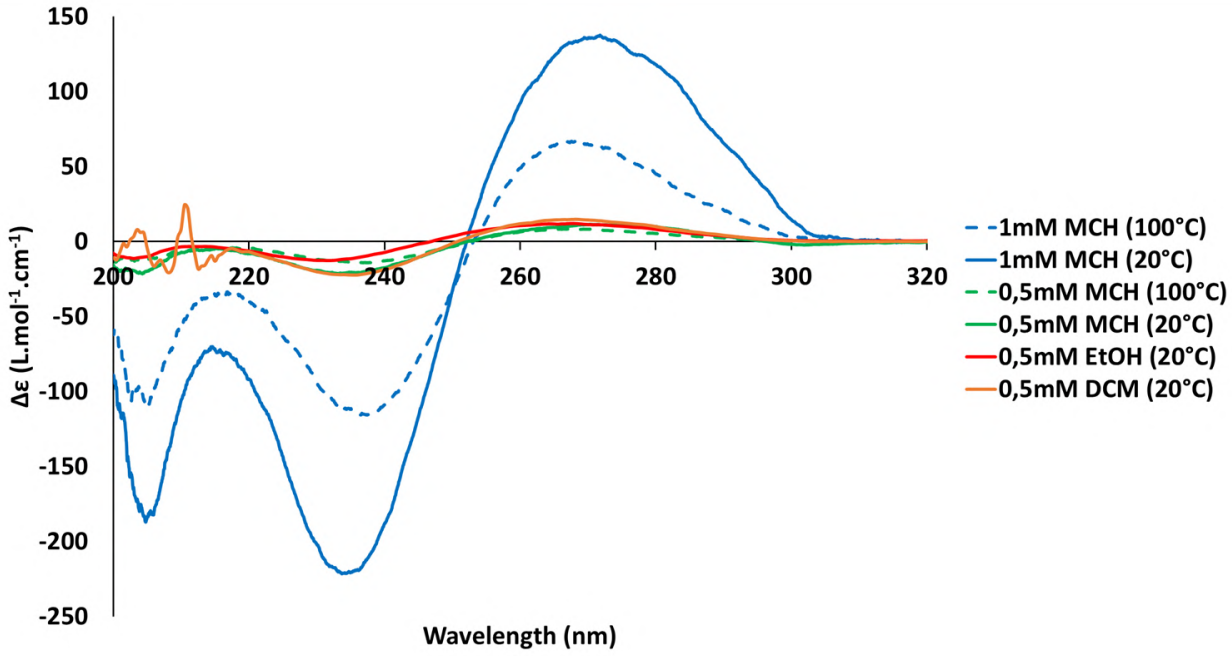

Figure III.10. CD spectra of gelator **18d** solutions at 0.5mM in methylcyclohexane, ethanol and dichloromethane and 1mM in methylcyclohexane; the spectra at 20°C are in bold lines and the spectra at 100°C are in dotted lines

Moreover, at 0.5mM, the CD spectrum is not affected significantly by heating to 100°C or by the nature of the solvent (dichloromethane and ethanol are good solvents for **18d**). This proves that **18d** is no longer self-assembled but in the monomeric state at 0.5mM in methylcyclohexane.

II.4.4. Viscometry

In order to corroborate the spectroscopy data, the temperature evolution of the relative viscosity of **18d** solutions in methylcyclohexane has been measured (**Figure III.11**).

At 0.5mM the solution is not more viscous than the solvent. At 1mM, the relative viscosity is slightly higher than at 0.5mM and it increases further at higher concentrations. These results are in perfect agreement with the spectroscopy data: at 20°C, self-assembly starts at a concentration between 0.5 and 1mM. Moreover, the viscosity of the solutions decreases at high temperatures indicating the breakdown of the assemblies.

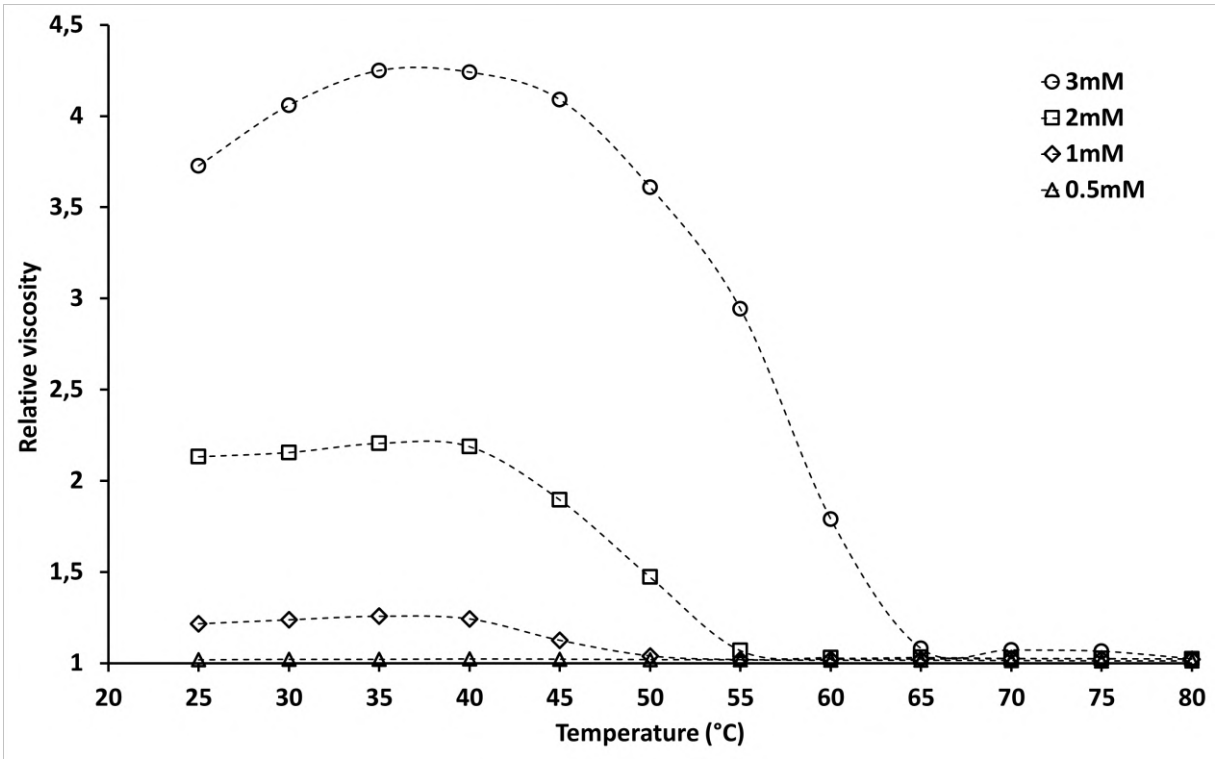

Figure III.11. Relative viscosity of gelator **18d** solutions at different concentrations in methylcyclohexane depending on the temperature, 3mM (○), 2mM (□), 1mM (◊) and 0.5mM (Δ).

II.4.5. Wide Angle X-Ray Scattering (WAXS)

In order to determine the characteristic intermolecular distances of the assembly, WAXS has been carried out. In order to perform this analysis, a gel was first formed and then the solvent was removed by filtration to obtain the dry fibers, which were then analyzed. The results are displayed on **Figure III.12**.

The peaks 1, 2 and 3 are associated with distances in the plane: **1**: 16.33 Å; **2**: 9.38 Å; **3**: 4.69 Å, with the intense peak 3 being a second harmonic of peak 2. Therefore, in the plane, the X-ray pattern showed two independent distances: 16.33 Å and 9.38 Å.

In the perpendicular plane to the source, two peaks have been observed: **4**: 16.98 Å; **5**: 8.47 Å. Peak 5 is therefore a second harmonic of peak 4, so there is only one independent distance: 16.98 Å.

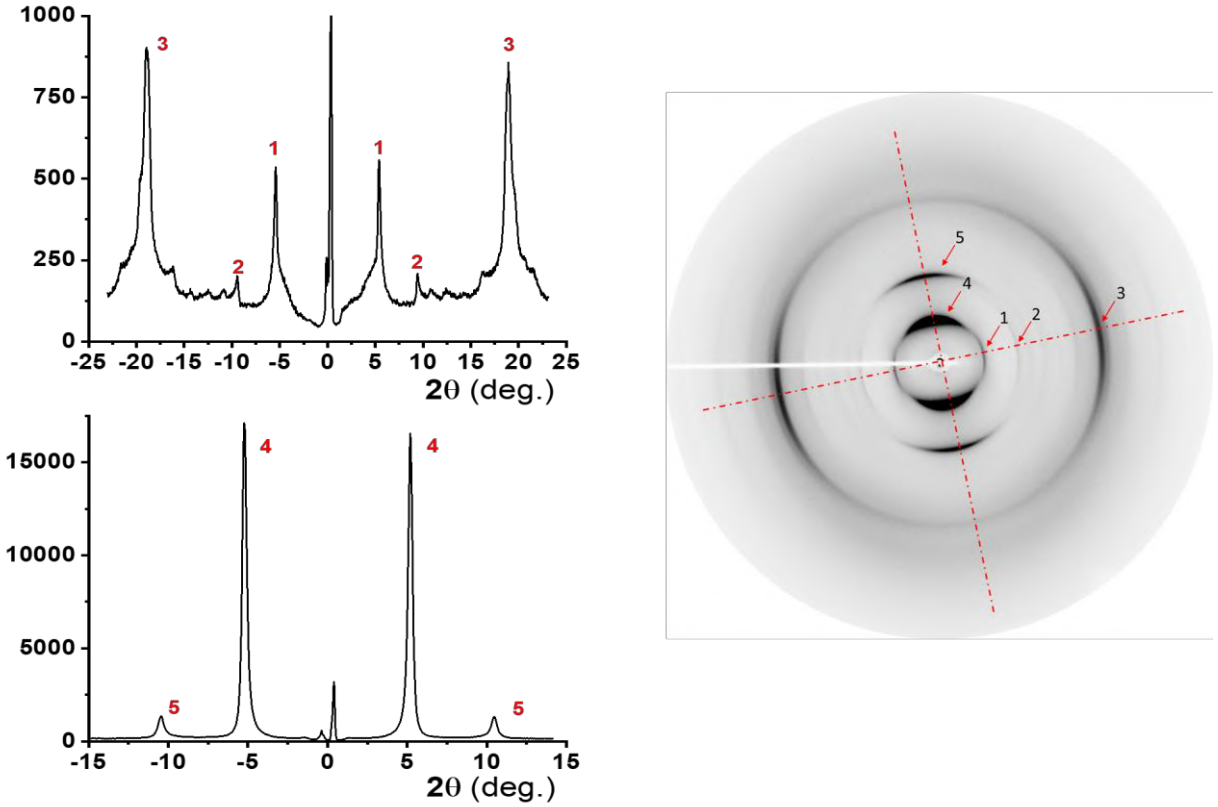

Figure III.12. Left) WAXS diffraction patterns of gelator **18d** dry fibers; Right) 2D-WAXS pattern

Nevertheless, without a crystallographic model, it is not possible to determine what these intermolecular distances correspond to.

Generally speaking, it is the "densest" family of reticular planes that will be perpendicular to the substrate. Reflection 4 is indeed very intense, which confirms that it is associated with X-ray reflection from planes of high electron density, i.e., planes that contain many molecules per unit area.

III. Conclusion

In this study, we used furan-2,5-dicarboxylic acid (FDCA) as bio-sourced platform to synthesize new organogelators. In order to provide hydrogen bond donor/acceptor functions, amide functions were chosen. Numerous molecules have been synthesized, and we discovered that molecules with amino acids functionalized with alkyl chains provide a good balance of solubility and self-association resulting in interesting gelling properties.

The assembly of the supramolecular gels has been characterized. Through the various characterization techniques, we determined that microscale assembly starts at a concentration of 1mM in methylcyclohexane. On a macroscopic scale, rheology shows a supramolecular gel behavior from 14.8mM i.e., 1wt% in rapeseed oil.

In conclusion, we have developed the first bio-sourced organogelators based on FDCA. These could be a green alternative to gelators derived from petrochemicals to increase the viscosity of polar or apolar media such as essential oils or mineral oils and perhaps use them in fields such as cosmetics, pharmaceutics or food industry.

IV. Additional results

In the diamide section, the unexpected formation of monoamides was observed due to the low concentration of the reaction medium. The synthesis of monoamides with longer alkyl chains than for diamides was performed by adapting the method from Ravasco et al.[20], and the resulting molecules are shown in **Figure III.13**.

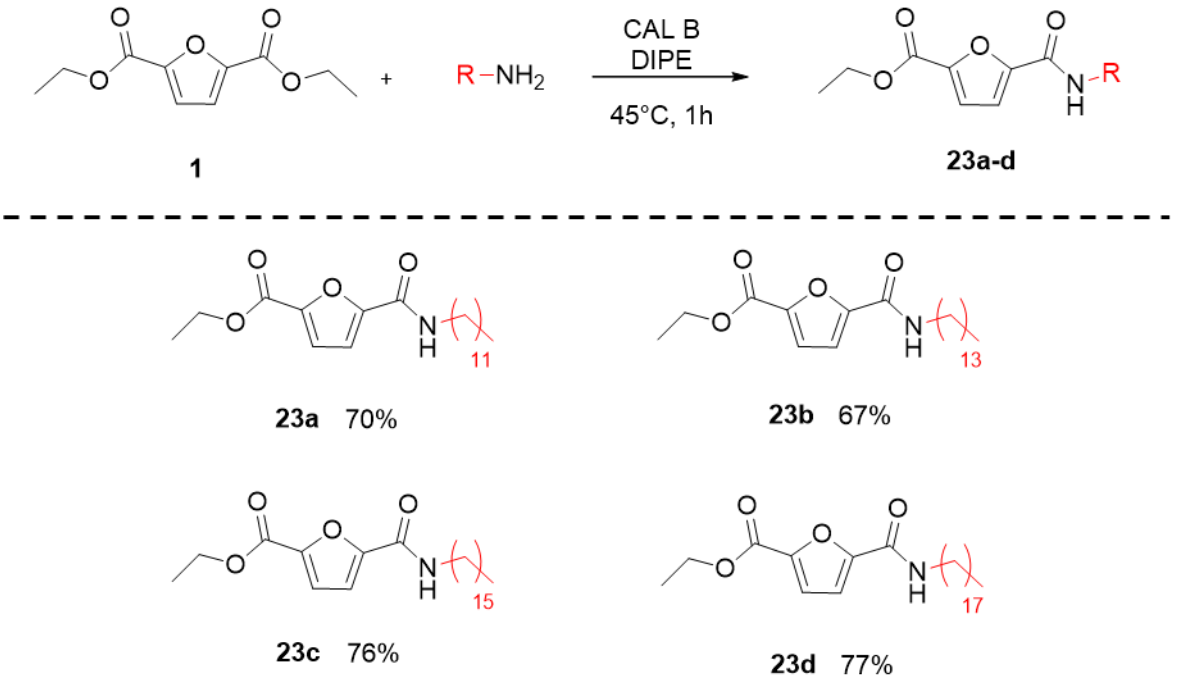

Figure III.13. Synthesis of alkyl monoamides

The yields obtained were very good, around 70-80%. This implies that under these conditions, the main product is the monoamide.

The yields obtained were very good, around 70-80%. This implies that under these conditions, the main product is the monoamide.

As for the other molecules, gelation tests were performed in the same range of liquids. The results are displayed on **Table III.5**.

Table III.5. Gelation tests of alkyl monoamides at 1wt% [a]

Compound	propylene carbonate	diacetone alcohol	benzyl acetate	1,4-dioxane	*m*-xylene	*R*(+)-limonene	rapeseed oil	n-hexadecane
23a	S	S	S	S	S	S	S	S
23b	S	S	S	S	S	S	S	P
23c	P	S	S	S	S	S	S	P
23d	P	S	S	S	S	S	P	P

[a] P: precipitate; S: soluble.

As displayed, no gel was obtained. Furthermore, the monoamides were soluble or precipitated in every liquid. In comparison with the diamides, the solubility of the monoamides is much higher. The compounds **2a** and **23a** with the dodecyl chain showed very different solubilities. This may be due to the non-symmetry of the molecule and the ethyl ester function.

V. References

[1] T. Werpy, G. Petersen, *Top Value-Added Chemicals from Biomass: Volume I -- Results of Screening for Potential Candidates from Sugars and Synthesis Gas*, **2004**.

[2] M. G. Davidson, S. Elgie, S. Parsons, T. J. Young, *Green Chem.* **2021**, 23, 3154–3171.

[3] A. F. Sousa, C. Vilela, A. C. Fonseca, M. Matos, C. S. R. Freire, G.-J. M. Gruter, J. F. J. Coelho, A. J. D. Silvestre, *Polym. Chem.* **2015**, 6, 5961–5983.

[4] M. Gomes, A. Gandini, A. J. D. Silvestre, B. Reis, *Journal of Polymer Science Part A: Polymer Chemistry* **2011**, 49, 3759–3768.

[5] M. Jiang, Q. Liu, Q. Zhang, C. Ye, G. Zhou, *Journal of Polymer Science Part A: Polymer Chemistry* **2012**, 50, 1026–1036.

[6] S. Thiyagarajan, W. Vogelzang, R. J. I. Knoop, A. E. Frissen, J. van Haveren, D. S. van Es, *Green Chem.* **2014**, 16, 1957–1966.

[7] V. Tsanaktsis, G. Z. Papageorgiou, D. N. Bikiaris, *Journal of Polymer Science Part A: Polymer Chemistry* **2015**, 53, 2617–2632.

[8] A. Gandini, A. J. D. Silvestre, C. P. Neto, A. F. Sousa, M. Gomes, *Journal of Polymer Science Part A: Polymer Chemistry* **2009**, 47, 295–298.

[9] S. Camiolo, P. A. Gale, M. B. Hursthouse, M. E. Light, C. N. Warriner, *Tetrahedron Letters* **2003**, 44, 1367–1369.

[10] T.-G. Qu, X.-M. Hao, H. Wang, X.-G. Cui, F. Chen, Y.-B. Wu, D. Yang, M. Zhang, W.-L. Guo, *Polyhedron* **2018**, 156, 208–217.

[11] S. Ottens-Hildebrandt, M. Nieger, K. Rissanen, J. Rouvinen, S. Meier, G. Harder, F. Vögtle, *J. Chem. Soc., Chem. Commun.* **1995**, 777–778.

[12] P. Terech, R. G. Weiss, *Chem. Rev.* **1997**, 97, 3133–3160.

[13] L. A. Estroff, A. D. Hamilton, *Chem. Rev.* **2004**, 104, 1201–1218.

[14] N. M. Sangeetha, U. Maitra, *Chem. Soc. Rev.* **2005**, 34, 821–836.

[15] R. G. Weiss, *J. Am. Chem. Soc.* **2014**, 136, 7519–7530.

[16] X. Du, J. Zhou, J. Shi, B. Xu, *Chem. Rev.* **2015**, 115, 13165–13307.

[17] J. H. van Esch, B. L. Feringa, *Angewandte Chemie International Edition* **2000**, 39, 2263–2266.

[18] B. O. Okesola, V. M. P. Vieira, D. J. Cornwell, N. K. Whitelaw, D. K. Smith, *Soft Matter* **2015**, 11, 4768–4787.

[19] A.-L. Fameau, M. A. Rogers, *Current Opinion in Colloid & Interface Science* **2020**, 45, 68–82.

[20] J. M. J. M. Ravasco, C. M. Monteiro, F. Siopa, A. F. Trindade, J. Oble, G. Poli, S. P. Simeonov, C. A. M. Afonso, *ChemSusChem* **2019**, 12, 4629–4635.

[21] S. Quattrosoldi, N. Lotti, M. Soccio, C. Schick, R. Androsch, *Polymers* **2020**, 12, 1099.

VI. Experimental part

VI.1. Materials and methods

VI.1.1. Reagents

All chemicals, reagents and solvents were of analytical grade, purchased from Sigma-Aldrich, Fluorochem, Alfa Aesar, Acros Organics and unless stated otherwise used without further purification. Deionized water was used for preparing aqueous solutions.

VI.1.2. Characterization

VI.1.2.1. ^{1}H and ^{13}C NMR

Proton nuclear magnetic resonance (^{1}H NMR) and carbon nuclear magnetic resonance (^{13}C NMR) analyses were performed in the same conditions as described in **Chapter II**.

VI.1.2.2. FTIR spectroscopy

Fourier-Transform Infrared (FTIR) measurements of solutions were performed on a Nicolet iS10 spectrometer. Spectra were measured in a CaF_2 cell of various pathlength (0.5, 1 or 2 mm according to the concentration) and were corrected for air, solvent and cell absorption.

The Attenuated Total Reflectance (ATR) FTIR spectra were recorded in the same conditions as described in **Chapter II**.

VI.1.2.3. Gelation tests

Gelation tests were carried out in the same conditions as described in **Chapter II**.

VI.1.2.4. Circular Dichroism spectroscopy (CD)

Circular dichroism (CD) measurements were performed on a Jasco J-1500 spectrometer equipped with a Peltier thermostated cell holder and Xe laser. Data were recorded with the following parameters: 50 $nm.min^{-1}$ sweep rate, 0.05 nm data pitch, 2 nm bandwidth, and between 400 and 200 nm. Spectra were corrected for air, solvent, and cell contribution at the

same temperature. Molar CD values are reported in $L.mol^{-1}.cm^{-1}$ and expressed as follows: $\Delta\varepsilon = \theta/(32980 \times l \times c)$ where θ is the measured ellipticity in mdeg, l is the optical pathlength in cm, and c is the concentration in $mol.L^{-1}$.

VI.1.2.5. Viscometry

An automated micro viscosimeter AMVn Anton Paar equipped with a capillary tube of diameter 1.6mm with a 1.5mm diameter steel ball was used for viscometry measurements. The falling time of the ball inside the capillary tube filled with the studied solution, for a given angle of inclination of the tube, was measured. The ratio between the falling time of the ball in the solution versus falling time of the ball in solvent (i.e., relative viscosity) was plotted versus temperature. Every sample was measured at an angle of 50° and at different temperatures (every 5°C between 25 and 80°C).

VI.1.2.6. Rheology

Preparation of the sample: In order to erase its thermo-mechanical history, the solution was stirred on a heating plate at 110°C for 15 minutes to make it fluid. Then the solution was poured on the rheometer plate at 25°C. The sample was then kept at 25°C for 2 hours to allow the gel to stabilize before performing the measurements.

The rheological measurements were carried out at 25°C. Viscoelastic moduli G' and G'' and yield stress were measured on a stress-controlled rheometer TA Instruments DHR 3 equipped with a sanded stainless-steel cone-plane geometry (diameter: 40 mm, gap: 54 μm, α: 2°). First, an oscillating strain sweep was performed at 1 Hz to determine the viscoelastic linear plateau. The measurement was stopped before reaching the maximum strain corresponding to end of the linear regime, in order to preserve the sample. Then, a frequency sweep was performed covering a pulsation (ω) range from 0.1 to 100 rad/s in the linear viscoelastic regime, the set strain value depended on the concentration of the sample. Finally, the sample was subjected to a total oscillating strain sweep over the linear and non-linear domain until 1000% strain to evaluate the yield stress. Measurements were repeated on several samples to check the reproducibility.

VI.1.2.7. Wide Angle X-Ray Scattering (WAXS)

Gel samples were dried under vacuum in order to obtain dry fibers. The two-dimensional wide-angle X-ray scattering (WAXS) patterns were collected on a MAR345 detector using Cu-K α radiation (wavelength: 1.542 Å) of a rotating anode X-ray source (40 kV, 40 mA; multilayer graded monochromator). Exposure time was 1200s.

VI.1.2.8. High Resolution Mass Spectrometry (HRMS)

Exact mass measurements (HRMS) were obtained on TQ R30-10 HRMS spectrometer by ESI^+ ionization and are reported in *m/z* for the major signal.

VI.1.2.9. Differential Scanning Calorimetry (DSC)

The analyses were carried out using a Q2000 instrument (TA Instruments). The products (about 5-10 mg) were introduced in sealed aluminum capsules. Two heating and cooling cycles were performed at a rate of 10°C.min^{-1}. The first heating from -50°C to 220-250°C and the first cooling from 250-220°C to -50°C were performed to remove the thermal history of the material. An isotherm of 2 min was maintained at the end of each heating and cooling step. The crystallization and melting temperatures were measured during the second cycle.

VI.1.2.10. Thermogravimetric analysis (TGA)

TGA spectra were recorded in the same conditions as described in **Chapter II**.

VI.2. Synthetic methods

VI.2.1. Synthesis of ester ammonium tosylate salts (Method A)

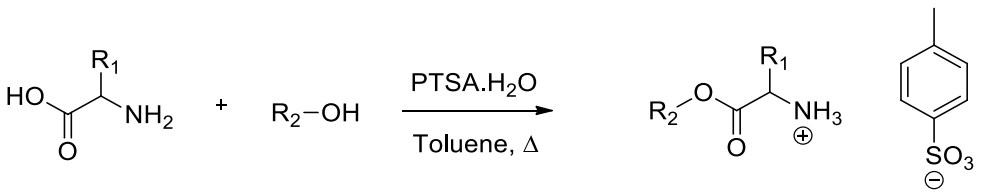

This synthesis was reproduced from: A. Desmarchelier, M. Raynal, P. Brocorens, N. Vanthuyne, L. Bouteiller, *Chem. Commun.* **2015**, *51*, 7397–7400.

In a Dean-Stark apparatus-mounted flask, 1 eq of amino acid, 1.1 eq of alcohol and 1.1 eq of PTSA.H_2O were added to toluene (0.1M) and the mixture was stirred under reflux overnight. The mixture was then concentrated under reduced pressure and diluted in Et_2O. The solution was gently heated to 35°C, and let cool in an ice bath to precipitate for a couple of hours. Then, the precipitate was filtered, washed with cold Et_2O and dried under vacuum.

VI.2.2. Synthesis of ester ammonium chloride salts (Method B)

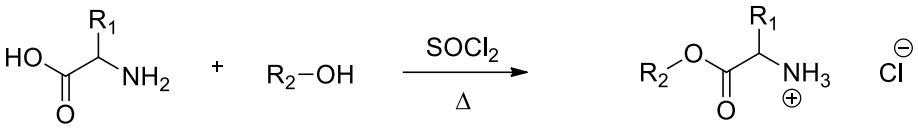

This synthesis was reproduced from: O. I. Shmatova, N. E. Shevchenko, E. S. Balenkova, G.-V. Röschenthaler, V. G. Nenajdenko, *Mendeleev Communications* **2013**, *23*, 92–93.

To a solution of amino acid (1 eq) in corresponding alcohol (20 mL), 1.2 eq of thionyl chloride was added under stirring. The reaction was put under argon atmosphere and refluxed overnight. The solvent was removed under reduced pressure and the white solid was dried under vacuum.

VI.2.3. Synthesis of ester ammonium chloride salts (Method C)

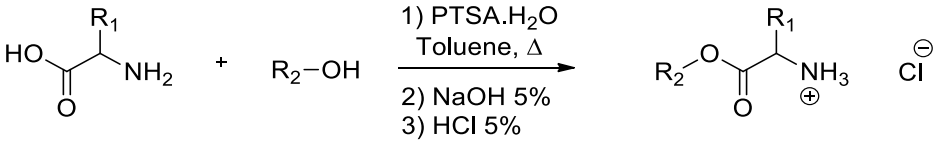

This synthesis was adapted from: J. L. Nichol, N. L. Morozowich, H. R. Allcock, *Polym. Chem.* **2013**, *4*, 600–606.

In a Dean-Stark apparatus-mounted flask, 1 eq of amino acid, 1.1 eq of alcohol and 1.1 eq of PTSA.H_2O were added to toluene (0.1M) and the mixture was stirred under reflux overnight. The solvent was evaporated under vacuum, the crude solid was redissolved in DCM and washed with NaOH 5% (3x30 mL) and HCl 5% (30 mL). The organic phase was evaporated under reduce pressure and the crude product was purified by sublimation to obtain white crystals.

VI.2.4. Synthesis of diamides (Method D)

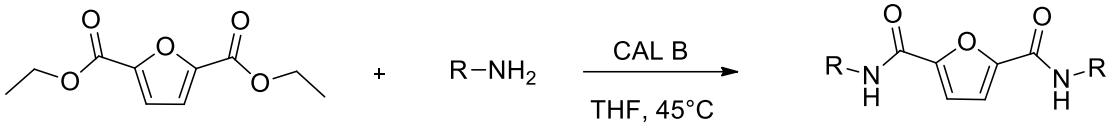

This synthesis was adapted from: J. M. J. M. Ravasco, C. M. Monteiro, F. Siopa, A. F. Trindade, J. Oble, G. Poli, S. P. Simeonov, C. A. M. Afonso, *ChemSusChem* **2019**, *12*, 4629-4635.

To a 1M solution of **1** (50 mg, 235.63 µmol) in anhydrous THF (236 µL) was added the amine (46 µL, 468 µmol, 2 equiv.) followed by CAL B (10 mg) and the mixture was stirred under reflux at 45˚C for 24h. The solvent was evaporated and the crude product was purified by column chromatography on silica gel, eluting with hexane/EtOAc 90:10 – 50:50 gradient.

VI.2.5. Synthesis of mono-amides (Method E)

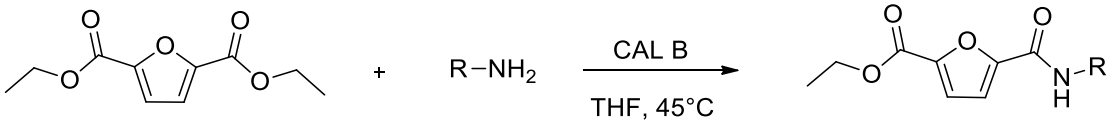

This synthesis was adapted from: J. M. J. M. Ravasco, C. M. Monteiro, F. Siopa, A. F. Trindade, J. Oble, G. Poli, S. P. Simeonov, C. A. M. Afonso, *ChemSusChem* **2019**, *12*, 4629-4635.

To a 0.85M solution of diethyl furan-2,5-dicarboxylate (50 mg, 235.63 µmol) in DIPE (0,2 mL) was added the amine (281.45 µmol, 1.2 equiv.) followed by CAL B (10 mg) and the mixture was stirred under reflux at 45˚C for 1h. The solvent was evaporated and the crude product was purified by column chromatography on silica gel, eluting with hexane/EtOAc 80:20 as eluent.

VI.2.6. Synthesis of di(amido-esters) (Method F)

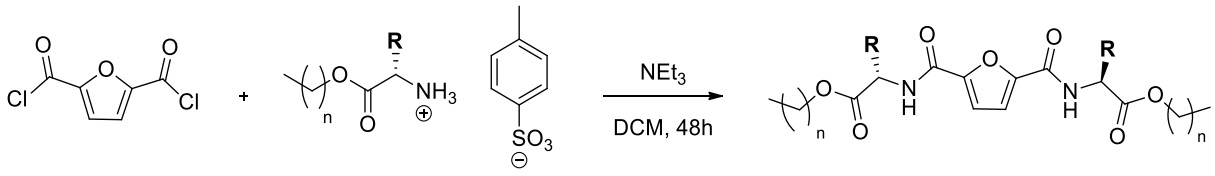

This synthesis was adapted from: A. Desmarchelier, M. Raynal, P. Brocorens, N. Vanthuyne, L. Bouteiller, *Chem. Commun.* **2015**, *51*, 7397–7400.

In a flame-dried round-bottom flask under argon atmosphere, furan-2,5-dicarbonyl dichloride (100 mg, 0.52 mmol, 1 eq) was dissolved in dry DCM (20 mL) at room temperature. The

ammonium salt (1.56 mmol, 3 eq) was then added in one portion, and the resulting mixture was cooled to 0°C with an ice/water bath. NEt_3 (0.52 mL, 3.64 mmol, 7 eq) was then added dropwise, the reaction was let warm to room temperature and stirred for 48h. Brine was then added to the flask, and the crude mixture was extracted twice with DCM. The combined organic phases were dried over $MgSO_4$, filtered, and the solvent was evaporated under reduced pressure. The resulting solid was then purified by column chromatography on silica gel, eluting with hexane/EtOAc 90:10 – 50:50 gradient.

VI.2.7. Synthesis of amino-amides (Method G)

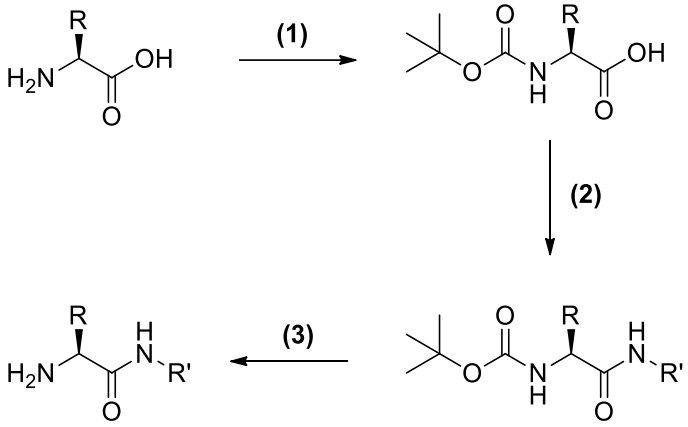

(1) $(Boc)_2O$, aq. NaOH (1M), dioxane:H_2O (1:1), 6 h, RT;
(2) $R'NH_2$, EDC.HCl, DMAP, HOBt, CH_2Cl_2, 12 h, RT;
(3) TFA, CH_2Cl_2, 30 min, RT.

This synthesis was adapted from: S. Datta, S. Bhattacharya, *Chem. Eur. J.* **2016**, *22*, 7524–7532.

Synthesis of N-(tert-butoxycarbonyl)-L-amino acid (1)

An *L*-amino acid (23 mmol, 1 eq) was dissolved in dioxane/water (2:1, 50 mL), which was made alkaline with NaOH (1 M, 23 mL) and cooled in an ice-bath. Then, $(Boc)_2O$ (1.3 eq) and $NaHCO_3$ (1 eq) were added. The reaction mixture was stirred overnight at room temperature and was then evaporated to half of the original volume. The residue was diluted with EtOAc (40 mL), cooled in an ice-bath and acidified to pH = 2.5-3 with HCl (1 M). The layers were separated and the aqueous fraction was extracted with EtOAc (2x30 mL). The combined organic phases were dried over $MgSO_4$, filtered and the solvent was evaporated under reduced pressure.

Amidation of N-(tert-butoxycarbonyl)-L-amino acid (2)

The alkyl amine (7.53 mmol) was added to the boc-protected amino acid (7.53 mmol) predissolved in dried DCM (20 mL). The mixture was cooled in an ice-bath followed by successive addition of EDC.HCl (1.44 g, 7.53 mmol), HOBt (1.98 g, 7.53 mmol) and DMAP (0.092 g, 0.75 mmol). After the solution was stirred at room temperature overnight, it was washed with acetic acid (10%, 10 mL), water, aq. $NaHCO_3$ and again with water, dried over $MgSO_4$ and evaporated, leaving a product as a colorless oil that was further purified by column chromatography on silica gel ($CHCl_3$/MeOH = 99:1).

Deprotection of N-(tert-butoxycarbonyl)-L-amino amide (3)

In a 100 mL round-bottom flask, a boc-protected amino amide (3.37 mmol, 1 eq) was solubilized with a mixture of TFA and DCM (1:1, 20 mL). The mixture was stirred for 30 minutes at room temperature. The solvent was then evaporated under reduced pressure and the crude liquid was diluted with 6M NaOH (10 mL) and extracted with DCM (15 mL). The organic layer was washed with water (2x20 mL), brine (20 mL), dried over $MgSO_4$, filtered and the solvent was evaporated under reduced pressure.

VI.2.8. Synthesis of di(amido-amides (Method H)

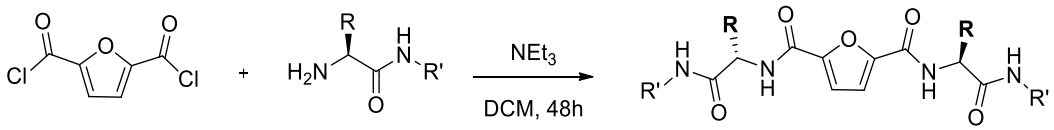

This synthesis was adapted from: A. Desmarchelier, M. Raynal, P. Brocorens, N. Vanthuyne, L. Bouteiller, *Chem. Commun.* **2015**, *51*, 7397–7400.

In a flame-dried round-bottom flask under argon atmosphere, furan-2,5-dicarbonyl dichloride (100 mg, 0.52 mmol, 1 eq) was dissolved in dry dichloromethane (10 mL) at room temperature. The amino-amide (1.14 mmol, 2.2 eq) was then added in one portion, and the resulting mixture was cooled to 0°C with an ice/water bath. NEt_3 (0.37 mL, 2.6 mmol, 5 eq) was then added dropwise, the reaction was let warm to room temperature and stirred for 48h. Brine (30 mL) was then added to the flask, and the crude mixture was extracted twice with DCM (30 mL). The combined organic phases were dried over $MgSO_4$, filtered, and the solvent was evaporated under reduced pressure to give a yellow mixture. Acetonitrile was then added to the crude product and a white precipitate appeared. The solid was filtered, washed three times with acetonitrile and dried under vacuum.

VI.3. Experimental data

VI.3.1. Precursors

*diethyl furan-2,5-dicarboxylate (**1**)*

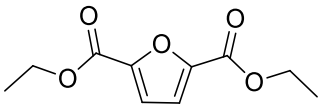

This synthesis was reproduced from: J. M. J. M. Ravasco, C. M. Monteiro, F. Siopa, A. F. Trindade, J. Oble, G. Poli, S. P. Simeonov, C. A. M. Afonso, *ChemSusChem* **2019**, *12*, 4629-4635.

To a solution of FDCA (600 mg) in anhydrous ethanol (20 mL), 30 µL of H_2SO_4 was added under stirring. The reaction was refluxed overnight. The solvent was evaporated under vacuum and the crude solid was redissolved in DCM and washed with water (3x30 mL). The organic phase was dried over $MgSO_4$ and evaporated under vacuum to give a solid which after recrystallization in hot hexane afforded 707 mg of the product as a white solid.

87%; white powder; **^{1}H NMR** (300 MHz, DMSO-d_6), δ (ppm): 7.39 (s, 2H, C**H** furan), 4.33 (q, *J* = 7.1 Hz, 4H, OC**H$_2$**), 1.31 (t, *J* = 7.1 Hz, 6H, C**H$_3$**); **^{13}C NMR** (101 MHz, DMSO-d_6), δ (ppm): 157.37 (**C**=O), 146.19 (**C**-C=O), 118.87 (**C**H), 61.31 (O**C**H_2), 14.01 (**C**H_3).

*furan-2,5-dicarbonyl dichloride (FDCDCl) (**7**)*

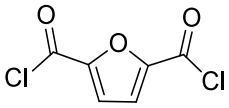

To a solution of FDCA (500 mg) in thionyl chloride (10 mL), 3 drops of DMF was added under stirring. The reaction is put under argon atmosphere and refluxed for 3h. The solvent was removed under reduce pressure and the white solid was dried under vacuum.

99%; white powder; **^{1}H NMR** (300 MHz, CD_2Cl_2-d_2), δ (ppm): 7.59 (s, 2H, C**H** furan); **^{13}C NMR** (75 MHz, CD_2Cl_2-d_2), δ (ppm): 156.45 (**C**=O), 149.79 (**C**-C=O), 124.29 (**C**H).

VI.3.2. Mono-amides

*ethyl 5-(dodecylcarbamoyl)furan-2-carboxylate (**23a**)*

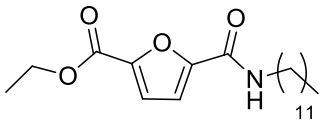

Preparation was achieved following the method E using commercially available dodecylamine and synthesized diethyl furan-2,5-dicarboxylate.

70%; white powder; **Tf:** 62,5°C; **^{1}H NMR** (300 MHz, DMSO-d_6), δ (ppm): 8.56 (t, *J* = 5.8 Hz, 1H, N**H**), 7.35 (d, *J* = 3.6 Hz, 1H, C**H** furan), 7.20 (d, *J* = 3.6 Hz, 1H, C**H** furan),), 4.32 (q, *J* = 7.1 Hz, 2H, C**H$_2$**-O), 3.21 (q, *J* = 6.7 Hz, 2H, C**H$_2$**-NH), 1.49 (p, *J* = 7.0 Hz, 2H, C**H$_2$**-CH_2-NH), 1.39-1.10 (m, 21H, (C**H$_2$**)$_9$ + OCH_2-C**H$_3$**), 0.83 (t, 3H, C**H$_3$**); **^{13}C NMR** (101 MHz, DMSO-d_6), δ (ppm): 157.63 (**C**=O ester), 156.85 (**C**=O amide), 150.55 (O-**C**-CO furan amide), 144.42 (O-**C**-CO furan ester), 119.04 (**C**H furan ester), 114.09 (**C**H furan amide), 61.00 (**C**H_2-O), 38.66 (**C**H_2-NH), 31.27, 29.02, 29.00, 28.96, 28.94, 28.69, 26.36, 22.07, 14.11, 13.91.

*ethyl 5-(tetradecylcarbamoyl)furan-2-carboxylate (**23b**)*

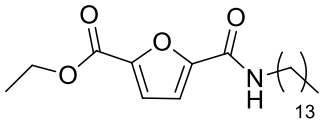

Preparation was achieved following the method E using commercially available tetradecylamine and synthesized diethyl furan-2,5-dicarboxylate.

67%; white powder; **Tf:** 72,2°C; **^{1}H NMR** (300 MHz, DMSO-d_6), δ (ppm): 8.56 (t, *J* = 5.7 Hz, 1H, N**H**), 7.35 (d, *J* = 3.7 Hz, 1H, C**H** furan), 7.20 (d, *J* = 3.7 Hz, 1H, C**H** furan),), 4.32 (q, *J* = 7.1 Hz, 2H, C**H$_2$**-O), 3.21 (q, *J* = 6.6 Hz, 2H, C**H$_2$**-NH), 1.50 (p, *J* = 6.8 Hz, 2H, C**H$_2$**-CH_2-NH), 1.38-1.13 (m, 25H, (C**H$_2$**)$_{11}$ + OCH_2-C**H$_3$**), 0.83 (t, 3H, C**H$_3$**); **^{13}C NMR** (101 MHz, DMSO-d_6), δ (ppm): 157.63 (**C**=O ester), 156.84 (**C**=O amide), 150.54 (O-**C**-CO furan amide), 144.42 (O-**C**-CO furan ester), 119.05 (**C**H furan ester), 114.09 (**C**H furan amide), 61.01 (**C**H_2-O), 38.66 (**C**H_2-NH), 31.27, 29.02, 29.00, 28.99, 28.96, 28.93, 28.68, 26.35, 22.07, 14.12, 13.92.

*ethyl 5-(hexadecylcarbamoyl)furan-2-carboxylate (**23c**)*

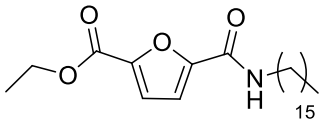

Preparation was achieved following the method E using commercially available hexadecylamine and synthesized diethyl furan-2,5-dicarboxylate.

76%; white powder; **Tf:** 78,2°C; **^{1}H NMR** (300 MHz, DMSO-d_6), δ (ppm): 8.56 (t, *J* = 5.8 Hz, 1H, N**H**), 7.34 (d, *J* = 3.7 Hz, 1H, C**H** furan), 7.20 (d, *J* = 3.6 Hz, 1H, C**H** furan), 4.32 (q, *J* = 7.1 Hz, 2H, C**H$_2$**-O), 3.21 (q, *J* = 6.7 Hz, 2H, C**H$_2$**-NH), 1.49 (p, *J* = 6.9 Hz, 2H, C**H$_2$**-CH_2-NH), 1.37-1.13 (m, 29H, (C**H$_2$**)$_{13}$ + OCH_2-C**H$_3$**), 0.83 (t, 3H, C**H$_3$**); **^{13}C NMR** (101 MHz, DMSO-d_6), δ (ppm): 158.10 (**C**=O ester), 157.35 (**C**=O amide), 151.10 (O-**C**-CO furan amide), 144.93 (O-**C**-CO furan ester), 119.20 (**C**H furan ester), 114.38 (**C**H furan amide), 61.35 (**C**H_2-O), 39.18 (**C**H_2-NH), 31.78, 29.53, 29.49, 29.24, 29.19, 26.90, 22.57, 14.48, 14.27.

*ethyl 5-(octadecylcarbamoyl)furan-2-carboxylate (**23d**)*

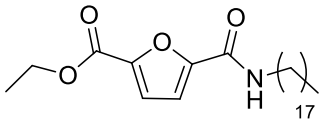

Preparation was achieved following the method E using commercially available octadecylamine and synthesized diethyl furan-2,5-dicarboxylate.

77%; white powder; **Tf:** 83,6°C; **^{1}H NMR** (300 MHz, DMSO-d_6 /CD_2Cl_2-d_2), δ (ppm): 8.10 (s, 1H, N**H**-CH_2), 7.25-7.04 (m, 2H, C**H** furan), 4.33 (q, *J* = 7.01 Hz, 2H, C**H$_2$**-O), 3.27 (q, *J* = 6.47 Hz, 2H, C**H$_2$**-NH), 1.54 (m, 2H, C**H$_2$**-CH_2-NH), 1.41-1.14 (m, 33H, (C**H$_2$**)$_{15}$ + OCH_2-C**H$_3$**), 0.86 (t, *J* = 6.48 Hz, 3H, C**H$_3$**); **^{13}C NMR** (101 MHz, DMSO-d_6 / CD_2Cl_2-d_2), δ (ppm): 158.09 (**C**=O ester), 157.40 (**C**=O amide), 151.12 (O-**C**-CO furan amide), 144.98 (O-**C**-CO furan ester), 118.72 (**C**H furan ester), 114.11 (**C**H furan amide), 61.24 (**C**H_2-O), 39.26 (**C**H_2-NH), 31.83, 29.59, 29.55, 29.31, 29.25, 26.95, 22.60, 14.24, 14.05.

VI.3.3. Furan-dicarboxamide with amines

*N^2, N^5-dioctylfuran-2,5-dicarboxamide (**2a**)*

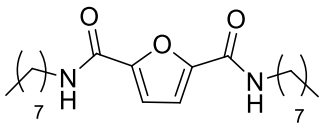

Preparation was achieved following the method D at 1M using commercially available octylamine and synthesized diethyl furan-2,5-dicarboxylate.

61%; white powder; **Tf:** 75,2°C; **^{1}H NMR** (300 MHz, DMSO-d_6), δ (ppm): 8.42 (t, *J* = 5.9 Hz, 2H, N**H**), 7.09 (s, 2H, C**H** furan), 3.25 (q, *J* = 6.7 Hz, 4H, C**H$_2$**-NH), 1.50 (m, *J* = 7.0 Hz, 4H, C**H$_2$**-CH_2-NH), 1.26 (m, 20H, (C**H$_2$**)$_5$), 0.84 (t, 6H, C**H$_3$**); **^{13}C NMR** (101 MHz, DMSO-d_6, 340K), δ (ppm): 157.07 (**C**=O), 148.16, 114.17, 38.47, 38.35, 31.22, 29.26, 28.70, 28.61, 26.43, 22.06, 13.89.

*N^2, N^5-dinonylfuran-2,5-dicarboxamide (**2b**)*

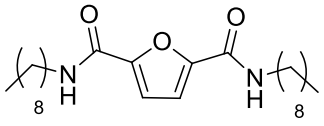

Preparation was achieved following the method D at 1M using commercially available nonylamine and synthesized diethyl furan-2,5-dicarboxylate.

86%; white powder; **Tf:** 77,3-83,7°C; **^{1}H NMR** (300 MHz, CD_2Cl_2-d_2 / DMSO-d_6), δ (ppm): 8.21 (t, *J* = 5.9 Hz, 2H, N**H**), 7.01 (d, *J* = 4.1 Hz, 2H, C**H** furan), 3.29 (q, *J* = 6.6 Hz, 4H, C**H$_2$**-NH), 1.55 (p, *J* = 6.7 Hz, 4H, C**H$_2$**-CH_2-NH), 1.26 (m, 24H, (C**H$_2$**)$_6$), 0.85 (t, 6H, C**H$_3$**); **^{13}C NMR** (101 MHz, CD_2Cl_2-d_2 / DMSO-d_6), δ (ppm): 157.04 (**C**=O), 148.08, 113.71, 38.45, 31.22, 29.26, 28.89, 28.74, 28.61, 26.42, 22.02, 13.58.

*N^2, N^5-didecylfuran-2,5-dicarboxamide (**2c**)*

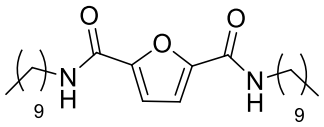

Preparation was achieved following the method D at 1M using commercially available decylamine and synthesized diethyl furan-2,5-dicarboxylate.

43%; white powder; **Tf:** 88,8°C; **^{1}H NMR** (300 MHz, DMSO-d_6), δ (ppm): 8.41 (t, *J* = 5.9 Hz, 2H, N**H**), 7.09 (s, 2H, C**H** furan), 3.30-3.22 (q, 4H, C**H$_2$**-NH), 1.50 (m, *J* = 7.0 Hz, 4H, C**H$_2$**-CH_2-NH), 1.26 (m, 28H, (C**H$_2$**)$_7$), 0.84 (t, 6H, C**H$_3$**); **^{13}C NMR** (151 MHz, DMSO-d_6, 340K), δ (ppm): 156.89 (**C**=O), 156.82 (**C**=O), 148.09, 113.72, 38.31, 38.19, 30.92, 28.90, 28.88, 28.58, 28.57, 28.38, 28.28, 26.11, 21.67, 13.47.

*N^2, N^5-diundecylfuran-2,5-dicarboxamide (**2d**)*

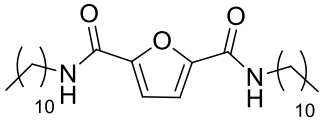

Preparation was achieved following the method D at 1M using commercially available undecylamine and synthesized diethyl furan-2,5-dicarboxylate.

73%; white powder; **Tf:** 91,7°C; **^{1}H NMR** (300 MHz, CD_2Cl_2-d_2 / DMSO-d_6), δ (ppm): 8.13 (q, *J* = 5.6 Hz, 2H, N**H**), 7.00 (s, 2H, C**H** furan), 3.31 (q, *J* = 6.7 Hz, 4H, C**H$_2$**-NH), 1.55 (q, *J* = 7.1 Hz, 4H, C**H$_2$**-CH_2-NH), 1.27 (m, 32H, (C**H$_2$**)$_8$), 0.86 (t, 6H, C**H$_3$**); **^{13}C NMR** (101 MHz, CD_2Cl_2-d_2 / DMSO-d_6), δ (ppm): 157.02 (**C**=O), 148.08, 113.74, 38.43, 31.22, 29.24, 28.93, 28.71, 28.64, 26.40, 22.01, 13.62.

*N^2, N^5-didodecylfuran-2,5-dicarboxamide (**2e**)*

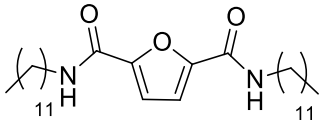

Preparation was achieved following the method D at 0.5M using commercially available dodecylamine and synthesized diethyl furan-2,5-dicarboxylate.

25%; white powder; **Tf:** 96,3°C; **^{1}H NMR** (400 MHz, CD_2Cl_2-d_2 / DMSO-d_6), δ (ppm): 8.15 (t, *J* = 5.9 Hz, 2H, N**H**), 7.01 (s, 2H, C**H** furan), 3.30 (q, *J* = 6.8 Hz, 4H, C**H$_2$**-NH), 1.56 (m, *J* = 7.2 Hz, 4H, C**H$_2$**-CH_2-NH), 1.46-1.11 (m, 36H, (C**H$_2$**)$_9$), 0.86 (t, *J* = 6.7 Hz, 6H, C**H$_3$**); **^{13}C NMR** (151 MHz, DMSO-d_6, 340K), δ (ppm): 156.85 (**C**=O), 148.07, 113.68, 38.28, 30.90, 28.88, 28.63, 28.60, 28.58, 28.56, 28.35, 28.28, 26.09, 21.66, 13.46.

*N^2, N^5-bis(2-ethylhexyl)furan-2,5-dicarboxamide (**2f**)*

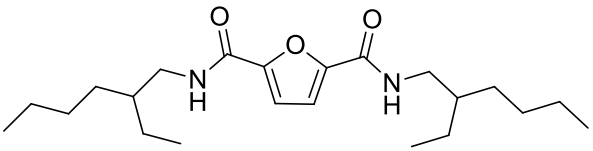

Preparation was achieved following the method D at 1M using commercially available 2-ethylhexylamine and synthesized diethyl furan-2,5-dicarboxylate.

86%; white powder; **^{1}H NMR** (300 MHz, CD_2Cl_2-d_2 / DMSO-d_6), δ (ppm): 8.35 (t, *J* = 6.0 Hz, 2H, N**H**), 7.11 (s, 2H, C**H** furan), 3.19 (t, *J* = 6.4 Hz, 4H, C**H$_2$**-NH), 1.52 (p, *J* = 6.0 Hz, 2H, C**H**), 1.27 (m, 16H, C**H$_2$**), 0.86 (m, 12H, C**H$_3$**); **^{13}C NMR** (101 MHz, DMSO-d_6), δ (ppm): 157.22, 148.20, 114.18, 41.81, 30.31, 28.28, 23.61, 22.43, 13.85, 10.60.

*N^2, N^5-dibenzhydrylfuran-2,5-dicarboxamide (**2g**)*

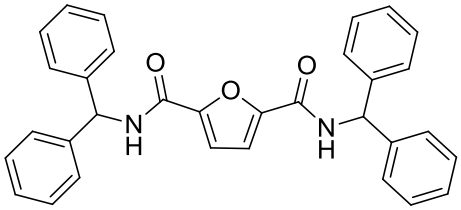

Preparation was achieved following the method D at 1M using commercially available benzhydrylamine and synthesized diethyl furan-2,5-dicarboxylate.

30%; white powder; **^{1}H NMR** (300 MHz, DMSO-d_6), δ (ppm): 9.26 (d, *J* = 8.7 Hz, 2H, N**H**), 7.33 (m, 22H, C**H** furan + Ar-**H**), 6.38 (d, *J* = 8.6 Hz, 2H, C**H**); **^{13}C NMR** (101 MHz, DMSO-d_6), δ (ppm): 156.78 (**C**=O), 148.12 (**C**-C=O), 141.52 (**C(i)** Ph), 128.40 (**C(m)** Ph), 127.66 (**C(o)** Ph), 127.21 (**C(p)** Ph), 115.11 (**C**H furan), 55.71 (NH-**C**H).

*N^2, N^5-dibenzylfuran-2,5-dicarboxamide (**2h**)*

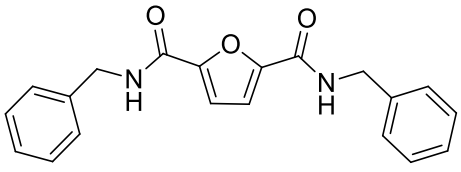

Preparation was achieved following the method D at 1M using commercially available benzylamine and synthesized diethyl furan-2,5-dicarboxylate.

66%; white powder; **^{1}H NMR** (300 MHz, DMSO-d_6), δ (ppm): 9.00 (t, *J* = 6.2 Hz, 2H, N**H**), 7.39-7.23 (m, 10H, Ar-**H**), 7.20 (s, 2H, C**H** furan), 4.51 (d, *J* = 6.1 Hz, 2H, C**H$_2$**); ^{13}C NMR

(101 MHz, DMSO-d_6), δ (ppm): 157.71 (C=O), 148.54 (O-**C**-CO furan), 139.46, 128.89, 127.71, 127.47, 115.24 (**C**H furan), 42.34 (**C**H_2-NH).

*N^2, N^5-diphenethylfuran-2,5-dicarboxamide (**2i**)*

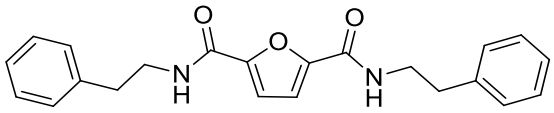

Preparation was achieved following the method D at 1M using commercially available phenethylamine and synthesized diethyl furan-2,5-dicarboxylate.

77%; yellow oil; **^{1}H NMR** (300 MHz, DMSO-d_6), δ (ppm): 8.59 (t, *J* = 5.9 Hz, 2H, N**H**), 7.37-7.16 (m, 10H, Ar-**H**), 7.12 (s, 2H, C**H** furan), 3.50 (dt, *J* = 8.1, 6.2 Hz, 4H, C**H**$_2$-NH), 2.85 (t, 4H, C**H**$_2$-CH_2-NH); **^{13}C NMR** (101 MHz, DMSO-d_6), δ (ppm): 157.13 (**C**=O), 148.12, 139.15, 128.61, 128.37, 126.17, 114.29, 35.22.

VI.3.4. Ester ammonium salts

VI.3.4.1. Synthesized from L-alanine

*ethyl L-alaninate ammonium chloride salt (**3a**)*

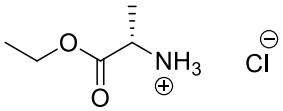

Preparation was achieved following the method B using commercially available ethanol and *L*-Ala.

99%; white powder; **^{1}H NMR** (400 MHz, DMSO-d_6), δ (ppm): 8.74 (s, 3H, N**H**$_3$), 4.17 (m, 2H, C**H**$_2$-O), 3.98 (q, *J* = 7.1 Hz, 1H, C**H**), 1.42 (d, *J* = 7.1 Hz, 3H, C**H**$_3$-CH-NH_3), 1.21 (t, *J* = 7.1 Hz, 3H, C**H**$_3$-CH_2); **^{13}C NMR** (75 MHz, DMSO-d_6), δ (ppm): 169.88 (**C**=O), 61.60 (**C**H_2-O), 47.80 (**C**H), 15.64, 13.92.

*octyl L-alaninate ammonium chloride salt (**3c**)*

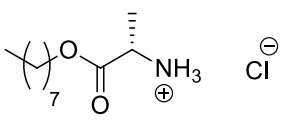

Preparation was achieved following the method C using commercially available octanol and *L*-Ala.

37%; white powder; **^{1}H NMR** (300 MHz, DMSO-d_6), δ (ppm): 8.64 (s, 3H, N**H**$_3$), 4.21-3.97 (m, 3H, C**H**$_2$-O + C**H**-NH_3), 1.60 (p, *J* = 6.6 Hz, 2H, C**H**$_2$-CH_2-O), 1.42 (d, *J* = 7.1 Hz, 3H, C**H**$_3$-CH-NH_3), 1.25 (m, 10H, CH_3-(C**H**$_2$)$_5$), 0.84 (t, 3H, C**H**$_3$-CH_2); **^{13}C NMR** (101 MHz, DMSO-d_6), δ (ppm): 170.00 (**C**=O), 65.51 (**C**H_2-O), 47.83 (**C**H), 31.20, 28.57, 27.95, 25.17, 22.08, 15.71, 13.95.

*dodecyl L-alaninate ammonium tosylate salt (**3d**)*

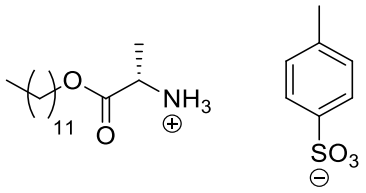

Preparation was achieved following the method A using commercially available dodecan-1-ol and *L*-Ala.

90%; white powder; **^{1}H NMR** (300 MHz, DMSO-d_6), δ (ppm): 8.15 (s, 3H, N**H**$_3$), 7.49 (d, *J* = 8.1 Hz, 2H, Ar-**H**), 7.12 (d, *J* = 7.9 Hz, 2H, Ar-**H**), 4.21-4.05 (m, 3H, C**H**$_2$-O + C**H**-NH_3), 2.29 (s, 3H, Ar-C**H**$_3$), 1.59 (m, *J* = 6.7 Hz, 2H, C**H**$_2$-CH_2-O), 1.38 (d, *J* = 7.2 Hz, 3H, C**H**$_3$-CH-NH_3), 1.24 (m, 18H, CH_3-(C**H**$_2$)$_9$), 0.85 (t, 3H, C**H**$_3$-CH_2); **^{13}C NMR** (75 MHz, DMSO-d_6), δ (ppm): 169.92 (**C**=O), 145.23, 138.00, 128.18, 125.56, 65.69 (**C**H_2-O), 47.86 (**C**H), 31.37, 29.11, 29.08, 29.04, 28.99, 28.78, 28.68, 27.99, 25.23, 22.16, 20.82, 15.62, 15.59, 13.97.

*tridecyl L-alaninate ammonium tosylate salt (**3e**)*

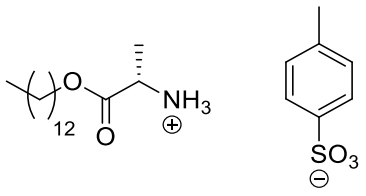

Preparation was achieved following the method A using commercially available tridecan-1-ol and *L*-Ala.

97%; white powder; **^{1}H NMR** (300 MHz, DMSO-d_6), δ (ppm): 8.32 (s, 3H, N**H**$_3$), 7.51 (d, *J* = 8.1 Hz, 2H, Ar-**H**), 7.13 (d, *J* = 8.0 Hz, 2H, Ar-**H**), 4.21-4.05 (m, 3H, C**H**$_2$-O + C**H**-NH_3), 2.30 (s, 3H, Ar-C**H**$_3$), 1.60 (t, *J* = 7.0 Hz, 2H, C**H**$_2$-CH_2-O), 1.40 (d, *J* = 7.2 Hz, 3H, C**H**$_3$-CH-NH_3), 1.25 (m, 20H, CH_3-(C**H**$_2$)$_{10}$), 0.86 (t, 3H, C**H**$_3$-CH_2); **^{13}C NMR** (75 MHz, DMSO-d_6), δ (ppm):

169.94 (**C**=O), 145.33, 137.79, 128.06, 125.48, 65.57 (**C**H_2-O), 47.93 (**C**H), 31.29, 29.06, 29.03, 29.01, 28.97, 28.92, 28.71, 28.61, 27.92, 25.15, 22.08, 20.74, 15.67, 13.90.

*pentadecyl L-alaninate ammonium tosylate salt (**3f**)*

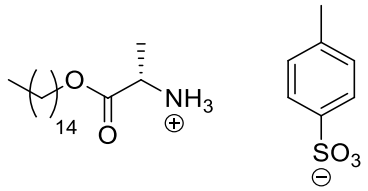

Preparation was achieved following the method A using commercially available pentadecan-1-ol and *L*-Ala.

98%; white powder; **^{1}H NMR** (400 MHz, DMSO-d_6), δ (ppm): 8.33 (s, 3H, N**H₃**), 7.52 (d, *J* = 7.9 Hz, 2H, Ar-**H**), 7.13 (d, *J* = 7.8 Hz, 2H, Ar-**H**), 4.21-4.07 (m, 3H, C**H₂**-O + C**H**-NH_3), 2.30 (s, 3H, Ar-C**H₃**), 1.59 (t, *J* = 6.7 Hz, 2H, C**H₂**-CH_2-O), 1.40 (d, *J* = 7.2 Hz, 3H, C**H₃**-CH-NH_3), 1.25 (m, 24H, CH_3-(C**H₂**)$_{12}$), 0.86 (t, 3H, C**H₃**-CH_2); **^{13}C NMR** (101 MHz, DMSO-d_6), δ (ppm): 169.94 (**C**=O), 145.26, 137.83, 128.07, 125.49, 65.56, 47.94, 31.32, 29.08, 29.06, 29.04, 29.01, 28.95, 28.74, 28.65, 27.94, 25.18, 22.10, 20.75, 15.67, 13.89.

*hexadecyl L-alaninate ammonium tosylate salt (**3g**)*

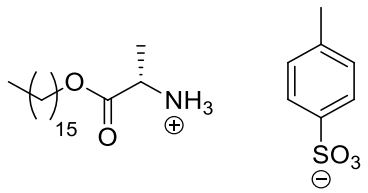

Preparation was achieved following the method A using commercially available hexadecan-1-ol and *L*-Ala.

99%; white powder; **^{1}H NMR** (300 MHz, DMSO-d_6), δ (ppm): 8.31 (s, 3H, N**H₃**), 7.50 (d, 2H, Ar-**H**), 7.12 (d, *J* = 7.8 Hz, 2H, Ar-**H**), 4.24-4.02 (m, 3H, C**H₂**-O + C**H**-NH_3), 2.29 (s, 3H, Ar-C**H₃**), 1.59 (t, *J* = 7.0 Hz, 2H, C**H₂**-CH_2-O), 1.39 (d, *J* = 7.2 Hz, 3H, C**H₃**-CH-NH_3), 1.24 (m, 26H, CH_3-(C**H₂**)$_{13}$), 0.86 (t, 3H, C**H₃**-CH_2); **^{13}C NMR** (75 MHz, DMSO-d_6), δ (ppm): 169.93 (**C**=O), 145.35, 137.74, 128.03, 125.48, 65.55, 47.92, 31.31, 29.08, 29.04, 29.01, 28.95, 28.73, 28.64, 27.94, 25.17, 22.09, 20.73, 15.65, 13.86.

*octadecyl L-alaninate ammonium tosylate salt (**3h**)*

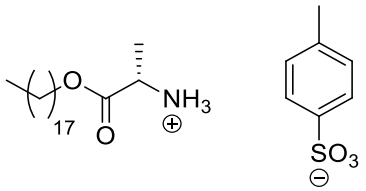

Preparation was achieved following the method A using commercially available octadecan-1-ol and *L*-Ala.

99%; white powder; **^{1}H NMR** (400 MHz, DMSO-d_6), δ (ppm): 8.32 (s, 3H, N**H$_3$**), 7.49 (d, *J* = 7.8 Hz, 2H, Ar-**H**), 7.11 (d, *J* = 7.8 Hz, 2H, Ar-**H**), 4.20-4.05 (m, 3H, C**H$_2$**-O + C**H**-NH_3), 2.29 (s, 3H, Ar-C**H$_3$**), 1.59 (m, *J* = 6.7 Hz, 2H, C**H$_2$**-CH_2-O), 1.38 (d, *J* = 7.2 Hz, 3H, C**H$_3$**-CH-NH_3), 1.23 (m, 30H, CH_3-(C**H$_2$**)$_{15}$), 0.85 (t, 3H, C**H$_3$**-CH_2). **^{13}C NMR** (75 MHz, CD_2Cl_2-d_2 / DMSO-d_6), δ (ppm): 169.72 (**C**=O), 144.18, 138.23, 127.86, 125.29, 65.57, 48.06, 31.27, 29.03, 28.99, 28.95, 28.87, 28.69, 28.57, 27.82, 25.11, 22.05, 20.48, 15.43, 13.48.

VI.3.4.2. Synthesized from L-phenylalanine

*ethyl L-phenylalaninate ammonium chloride salt (**4a**)*

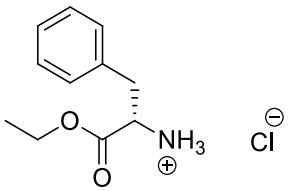

Preparation was achieved following the method B using commercially available ethanol and *L*-Phe.

99%; white powder; **^{1}H NMR** (300 MHz, DMSO-d_6), δ (ppm): 8.84 (s, 3H, N**H$_3$**), 7.40-7.18 (m, 5H, Ar-**H**), 4.18 (dd, *J* = 8.1, 5.4 Hz, 1H, NH_3-C**H**), 4.08 (qd, *J* = 7.1, 2.1 Hz, 2H, C**H$_2$**-O), 3.33-3.01 (m, 2H, NH_3-CH-C**H$_2$**), 1.08 (t, *J* = 7.1 Hz, 3H, C**H$_3$**-CH_2); **^{13}C NMR** (75 MHz, DMSO-d_6), δ (ppm): 168.84 (**C**=O), 134.61 (**C(i)** Ph), 129.42 (**C**H**(m)** Ph), 128.47 (**C**H**(o)** Ph), 127.15 (**C**H**(p)** Ph), 61.45 (**C**H_2-O), 53.23 (**C**H), 35.91 (**C**H_2-Ph), 13.72 (**C**H_3).

*hexyl L-phenylalaninate ammonium tosylate salt (**4b**)*

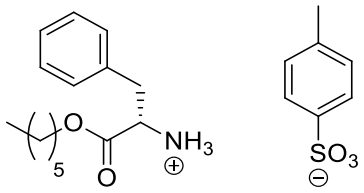

Preparation was achieved following the method A using commercially available hexan-1-ol and *L*-Phe.

90%; white powder; **^{1}H NMR** (300 MHz, DMSO-d_6), δ (ppm): 8.45 (s, 3H, N**H**$_3$), 7.51 (d, *J* = 8.1 Hz, 2H, Ar-**H**), 7.39-7.18 (m, 5H, Ar-**H**), 7.13 (d, *J* = 7.9 Hz, 2H, Ar-**H**), 4.28 (t, *J* = 6.9 Hz, 1H, NH_3-C**H**), 4.02 (t, *J* = 6.5 Hz, 2H, C**H**$_2$-O), 3.24-2.94 (m, 2H, NH_3-CH-C**H**$_2$), 2.29 (s, 3H, Ar-C**H**$_3$), 1.42 (p, *J* = 6.7 Hz, 2H, C**H**$_2$-CH_2-O), 1.31-1.06 (m, 6H, CH_3-(C**H**$_2$)$_3$), 0.85 (t, *J* = 6.9 Hz, 3H, C**H**$_3$-CH_2); **^{13}C NMR** (75 MHz, DMSO-d_6), δ (ppm): 169.05 (**C**=O), 145.37, 137.81, 134.61, 129.29, 128.53, 128.09, 127.23, 125.49, 65.56 (**C**H_2-O), 53.24 (**C**H), 36.15 (**C**H_2-Ph), 30.77, 27.72, 24.75, 21.90, 20.76, 13.84.

*octyl L-phenylalaninate ammonium tosylate salt (**4c**)*

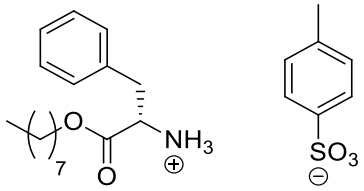

Preparation was achieved following the method A using commercially available octan-1-ol and *L*-Phe.

92%; white powder; **^{1}H NMR** (300 MHz, DMSO-d_6), δ (ppm): 8.44 (s, 3H, N**H**$_3$), 7.51 (d, *J* = 8.1 Hz, 2H, Ar-**H**), 7.39-7.18 (m, 5H, Ar-**H**), 7.12 (d, *J* = 7.8 Hz, 2H, Ar-**H**), 4.28 (dd, *J* = 8.0, 5.8 Hz, 1H, NH_3-C**H**), 4.02 (t, *J* = 6.5 Hz, 2H, C**H**$_2$-O), 3.26-2.91 (m, 2H, NH_3-CH-C**H**$_2$), 2.29 (s, 3H, Ar-C**H**$_3$), 1.42 (p, *J* = 6.8 Hz, 2H, C**H**$_2$-CH_2-O), 1.18 (m, 10H, CH_3-(C**H**$_2$)$_5$), 0.86 (t, *J* = 6.6 Hz, 3H, C**H**$_3$-CH_2); **^{13}C NMR** (75 MHz, DMSO-d_6), δ (ppm): 169.05 (**C**=O), 145.43, 137.75, 134.60, 129.29, 128.52, 128.06, 127.21, 125.48, 65.56 (**C**H_2-O), 53.22 (**C**H), 36.15 (**C**H_2-Ph), 31.17, 28.52, 28.49, 27.75, 25.09, 22.05, 20.75, 13.91.

dodecyl L-phenylalaninate ammonium tosylate salt ***(4d)***

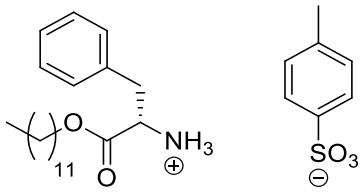

Preparation was achieved following the method A using commercially available dodecan-1-ol and *L*-Phe.

96%; white powder; **^{1}H NMR** (300 MHz, DMSO-d_6), δ (ppm): 8.49 (s, 3H, N**H**$_3$), 7.50 (d, *J* = 8.2 Hz, 2H, Ar-**H**), 7.37-7.19 (m, 5H, Ar-**H**), 7.12 (d, *J* = 7.9 Hz, 2H, Ar-**H**), 4.29 (m, *J* = 7.9, 5.9 Hz, 1H, NH_3-C**H**), 4.03 (t, *J* = 6.4 Hz, 2H, C**H**$_2$-O), 3.19-2.98 (m, 2H, NH_3-CH-C**H**$_2$), 2.29 (s, 3H, Ar-C**H**$_3$), 1.42 (m, *J* = 6.8 Hz, 2H, C**H**$_2$-CH_2-O), 1.22 (m, 18H, CH_3-(C**H**$_2$)$_9$), 0.85 (t, 3H, C**H**$_3$-CH_2); **^{13}C NMR** (101 MHz, DMSO-d_6), δ (ppm): 169.01 (**C**=O), 145.23, 137.94, 134.65, 129.32, 128.53, 128.13, 127.21, 125.53, 65.58, 53.19, 36.11, 31.34, 29.08, 29.05, 29.00, 28.90, 28.75, 28.62, 27.79, 25.14, 22.13, 20.78, 13.95.

tridecyl L-phenylalaninate ammonium tosylate salt ***(4e)***

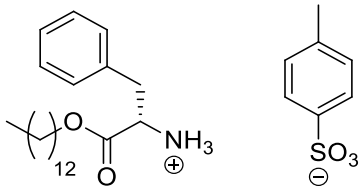

Preparation was achieved following the method A using commercially available tridecan-1-ol and *L*-Phe.

99%; white powder; **^{1}H NMR** (300 MHz, DMSO-d_6), δ (ppm): 8.46 (s, 3H, N**H**$_3$), 7.52 (d, 2H, Ar-**H**), 7.42-7.18 (m, 5H, Ar-**H**), 7.13 (d, *J* = 7.9 Hz, 2H, Ar-**H**), 4.28 (m, *J* = 7.0 Hz, 1H, NH_3-C**H**), 4.02 (t, *J* = 6.4 Hz, 2H, C**H**$_2$-O), 3.26-2.94 (m, 2H, NH_3-CH-C**H**$_2$), 2.30 (s, 3H, Ar-C**H**$_3$), 1.43 (m, *J* = 6.4 Hz, 2H, C**H**$_2$-CH_2-O), 1.25 (m, 20H, CH_3-(C**H**$_2$)$_{10}$), 0.86 (t, 3H, C**H**$_3$-CH_2); **^{13}C NMR** (75 MHz, DMSO-d_6), δ (ppm): 169.03 (**C**=O), 145.36, 137.78, 134.62, 129.29, 128.49, 128.06, 127.17, 125.49, 65.54, 53.24, 36.15, 31.29, 29.05, 29.03, 29.01, 28.96, 28.86, 28.71, 28.58, 27.76, 25.10, 22.08, 20.75, 13.90.

*pentadecyl L-phenylalaninate ammonium tosylate salt **(4f)***

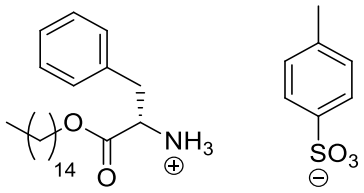

Preparation was achieved following the method A using commercially available pentadecan-1-ol and *L*-Phe.

99%; white powder; **^{1}H NMR** (400 MHz, DMSO-d_6), δ (ppm): 8.46 (s, 3H, N**H**$_3$), 7.53 (d, *J* = 7.9 Hz, 2H Ar-**H**), 7.38 – 7.18 (m, 5H, Ar-**H**), 7.14 (d, *J* = 7.8 Hz, 2H Ar-**H**), 4.28 (m, 1H, NH_3-C**H**), 4.02 (t, *J* = 6.4 Hz, 2H, C**H**$_2$-O), 3.26 – 2.94 (m, 2H, NH_3-CH-C**H**$_2$), 2.30 (s, 3H, Ar-C**H**$_3$), 1.42 (m, *J* = 6.6 Hz, 2H, C**H**$_2$-CH_2-O), 1.25 (m, 24H, CH_3-(C**H**$_2$)$_{12}$), 0.86 (t, 3H, C**H**$_3$-CH_2); **^{13}C NMR** (101 MHz, DMSO-d_6), δ (ppm): 169.04 (**C**=O), 145.22, 137.90, 134.65, 129.30, 128.49, 128.11, 127.17, 125.51, 65.53, 53.26, 36.16, 31.31, 29.07, 29.03, 29.00, 28.89, 28.73, 28.62, 27.78, 25.13, 22.10, 20.76, 13.91.

*hexadecyl L-phenylalaninate ammonium tosylate salt **(4g)***

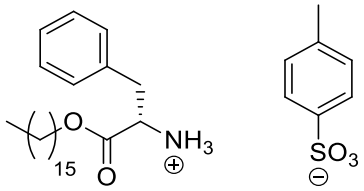

Preparation was achieved following the method A using commercially available hexadecan-1-ol and *L*-Phe.

99%; white powder; **^{1}H NMR** (300 MHz, DMSO-d_6), δ (ppm): 8.45 (s, 3H, N**H**$_3$), 7.52 (d, 2H Ar-**H**), 7.38-7.18 (m, 5H, Ar-**H**), 7.12 (d, *J* = 7.8 Hz, 2H Ar-**H**), 4.27 (m, 1H, NH_3-C**H**), 4.01 (m, 2H, C**H**$_2$-O), 3.26-2.92 (m, 2H, NH_3-CH-C**H**$_2$), 2.29 (s, 3H, Ar-C**H**$_3$), 1.40 (d, *J* = 6.9 Hz, 2H, C**H**$_2$-CH_2-O), 1.24 (m, 26H, CH_3-(C**H**$_2$)$_{13}$), 0.84 (t, 3H, C**H**$_3$-CH_2); **^{13}C NMR** (75 MHz, DMSO-d_6), δ (ppm): 169.03 (**C**=O), 145.30, 137.81, 134.64, 129.29, 128.47, 128.07, 127.15, 125.50, 65.51, 53.25, 36.15, 31.31, 29.07, 29.03, 29.00, 28.89, 28.73, 28.62, 27.77, 25.12, 22.09, 20.74, 13.88.

*octadecyl L-phenylalaninate ammonium tosylate salt (**4h**)*

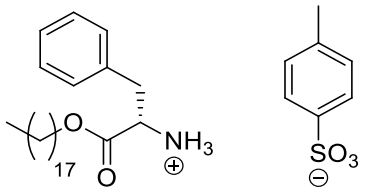

Preparation was achieved following the method A using commercially available octadecan-1-ol and *L*-Phe.

99%; white powder; **^{1}H NMR** (400 MHz, DMSO-d_6), δ (ppm): 8.49 (s, 3H, N**H$_3$**), 7.50 (d, *J* = 8.2 Hz, 2H, Ar-**H**), 7.37-7.19 (m, 5H, Ar-**H**), 7.12 (d, *J* = 7.8 Hz, 2H, Ar-**H**), 4.29 (t, *J* = 7.0 Hz, 1H, NH_3-C**H**), 4.03 (t, *J* = 6.4 Hz, 2H, C**H$_2$**-O), 3.19-2.98 (m, 2H, NH_3-CH-C**H$_2$**), 2.29 (s, 3H, Ar-C**H$_3$**), 1.42 (m, *J* = 6.8 Hz, 2H, C**H$_2$**-CH_2-O), 1.22 (m, 30H, CH_3-(C**H$_2$**)$_{15}$), 0.85 (t, 3H, C**H$_3$**-CH_2). **^{13}C NMR** (75 MHz, CD_2Cl_2-d_2 / DMSO-d_6), δ (ppm): 168.77, (**C**=O), 144.31, 138.16, 134.25, 129.01, 128.18, 127.85, 126.91, 125.31, 65.53, 53.39, 36.01, 31.26, 29.01, 28.97, 28.93, 28.82, 28.67, 28.54, 27.67, 25.41, 25.06, 22.03, 13.50.

VI.3.4.3. Synthesized from L-leucine

*ethyl L-leucinate ammonium chloride salt (**5a**)*

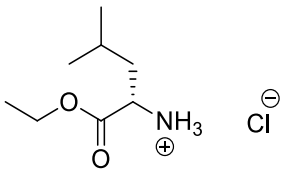

Preparation was achieved following the method B using commercially available ethanol and *L*-Leu.

99%; white powder; **^{1}H NMR** (300 MHz, DMSO-d_6), δ (ppm): 8.75 (s, 3H, N**H$_3$**), 4.18 (m, *J* = 7.1, 2.7 Hz, 2H, C**H$_2$**-O), 3.84 (q, *J* = 6.9 Hz, 1H, NH_3-C**H**), 1.87-1.56 (m, 5H, $(CH_3)_2$-C**H**-C**H$_2$** + C**H$_2$**-CH_2-O), 1.22 (t, *J* = 7.1 Hz, 3H, C**H$_3$**-CH_2), 0.88 (d, *J* = 6.2 Hz, 6H, (C**H$_3$**)$_2$-CH); **^{13}C NMR** (75 MHz, DMSO-d_6), δ (ppm): 169.73 (**C**=O), 61.58 (**C**H_2-O), 50.48 (**C**H-NH), 39.11 (**C**H_2-$(CH_3)_2$), 23.73, 22.19, 21.92, 13.90.

*octyl L-leucinate ammonium tosylate salt (**5c**)*

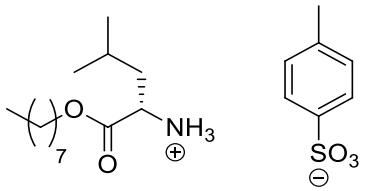

Preparation was achieved following the method A using commercially available octan-1-ol and *L*-Leu.

40%; white powder; **^{1}H NMR** (300 MHz, DMSO-d_6), δ (ppm): 8.33 (s, 3H, N**H$_3$**), 7.50 (d, *J* = 8.0 Hz, 2H, Ar-**H**), 7.12 (d, *J* = 7.8 Hz, 2H Ar-**H**), 4.15 (m, 2H, C**H$_2$**-O), 3.96 (q, *J* = 6.2 Hz, 1H, NH_3-C**H**), 2.29 (s, 3H, Ar-C**H$_3$**), 1.83-1.50 (m, 5H, $(CH_3)_2$-C**H**-C**H$_2$** + C**H$_2$**-CH_2-O), 1.26 (m, 10H, (C**H$_2$**)$_5$), 0.88 (m, 9H, C**H$_3$**); **^{13}C NMR** (75 MHz, DMSO-d_6), δ (ppm): 169.89 (**C**=O), 145.33 (**C(i)** Tosyl), 137.81 (**C(p)** Tosyl), 128.07 (**C(m)** Tosyl), 125.48 (**C(o)** Tosyl), 65.60 (**C**H_2-O), 50.63 (**C**H-NH), 39.21 (**C**H_2-$(CH_3)_2$), 31.15, 28.54, 28.48, 27.86, 25.18, 23.79, 22.10, 22.05, 21.87, 20.75, 13.90.

*dodecyl L-leucinate ammonium tosylate salt (**5d**)*

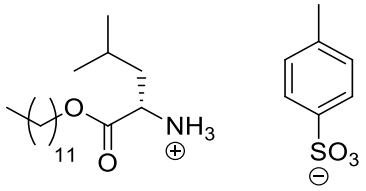

Preparation was achieved following the method A using commercially available dodecan-1-ol and *L*-Leu.

99%; white powder; **^{1}H NMR** (400 MHz, DMSO-d_6), δ (ppm): 8.34 (s, 3H, N**H$_3$**), 7.51 (d, *J* = 7.8 Hz, 2H, Ar-**H**), 7.13 (d, *J* = 7.8 Hz, 2H Ar-**H**), 4.14 (m, *J* = 10.8, 6.4 Hz, 2H, C**H$_2$**-O), 3.97 (q, *J* = 6.0 Hz, 1H, NH_3-C**H**), 2.30 (s, 3H, Ar-C**H$_3$**), 1.82-1.51 (m, 5H, $(CH_3)_2$-C**H**-C**H$_2$** + C**H$_2$**-CH_2-O), 1.25 (m, 18H, (C**H$_2$**)$_9$), 0.88 (m, 9H, C**H$_3$**); **^{13}C NMR** (75 MHz, DMSO-d_6), δ (ppm): 169.88 (**C**=O), 145.34 (**C(i)** Tosyl), 137.78 (**C(p)** Tosyl), 128.05 (**C(m)** Tosyl), 125.48 (**C(o)** Tosyl), 65.59 (**C**H_2-O), 50.62 (**C**H-NH), 39.21 (**C**H_2-$(CH_3)_2$), 31.29, 29.03, 29.00, 28.92, 28.90, 28.69, 28.54, 27.87, 25.19, 23.78, 22.10, 22.08, 21.86, 20.75, 13.90.

*tridecyl L-leucinate ammonium tosylate salt (**5e**)*

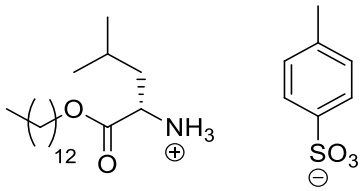

Preparation was achieved following the method A using commercially available tridecan-1-ol and *L*-Leu.

99%; white powder; **^{1}H NMR** (400 MHz, DMSO-d_6), δ (ppm): 8.33 (s, 3H, N**H$_3$**), 7.50 (d, *J* = 7.9 Hz, 2H, Ar-**H**), 7.12 (d, *J* = 7.8 Hz, 2H Ar-**H**), 4.13 (m, *J* = 10.8, 6.5 Hz, 2H, C**H$_2$**-O), 3.96 (s, 1H, NH_3-C**H**), 2.29 (s, 3H, Ar-C**H$_3$**), 1.82-1.47 (m, 5H, $(CH_3)_2$-C**H**-C**H$_2$** + C**H$_2$**-CH_2-O), 1.24 (m, 20H, (C**H$_2$**)$_{10}$), 0.88 (m, 9H, C**H$_3$**); **^{13}C NMR** (75 MHz, DMSO-d_6), δ (ppm): 169.87 (**C**=O), 145.30 (**C(i)** Tosyl), 137.80 (**C(p)** Tosyl), 128.05 (**C(m)** Tosyl), 125.49 (**C(o)** Tosyl), 65.57 (**C**H_2-O), 50.63 (**C**H-NH), 39.20 (**C**H_2-$(CH_3)_2$), 31.29, 29.05, 29.03, 29.01, 28.93, 28.91, 28.71, 28.55, 27.87, 25.20, 23.78, 22.09, 21.84, 20.74, 13.89.

*pentadecyl L-leucinate ammonium tosylate salt (**5f**)*

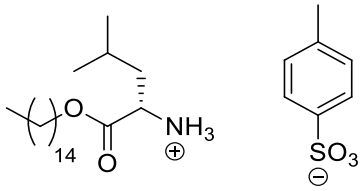

Preparation was achieved following the method A using commercially available pentadecan-1-ol and *L*-Leu.

99%; white powder; **^{1}H NMR** (400 MHz, DMSO-d_6), δ (ppm): 8.33 (s, 3H, N**H$_3$**), 7.50 (d, *J* = 7.8 Hz, 2H, Ar-**H**), 7.12 (d, *J* = 7.8 Hz, 2H Ar-**H**), 4.12 (m, 2H, C**H$_2$**-O), 3.96 (q, *J* = 6.0 Hz, 1H, NH_3-C**H**), 2.29 (s, 3H, Ar-C**H$_3$**), 1.82-1.50 (m, 5H, $(CH_3)_2$-C**H**-C**H$_2$** + C**H$_2$**-CH_2-O), 1.24 (m, 24H, (C**H$_2$**)$_{12}$), 0.87 (m, 9H, C**H$_3$**); **^{13}C NMR** (75 MHz, DMSO-d_6), δ (ppm): 169.87 (**C**=O), 145.33 (**C(i)** Tosyl), 137.78 (**C(p)** Tosyl), 128.04 (**C(m)** Tosyl), 125.49 (**C(o)** Tosyl), 65.57 (**C**H_2-O), 50.62 (**C**H-NH), 39.20 (**C**H_2-$(CH_3)_2$), 31.30, 29.06, 29.04, 29.01, 28.93, 28.91, 28.71, 28.55, 27.87, 25.21, 23.78, 22.09, 21.84, 20.74, 13.88.

*hexadecyl L-leucinate ammonium tosylate salt (**5g**)*

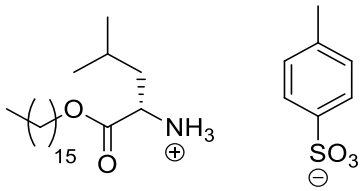

Preparation was achieved following the method A using commercially available hexadecan-1-ol and *L*-Leu.

93%; white powder; **^{1}H NMR** (400 MHz, DMSO-d_6), δ (ppm): 8.33 (s, 3H, N**H$_3$**), 7.50 (d, *J* = 7.9 Hz, 2H, Ar-**H**), 7.12 (d, *J* = 7.8 Hz, 2H Ar-**H**), 4.13 (m, *J* = 10.8, 6.4 Hz, 2H, C**H$_2$**-O), 3.96 (t, *J* = 7.0 Hz, 1H, NH_3-C**H**), 2.29 (s, 3H, Ar-C**H$_3$**), 1.82-1.50 (m, 5H, $(CH_3)_2$-C**H**-C**H$_2$** + C**H$_2$**-CH_2-O), 1.24 (m, 26H, (C**H$_2$**)$_{13}$), 0.88 (m, 9H, C**H$_3$**); **^{13}C NMR** (75 MHz, DMSO-d_6), δ (ppm): 169.87 (**C**=O), 145.37 (**C(i)** Tosyl), 137.74 (**C(p)** Tosyl), 128.03 (**C(m)** Tosyl), 125.48 (**C(o)** Tosyl), 65.57 (**C**H_2-O), 50.61 (**C**H-NH), 39.20 (**C**H_2-$(CH_3)_2$), 31.30, 29.04, 29.01, 28.94, 28.92, 28.71, 28.55, 27.87, 25.21, 23.78, 22.09, 21.84, 20.73, 13.88.

*octadecyl L-leucinate ammonium tosylate salt (**5h**)*

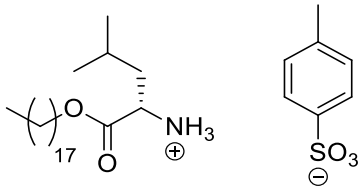

Preparation was achieved following the method A using commercially available octadecan-1-ol and *L*-Leu.

99%; white powder; **^{1}H NMR** (400 MHz, DMSO-d_6), δ (ppm): 8.33 (s, 3H, N**H$_3$**), 7.51 (d, *J* = 7.8 Hz, 2H, Ar-**H**), 7.12 (d, *J* = 7.8 Hz, 2H Ar-**H**), 4.14 (m, *J* = 11.1, 6.4 Hz, 2H, C**H$_2$**-O), 3.97 (t, *J* = 6.9 Hz, 1H, NH_3-C**H**), 2.30 (s, 3H, Ar-C**H$_3$**), 1.83-1.48 (m, 5H, $(CH_3)_2$-C**H**-C**H$_2$** + C**H$_2$**-CH_2-O), 1.24 (m, 30H, (C**H$_2$**)$_{15}$), 0.87 (m, 9H, C**H$_3$**); **^{13}C NMR** (75 MHz, DMSO-d_6), δ (ppm): 169.87 (**C**=O), 145.41 (**C(i)** Tosyl), 137.71 (**C(p)** Tosyl), 128.02 (**C(m)** Tosyl), 125.48 (**C(o)** Tosyl), 65.56 (**C**H_2-O), 50.60 (**C**H-NH), 39.20 (**C**H_2-$(CH_3)_2$), 31.30, 29.05, 29.02, 28.95, 28.93, 28.72, 28.57, 27.87, 25.21, 23.77, 22.08, 21.84, 20.73, 13.86.

VI.3.4.4. Synthesized from L-aspartic acid

*diethyl L-aspartate ammonium chloride salt (**6a**)*

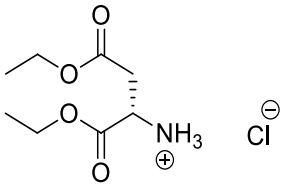

Preparation was achieved following the method B using commercially available ethanol and *L*-Asp.

99%; white powder; **^{1}H NMR** (300 MHz, DMSO-d_6), δ (ppm): 8.85 (s, 3H, N**H**$_3$), 4.37-3.98 (m, 5H, C**H**$_2$-O + C**H**), 3.01 (m, 2H, C**H**$_2$), 1.20 (td, *J* = 7.1, 1.8 Hz, 6H, C**H**$_3$); **^{13}C NMR** (75 MHz, DMSO-d_6), δ (ppm): 169.02 (**C**=O), 168.14 (**C**=O), 61.91 (**C**H_2-O), 60.84 (**C**H_2-O), 48.44 (**C**H), 34.18 (**C**H_2), 13.91 (**C**H_3), 13.79 (**C**H_3).

*dihexyl L-aspartate ammonium tosylate salt (**6b**)*

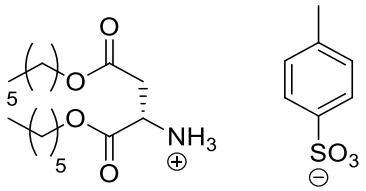

Preparation was achieved following the method A using commercially available hexan-1-ol and *L*-Asp.

63%; white powder; **^{1}H NMR** (300 MHz, DMSO-d_6), δ (ppm): 8.41 (s, 3H, N**H**$_3$), 7.50 (d, *J* = 8.1 Hz, 2H, Ar-**H**), 7.12 (d, *J* = 7.8 Hz, 2H Ar-**H**), 4.35 (t, *J* = 5.4 Hz, 1H, C**H**), 4.22-3.95 (m, 4H, C**H**$_2$-O), 2.91 (m, 2H, C**H**$_2$), 2.29 (s, 3H, Ar-C**H**$_3$), 1.56 (m, *J* = 7.1 Hz, 4H, C**H**$_2$-CH_2-O), 1.28 (m, 12H, (C**H**$_2$)$_3$), 0.87 (t, 6H, C**H**$_3$); **^{13}C NMR** (75 MHz, DMSO-d_6), δ (ppm): 169.13 (**C**=O), 168.31 (**C**=O), 145.31 (**C(i)** Tosyl), 137.83 (**C(p)** Tosyl), 128.07 (**C(m)** Tosyl), 125.49 (**C(o)** Tosyl), 65.89 (**C**H_2-O), 64.88 (**C**H_2-O), 48.58 (**C**H-NH), 34.26 (CH-**C**H_2), 30.87, 30.82, 27.92, 27.82, 24.95, 24.81, 21.97, 20.75, 13.82.

*didodecyl L-aspartate ammonium tosylate salt (**6d**)*

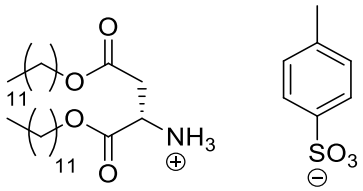

Preparation was achieved following the method A using commercially available dodecan-1-ol and *L*-Asp.

98%; white powder; **^{1}H NMR** (300 MHz, DMSO-d_6), δ (ppm): 8.44 (s, 3H, N**H**$_3$), 7.50 (d, 2H, Ar-**H**), 7.11 (d, *J* = 7.9 Hz, 2H Ar-**H**), 4.36 (t, *J* = 5.4 Hz, 1H, C**H**), 4.23-3.98 (m, 4H, C**H**$_2$-O), 2.92 (qd, *J* = 17.4, 5.4 Hz, 2H, C**H**$_2$), 2.29 (s, 3H, Ar-C**H**$_3$), 1.56 (m, *J* = 6.9 Hz, 4H, C**H**$_2$-CH_2-O), 1.24 (m, 36H, (C**H**$_2$)$_9$), 0.85 (t, 6H, C**H**$_3$); **^{13}C NMR** (75 MHz, DMSO-d_6), δ (ppm): 169.04, 168.19, 145.35, 137.74, 128.03, 125.49, 65.87, 64.84, 48.50, 34.15, 31.33, 29.13, 29.10, 29.06, 29.00, 28.76, 28.70, 27.99, 27.87, 25.32, 25.21, 22.10, 20.73, 13.85.

*ditridecyl L-aspartate ammonium tosylate salt (**6e**)*

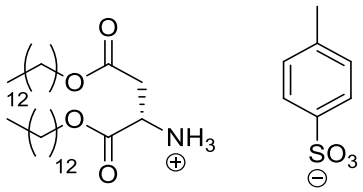

Preparation was achieved following the method A using commercially available tridecan-1-ol and *L*-Asp.

99%; white powder; **^{1}H NMR** (300 MHz, DMSO-d_6), δ (ppm): 8.44 (s, 3H, N**H**$_3$), 7.50 (d, 2H, Ar-**H**), 7.11 (d, *J* = 7.9 Hz, 2H Ar-**H**), 4.36 (t, *J* = 5.4 Hz, 1H, C**H**), 4.24-3.94 (m, 4H, C**H**$_2$-O), 2.92 (qd, *J* = 17.4, 5.4 Hz, 2H, C**H**$_2$), 2.29 (s, 3H, Ar-C**H**$_3$), 1.54 (m, *J* = 6.7 Hz, 4H, C**H**$_2$-CH_2-O), 1.24 (m, 40H, (C**H**$_2$)$_{10}$), 0.84 (t, 6H, C**H**$_3$); **^{13}C NMR** (75 MHz, DMSO-d_6), δ (ppm): 169.02, 168.19, 145.35, 137.73, 128.02, 125.49, 65.86, 64.82, 48.49, 34.14, 31.34, 29.14, 29.11, 29.07, 29.02, 28.76, 28.71, 28.00, 27.87, 25.32, 25.22, 22.10, 20.73, 13.83.

*dihexadecyl L-aspartate ammonium tosylate salt (**6g**)*

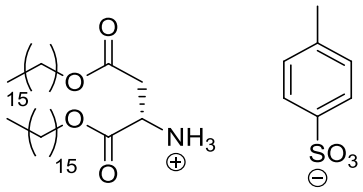

Preparation was achieved following the method A using commercially available hexadecan-1-ol and *L*-Asp.

99%; white powder; **^{1}H NMR** (300 MHz, CD_2Cl_2-d_2 / DMSO-d_6), δ (ppm): 8.47 (s, 3H, N**H**$_3$), 7.56 (d, 2H, Ar-**H**), 7.11 (d, *J* = 7.9 Hz, 2H Ar-**H**), 4.40-3.94 (m, 5H, C**H** + C**H**$_2$-O), 2.94 (m, 2H, C**H**$_2$), 2.31 (s, 3H, Ar-C**H**$_3$), 1.58 (p, *J* = 6.9 Hz, 4H, C**H**$_2$-CH_2-O), 1.24 (m, 52H, (C**H**$_2$)$_{13}$), 0.86 (t, 6H, C**H**$_3$). **^{13}C NMR** (101 MHz, CD_2Cl_2-d_2 / DMSO-d_6), δ (ppm): 168.96, 167.93, 144.14, 138.26, 127.89, 125.32, 65.94, 64.91, 48.53, 33.87, 31.29, 29.06, 29.01, 28.93, 28.71, 28.68, 28.62, 27.91, 27.77, 25.25, 25.14, 22.06, 20.51, 13.52.

*dioctadecyl L-aspartate ammonium tosylate salt (**6h**)*

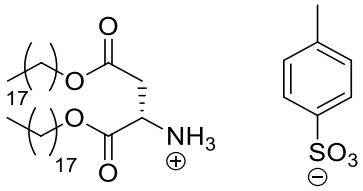

Preparation was achieved following the method A using commercially available octadecan-1-ol and *L*-Asp.

99%; white powder; **^{1}H NMR** (300 MHz, CD_2Cl_2-d_2 / DMSO-d_6), δ (ppm): 8.49 (s, 3H, N**H**$_3$), 7.59 (d, 2H, Ar-**H**), 7.11 (d, *J* = 7.8 Hz, 2H Ar-**H**), 4.32-3.99 (m, 5H, C**H** + C**H**$_2$-O), 2.97 (dd, *J* = 5.4, 3.0 Hz, 2H, C**H**$_2$), 2.32 (s, 3H, Ar-C**H**$_3$), 1.59 (m, *J* = 6.5 Hz, 4H, C**H**$_2$-CH_2-O), 1.24 (m, 60H, (C**H**$_2$)$_{15}$), 0.86 (t, 6H, C**H**$_3$). **^{13}C NMR** (101 MHz, CD_2Cl_2-d_2 / DMSO-d_6), δ (ppm): 169.01, 167.94, 143.96, 138.43, 127.95, 125.35, 66.02, 64.97, 48.55, 33.89, 31.30, 29.06, 28.72, 27.93, 27.80, 25.28, 25.17, 22.08, 20.54, 13.54.

VI.3.5. Di(amido-esters)

VI.3.5.1. Synthesized from L-alaninate ammonium salts

*N^2, N^5-di(ethyl L-alaninate)-furan-2,5-dicarboxamide (**8a**)*

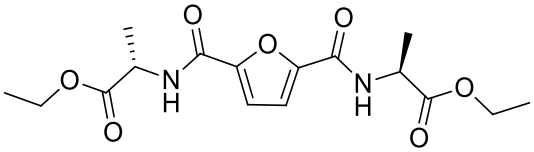

Preparation was achieved following the method F using synthesized ethyl *L*-alaninate ammonium chloride salt and furan-2,5-dicarbonyl dichloride.

84%; yellow solid; **Tf:** 109,6°C; **^{1}H NMR** (400 MHz, CD_2Cl_2-d_2 / DMSO-d_6), δ (ppm): 8.49 (d, *J* = 7.9 Hz, 2H, N**H**), 7.13 (s, 2H, C**H** furan), 4.58 (m, 2H, C**H**-NH), 4.23-4.05 (m, 4H, C**H$_2$**-O), 1.49 (d, *J* = 7.3 Hz, 6H, C**H$_3$**-CH-NH), 1.25 (t, *J* = 7.1 Hz, 6H, C**H$_3$**-CH_2); **^{13}C NMR** (75 MHz, CD_2Cl_2-d_2 / DMSO-d_6), δ (ppm): 172.00 (**C**=O ester), 156.84 (**C**=O amide), 147.69 (**C**-C=O amide), 114.65 (**C**H furan), 60.54 (**C**H_2-O), 47.42 (NH-**C**H), 16.77 (**C**H_3-CH), 13.47 (**C**H_3-CH_2).

*N^2, N^5-di(octyl L-alaninate)-furan-2,5-dicarboxamide (**8c**)*

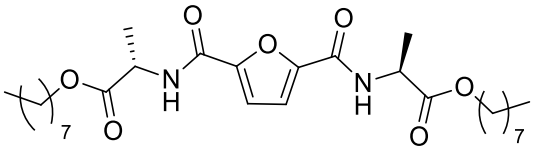

Preparation was achieved following the method F using synthesized octyl *L*-alaninate ammonium chloride salt and furan-2,5-dicarbonyl dichloride.

84%; yellow solid; **Tf:** 51,3°C; **^{1}H NMR** (300 MHz, CD_2Cl_2-d_2 / DMSO-d_6), δ (ppm): 8.53 (d, *J* = 7.6 Hz, 2H, N**H**), 7.13 (s, 2H, C**H** furan), 4.58 (p, *J* = 7.4 Hz, 2H, C**H**-NH), 4.22-3.94 (m, 4H, C**H$_2$**-O), 1.61 (p, *J* = 6.7 Hz, 4H, C**H$_2$**-CH_2-O), 1.48 (d, *J* = 7.3 Hz, 6H, C**H$_3$**-CH-NH), 1.26 (m, 20H, CH_3-(C**H$_2$**)$_5$), 0.84 (t, 6H, C**H$_3$**-CH_2); **^{13}C NMR** (75 MHz, CD_2Cl_2-d_2 / DMSO-d_6), δ (ppm): 172.09 (**C**=O ester), 156.90 (**C**=O amide), 147.72 (**C**-C=O amide), 114.68 (**C**H furan), 64.63 (**C**H_2-O), 47.50 (NH-**C**H), 31.12, 28.52, 27.98, 25.20, 22.00, 16.78, 13.46.

*N^2, N^5-di(dodecyl L-alaninate)-furan-2,5-dicarboxamide (**8d**)*

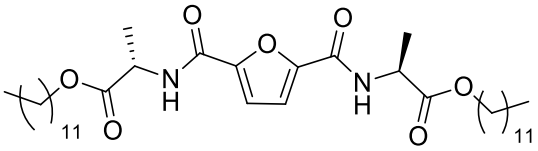

Preparation was achieved following the method F using synthesized dodecyl *L*-alaninate ammonium tosylate salt and furan-2,5-dicarbonyl dichloride.

75%; yellow paste; **^{1}H NMR** (300 MHz, CD_2Cl_2-d_2 / DMSO-d_6), δ (ppm): 8.44 (d, *J* = 7.8 Hz, 2H, N**H**), 7.11 (s, 2H, C**H** furan), 4.61 (p, *J* = 7.3 Hz, 2H, C**H**-NH), 4.18-4.04 (m, 4H, C**H$_2$**-O), 1.62 (p, *J* = 6.9 Hz, 4H, C**H$_2$**-CH_2-O), 1.49 (d, *J* = 7.3 Hz, 6H, C**H$_3$**-CH-NH), 1.25 (m, 36H, CH_3-(C**H$_2$**)$_9$), 0.86 (t, *J* = 6.5 Hz, 6H, C**H$_3$**-CH_2); **^{13}C NMR** (101 MHz, CD_2Cl_2-d_2 / DMSO-d_6), δ (ppm): 172.07 (**C**=O ester), 156.84 (**C**=O amide), 147.71 (**C**-C=O amide), 114.63 (**C**H

furan), 64.63 (**C**H_2-O), 47.44 (NH-**C**H), 31.27, 28.99, 28.97, 28.91, 28.87, 28.69, 28.57, 27.97, 25.20, 22.04, 16.80, 13.43.

*N^2, N^5-di(tridecyl L-alaninate)-furan-2,5-dicarboxamide (**8e**)*

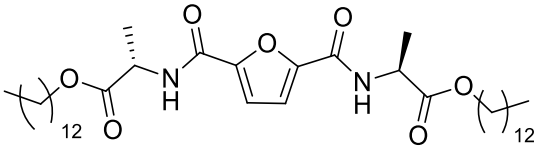

Preparation was achieved following the method F using synthesized tridecyl *L*-alaninate ammonium tosylate salt and furan-2,5-dicarbonyl dichloride.

80%; yellow paste; **^{1}H NMR** (400 MHz, CD_2Cl_2-d_2 / DMSO-d_6), δ (ppm): 8.52 (d, *J* = 7.7 Hz, 2H, N**H**), 7.12 (s, 2H, C**H** furan), 4.59 (p, *J* = 7.4 Hz, 2H, C**H**-NH), 4.09 (m, *J* = 10.8, 6.6 Hz, 4H, C**H_2**-O), 1.61 (p, *J* = 6.7 Hz, 4H, C**H_2**-CH_2-O), 1.48 (d, *J* = 7.3 Hz, 6H, C**H_3**-CH-NH), 1.24 (m, 40H, CH_3-(C**H_2**)$_{10}$), 0.86 (t, *J* = 6.7 Hz, 6H, C**H_3**-CH_2); **^{13}C NMR** (101 MHz, CD_2Cl_2-d_2 / DMSO-d_6), δ (ppm): 172.04 (**C**=O ester), 156.83 (**C**=O amide), 147.63 (**C**-C=O amide), 114.63 (**C**H furan), 64.58 (**C**H_2-O), 47.45 (NH-**C**H), 31.25, 28.99, 28.96, 28.89, 28.85, 28.67, 28.55, 27.96, 25.18, 22.02, 16.77, 13.47.

*N^2, N^5-di(pentadecyl L-alaninate)-furan-2,5-dicarboxamide (**8f**)*

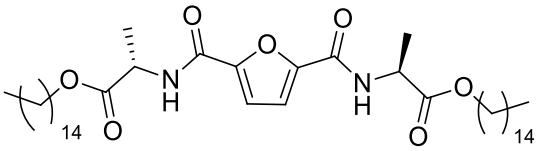

Preparation was achieved following the method F using synthesized pentadecyl *L*-alaninate ammonium tosylate salt and furan-2,5-dicarbonyl dichloride.

63%; yellow paste; **^{1}H NMR** (400 MHz, CD_2Cl_2-d_2 / DMSO-d_6), δ (ppm): 8.50 (d, *J* = 7.7 Hz, 2H, N**H**), 7.12 (s, 2H, C**H** furan), 4.59 (p, *J* = 7.3 Hz, 2H, C**H**-NH), 4.09 (m, *J* = 10.8, 6.5 Hz, 4H, C**H_2**-O), 1.61 (p, *J* = 6.8 Hz, 4H, C**H_2**-CH_2-O), 1.48 (d, *J* = 7.3 Hz, 6H, C**H_3**-CH-NH), 1.24 (m, 48H, CH_3-(C**H_2**)$_{12}$), 0.86 (t, *J* = 6.5 Hz, 6H, C**H_3**-CH_2); **^{13}C NMR** (101 MHz, CD_2Cl_2-d_2 / DMSO-d_6), δ (ppm): 172.04 (**C**=O ester), 156.82 (**C**=O amide), 147.70 (**C**-C=O amide), 114.62 (**C**H furan), 64.58 (**C**H_2-O), 47.43 (NH-**C**H), 31.25, 29.01, 28.99, 28.97, 28.89, 28.85, 28.67, 28.55, 27.96, 25.18, 22.02, 16.77, 13.46.

*N^2, N^5-di(hexadecyl L-alaninate)-furan-2,5-dicarboxamide (**8g**)*

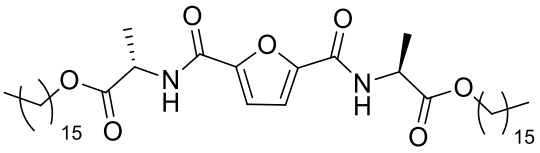

Preparation was achieved following the method F using synthesized hexadecyl *L*-alaninate ammonium tosylate salt and furan-2,5-dicarbonyl dichloride.

71%; yellow solid; **Tf:** 32°C; **^{1}H NMR** (400 MHz, CD_2Cl_2-d_2 / DMSO-d_6), δ (ppm): 8.51 (d, *J* = 7.6 Hz, 2H, N**H**), 7.12 (s, 2H, C**H** furan), 4.60 (p, *J* = 7.3 Hz, 2H, C**H**-NH), 4.09 (m, 4H, C**H$_2$**-O), 1.61 (p, *J* = 6.9 Hz, 4H, C**H$_2$**-CH_2-O), 1.48 (d, *J* = 7.3 Hz, 6H, C**H$_3$**-CH-NH), 1.24 (m, 52H, CH_3-(C**H$_2$**)$_{13}$), 0.86 (t, *J* = 6.7 Hz, 6H, C**H$_3$**-CH_2); **^{13}C NMR** (101 MHz, CD_2Cl_2-d_2 / DMSO-d_6), δ (ppm): 172.19 (**C**=O ester), 172.04 (**C**=O ester), 156.82 (**C**=O amide), 147.70 (**C**-C=O amide), 147.66 (**C**-C=O amide), 114.61 (**C**H furan), 64.58 (**C**H_2-O), 47.43 (NH-**C**H), 47.36 (NH-**C**H), 31.25, 29.12 – 28.44 (m), 27.96, 25.18, 22.02, 16.77 (CH-**C**H_3), 16.69 (CH-**C**H_3), 13.45.

*N^2, N^5-di(octadecyl L-alaninate)-furan-2,5-dicarboxamide (**8h**)*

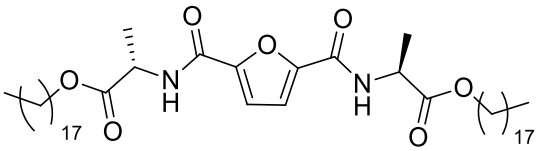

Preparation was achieved following the method F using synthesized octadecyl *L*-alaninate ammonium tosylate salt and furan-2,5-dicarbonyl dichloride.

88%; white solid; **Tf:** 45,3°C; **^{1}H NMR** (400 MHz, CD_2Cl_2-d_2 / DMSO-d_6), δ (ppm): 8.49 (dd, *J* = 13.4, 7.7 Hz, 2H, N**H**), 7.12 (d, *J* = 2.3 Hz, 2H, C**H** furan), 4.62 (pd, *J* = 7.4, 3.1 Hz, 2H, C**H**-NH), 4.18-4.04 (m, 4H, C**H$_2$**-O), 1.62 (m, 4H, C**H$_2$**-CH_2-O), 1.50 (dd, *J* = 7.4, 1.7 Hz, 6H, C**H$_3$**-CH-NH_3), 1.26 (m, 60H, CH_3-(C**H$_2$**)$_{15}$), 0.87 (t, *J* = 6.6 Hz, 6H, C**H$_3$**-CH_2); **^{13}C NMR** (101 MHz, CD_2Cl_2-d_2 / DMSO-d_6), δ (ppm): 172.03 (**C**=O ester), 156.80 (**C**=O amide), 147.67 (**C**-C=O amide), 114.59 (**C**H furan), 64.59, 47.40, 31.23, 28.99, 28.95, 28.88, 28.83, 28.65, 28.54, 27.94, 25.16, 22.01, 16.78, 16.69, 13.41.

VI.3.5.2. Synthesized from L-phenylalaninate ammonium salts

*N^2, N^5-di(ethyl L-phenylalaninate)-furan-2,5-dicarboxamide (**9a**)*

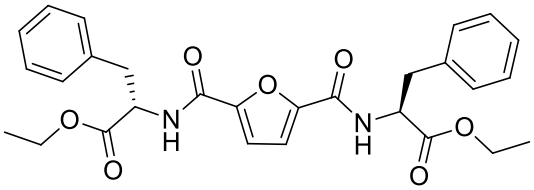

Preparation was achieved following the method F using synthesized ethyl *L*-phenylalaninate ammonium chloride salt and furan-2,5-dicarbonyl dichloride.

62%; yellow solid; **^{1}H NMR** (300 MHz, CD_2Cl_2-d_2 / DMSO-d_6), δ (ppm): 8.56 (d, *J* = 8.1 Hz, 2H, N**H**), 7.32-7.15 (m, 10H, Ar-**H**), 7.10 (s, 2H, C**H** furan), 4.77 (td, *J* = 8.5, 6.0 Hz, 2H, C**H**-NH), 4.14 (q, *J* = 7.1 Hz, 4H, C**H$_2$**-O), 3.30-3.07 (m, 4H, C**H$_2$**-Ph), 1.19 (t, *J* = 7.1 Hz, 6H, C**H$_3$**); **^{13}C NMR** (75 MHz, CD_2Cl_2-d_2 / DMSO-d_6), δ (ppm): 170.91 (**C**=O ester), 156.93 (**C**=O amide), 147.65 (**C**-C=O amide), 136.73 (**C(i)** Ph), 128.74 (**C**H**(m)** Ph), 127.88 (**C**H**(o)** Ph), 126.20 (**C**H**(p)** Ph), 114.67 (**C**H furan), 60.63 (**C**H_2-O), 53.39 (NH-**C**H), 36.75 (**C**H_2-Ph), 13.49 (**C**H_3).

*N^2, N^5-di(hexyl L-phenylalaninate)-furan-2,5-dicarboxamide (**9b**)*

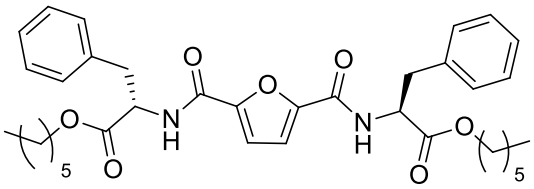

Preparation was achieved following the method F using synthesized hexyl *L*-phenylalaninate ammonium tosylate salt and furan-2,5-dicarbonyl dichloride.

81%; yellow oil; **^{1}H NMR** (400 MHz, CD_2Cl_2-d_2 / DMSO-d_6), δ (ppm): 8.61 (q, *J* = 7.5, 6.1 Hz, 2H, N**H**), 7.38-7.15 (m, 10H, Ar-**H**), 7.11 (s, 2H, C**H** furan), 4.76 (q, *J* = 7.3, 6.8 Hz, 2H C**H**-NH), 4.07 (t, *J* = 6.5 Hz, 4H, C**H$_2$**-O), 3.38-3.03 (m, 4H, C**H$_2$**-Ph), 1.54 (m, 4H, C**H$_2$**-CH_2-O), 1.26 (m, 12H, (C**H$_2$**)$_3$), 0.85 (t, *J* = 6.1 Hz, 6H, C**H$_3$**); **^{13}C NMR** (101 MHz, CD_2Cl_2-d_2 / DMSO-d_6), δ (ppm): 171.01 (**C**=O ester), 156.95 (**C**=O amide), 147.66 (**C**-C=O amide), 136.80 (**C(i)** Ph), 128.72 (**C**H**(m)** Ph), 127.91 (**C**H**(o)** Ph), 126.22 (**C**H**(p)** Ph), 114.67 (**C**H furan), 64.70 (**C**H_2-O), 53.40 (NH-**C**H), 36.73 (**C**H_2-Ph), 30.73, 27.85, 24.83, 21.86, 13.36.

*N^2, N^5-di(octyl L-phenylalaninate)-furan-2,5-dicarboxamide (**9c**)*

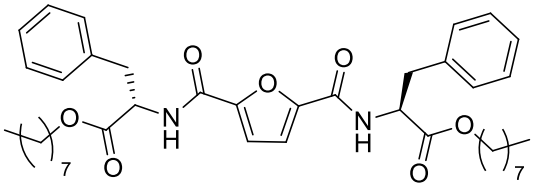

Preparation was achieved following the method F using synthesized octyl *L*-phenylalaninate ammonium tosylate salt and furan-2,5-dicarbonyl dichloride.

80%; yellow oil; **^{1}H NMR** (400 MHz, CD_2Cl_2-d_2 / DMSO-d_6), δ (ppm): 8.65 (d, *J* = 8.3 Hz, N**H (R,S)**), 8.59 (d, *J* = 8.1 Hz, 2H, N**H (S,S)**), 7.41-7.14 (m, 10H, Ar-**H**), 7.10 (s, 2H, C**H** furan **(S,S)**), 7.05 (s, C**H** furan **(R,S)**), 4.76 (m, *J* = 6.1 Hz, 2H, C**H**-NH), 4.08 (m, *J* = 6.5 Hz, 4H, C**H$_2$**-O), 3.39-2.96 (m, 4H, C**H$_2$**-Ph), 1.55 (h, *J* = 6.5 Hz, 4H, C**H$_2$**-CH_2-O), 1.25 (m, 20H, (C**H$_2$**)$_5$), 0.86 (t, *J* = 6.8 Hz, 6H, C**H$_3$**); **^{13}C NMR** (101 MHz, CD_2Cl_2-d_2 / DMSO-d_6), δ (ppm): 171.30 (**C**=O ester **(R,S)**), 170.99 (**C**=O ester **(S,S)**), 156.97 (**C**=O amide **(R,S)**), 156.92 (**C**=O amide **(S,S)**), 147.64 (**C**-C=O amide **(S,S)**), 147.49 (**C**-C=O amide **(R,S)**), 136.80 (**C(i)** Ph **(R,S)**), 136.77 (**C(i)** Ph **(S,S)**), 128.71 (**C**H**(m)** Ph), 127.92 (**C**H**(o)** Ph **(R,S)**), 127.89 (**C**H**(o)** Ph **(S,S)**), 126.24 (**C**H**(p)** Ph **(R,S)**), 126.20 (**C**H**(p)** Ph **(S,S)**), 114.65 (**C**H furan), 64.78 (**C**H_2-O **(R,S)**), 64.70 (**C**H_2-O **(S,S)**), 53.43 (NH-**C**H **(R,S)**), 53.38 (NH-**C**H **(S,S)**), 36.74 (**C**H_2-Ph **(S,S)**), 36.69 (**C**H_2-Ph **(R,S)**), 31.11, 28.49, 28.47, 27.91, 27.87, 25.16, 21.98, 13.46.

*N^2, N^5-di(dodecyl L-phenylalaninate)-furan-2,5-dicarboxamide (**9d**)*

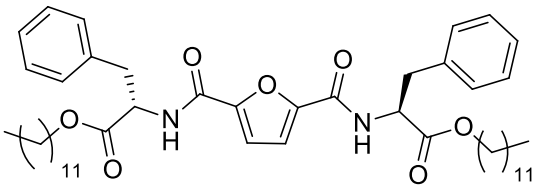

Preparation was achieved following the method F using synthesized dodecyl *L*-phenylalaninate ammonium tosylate salt and furan-2,5-dicarbonyl dichloride.

77%; yellow oil; **^{1}H NMR** (400 MHz, CD_2Cl_2-d_2 / DMSO-d_6), δ (ppm): 8.60 (d, *J* = 8.3 Hz, N**H (R,S)**), 8.50 (d, *J* = 8.1 Hz, 2H, N**H (S,S)**), 7.37-7.14 (m, 10H, Ar-**H**), 7.09 (s, 2H, C**H** furan **(S,S)**), 7.04 (s, C**H** furan **(R,S)**), 4.78 (m, *J* = 6.0 Hz, 2H, C**H**-NH), 4.07 (t, *J* = 6.7 Hz, 4H, C**H$_2$**-O), 3.31-3.08 (m, 4H, C**H$_2$**-Ph), 1.55 (p, *J* = 6.4 Hz, 4H, C**H$_2$**-CH_2-O), 1.25 (m, 36H, (C**H$_2$**)$_9$), 0.86 (t, 6H, C**H$_3$**); **^{13}C NMR** (101 MHz, CD_2Cl_2-d_2 / DMSO-d_6), δ (ppm): 171.30 (**C**=O ester **(R,S)**), 171.01 (**C**=O ester **(S,S)**), 156.98 (**C**=O amide **(R,S)**), 156.95 (**C**=O amide

(S,S)), 147.68 (**C**-C=O amide **(S,S)**), 147.53 (**C**-C=O amide **(R,S)**), 136.84 (**C(i)** Ph), 128.74 (**C**H**(m)** Ph), 127.93 (**C**H**(o)** Ph), 126.23 (**C**H**(p)** Ph), 114.69 (**C**H furan), 64.77 (**C**H_2-O **(R,S)**), 64.68 (**C**H_2-O **(S,S)**), 53.44 (NH-**C**H), 36.70 (**C**H_2-Ph), 31.26, 28.99, 28.97, 28.91, 28.84, 28.68, 28.56, 27.91, 25.18, 22.04, 13.54.

*N^2, N^5-di(tridecyl L-phenylalaninate)-furan-2,5-dicarboxamide (**9e**)*

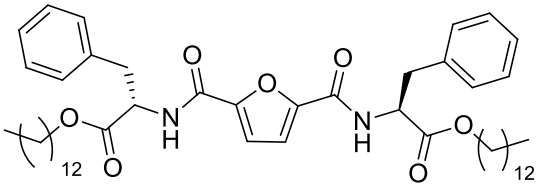

Preparation was achieved following the method F using synthesized tridecyl *L*-phenylalaninate ammonium tosylate salt and furan-2,5-dicarbonyl dichloride.

78%; yellow oil; **^{1}H NMR** (400 MHz, CD_2Cl_2-d_2 / DMSO-d_6), δ (ppm): 8.59 (d, *J* = 8.1 Hz, 2H, N**H**), 7.31-7.16 (m, 10H, Ar-**H**), 7.10 (s, 2H, C**H** furan), 4.77 (td, *J* = 8.4, 6.0 Hz, 2H, C**H**-NH), 4.06 (t, *J* = 6.6 Hz, 4H, C**H$_2$**-O), 3.28-3.10 (m, 4H, C**H$_2$**-Ph), 1.55 (p, *J* = 6.6 Hz, 4H, C**H$_2$**-CH_2-O), 1.25 m, 40H, (C**H$_2$**)$_{10}$), 0.87 (t, *J* = 6.6 Hz, 6H, C**H$_3$**); **^{13}C NMR** (101 MHz, CD_2Cl_2-d_2 / DMSO-d_6), δ (ppm): 170.99 (**C**=O ester), 156.92 (**C**=O amide), 147.66 (**C**-C=O amide), 136.77 (**C(i)** Ph), 128.71 (**C**H**(m)** Ph), 127.89 (**C**H**(o)** Ph), 126.20 (**C**H**(p)** Ph), 114.65 (**C**H furan), 64.69 (**C**H_2-O), 53.39 (NH-**C**H), 36.76 (**C**H_2-Ph), 31.25, 29.01, 28.97, 28.90, 28.83, 28.67, 28.55, 27.89, 25.17, 22.03, 13.49.

*N^2, N^5-di(pentadecyl L-phenylalaninate)-furan-2,5-dicarboxamide (**9f**)*

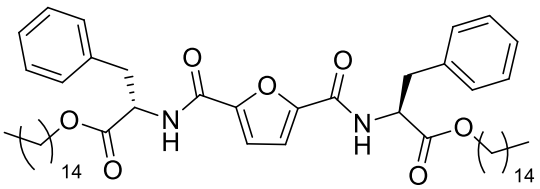

Preparation was achieved following the method F using synthesized pentadecyl *L*-**65%**; yellow solid; **^{1}H NMR** (400 MHz, CD_2Cl_2-d_2 / DMSO-d_6), δ (ppm): 8.59 (d, *J* = 8.1 Hz, 2H, N**H**), 7.32-7.15 (m, 10H, Ar-**H**), 7.10 (s, 2H, C**H** furan), 4.77 (td, *J* = 8.4, 6.0 Hz, 2H, C**H**-NH), 4.07 (t, *J* = 6.6 Hz, 4H, C**H$_2$**-O), 3.30-3.09 (m, 4H, C**H$_2$**-Ph), 1.55 (p, *J* = 6.6 Hz, 4H, C**H$_2$**-CH_2-O), 1.25 m, 48H, (C**H$_2$**)$_{12}$), 0.87 (t, *J* = 6.7 Hz, 6H, C**H$_3$**); **^{13}C NMR** (101 MHz, CD_2Cl_2-d_2 / DMSO-d_6), δ (ppm): 171.02 (**C**=O ester), 156.97 (**C**=O amide), 147.71 (**C**-C=O amide), 136.89 (**C(i)** Ph), 128.77 (**C**H**(m)** Ph), 127.94 (**C**H**(o)** Ph), 126.25 (**C**H**(p)** Ph), 114.71 (**C**H furan), 64.68

(**C**CH_2-O), 53.47 (NH-**C**H), 36.72 (**C**H_2-Ph), 31.29, 29.06, 29.02, 28.95, 28.88, 28.72, 28.60, 27.94, 25.21, 22.07, 13.57.

*N^2, N^5-di(hexadecyl L-phenylalaninate)-furan-2,5-dicarboxamide (**9g**)*

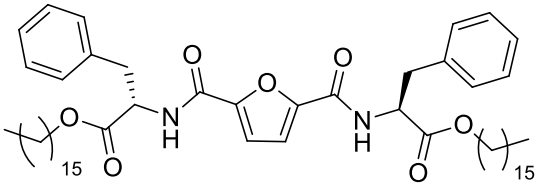

Preparation was achieved following the method F using synthesized hexadecyl *L*-phenylalaninate ammonium tosylate salt and furan-2,5-dicarbonyl dichloride.

70%; yellow paste; **Tf:** 8°C; **^{1}H NMR** (400 MHz, CD_2Cl_2-d_2 / DMSO-d_6), δ (ppm): 8.66 (d, *J* = 8.3 Hz, N**H (R,S)**), 8.60 (d, *J* = 8.1 Hz, 2H, N**H (S,S)**), 7.32 – 7.16 (m, 10H, Ar-**H**), 7.10 (s, 2H, C**H** furan **(S,S)**), 7.05 (s, C**H** furan **(R,S)**), 4.76 (td, *J* = 8.4, 6.0 Hz, 2H, C**H**-NH), 4.06 (t, *J* = 6.7 Hz, 4H, C**H$_2$**-O), 3.31-3.07 (m, 4H, C**H$_2$**-Ph), 1.55 (p, *J* = 6.5 Hz, 4H, C**H$_2$**-CH_2-O), 1.24 (m, 52H, (C**H$_2$**)$_{13}$), 0.86 (t, *J* = 6.6 Hz, 6H, C**H$_3$**); **^{13}C NMR** (101 MHz, CD_2Cl_2-d_2 / DMSO-d_6), δ (ppm): 171.29 (**C**=O ester **(R,S)**), 170.98 (**C**=O ester **(S,S)**), 156.96 (**C**=O amide **(R,S)**), 156.92 (**C**=O amide **(S,S)**), 147.67 (**C**-C=O amide **(S,S)**), 147.51 (**C**-C=O amide **(R,S)**), 136.80 (**C(i)** Ph), 128.72 (**C**H**(m)** Ph), 127.89 (**C**H**(o)** Ph), 126.25 (**C**H**(p)** Ph), 114.65 (**C**H furan), 64.77 (**C**H_2-O **(R,S)**), 64.68 (**C**H_2-O **(S,S)**), 53.40 (NH-**C**H), 36.75 (**C**H_2-Ph), 31.26, 29.02, 28.98, 28.91, 28.84, 28.68, 28.56, 27.90, 25.17, 22.03, 13.50.

*N^2, N^5-di(octadecyl L-phenylalaninate)-furan-2,5-dicarboxamide (**9h**)*

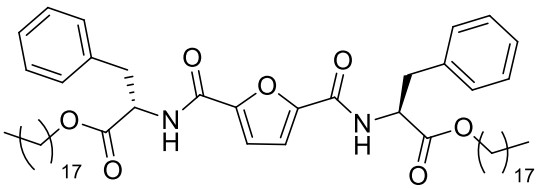

Preparation was achieved following the method F using synthesized octadecyl *L*-phenylalaninate ammonium tosylate salt and furan-2,5-dicarbonyl dichloride.

90%; white solid; **Tf:** 32,7°C; **^{1}H NMR** (400 MHz, CD_2Cl_2-d_2 / DMSO-d_6), δ (ppm): 8.62 (d, *J* = 8.3 Hz, N**H (R,S)**), 8.54 (d, *J* = 8.1 Hz, 2H, N**H (S,S)**), 7.35-7.16 (m, 10H, Ar-**H**), 7.10 (s, 2H, C**H** furan **(S,S)**), 7.05 (s, C**H** furan **(R,S)**), 4.79 (td, *J* = 8.4, 6.1 Hz, 2H, C**H**-NH), 4.10 (dt, *J* = 16.0, 6.7 Hz, 4H, C**H$_2$**-O **(S,S)**), 3.94 (m, C**H$_2$**-O **(R,S)**), 3.44 (q, *J* = 6.3 Hz, C**H$_2$**-Ph **(R,S)**), 3.31-3.11 (m, 4H, C**H$_2$**-Ph **(S,S)**), 1.58 (p, *J* = 6.6 Hz, 4H, C**H$_2$**-CH_2-O), 1.26 (m, 60H, (C**H$_2$**)$_{15}$),

0.86 (t, *J* = 6.6 Hz, 6H, C**H**$_3$); **^{13}C NMR** (101 MHz, CD_2Cl_2-d_2 / DMSO-d_6), δ (ppm): 171.27 (**C**=O ester **(R,S)**), 170.95 (**C**=O ester **(S,S)**), 156.93 (**C**=O amide **(R,S)**), 156.88 (**C**=O amide **(S,S)**), 147.63 (**C**-C=O amide **(S,S)**), 147.47 (**C**-C=O amide **(R,S)**), 136.73 (**C(i)** Ph **(R,S)**), 136.69 (**C(i)** Ph **(R,S)**), 128.67 (**C**H**(m)** Ph), 127.87 (**C**H**(o)** Ph **(R,S)**), 127.85 (**C**H**(o)** Ph **(S,S)**), 126.20 (**C**H**(p)** Ph **(R,S)**), 126.17 (**C**H**(p)** Ph **(S,S)**), 114.61 (**C**H furan), 64.77 (**C**H_2-O **(R,S)**), 64.69 (**C**H_2-O **(S,S)**), 53.39 (NH-**C**H **(R,S)**), 53.34 (NH-**C**H **(R,S)**), 36.79 (**C**H_2-Ph), 31.23, 28.99, 28.96, 28.89, 28.82, 28.65, 28.54, 27.90, 27.86, 25.15, 22.00, 13.43.

VI.3.5.3. Synthesized from L-leucinate ammonium tosylate salts

*N^2, N^5-di(ethyl L-leucinate)-furan-2,5-dicarboxamide (**10a**)*

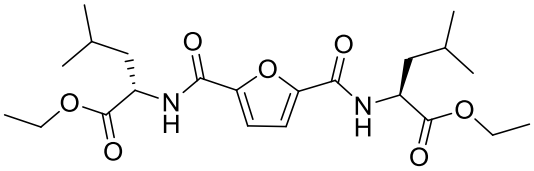

Preparation was achieved following the method F using synthesized ethyl *L*-leucinate ammonium chloride salt and furan-2,5-dicarbonyl dichloride.

85%; yellow oil; **^{1}H NMR** (400 MHz, CD_2Cl_2-d_2 / DMSO-d_6), δ (ppm): 8.51 (dd, *J* = 8.4, 2.6 Hz, 2H, N**H**), 7.17 (d, 2H, C**H** furan), 4.63 (m, 2H, C**H**-NH_3), 4.16 (m, 4H, C**H$_2$**-O), 1.72 (m, 10H, $(CH_3)_2$-C**H**-C**H$_2$**), 1.25 (m, 6H, C**H$_3$**), 0.94 (m, 12H, CH-(C**H$_3$**)$_2$); **^{13}C NMR** (101 MHz, CD_2Cl_2-d_2 / DMSO-d_6), δ (ppm): 172.02 (**C**=O ester), 157.12 (**C**=O amide), 147.77 (**C**-C=O amide), 114.74 (**C**H furan), 60.49 (**C**H_2-O), 50.07 (NH-**C**H), 39.81 (**C**H-$(CH_3)_2$), 24.27, 22.33, 20.93, 13.63.

*N^2, N^5-di(octyl L-leucinate)-furan-2,5-dicarboxamide (**10c**)*

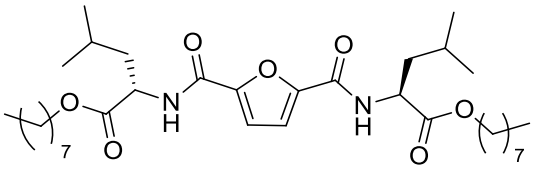

Preparation was achieved following the method F using synthesized octyl *L*-leucinate ammonium tosylate salt and furan-2,5-dicarbonyl dichloride.

89%; yellow oil; **^{1}H NMR** (400 MHz, CD_2Cl_2-d_2 / DMSO-d_6), δ (ppm): 8.47 (d, *J* = 8.3 Hz, 2H, N**H**), 7.15 (s, 2H, C**H** furan), 4.62 (m, 2H, C**H**-NH_3), 4.09 (m, 4H, C**H$_2$**-O), 1.83-1.55 (m,

10H, $(CH_3)_2$-C**H**-C**H₂** + C**H₂**-CH_2-O), 1.26 (m, 20H, CH_3-(C**H₂**)$_5$), 0.94 (dd, *J* = 11.9, 5.1 Hz, 12H, CH-(C**H₃**)$_2$), 0.85 (t, *J* = 6.7 Hz, 6H, C**H₃**-CH_2); **^{13}C NMR** (101 MHz, CD_2Cl_2-d_2 / DMSO-d_6), δ (ppm): 172.06 (**C**=O ester), 157.08 (**C**=O amide), 147.77 (**C**-C=O amide), 114.70 (**C**H furan), 64.52 (**C**H_2-O), 50.09 (NH-**C**H), 39.87 (**C**H-$(CH_3)_2$), 31.08, 28.49, 28.46, 27.93, 25.19, 24.28, 22.26, 21.97, 20.97, 13.47.

*N^2, N^5-di(dodecyl L-leucinate)-furan-2,5-dicarboxamide (**10d**)*

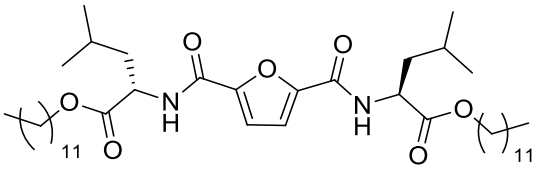

Preparation was achieved following the method F using synthesized dodecyl *L*-leucinate ammonium tosylate salt and furan-2,5-dicarbonyl dichloride.

88%; yellow oil; **^{1}H NMR** (400 MHz, CD_2Cl_2-d_2 / DMSO-d_6), δ (ppm): 8.47 (d, *J* = 8.3 Hz, 2H, N**H**), 7.15 (s, 2H, C**H** furan), 4.62 (m, 2H, C**H**-NH_3), 4.09 (m, 4H, C**H₂**-O), 1.84-1.52 (m, 10H, $(CH_3)_2$-C**H**-C**H₂** + C**H₂**-CH_2-O), 1.25 (m, 36H, CH_3-(C**H₂**)$_9$), 0.94 (dd, *J* = 11.7, 5.3 Hz, 12H, CH-(C**H₃**)$_2$), 0.86 (t, *J* = 6.6 Hz, 6H, C**H₃**-CH_2); **^{13}C NMR** (101 MHz, CD_2Cl_2-d_2 / DMSO-d_6), δ (ppm): 172.04 (**C**=O ester), 157.07 (**C**=O amide), 147.78 (**C**-C=O amide), 114.69 (**C**H furan), 64.50 (**C**H_2-O), 50.10 (NH-**C**H), 39.88 (**C**H-$(CH_3)_2$), 31.24, 28.96, 28.94, 28.87, 28.84, 28.66, 28.52, 27.94, 25.20, 24.28, 22.27, 22.02, 20.99, 13.49.

*N^2, N^5-di(tridecyl L-leucinate)-furan-2,5-dicarboxamide (**10e**)*

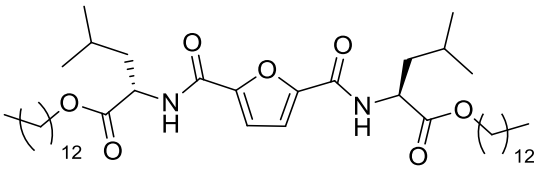

Preparation was achieved following the method F using synthesized tridecyl *L*-leucinate ammonium tosylate salt and furan-2,5-dicarbonyl dichloride.

73%; yellow oil; **^{1}H NMR** (300 MHz, CD_2Cl_2-d_2 / DMSO-d_6), δ (ppm): 8.47 (d, *J* = 8.3 Hz, 2H, N**H**), 7.15 (s, 2H, C**H** furan), 4.62 (m, 2H, C**H**-NH_3), 4.08 (m, 4H, C**H₂**-O), 1.85-1.52 (m, 10H, $(CH_3)_2$-C**H**-C**H₂** + C**H₂**-CH_2-O), 1.24 (m, 40H, CH_3-(C**H₂**)$_{10}$), 0.94 (dd, *J* = 8.7, 5.7 Hz, 12H, CH-(C**H₃**)$_2$), 0.85 (t, *J* = 6.7 Hz, 6H, C**H₃**-CH_2); **^{13}C NMR** (75 MHz, CD_2Cl_2-d_2 / DMSO-d_6), δ (ppm): 172.02 (**C**=O ester), 157.06 (**C**=O amide), 147.77 (**C**-C=O amide), 114.67 (**C**H

furan), 64.49 (**C**H_2-O), 50.09 (NH-**C**H), 39.87 (**C**H-$(CH_3)_2$), 31.23, 28.97, 28.94, 28.85, 28.82, 28.64, 28.50, 27.93, 25.18, 24.27, 22.25, 22.00, 20.98, 13.48.

N^2, N^5-di(pentadecyl L-leucinate)-furan-2,5-dicarboxamide ***(10f)***

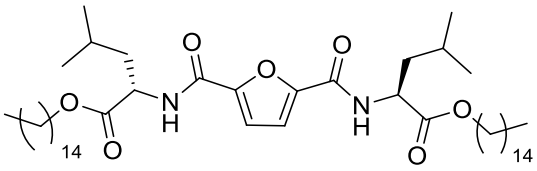

Preparation was achieved following the method F using synthesized pentadecyl *L*-leucinate ammonium tosylate salt and furan-2,5-dicarbonyl dichloride.

65%; yellow oil; **Tf:** -1°C; **^{1}H NMR** (300 MHz, CD_2Cl_2-d_2 / DMSO-d_6), δ (ppm): 8.53 (d, N**H (R,S)**), 8.47 (d, *J* = 8.3 Hz, 2H, N**H (S,S)**), 7.15 (s, 2H, C**H** furan **(S,S)**), 7.12 (s, C**H** furan **(R,S)**), 4.62 (m, 2H, C**H**-NH_3), 4.08 (m, 4H, C**H$_2$**-O), 1.85-1.52 (m, 10H, $(CH_3)_2$-C**H**-C**H$_2$** + C**H$_2$**-CH_2-O), 1.24 (m, 48H, CH_3-(C**H$_2$**)$_{12}$), 0.94 (dd, *J* = 8.7, 5.8 Hz, 12H, CH-(C**H$_3$**)$_2$), 0.85 (t, *J* = 6.6 Hz, 6H, C**H$_3$**-CH_2); **^{13}C NMR** (75 MHz, CD_2Cl_2-d_2 / DMSO-d_6), δ (ppm): 172.02 (**C**=O ester), 157.06 (**C**=O amide), 147.77 (**C**-C=O amide), 114.68 (**C**H furan), 64.49 (**C**H_2-O), 50.10 (NH-**C**H), 39.87 (**C**H-$(CH_3)_2$), 31.23, 28.98, 28.95, 28.86, 28.83, 28.65, 28.51, 27.93, 25.18, 24.28, 22.26, 22.01, 20.99, 13.49.

N^2, N^5-di(hexadecyl L-leucinate)-furan-2,5-dicarboxamide ***(10g)***

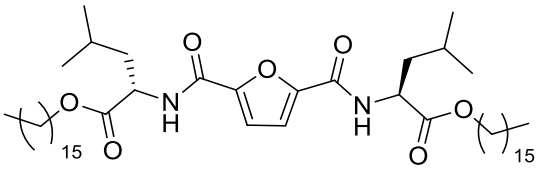

Preparation was achieved following the method F using synthesized hexadecyl *L*-leucinate ammonium tosylate salt and furan-2,5-dicarbonyl dichloride.

88%; yellow paste; **Tf:** 11,6°C; **^{1}H NMR** (400 MHz, CD_2Cl_2-d_2 / DMSO-d_6), δ (ppm): 8.50 (d, *J* = 8.2 Hz, N**H (R,S)**), 8.43 (d, *J* = 8.3 Hz, 2H, N**H (S,S)**), 7.14 (s, 2H, C**H** furan **(S,S)**), 7.11 (s, C**H** furan **(R,S)**), 4.63 (m, 2H, C**H**-NH), 4.09 (m, 4H, C**H$_2$**-O), 1.84-1.53 (m, 10H, $(CH_3)_2$-C**H**-C**H$_2$** + C**H$_2$**-CH_2-O), 1.24 (m, 52H, (C**H$_2$**)$_{13}$), 0.95 (m, 12H, CH-(C**H$_3$**)$_2$), 0.86 (t, *J* = 6.7 Hz, 6H, C**H$_3$**); **^{13}C NMR** (75 MHz, CD_2Cl_2-d_2 / DMSO-d_6), δ (ppm): 172.30 (**C**=O ester **(R,S)**), 172.04 (**C**=O ester **(S,S)**), 157.10 (**C**=O amide **(R,S)**), 157.05 (**C**=O amide **(S,S)**), 147.76 (**C**-C=O amide **(S,S)**), 147.63 (**C**-C=O amide **(R,S)**), 114.66 (**C**H furan **(S,S)**), 114.54 (**C**H furan **(R,S)**), 64.51 (**C**H_2-O), 50.20 (NH-**C**H **(R,S)**), 50.07 (NH-**C**H **(S,S)**), 39.63 (**C**H-$(CH_3)_2$),

31.24, 28.99, 28.96, 28.87, 28.83, 28.66, 28.51, 27.92, 25.18, 24.34, 24.27, 22.22, 22.01, 20.96, 20.84, 13.45.

*N^2, N^5-di(octadecyl L-leucinate)-furan-2,5-dicarboxamide (**10h**)*

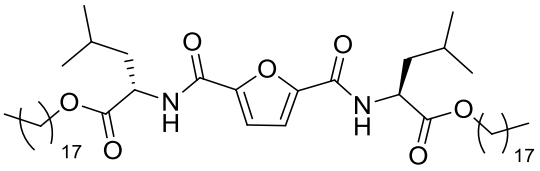

Preparation was achieved following the method F using synthesized octadecyl *L*-leucinate ammonium tosylate salt and furan-2,5-dicarbonyl dichloride.

77%; yellow solid; **Tf:** 26,9°C; **^{1}H NMR** (400 MHz, CD_2Cl_2-d_2 / DMSO-d_6), δ (ppm): 8.52 (d, *J* = 7.9Hz, N**H (R,S)**), 8.45 (d, *J* = 8.2 Hz, 2H, N**H (S,S)**), 7.14 (s, 2H, C**H** furan **(S,S)**), 7.11 (s, C**H** furan **(R,S)**), 4.62 (m, 2H, C**H**-NH), 4.09 (m, 4H, C**H$_2$**-O), 1.83-1.52 (m, 10H, $(CH_3)_2$-C**H**-C**H$_2$** + C**H$_2$**-CH_2-O), 1.24 (m, 60H, $(CH_2)_{15}$), 0.94 (dd, *J* = 11.5, 5.3 Hz, 12H, CH-(C**H$_3$**)$_2$), 0.85 (t, *J* = 6.5 Hz, 6H, C**H$_3$**-CH_2); **^{13}C NMR** (75 MHz, CD_2Cl_2-d_2 / DMSO-d_6), δ (ppm): 172.30 (**C**=O ester **(R,S)**), 172.05 (**C**=O ester **(S,S)**), 157.11 (**C**=O amide **(R,S)**), 157.06 (**C**=O amide **(S,S)**), 147.75 (**C**-C=O amide **(S,S)**), 147.63 (**C**-C=O amide **(R,S)**), 114.68 (**C**H furan **(S,S)**), 114.57 (**C**H furan **(R,S)**), 64.51 (**C**H_2-O), 50.20 (NH-**C**H **(R,S)**), 50.08 (NH-**C**H **(S,S)**), 39.90 (**C**H-$(CH_3)_2$), 31.25, 29.00, 28.96, 28.87, 28.84, 28.67, 28.52, 27.93, 25.19, 24.34, 24.27, 22.25, 22.02, 20.97, 20.85, 13.48.

VI.3.5.4. Synthesized from L-aspartate ammonium salts

*N^2, N^5-bis(diethyl L-aspartate)-furan-2,5-dicarboxamide (**11a**)*

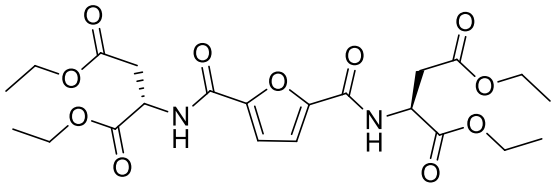

Preparation was achieved following the method F using synthesized diethyl *L*-aspartate ammonium chloride salt and furan-2,5-dicarbonyl dichloride.

82%; yellow oil; **^{1}H NMR** (400 MHz, CD_2Cl_2-d_2 / DMSO-d_6), δ (ppm): 8.73 (d, *J* = 8.2 Hz, 2H, N**H**), 7.16 (s, 2H, C**H** furan), 4.88 (qd, *J* = 7.4, 6.6, 1.3 Hz, 2H, C**H**-NH), 4.25-4.01 (m, 8H, C**H$_2$**-O), 3.08-2.72 (m, 4H, C**H$_2$**-C=O), 1.21 (q, *J* = 7.2 Hz, 12H, C**H$_3$**-CH_2); **^{13}C NMR**

(101 MHz, CD_2Cl_2-d_2 / DMSO-d_6), δ (ppm): 169.98 (**C**=O ester), 169.74 (**C**=O ester), 156.90 (**C**=O amide), 147.66 (**C**-C=O amide), 114.89 (**C**H furan), 60.97 (**C**H_2-O), 60.20 (**C**H_2-O), 48.54 (NH-**C**H), 35.56 (C**H₂**), 13.55 (C**H₃**), 13.53 (C**H₃**).

*N^2, N^5-bis(dihexyl L-aspartate)-furan-2,5-dicarboxamide (**11b**)*

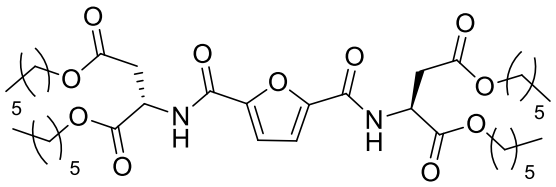

Preparation was achieved following the method F using synthesized dihexyl *L*-aspartate ammonium tosylate salt and furan-2,5-dicarbonyl dichloride.

86%; yellow oil; **^{1}H NMR** (400 MHz, CD_2Cl_2-d_2 / DMSO-d_6), δ (ppm): 8.74 (d, *J* = 8.1 Hz, 2H, N**H**), 7.16 ((d, *J* = 8.1 Hz, 2H, C**H** furan), 4.89 (q, *J* = 7.4 Hz, 2H, C**H**-NH), 4.07 (m, 8H, C**H₂**-O), 3.07-2.79 (m, 4H, C**H₂**-C=O), 1.57 (m, 8H, C**H₂**-CH_2-O), 1.27 (m, 24H, CH_3-(C**H₂**)$_3$), 0.84 (t, *J* = 7.0 Hz, 12H, C**H₃**-CH_2); **^{13}C NMR** (101 MHz, CD_2Cl_2-d_2 / DMSO-d_6), δ (ppm): 170.03 (d, *J* = 4.2 Hz, **C**=O ester), 169.79 (**C**=O ester), 156.86 (**C**=O amide), 147.66 (**C**-C=O amide), 114.81 (**C**H furan), 64.99 (**C**H_2-O), 64.29 (**C**H_2-O), 48.53 (NH-**C**H), 35.52, 30.75, 30.70, 27.89, 27.83, 24.87, 24.80, 21.85, 13.37, 13.34.

*N^2, N^5-bis(didodecyl L-aspartate)-furan-2,5-dicarboxamide (**11d**)*

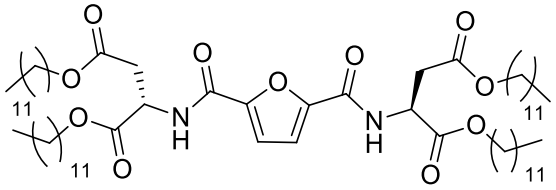

Preparation was achieved following the method F using synthesized didodecyl *L*-aspartate ammonium tosylate salt and furan-2,5-dicarbonyl dichloride.

75%; yellow paste; **Tf:** -1,1°C; **^{1}H NMR** (400 MHz, CD_2Cl_2-d_2 / DMSO-d_6), δ (ppm): 8.69 (d, *J* = 8.1 Hz, 2H, N**H**), 7.14 (s, 2H, C**H** furan), 4.89 (q, *J* = 7.0 Hz, 2H, C**H**-NH), 4.15-4.01 (m, 8H, C**H₂**-O), 3.07-2.76 (m, 4H, C**H₂**-C=O), 1.58 (m, 8H, C**H₂**-CH_2-O), 1.25 (m, 72H, CH_3-(C**H₂**)$_9$), 0.86 (t, *J* = 6.7 Hz, 12H, C**H₃**-CH_2); **^{13}C NMR** (75 MHz, CD_2Cl_2-d_2 / DMSO-d_6), δ (ppm): 169.95 (**C**=O ester), 169.75 (**C**=O ester), 156.82 (**C**=O amide), 147.66 (**C**-C=O amide), 114.79 (**C**H furan), 64.98 (**C**H_2-O), 64.29 (**C**H_2-O), 48.50 (NH-**C**H), 35.56, 31.24, 28.98, 28.95, 28.91, 28.85, 28.66, 28.59, 28.56, 27.94, 27.88, 25.22, 25.17, 22.01, 13.45.

*N^2, N^5-bis(ditridecyl L-aspartate)-furan-2,5-dicarboxamide (**11e**)*

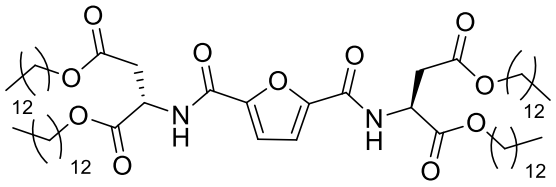

Preparation was achieved following the method F using synthesized ditridecyl *L*-aspartate ammonium tosylate salt and furan-2,5-dicarbonyl dichloride.

74%; yellow paste; **Tf:** 10,3°C; **^{1}H NMR** (400 MHz, CD_2Cl_2-d_2 / DMSO-d_6), δ (ppm): 8.74 (d, *J* = 8.1 Hz, 2H, N**H**), 7.15 (s, 2H, C**H** furan), 4.88 (q, *J* = 7.0 Hz, 2H, C**H**-NH), 4.18-3.98 (m, 8H, C**H$_2$**-O), 3.07-2.76 (m, 4H, C**H$_2$**-C=O), 1.57 (m, 8H, C**H$_2$**-CH_2-O), 1.25 (m, 80H, CH_3-(C**H$_2$**)$_{10}$), 0.86 (t, *J* = 6.7 Hz, 12H, C**H$_3$**-CH_2); **^{13}C NMR** (75 MHz, CD_2Cl_2-d_2 / DMSO-d_6), δ (ppm): 169.97 (**C**=O ester), 169.74 (**C**=O ester), 156.83 (**C**=O amide), 147.69 (**C**-C=O amide), 114.84 (**C**H furan), 64.94 (**C**H_2-O), 64.26 (**C**H_2-O), 48.54 (NH-**C**H), 35.56, 31.25, 29.01, 28.98, 28.93, 28.87, 28.68, 28.61, 28.57, 27.97, 27.90, 25.24, 25.19, 22.02, 13.53.

*N^2, N^5-bis(dihexadecyl L-aspartate)-furan-2,5-dicarboxamide (**11g**)*

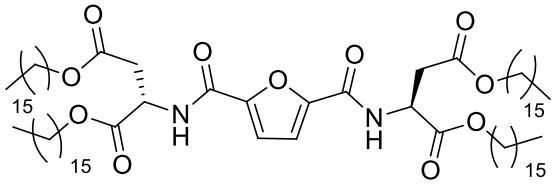

Preparation was achieved following the method F using synthesized dihexadecyl *L*-aspartate ammonium tosylate salt and furan-2,5-dicarbonyl dichloride.

47%; white solid; **Tf:** 37,6°C; **^{1}H NMR** (300 MHz, CD_2Cl_2-d_2 / DMSO-d_6), δ (ppm): 8.68 (d, *J* = 8.1 Hz, 2H, N**H**), 7.14 (s, 2H, C**H** furan), 4.89 (m, 2H, C**H**-NH), 4.19-3.95 (m, 8H, C**H$_2$**-O), 3.07-2.76 (m, 4H, C**H$_2$**-C=O), 1.59 (m, 8H, C**H$_2$**-CH_2-O), 1.24 (m, 104H, CH_3-(C**H$_2$**)$_{13}$), 0.84 (t, 12H, C**H$_3$**-CH_2); **^{13}C NMR** (75 MHz, CD_2Cl_2-d_2 / DMSO-d_6), δ (ppm): 169.94 (**C**=O ester), 169.75 (**C**=O ester), 156.81 (**C**=O amide), 147.66 (**C**-C=O amide), 114.80 (**C**H furan), 64.97 (**C**H_2-O), 64.28 (**C**H_2-O), 48.49 (NH-**C**H), 35.56, 31.25, 29.03, 28.99, 28.93, 28.87, 28.68, 28.61, 28.57, 27.95, 27.89, 25.24, 25.18, 22.02, 13.45.

*N^2, N^5-bis(dioctadecyl L-aspartate)-furan-2,5-dicarboxamide (**11h**)*

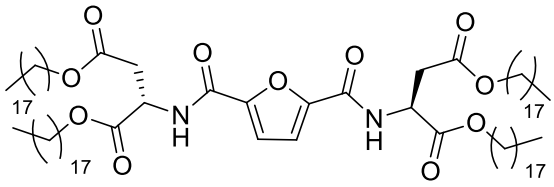

Preparation was achieved following the method F using synthesized dioctadecyl *L*-aspartate ammonium tosylate salt and furan-2,5-dicarbonyl dichloride.

64%; white solid; **Tf:** 50,5°C; **^{1}H NMR** (300 MHz, CD_2Cl_2-d_2 / DMSO-d_6), δ (ppm): 8.68 (d, *J* = 8.1 Hz, 2H, N**H**), 7.14 (s, 2H, C**H** furan), 4.88 (q, 2H, C**H**-NH), 4.19-3.98 (m, 8H, C**H$_2$**-O), 3.07-2.76 (m, 4H, C**H$_2$**-C=O), 1.58 (m, 8H, C**H$_2$**-CH_2-O), 1.24 (m, 120H, CH_3-(C**H$_2$**)$_{15}$), 0.85 (t, 12H, C**H$_3$**-CH_2); **^{13}C NMR** (75 MHz, CD_2Cl_2-d_2 / DMSO-d_6), δ (ppm): 169.94 (**C**=O ester), 169.74 (**C**=O ester), 156.81 (**C**=O amide), 147.66 (**C**-C=O amide), 114.80 (**C**H furan), 64.97 (**C**H_2-O), 64.28 (**C**H_2-O), 48.49 (NH-**C**H), 35.56, 31.26, 29.03, 28.99, 28.94, 28.88, 28.68, 28.62, 28.58, 27.96, 27.89, 25.24, 25.18, 22.02, 13.46.

VI.3.6. Amino-amides

VI.3.6.1. Synthesized from L-alanine

*N-hexyl-L-alaninamide (**12a**)*

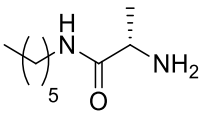

Preparation was achieved following the method G using commercially available hexylamine and *L*-Ala.

95%; white solid; **^{1}H NMR** (300 MHz, DMSO-d_6), δ (ppm): 7.75 (t, *J* = 5.9 Hz, 1H, N**H**), 3.21 (q, *J* = 6.8 Hz, 1H, C**H**), 3.04 (dt, *J* = 7.8, 6.0 Hz, 2H, C**H$_2$**-NH), 2.01 (s, 2H, N**H$_2$**), 1.39 (p, *J* = 7.3 Hz, 2H, C**H$_2$**-CH_2-NH), 1.25 (m, 6H, (C**H$_2$**)$_3$), 1.10 (d, *J* = 6.9 Hz, 3H, C**H$_3$**-CH), 0.84 (t, 3H, C**H$_3$**); **^{13}C NMR** (75 MHz, DMSO-d_6), δ (ppm): 175.44 (**C**=O), 50.25 (**C**H), 38.21 (**C**H_2-NH), 30.97, 29.12, 26.00, 22.02, 21.68, 13.81.

*N-dodecyl-L-alaninamide (**12d**)*

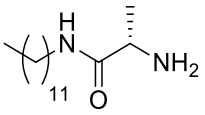

Preparation was achieved following the method G using commercially available dodecylamine and *L*-Ala.

60%; white solid; **^{1}H NMR** (300 MHz, DMSO-d_6), δ (ppm): 7.77 (t, *J* = 5.9 Hz, 1H, N**H**), 3.25 (q, *J* = 6.9 Hz, 1H, C**H**), 3.03 (m 2H, C**H$_2$**-NH), 2.63 (s, 2H, N**H$_2$**), 1.38 (m, 2H, C**H$_2$**-CH_2-NH), 1.26 (m, 18H, (C**H$_2$**)$_9$), 1.11 (d, *J* = 6.9 Hz, 3H, C**H$_3$**-CH), 0.84 (t, 3H, C**H$_3$**); **^{13}C NMR** (75 MHz, DMSO-d_6), δ (ppm): 174.90 (**C**=O), 50.07 (**C**H), 38.22 (**C**H_2-NH), 31.26, 29.11, 29.01, 28.98, 28.96, 28.71, 28.67, 26.31, 22.05, 21.34, 13.90.

VI.3.6.2. Synthesized from L-phenylalanine

*N-hexyl-L-phenylalaninamide (**13a**)*

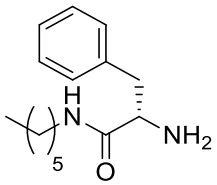

Preparation was achieved following the method G using commercially available hexylamine and *L*-Phe.

98%; white solid; **^{1}H NMR** (300 MHz, DMSO-d_6), δ (ppm): 7.75 (t, *J* = 5.7 Hz, 1H, N**H**), 7.34-7.12 (m, 5H, Ar-**H**), 3.36 (dd, *J* = 7.8, 5.5 Hz, 1H, C**H**), 3.02 (h, *J* = 6.4 Hz, 2H, C**H$_2$**-NH), 2.93-2.56 (m, 2H, C**H$_2$**-Ph), 1.85 (s, 2H, N**H$_2$**), 1.33 (m, 2H, C**H$_2$**-CH_2-NH), 1.21 (m, 6H, (C**H$_2$**)$_3$), 0.84 (t, *J* = 6.8 Hz, 3H, C**H$_3$**); **^{13}C NMR** (75 MHz, DMSO-d_6), δ (ppm): 173.86 (**C**=O amide), 138.68 (**C(i)** Ph), 129.25 (**C**H**(m)** Ph), 128.00 (**C**H**(o)** Ph), 126.01 (**C**H**(p)** Ph), 56.23 (NH_2-**C**H), 41.22 (**C**H_2-NH), 38.29 (**C**H_2-Ph), 30.97, 29.02, 25.99, 22.01, 13.89.

*N-2-ethylhexyl-L-phenylalaninamide (**13b**)*

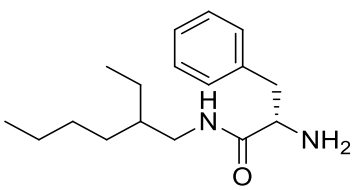

Preparation was achieved following the method G using commercially available 2-ethylhexylamine and *L*-Phe.

99%; white solid; **^{1}H NMR** (300 MHz, DMSO-d_6), δ (ppm): 7.88 (t, *J* = 5.8 Hz, 1H, N**H**), 7.36-7.09 (m, 5H, Ar-**H**), 3.63-3.56 (m, 1H, C**H**), 3.13-2.68 (m, 4H, C**H$_2$**-Ph + NH-C**H$_2$**), 1.42-0.96 (m, 9H, C**H**-C**H$_2$** + (C**H$_2$**)$_3$), 0.82 (m, 6H, C**H$_3$**).

*N-dodecyl-L-phenylalaninamide (**13d**)*

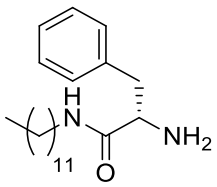

Preparation was achieved following the method G using commercially available dodecylamine and *L*-Phe.

98%; white solid; **^{1}H NMR** (300 MHz, DMSO-d_6), δ (ppm): 7.74 (t, *J* = 5.8 Hz, 1H, N**H**), 7.31-7.13 (m, 5H, Ar-**H**), 3.35 (dd, *J* = 7.9, 5.4 Hz, 1H, C**H**), 3.01 (m, 2H, C**H$_2$**-NH), 2.95-2.54 (m, 2H, C**H$_2$**-Ph), 1.90 (s, 2H, N**H$_2$**), 1.31 (m, 2H, C**H$_2$**-CH$_2$-NH), 1.24 (m, 18H, (C**H$_2$**)$_9$), 0.84 (t, 3H, C**H$_3$**); **^{13}C NMR** (75 MHz, DMSO-d_6), δ (ppm): 173.90 (**C**=O amide), 138.72 (**C(i)** Ph), 129.23 (**C**H**(m)** Ph), 127.97 (**C**H**(o)** Ph), 125.97 (**C**H**(p)** Ph), 56.25 (NH$_2$-**C**H), 41.26 (**C**H$_2$-NH), 38.26 (**C**H$_2$-Ph), 31.27, 29.05, 29.02, 28.97, 28.94, 28.73, 28.68, 26.30, 22.06, 13.91.

*N-octadecyl-L-phenylalaninamide (**13f**)*

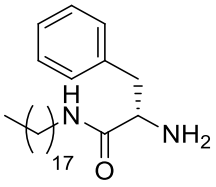

Preparation was achieved following the method G using commercially available octadecylamine and *L*-Phe.

91%; white solid; **^{1}H NMR** (300 MHz, CD_2Cl_2-d_2 / DMSO-d_6), δ (ppm): 7.57 (t, *J* = 5.2 Hz, 1H, N**H**), 7.33-7.09 (m, 5H, Ar-**H**), 3.43 (dd, *J* = 8.4, 4.9 Hz, 1H, C**H**), 3.09 (m, 2H, C**H$_2$**-NH), 3.04-2.61 (m, 2H, C**H$_2$**-Ph), 1.39 (m, 2H, C**H$_2$**-CH$_2$-NH), 1.24 (m, 30H, (C**H$_2$**)$_{15}$), 0.85 (t, 3H, C**H$_3$**). **^{13}C NMR** (101 MHz, CD_2Cl_2-d_2 / DMSO-d_6), δ (ppm): 170.15 (**C**=O amide), 136.28 (**C(i)** Ph), 129.50 (**C**H**(m)** Ph), 128.34 (**C**H**(o)** Ph), 126.78 (**C**H**(p)** Ph), 54.91 (NH$_2$-**C**H), 39.00 (**C**H$_2$-NH), 38.73 (**C**H$_2$-Ph), 31.60, 29.37, 29.35, 29.31, 29.06, 29.01, 26.65, 22.39, 13.86.

VI.3.6.3. Synthesized from L-leucine

*N-hexyl-L-leucinamide (**14a**)*

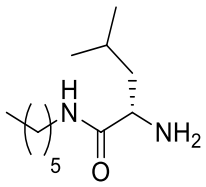

Preparation was achieved following the method G using commercially available hexylamine and *L*-Leu.

77%; white solid; **^{1}H NMR** (300 MHz, DMSO-d_6), δ (ppm): 7.79 (t, *J* = 5.9 Hz, 1H, N**H**), 3.17-2.91 (m, 3H, C**H** + NH-C**H$_2$**), 1.69 (m, 1H, C**H**), 1.37 (m, 2H, C**H$_2$**-CH$_2$-NH), 1.33-1.12 (m, 8H, CH-C**H$_2$** + (C**H$_2$**)$_3$), 0.86 (m, 9H, C**H$_3$**); **^{13}C NMR** (75 MHz, DMSO-d_6), δ (ppm): 175.40 (**C**=O amide), 53.18 (NH$_2$-**C**H), 44.59 (CH-**C**H$_2$), 38.18 (NH-**C**H$_2$), 30.95, 29.10, 25.99, 24.15, 23.13, 22.03, 21.92, 13.85.

*N-2-ethylhexyl-L-leucinamide (**14b**)*

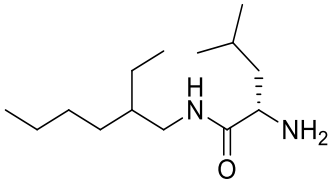

Preparation was achieved following the method G using commercially available 2-ethylhexylamine and *L*-Leu.

88%; white solid; **^{1}H NMR** (300 MHz, DMSO-d_6), δ (ppm): 7.85 (t, *J* = 5.9 Hz, 1H, N**H**), 3.24 (dd, *J* = 8.3, 5.9 Hz, 1H, C**H**), 3.13-2.88 (m, 2H, NH-C**H$_2$**), 1.67 (m, 1H, C**H**), 1.47-1.12 (m, 11H, C**H**-C**H$_2$** + (C**H$_2$**)$_4$), 0.85 (m, 12H, C**H$_3$**); **^{13}C NMR** (75 MHz, DMSO-d_6), δ (ppm): 174.24 (**C**=O amide), 52.77 (NH$_2$-**C**H), 43.81 (CH-**C**H$_2$), 41.16 + 41.13 (NH-**C**H$_2$ **R+S**), 38.85, 38.82, 30.33, 28.36, 28.28, 24.09, 23.62, 22.95, 22.47, 21.99, 13.91, 10.72, 10.67.

*N-decyl-L-leucinamide (**14c**)*

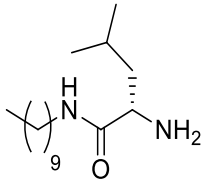

Preparation was achieved following the method G using commercially available decylamine and *L*-Leu.

98%; white solid; **^{1}H NMR** (400 MHz, DMSO-d_6), δ (ppm): 7.78 (t, *J* = 5.8 Hz, 1H, N**H**), 3.15-2.92 (m, 3H, C**H**-NH_2 + NH-C**H$_2$**), 1.67 (m, 1H, C**H**), 1.37 (m, 2H, C**H$_2$**-CH_2-NH), 1.31-1.14 (m, 16H, CH-C**H$_2$** + (C**H$_2$**)$_7$), 0.85 (m, 9H, C**H$_3$**); **^{13}C NMR** (101 MHz, DMSO-d_6), δ (ppm): 174.91 (**C**=O amide), 53.03 (NH_2-**C**H), 44.27 (CH-**C**H_2), 38.23 (NH-**C**H_2), 31.31, 29.10, 29.01, 28.94, 28.73, 28.72, 28.70, 26.33, 24.14, 23.07, 22.10, 21.97, 13.94.

*N-dodecyl-L-leucinamide (**14d**)*

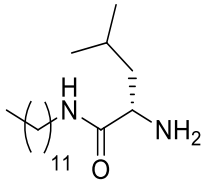

Preparation was achieved following the method G using commercially available dodecylamine and *L*-Leu.

91%; white solid; **^{1}H NMR** (400 MHz, DMSO-d_6), δ (ppm): 7.81 (t, *J* = 5.8 Hz, 1H, N**H**), 3.17-2.94 (m, 3H, C**H** + NH-C**H$_2$**), 1.67 (m, 1H, C**H**), 1.38 (m, 2H, C**H$_2$**-CH_2-NH), 1.32-1.16 (m, 20H, CH-C**H$_2$** + (C**H$_2$**)$_9$), 0.85 (m, 9H, C**H$_3$**); **^{13}C NMR** (101 MHz, DMSO-d_6), δ (ppm): 175.08 (**C**=O amide), 53.08 (NH_2-**C**H), 44.40 (CH-**C**H_2), 38.18 (NH-**C**H_2), 31.29, 29.10, 29.05, 29.01, 28.99, 28.96, 28.72, 28.70, 26.32, 24.13, 23.08, 22.08, 21.93, 13.91.

*N-tetradecyl-L-leucinamide (**14e**)*

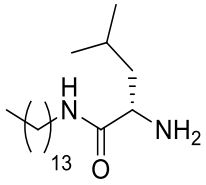

Preparation was achieved following the method G using commercially available tetradecylamine and *L*-Leu.

72%; white solid; **^{1}H NMR** (300 MHz, DMSO-d_6), δ (ppm): 8.49 (t, *J* = 5.6 Hz, 1H, N**H**), 7.59 (s, 2H, N**H$_2$**), 3.61 (t, *J* = 7.1 Hz, 1H, C**H**-NH), 3.08 (m, 2H, NH-C**H$_2$**), 1.60 (m, 1H, C**H**), 1.50 (m, 2H, C**H$_2$**-CH_2-NH), 1.41 (m, 2H, CH-C**H$_2$**), 1.23 (m, 22H, (C**H$_2$**)$_{11}$), 0.87 (m, 9H, C**H$_3$**); **^{13}C NMR** (101 MHz, DMSO-d_6), δ (ppm): 169.44 (**C**=O amide), 51.30 (NH_2-**C**H), 40.82 (CH-

CH_2), 38.57 (NH-**C**H_2), 31.30, 29.06, 29.02, 29.00, 28.98, 28.78, 28.71, 26.32, 23.80, 22.44, 22.30, 22.10, 13.95.

*N-octadecyl-L-leucinamide (**14f**)*

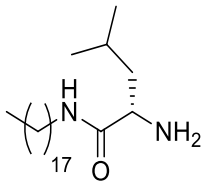

Preparation was achieved following the method G using commercially available octadecylamine and *L*-Leu.

80%; white solid; **^{1}H NMR** (300 MHz, CD_2Cl_2-d_2 / DMSO-d_6), δ (ppm): 7.58 (t, *J* = 7.0 Hz, 1H, N**H**), 3.24-3.02 (m, 3H, C**H** + NH-C**H$_2$**), 1.70 (m, 1H, C**H**-$(CH_3)_2$), 1.61-1.35 (m, 4H, C**H$_2$**-CH_2-NH + CH-C**H$_2$**), 1.24 (m, 30H, $(CH_2)_{15}$), 0.89 (m, 9H, C**H$_3$**); **^{13}C NMR** (75 MHz, CD_2Cl_2-d_2 / DMSO-d_6), δ (ppm): 175.05 (**C**=O amide), 53.01 (NH_2-**C**H), 44.08 (CH-**C**H_2), 38.19 (NH-**C**H_2), 31.22, 29.05, 28.98, 28.92, 28.68, 28.64, 26.30, 24.08, 22.72, 22.00, 21.18, 13.46.

VI.3.6.4. Synthesized from L-aspartic acid

*N-dihexyl-L-aspartamide (**15a**)*

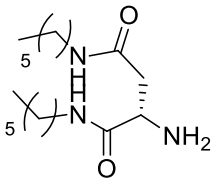

Preparation was achieved following the method G using commercially available hexylamine and *L*-Asp.

76%; white solid; **^{1}H NMR** (400 MHz, DMSO-d_6), δ (ppm): 7.90 (q, *J* = 5.8 Hz, 2H, N**H**), 3.52 (dd, *J* = 8.8, 4.4 Hz, 1H, C**H**), 3.16-2.91 (m, 4H, NH-C**H$_2$**), 2.46-2.12 (m, 2H, CH-C**H$_2$**), 1.28 (m, 16H, $(CH_2)_4$), 0.85 (m, 6H, C**H$_3$**).

*N-bis(2-ethylhexyl)-L-aspartamide (**15b**)*

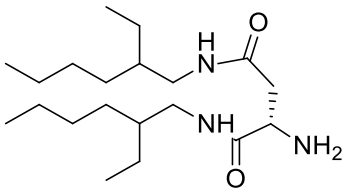

Preparation was achieved following the method G using commercially available 2-ethylhexylamine and *L*-Asp.

49%; white solid; **^{1}H NMR** (300 MHz, DMSO-d_6), δ (ppm): 7.87 (t, J = 5.8 Hz, 1H, N**H**), 7.79 (t, J = 6.0 Hz, 1H, N**H**), 3.49 (dd, J = 9.0, 4.2 Hz, 1H, C**H**), 3.11-2.87 (m, 4H, NH-C**H$_2$**), 2.45-2.13 (m, 2H, NH-CH-C**H$_2$**), 1.48-1.09 (m, 18H, C**H**-C**H$_2$** + (C**H$_2$**)$_3$), 0.84 (m, 12H,C**H$_3$**).**^{13}C NMR** (75 MHz, DMSO-d_6), δ (ppm): 173.80 (**C**=O amide), 170.36 (**C**=O amide), 52.13 (NH_2-**C**H), 41.25 (NH-**C**H_2), 41.15 (NH-**C**H_2), 40.73, 38.79, 30.35, 30.30, 28.34, 28.31, 23.59, 23.54, 22.47, 13.92, 10.67.

VI.3.7. Di(amido-amides)

VI.3.7.1. Synthesized from L-alanine

*N^2, N^5-bis(hexyl L-alaninamide)-furan-2,5-dicarboxamide (**16a**)*

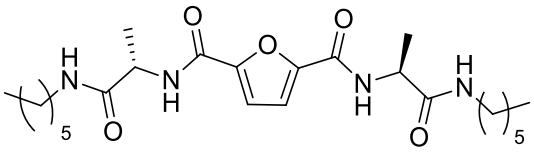

Preparation was achieved following the method H using synthesized *N*-hexyl-*L*-alaninamide and furan-2,5-dicarbonyl dichloride.

80%; white solid; **Tf:** 224°C;**^{1}H NMR** (300 MHz, CD_2Cl_2-d_2 / DMSO-d_6), δ (ppm): 8.38 (d, *J* = 8.0 Hz, 2H, N**H**), 7.77 (t, *J* = 5.8 Hz, 2H, N**H**), 7.10 (s, 2H, C**H** furan), 4.54 (p, *J* = 7.2 Hz, 2H, C**H**-NH), 3.09 (m, 4H, C**H$_2$**-NH), 1.43 (m, 4H, C**H$_2$**-CH_2-NH), 1.38 (d, *J* = 7.0 Hz, 6H, C**H$_3$**-CH-NH), 1.25 (m, 12H, CH_3-(C**H$_2$**)$_3$), 0.84 (t, 6H, C**H$_3$**-CH_2); **^{13}C NMR** (75 MHz, CD_2Cl_2-d_2 / DMSO-d_6), δ (ppm): 171.38 (**C**=O amide), 156.70 (**C**=O amide furan), 147.98 (**C**-C=O amide), 114.52 (**C**H furan), 48.09 (NH-**C**H), 38.62 (**C**H_2-NH), 30.88, 28.86, 25.94, 21.94, 17.98, 13.42; **HRMS (ESI, m/z):** 487.289 $[M + Na]^+$, 487.2891 calculated for $C_{24}H_{40}N_4O_5Na$.

*N^2, N^5-bis(dodecyl L-alaninamide)-furan-2,5-dicarboxamide (**16d**)*

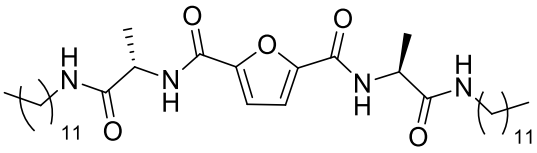

Preparation was achieved following the method H using synthesized *N*-dodecyl-*L*-alaninamide and furan-2,5-dicarbonyl dichloride.

17%; white solid; **Tf:** 202,3°C; **^{1}H NMR** (300 MHz, CD_2Cl_2-d_2 / DMSO-d_6), δ (ppm): 8.43 (d, *J* = 8.0 Hz, 2H, N**H**), 7.87 (t, *J* = 5.8 Hz, 2H, N**H**), 7.13 (s, 2H, C**H** furan), 4.52 (p, *J* = 7.3 Hz, 2H, C**H**-NH), 3.08 (m, 4H, C**H$_2$**-NH), 1.43 (m, 4H, C**H$_2$**-CH_2-NH), 1.37 (d, *J* = 7.1 Hz, 6H, C**H$_3$**-CH-NH), 1.24 (m, 36H, CH_3-(C**H$_2$**)$_9$), 0.85 (t, *J* = 6.5 Hz, 6H, C**H$_3$**-CH_2); **^{13}C NMR** (75 MHz, CD_2Cl_2-d_2 / DMSO-d_6), δ (ppm): 171.39 (**C**=O amide), 156.68 (**C**=O amide furan), 148.01 (**C**-C=O amide), 114.66 (**C**H furan), 48.10 (NH-**C**H), 38.55 (**C**H_2-NH), 31.24, 28.99, 28.94, 28.68, 28.65, 26.28, 22.02, 18.16, 13.66; **HRMS (ESI, m/z):** 655.477 $[M + Na]^+$, 655.4769 calculated for $C_{36}H_{64}N_4O_5Na$.

VI.3.7.2.Synthesized from L-phenylalanine

*N^2, N^5-bis(hexyl L-phenylalaninamide)-furan-2,5-dicarboxamide (**17a**)*

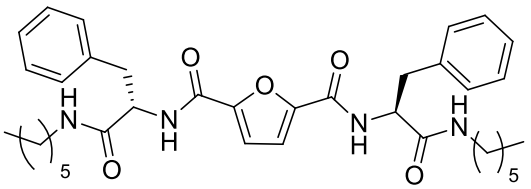

Preparation was achieved following the method H using synthesized *N*-hexyl-*L*-phenylalaninamide and furan-2,5-dicarbonyl dichloride.

37%; white solid; **^{1}H NMR** (300 MHz, CD_2Cl_2-d_2 / DMSO-d_6), δ (ppm): 8.80 (d, *J* = 8.8 Hz, 2H, N**H**), 8.08 (t, *J* = 5.7 Hz, 2H, N**H**), 7.35-7.10 (m, 10H, Ar-**H**), 7.08 (s, 2H, C**H** furan), 4.69 (td, *J* = 8.9, 5.8 Hz, 2H, C**H**-NH), 3.18-2.96 (m, 8H, C**H$_2$**-NH + C**H$_2$**-Ph), 1.38 (p, *J* = 6.8 Hz, 4H, C**H$_2$**-CH_2-NH), 1.22 (m, 12H, CH_3-(C**H$_2$**)$_3$), 0.84 (t, 6H, C**H$_3$**-CH_2); **^{13}C NMR** (75 MHz, CD_2Cl_2-d_2 / DMSO-d_6), δ (ppm): 170.39 (**C**=O amide), 156.78 (**C**=O amide furan), 147.90 (**C**-C=O amide), 137.80 (**C(i)** Ph), 129.04 (**C**H**(m)** Ph), 127.88 (**C**H**(o)** Ph), 126.08 (**C**H**(p)** Ph), 114.64 (**C**H furan), 54.45 (NH-**C**H), 37.75 (**C**H_2-NH), 30.94, 28.83, 25.99, 21.99, 13.68; **HRMS (ESI, m/z):** 639.3516 $[M + Na]^+$, 639.3517 calculated for $C_{36}H_{48}N_4O_5Na$.

*N^2, N^5-bis(2-ethylhexyl L-phenylalaninamide)-furan-2,5-dicarboxamide (**17b**)*

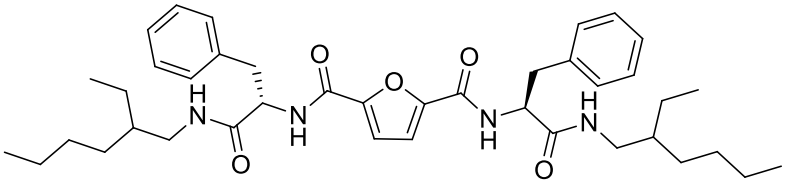

Preparation was achieved following the method H using synthesized *N*-2-ethylhexyl-*L*-phenylalaninamide and furan-2,5-dicarbonyl dichloride.

21%; white solid; **^{1}H NMR** (400 MHz, CD_2Cl_2-d_2 / DMSO-d_6), δ (ppm): 9.09 (d, *J* = 8.9 Hz, 2H, N**H**), 8.02 (t, *J* = 5.8 Hz, 2H, N**H**), 7.38-7.09 (m, 10H, Ar-**H**), 7.03 (s, 2H, C**H** furan), 4.74 (td, *J* = 9.0, 5.9 Hz, 2H, C**H**-NH), 3.19-2.95 (m, 8H, C**H$_2$**-NH + C**H$_2$**-Ph), 1.42 (p, *J* = 5.9 Hz, 2H, C**H**-CH_2-NH), 1.22 (m, 16H, C**H$_2$**-CH_3 + (C**H$_2$**)$_3$), 0.82 (t, *J* = 7.0 Hz, 12H, C**H$_3$**); **^{13}C NMR** (101 MHz, CD_2Cl_2-d_2 / DMSO-d_6), δ (ppm): 170.70 (**C**=O amide), 156.66 (**C**=O amide furan), 147.83 (**C**-C=O amide), 137.84 (**C(i)** Ph), 128.93 (**CH(m)** Ph), 127.72 (**CH(o)** Ph), 125.90 (**CH(p)** Ph), 114.38 (**C**H furan), 54.79 (NH-**C**H), 41.57, 38.64, 37.68, 30.27, 28.28, 28.22, 23.52, 22.39, 13.58, 10.39, 10.34; **HRMS (ESI, m/z):** 695.4143 $[M + Na]^+$, 695.4143 calculated for $C_{40}H_{56}N_4O_5Na$.

*N^2, N^5-bis(dodecyl L-phenylalaninamide)-furan-2,5-dicarboxamide (**17d**)*

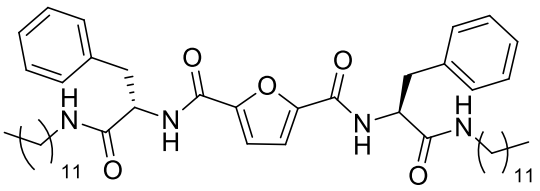

Preparation was achieved following the method H using synthesized *N*-dodecyl-*L*-phenylalaninamide and furan-2,5-dicarbonyl dichloride.

39%; white solid; **Tf:** 181,3°C; **^{1}H NMR** (300 MHz, CD_2Cl_2-d_2 / DMSO-d_6), δ (ppm): 8.57 (d, *J* = 8.6 Hz, 2H, N**H**), 8.01 (t, *J* = 5.7 Hz, 2H, N**H**), 7.35-7.11 (m, 10H, Ar-**H**), 7.09 (s, 2H, C**H** furan), 4.71 (td, *J* = 8.8, 5.7 Hz, 2H, C**H**-NH), 3.18-2.93 (m, 8H, C**H$_2$**-NH + C**H$_2$**-Ph), 1.36 (t, *J* = 6.8 Hz, 4H, C**H$_2$**-CH_2-NH), 1.22 (m, 36H, CH_3-(C**H$_2$**)$_9$), 0.85 (t, *J* = 6.5 Hz, 6H, C**H$_3$**-CH_2); **^{13}C NMR** (75 MHz, CD_2Cl_2-d_2 / DMSO-d_6), δ (ppm): 170.21 (**C**=O amide), 156.79 (**C**=O amide furan), 147.92 (**C**-C=O amide), 137.68 (**C(i)** Ph), 129.02 (**CH(m)** Ph), 127.87 (**CH(o)** Ph), 126.07 (**CH(p)** Ph), 114.64 (**C**H furan), 54.49 (NH-**C**H), 38.62 (**C**H_2-Ph), 37.84 (**C**H_2-

NH), 31.27, 29.03, 28.99, 28.95, 28.88, 28.72, 28.69, 26.31, 22.06, 13.73; **HRMS (ESI, m/z):** 807.5397 $[M + Na]^+$, 807.5395 calculated for $C_{48}H_{72}N_4O_5Na$.

*N^2, N^5-bis(octadecyl L-phenylalaninamide)-furan-2,5-dicarboxamide (**17f**)*

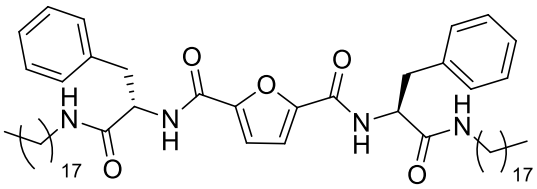

Preparation was achieved following the method H using synthesized *N*-octadecyl-*L*-phenylalaninamide and furan-2,5-dicarbonyl dichloride.

61%; white solid; **Tf:** 167,9°C; **^{1}H NMR** (300 MHz, CD_2Cl_2-d_2 / DMSO-d_6), δ (ppm): 8.60 (d, *J* = 8.7 Hz, 2H, N**H (S,S)**), 8.53 (d, *J* = 9.4 Hz, N**H (R,S)**), 7.88 (t, *J* = 5.7 Hz, 2H, N**H**),), 7.33-7.11 (m, 10H, Ar-**H**), 7.04 (s, 2H, C**H** furan **(S,S)**), 7.00 (s, C**H** furan **(R,S)**), 4.74 (td, *J* = 8.7, 6.0 Hz, 2H, C**H**-NH), 3.35-2.91 (m, 8H, C**H$_2$**-NH + C**H$_2$**-Ph), 1.36 (t, *J* = 6.8 Hz, 4H, C**H$_2$**-CH_2-NH), 1.42-1.21 (m, 64H, (C**H$_2$**)$_{16}$), 0.87 (t, 6H, C**H$_3$**-CH_2); **^{13}C NMR** (75 MHz, CD_2Cl_2-d_2 / DMSO-d_6), δ (ppm): 170.11 (**C**=O amide), 156.69 (**C**=O amide furan), 147.85 (**C**-C=O amide), 137.50 (**C(i)** Ph), 128.87 (**C**H**(m)** Ph), 127.66 (**C**H**(o)** Ph), 125.86 (**C**H**(p)** Ph), 114.38 (**C**H furan), 54.16 (NH-**C**H), 38.63 (**C**H_2-Ph), 37.82 (**C**H_2-NH), 31.23, 28.99, 28.95, 28.92, 28.81, 28.69, 28.65, 26.30, 22.01, 13.50; **HRMS (ESI, m/z):** 975.7275 $[M + Na]^+$, 975.7273 calculated for $C_{60}H_{96}N_4O_5Na$.

VI.3.7.3.Synthesized from L-leucine

*N^2, N^5-bis(hexyl L-leucinamide)-furan-2,5-dicarboxamide (**18a**)*

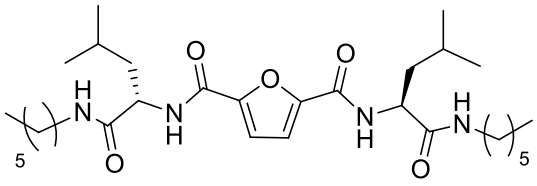

Preparation was achieved following the method H using synthesized *N*-hexyl-*L*-leucinamide and furan-2,5-dicarbonyl dichloride.

52%; white solid; **Tf:** 199,4°C; **^{1}H NMR** (300 MHz, DMSO-d_6), δ (ppm): 8.45 (d, *J* = 8.7 Hz, 2H, N**H**), 8.08 (t, *J* = 5.6 Hz, 2H, N**H**), 7.21 (s, 2H, C**H** furan), 4.53 (td, *J* = 13.9, 6.9 Hz, 2H, C**H**-NH), 3.05 (m, 4H, C**H$_2$**-NH), 1.60 (m, 6H, C**H$_2$**-C**H**-$(CH_3)_2$), 1.39 (p, *J* = 7.0 Hz, 4H, C**H$_2$**-

CH_2-NH), 1.24 (m, 12H, (C**H₂**)₃), 0.87 (m, 18H, C**H₃**); **^{13}C NMR** (101 MHz, DMSO-d_6), δ (ppm): 171.20 (**C**=O amide), 156.92 (**C**=O amide furan), 148.06 (**C**-C=O amide), 115.07 (**C**H furan), 50.95 (NH-**C**H), 40.99 (NH-CH-**C**H_2), 38.50 (**C**H_2-NH), 30.90, 28.90, 25.93, 24.40, 22.88, 22.02, 21.64, 13.83; **HRMS (ESI, m/z):** 571.3831 $[M + Na]^+$, 571.3830 calculated for $C_{30}H_{52}N_4O_5Na$.

*N^2, N^5-bis(2-ethylhexyl L-leucinamide)-furan-2,5-dicarboxamide (**18b**)*

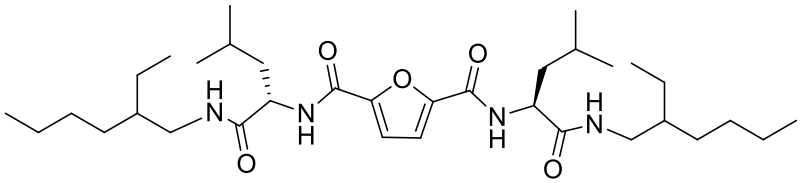

Preparation was achieved following the method H using synthesized *N*-2-ethylhexyl-*L*-leucinamide and furan-2,5-dicarbonyl dichloride.

46%; white solid; **Tf:** 182,3°C; **^{1}H NMR** (400 MHz, DMSO-d_6), δ (ppm): 8.44 (d, *J* = 8.7 Hz, 2H, N**H**), 8.01 (t, *J* = 5.8 Hz, 2H, N**H**), 7.21 (s, 2H, C**H** furan), 4.57 (td, *J* = 9.0, 4.4 Hz, 2H, C**H**-NH), 3.16-2.85 (m, 4H, C**H₂**-NH), 1.61 (m, 6H, C**H₂**-C**H**-$(CH_3)_2$), 1.38 (p, *J* = 6.1 Hz, 2H, C**H**-CH_2-NH), 1.22 (m, 16H, C**H₂**-CH_3 + (C**H₂**)₃), 0.86 (m, 24H, C**H₃**); **^{13}C NMR** (101 MHz, DMSO-d_6), δ (ppm): 171.40 (**C**=O amide), 156.88 (**C**=O amide furan), 148.08 (**C**-C=O amide), 115.06 (**C**H furan), 50.98 (NH-**C**H), 41.40 + 41.36 (**C**H_2-NH), 41.05 (NH-CH-**C**H_2), 38.79 + 38.76 (**C**H-CH_2-NH, **R** + **S**), 30.28, 28.35 + 28.24 (C**H₂** ethyl, **R** + **S**), 24.41, 23.65, 23.60, 22.85, 22.46, 21.70, 13.87, 10.77 + 10.64 (C**H₃** ethyl, **R** + **S**); **HRMS (ESI, m/z):** 627.4455 $[M + Na]^+$, 627.4456 calculated for $C_{34}H_{60}N_4O_5Na$.

*N^2, N^5-bis(decyl L-leucinamide)-furan-2,5-dicarboxamide (**18c**)*

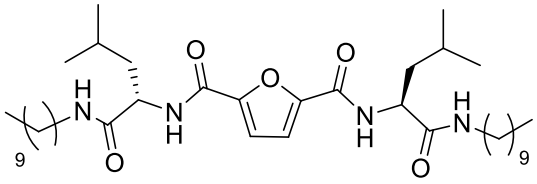

Preparation was achieved following the method H using synthesized *N*-decyl-*L*-leucinamide and furan-2,5-dicarbonyl dichloride.

36%; white solid; **Tf:** 175,4°C; **^{1}H NMR** (300 MHz, DMSO-d_6), δ (ppm): 8.44 (d, *J* = 8.7 Hz, 2H, N**H**), 8.08 (t, *J* = 5.6 Hz, 2H, N**H**), 7.20 (s, 2H, C**H** furan), 4.52 (m, 2H, C**H**-NH), 3.03 (m, 4H, C**H₂**-NH), 1.61 (m, 6H, C**H₂**-C**H**-$(CH_3)_2$), 1.39 (p, *J* = 6.8 Hz, 4H, C**H₂**-CH_2-NH), 1.22

(m, 28H, (C**H**$_2$)$_7$), 0.88 (m, 18H, C**H**$_3$); **^{13}C NMR** (101 MHz, DMSO-d$_6$), δ (ppm): 171.20 (**C**=O amide), 156.89 (**C**=O amide furan), 148.05 (**C**-C=O amide), 115.03 (**C**H furan), 51.01 (NH-**C**H), 41.00 (NH-CH-**C**H$_2$), 38.46 (**C**H$_2$-NH), 31.26, 28.96, 28.89, 28.67, 28.65, 26.23, 24.38, 22.85, 22.06, 21.64, 13.91; **HRMS (ESI, m/z):** 683.5082 [M + Na]$^+$, 683.5082 calculated for $C_{38}H_{68}N_4O_5Na$.

*N^2, N^5-bis(dodecyl L-leucinamide)-furan-2,5-dicarboxamide (**18d**)*

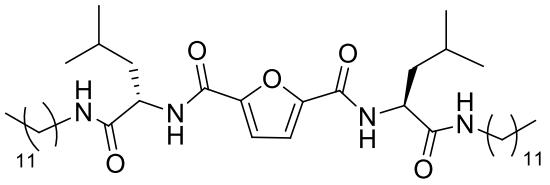

Preparation was achieved following the method H using synthesized *N*-dodecyl-*L*-leucinamide and furan-2,5-dicarbonyl dichloride.

57%; white solid; **Tf:** 156,5°C; **^{1}H NMR** (400 MHz, DMSO-d$_6$), δ (ppm): 8.54 (d, *J* = 8.8 Hz, 2H, N**H**), 8.10 (t, *J* = 5.6 Hz, 2H, N**H**), 7.19 (s, 2H, C**H** furan), 4.51 (td, *J* = 9.2, 4.8 Hz, 2H, C**H**-NH), 3.03 (m, 4H, C**H**$_2$-NH), 1.62 (m, 6H, C**H**$_2$-C**H**-(CH$_3$)$_2$), 1.38 (p, *J* = 6.7 Hz, 4H, C**H**$_2$-CH$_2$-NH), 1.22 (m, 36H, (C**H**$_2$)$_9$), 0.87 (m, 18H, C**H**$_3$); **^{13}C NMR** (101 MHz, DMSO-d$_6$), δ (ppm): 171.24 (**C**=O amide), 156.87 (**C**=O amide furan), 148.05 (**C**-C=O amide), 115.01 (**C**H furan), 51.13 (NH-**C**H), 40.99 (NH-CH-**C**H$_2$), 38.46 (**C**H$_2$-NH), 31.28, 29.03, 28.99, 28.96, 28.94, 28.88, 28.69, 28.66, 26.24, 24.39, 22.85, 22.08, 21.62, 13.92; **HRMS (ESI, m/z):** 739.571 [M + Na]$^+$, 739.5708 calculated for $C_{42}H_{76}N_4O_5Na$.

*N^2, N^5-bis(tetradecyl L-leucinamide)-furan-2,5-dicarboxamide (**18e**)*

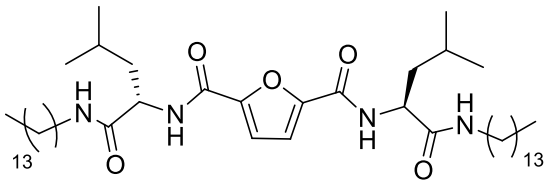

Preparation was achieved following the method H using synthesized *N*-tetradecyl-*L*-leucinamide and furan-2,5-dicarbonyl dichloride.

46%; white solid; **Tf:** 168,8°C; **^{1}H NMR** (300 MHz, CD_2Cl_2-d$_2$ / DMSO-d$_6$), δ (ppm): 8.72 (d, *J* = 8.9 Hz, 2H, N**H**), 8.04 (t, *J* = 5.6 Hz, 2H, N**H**), 7.12 (s, 2H, C**H** furan), 4.55 (td, *J* = 9.3, 4.8 Hz, 2H, C**H**-NH), 3.07 (m, 4H, C**H**$_2$-NH), 1.66 (m, 6H, C**H**$_2$-C**H**-(CH$_3$)$_2$), 1.42 (p, *J* = 6.8 Hz, 4H, C**H**$_2$-CH$_2$-NH), 1.22 (m, 44H, (C**H**$_2$)$_{11}$), 0.88 (m, 18H, C**H**$_3$); **^{13}C NMR** (75 MHz, CD_2Cl_2-

d_2 / DMSO-d_6), δ (ppm): 171.31 (**C**=O amide), 156.76 (**C**=O amide furan), 148.00 (**C**-C=O amide), 114.59 (**C**H furan), 51.35 (NH-**C**H), 41.00 (NH-CH-**C**H_2), 38.52 (**C**H_2-NH), 31.23, 28.99, 28.95, 28.92, 28.81, 28.65, 26.28, 24.28, 22.57, 22.02, 21.41, 13.63; **HRMS (ESI, m/z):** 795.6335 $[M + Na]^+$, 795.6334 calculated for $C_{46}H_{84}N_4O_5Na$.

*N^2, N^5-bis(octadecyl L-leucinamide)-furan-2,5-dicarboxamide (**18f**)*

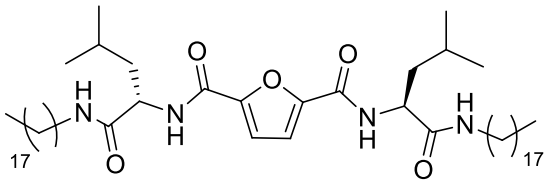

Preparation was achieved following the method H using synthesized *N*-octadecyl-*L*-leucinamide and furan-2,5-dicarbonyl dichloride.

67%; white solid; **Tf:** 163,6°C; **^{1}H NMR** (300 MHz, CD_2Cl_2-d_2 / DMSO-d_6), δ (ppm): 8.30 (d, *J* = 8.8 Hz, 2H, N**H**), 7.72 (t, *J* = 5.7 Hz, 2H, N**H**), 7.10 (s, 2H, C**H** furan), 4.60 (q, *J* = 7.5 Hz, 2H, C**H**-NH), 3.12 (m, 4H, C**H$_2$**-NH), 1.65 (m, 6H, C**H$_2$**-C**H**-$(CH_3)_2$), 1.44 (p, *J* = 6.5 Hz, 4H, C**H$_2$**-CH_2-NH), 1.24 (m, 64H, $(CH_2)_{16}$), 0.89 (m, 18H, C**H$_3$**); **^{13}C NMR** (75 MHz, CD_2Cl_2-d_2 / DMSO-d_6), δ (ppm): 171.11 (**C**=O amide), 156.83 (**C**=O amide furan), 147.97 (**C**-C=O amide), 114.51 (**C**H furan), 50.91 (NH-**C**H), 40.96 (NH-CH-**C**H_2), 38.59 (**C**H_2-NH), 31.24, 29.00, 28.95, 28.93, 28.84, 28.66, 26.29, 24.23, 22.37, 22.01, 21.35, 13.44; **HRMS (ESI, m/z):** 907.7589 $[M + Na]^+$, 907.7586 calculated for $C_{54}H_{100}N_4O_5Na$.

VI.3.7.4. Synthesized from L-aspartic acid

*N^2, N^5-bis(dihexyl L-aspartamide)-furan-2,5-dicarboxamide (**19a**)*

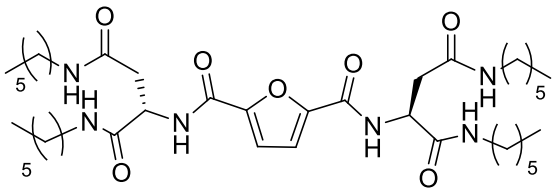

Preparation was achieved following the method H using synthesized *N*-hexyl-*L*-aspartamide and furan-2,5-dicarbonyl dichloride.

27%; white solid; **^{1}H NMR** (300 MHz, DMSO-d_6, 373K), δ (ppm): 8.46 (d, *J* = 8.2 Hz, 2H, N**H**), 7.86 (t, *J* = 5.7 Hz, 2H, N**H**), 7.76 (t, *J* = 5.6 Hz, 2H, N**H**), 7.18 (s, 2H, C**H** furan), 4.72 (td, *J* = 8.0, 5.9 Hz, 2H, C**H**-NH), 3.02 (m, 8H, C**H$_2$**-NH), 2.59 (m, 2H, C**H$_2$**-C=O), 1.46-1.10

(m, 32H, (C**H**$_2$)$_4$), 0.83 (m, 12H, C**H**$_3$); **^{13}C NMR** (101 MHz, CD_2Cl_2-d_2 / DMSO-d_6), δ (ppm): 169.84 (**C**=O amide), 169.26 (**C**=O amide), 156.76 (**C**=O amide furan), 147.97 (**C**-C=O amide), 114.47 (**C**H furan), 49.86 (NH-**C**H), 38.77 (**C**H$_2$-NH), 38.65 (**C**H$_2$-NH), 37.69, 30.91, 30.88, 28.90, 28.83, 26.00, 25.92, 21.93, 13.40; **HRMS (ESI, m/z):** 741.4886 $[M + Na]^+$, 741.4885 calculated for $C_{38}H_{66}N_6O_7Na$.

*N^2, N^5-bis(bis(2-ethylhexyl) L-aspartamide)-furan-2,5-dicarboxamide (**19b**)*

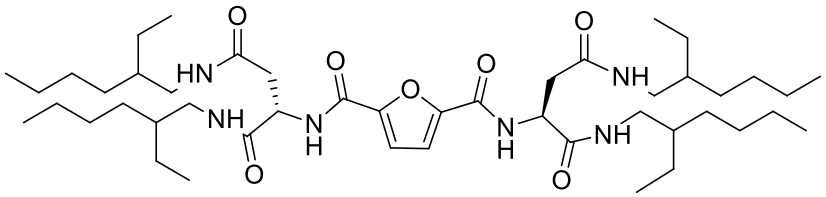

Preparation was achieved following the method H using synthesized *N*-2-ethylhexyl-*L*-aspartamide and furan-2,5-dicarbonyl dichloride.

18%; white solid; **Tf:** 172,8-200,6°C; **^{1}H NMR** (300 MHz, DMSO-d_6), δ (ppm): 8.50 (d, *J* = 8.2 Hz, 2H, N**H**), 7.87 (t, *J* = 5.2 Hz, 2H, N**H**), 7.73 (t, *J* = 4.7 Hz, 2H, N**H**), 7.19 (s, 2H, C**H** furan), 4.75 (q, *J* = 7.3 Hz, 2H, C**H**-NH), 2.97 (m, 8H, C**H**$_2$-NH), 2.59 (d, *J* = 6.9 Hz, 4H, C**H**$_2$-C=O), 1.46-1.01 (m, 36H, C**H**$_2$-C**H**-(C**H**$_2$)$_3$), 0.81 (m, 24H, C**H**$_3$); **^{13}C NMR** (101 MHz, DMSO-d_6), δ (ppm): 170.32 (**C**=O amide), 169.14 (**C**=O amide), 157.85 (**C**=O amide furan), 148.17 (**C**-C=O amide), 114.80 (**C**H furan), 50.11 (NH-**C**H), 41.56 (**C**H$_2$-NH), 41.42 (**C**H$_2$-NH), 38.76 + 38.74 (**C**H-CH$_2$-NH, **R** + **S**), 38.70, 37.73, 28.32 + 28.27 (C**H**$_2$ ethyl, **R** + **S**), 23.50, 23.48, 23.43, 22.47, 22.44, 13.92, 10.68, 10.62 + 10.60 (C**H**$_3$ ethyl, **R** + **S**), 10.55; **HRMS (ESI, m/z):** 853.6168 $[M + Na]^+$, 853.6137 calculated for $C_{46}H_{82}N_6O_7Na$.

VII.Annexes

VII.1. NMR spectra

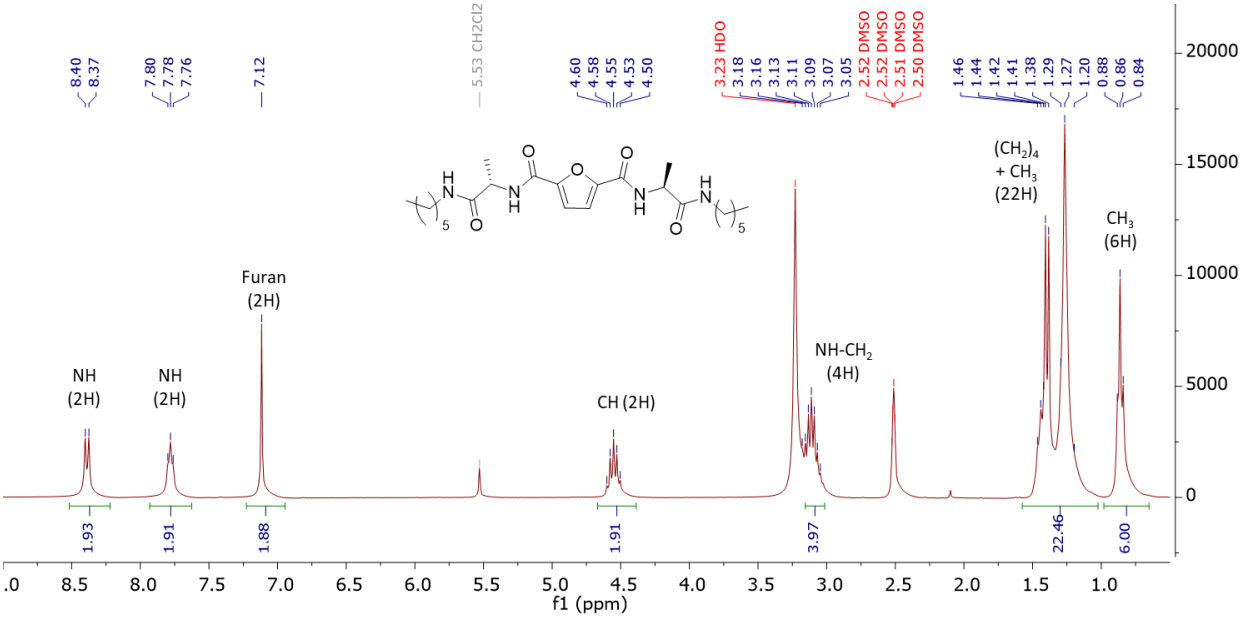

Figure III.14. ^{1}H NMR spectrum of compound **16a** in CD_2Cl_2/DMSO-D_6

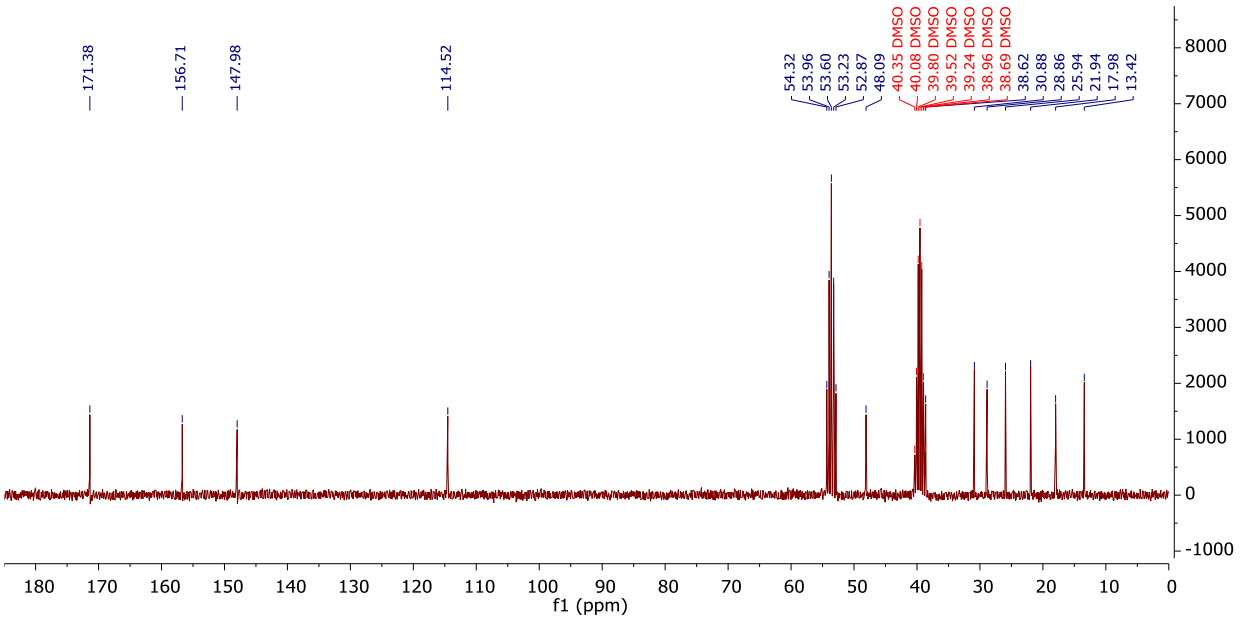

Figure III.15. ^{13}C NMR spectrum of compound **16a** in CD_2Cl_2/DMSO-D_6

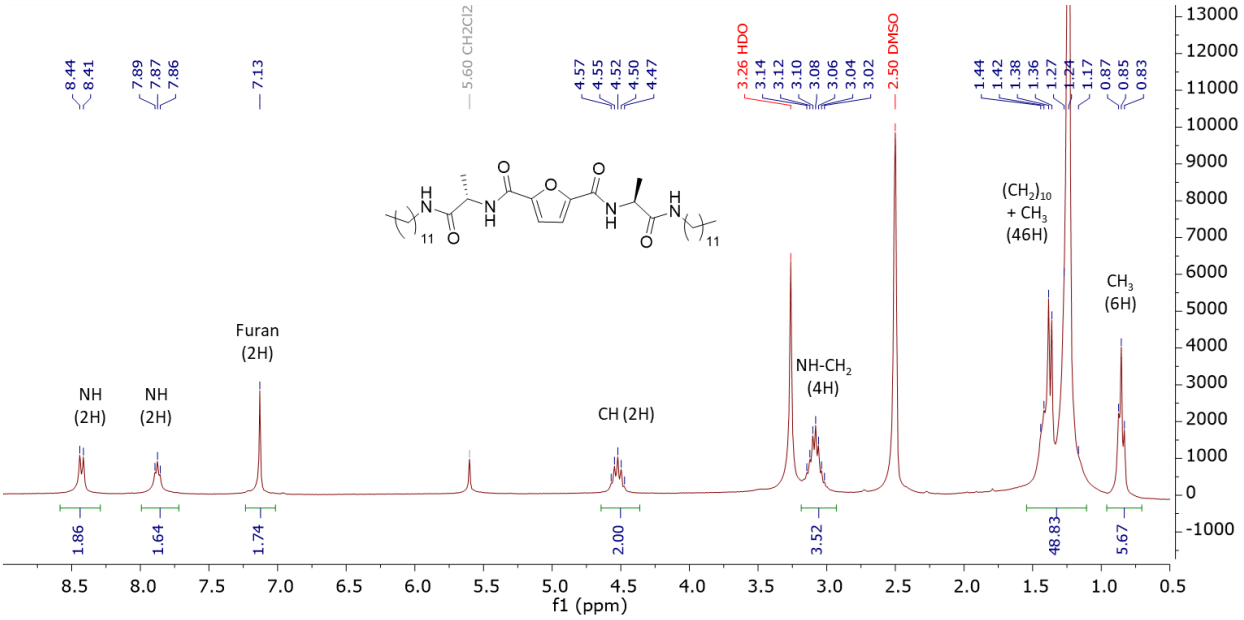

Figure III.16. ^{1}H NMR spectrum of compound **16d** in CD_2Cl_2/DMSO-D_6

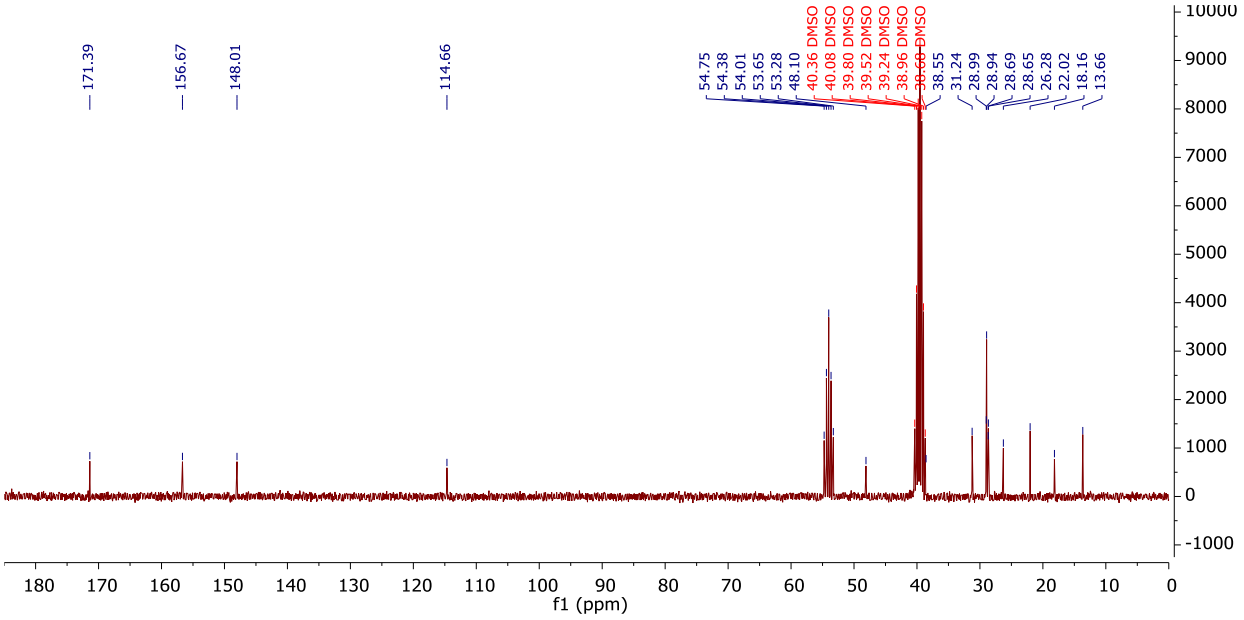

Figure III.17. ^{13}C NMR spectrum of compound **16d** in CD_2Cl_2/DMSO-D_6

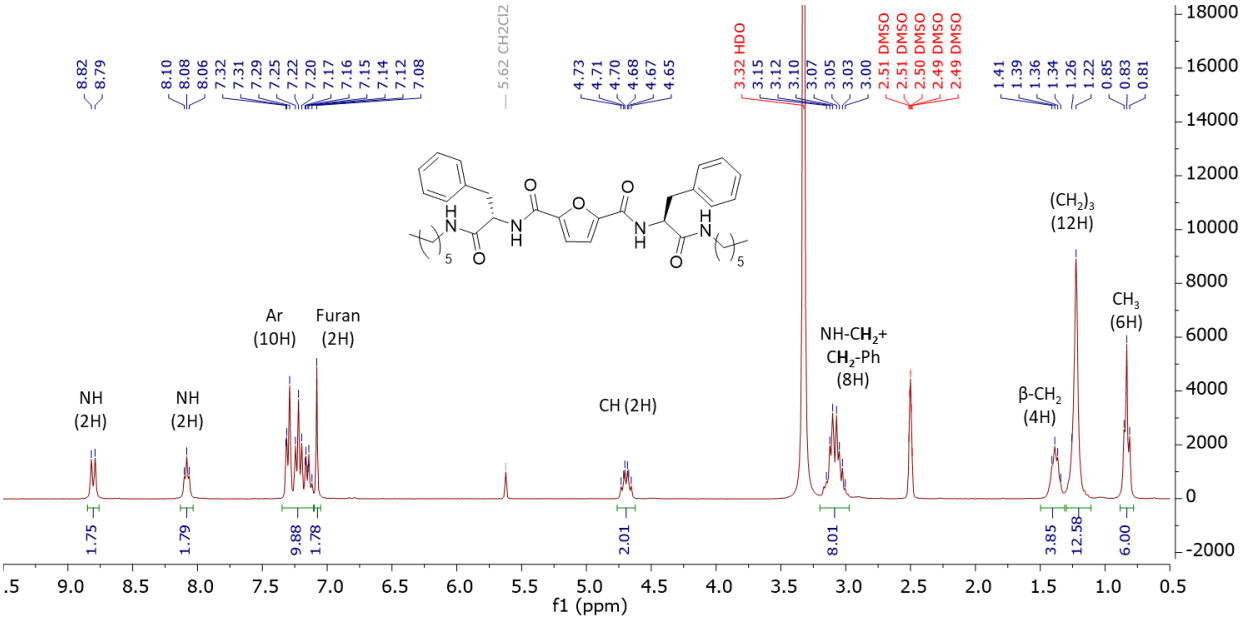

Figure III.18. ^{1}H NMR spectrum of compound **17a** in CD_2Cl_2/DMSO-D_6

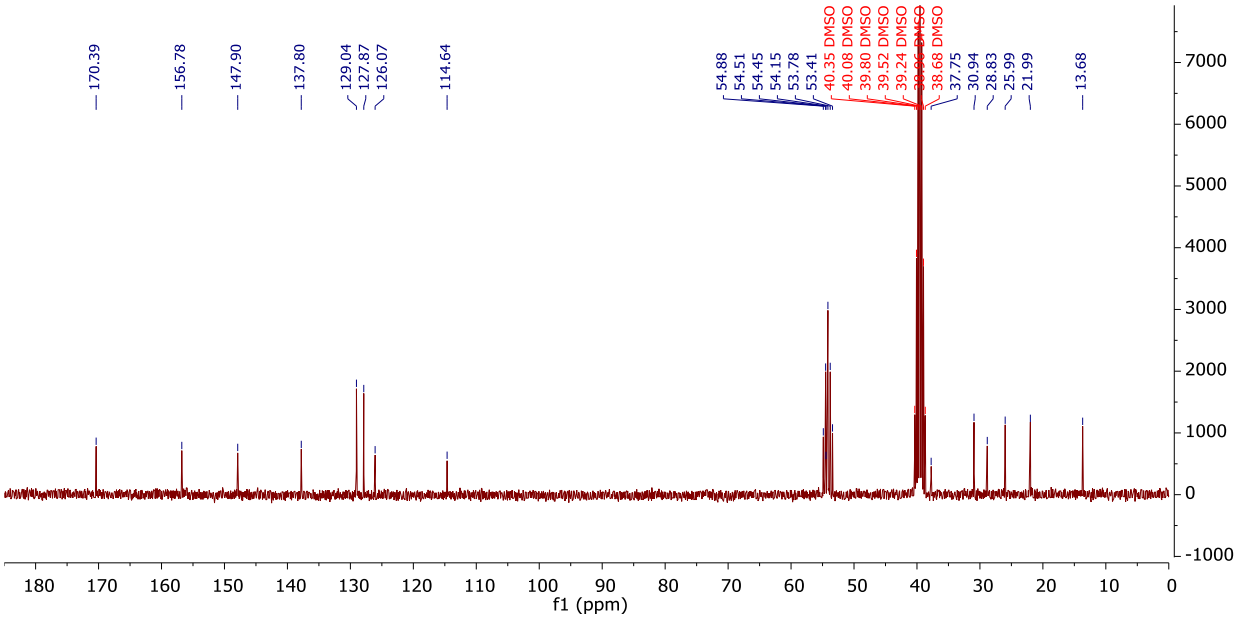

Figure III.19. ^{13}C NMR spectrum of compound **17a** in CD_2Cl_2/DMSO-D_6

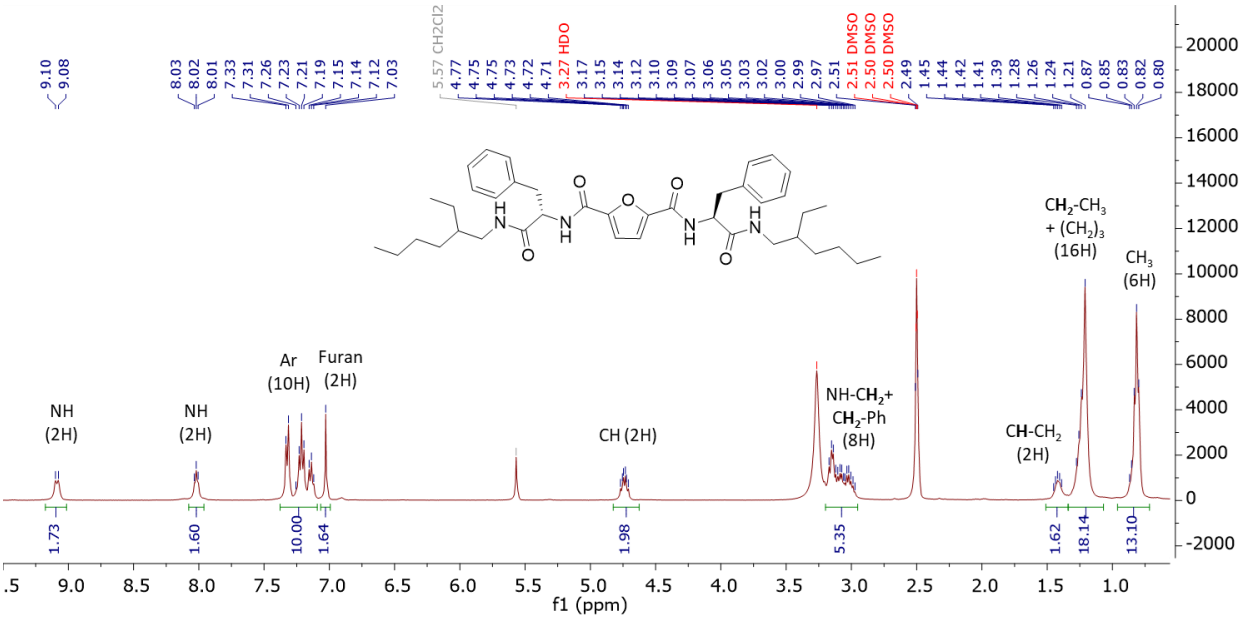

Figure III.20. ^{1}H NMR spectrum of compound **17b** in CD_2Cl_2/DMSO-D_6

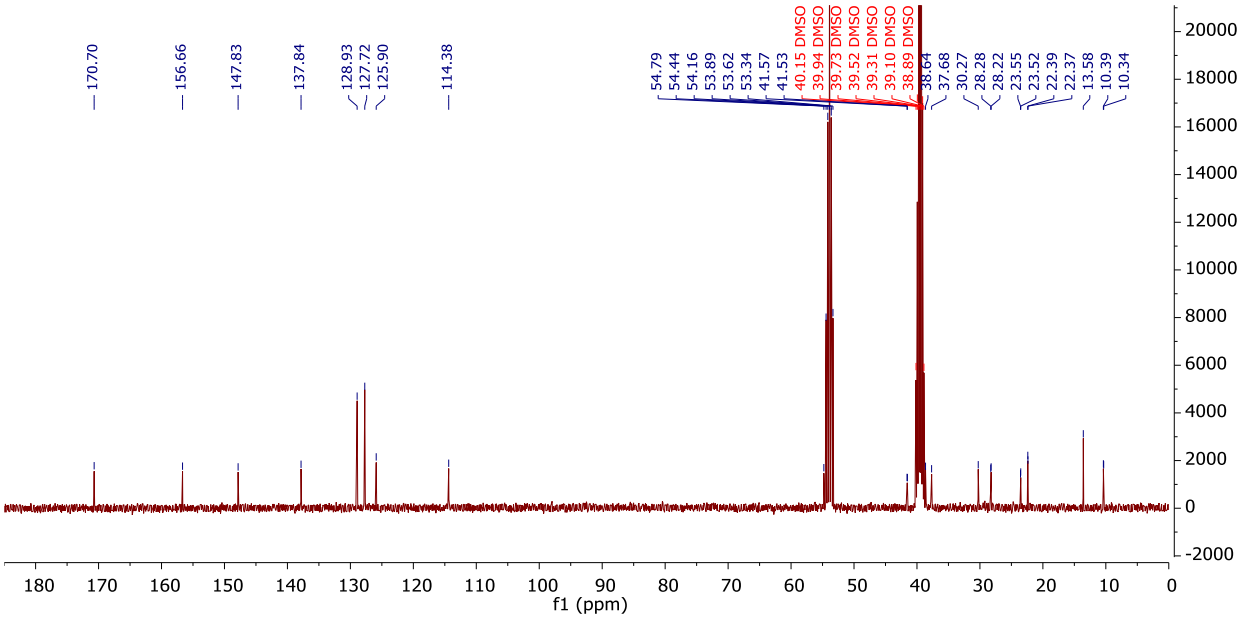

Figure III.21. ^{13}C NMR spectrum of compound **17b** in CD_2Cl_2/DMSO-D_6

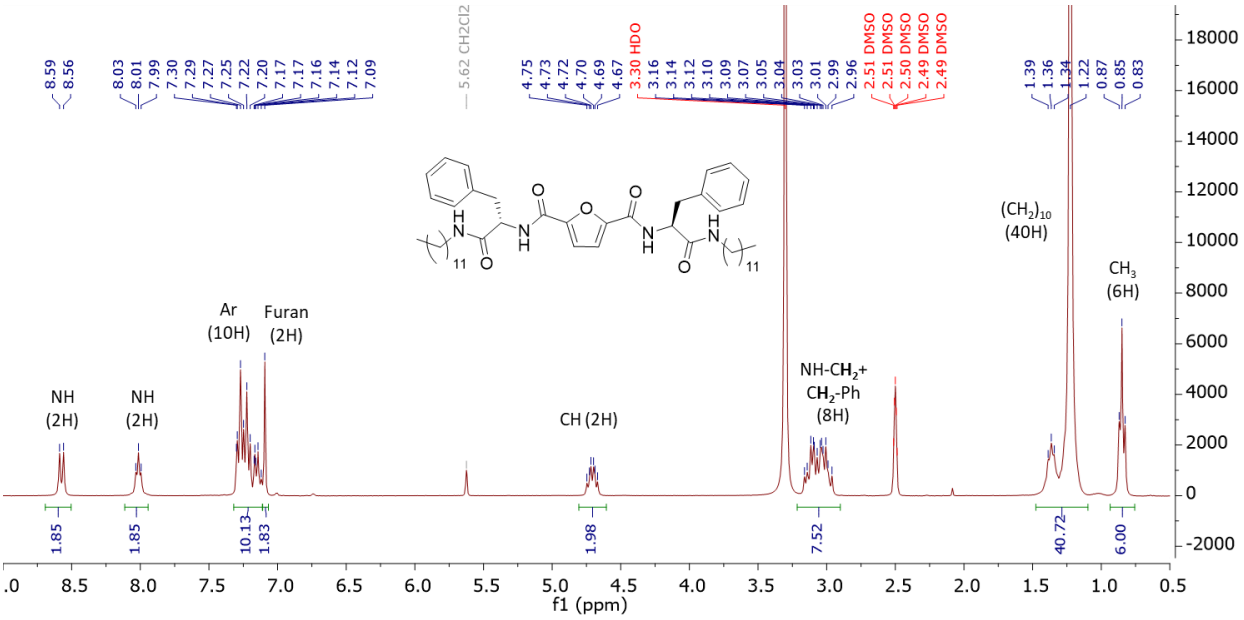

Figure III.22. ^{1}H NMR spectrum of compound **17d** in CD_2Cl_2/DMSO-D_6

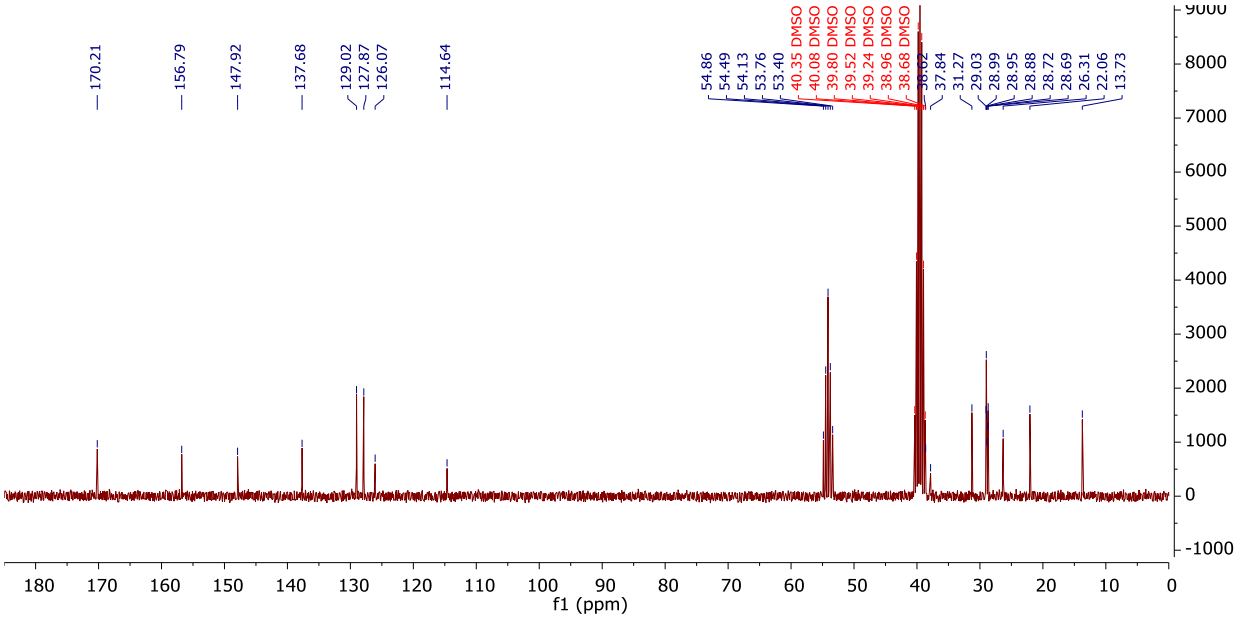

Figure III.23. ^{13}C NMR spectrum of compound **17d** in CD_2Cl_2/DMSO-D_6

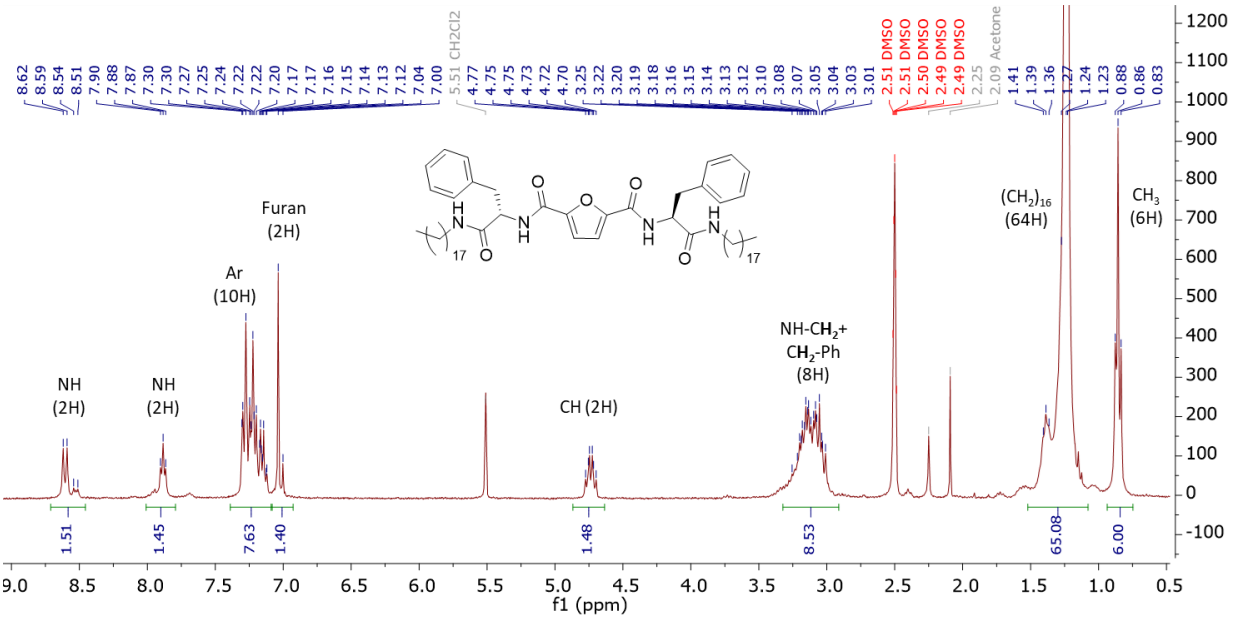

Figure III.24. ^{1}H NMR spectrum of compound **17f** in CD_2Cl_2/DMSO-D_6

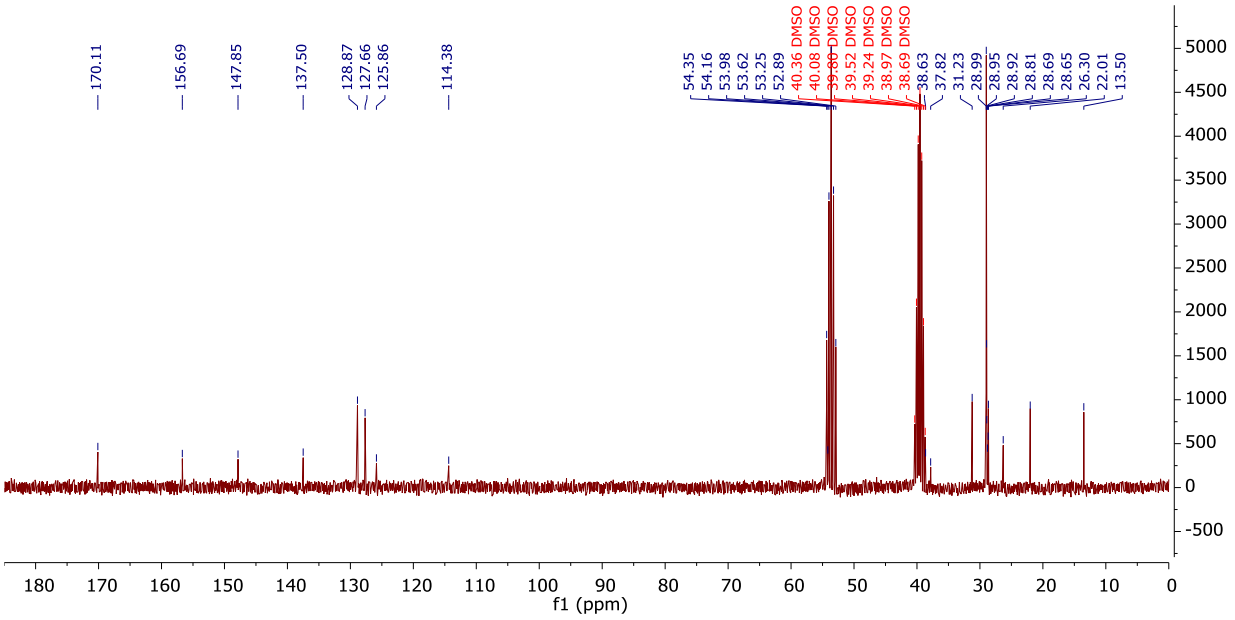

Figure III.25. ^{13}C NMR spectrum of compound **17f** in CD_2Cl_2/DMSO-D_6

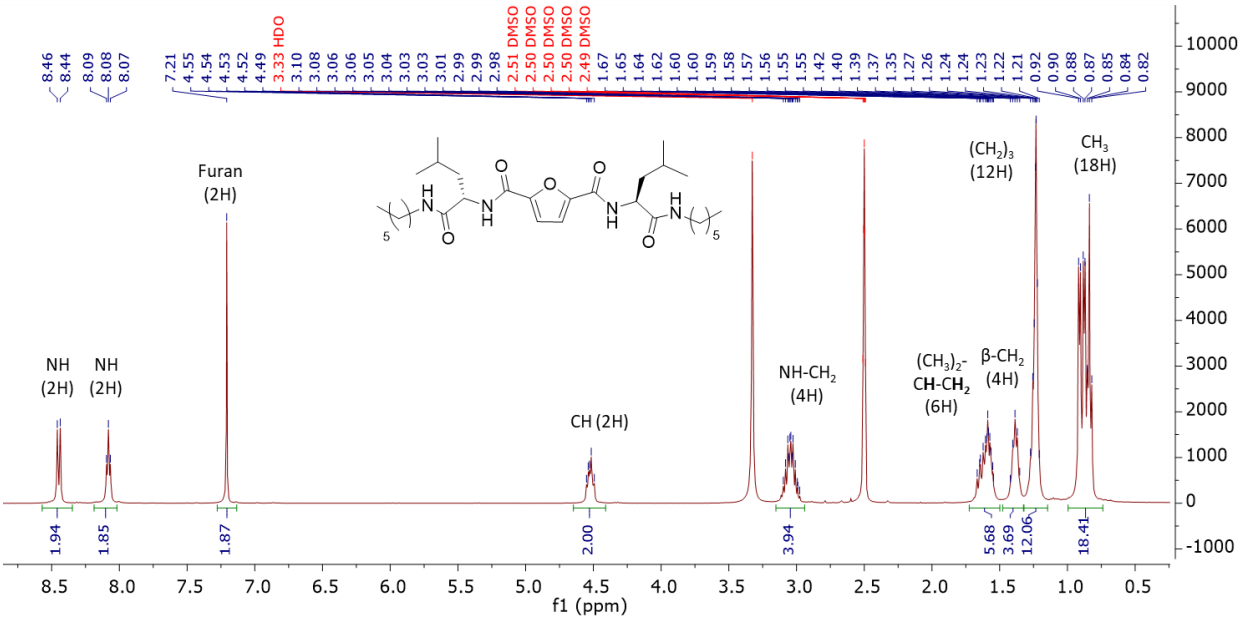

Figure III.26. ^{1}H NMR spectrum of compound **18a** in DMSO-D_6

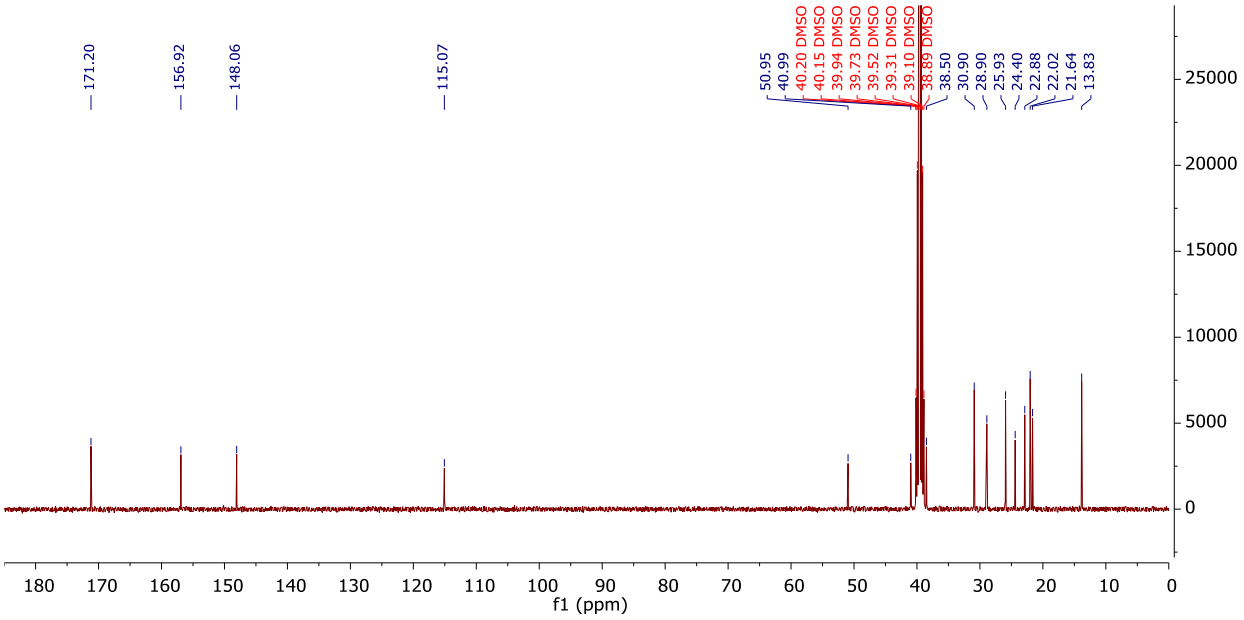

Figure III.27. ^{13}C NMR spectrum of compound **18a** in DMSO-D_6

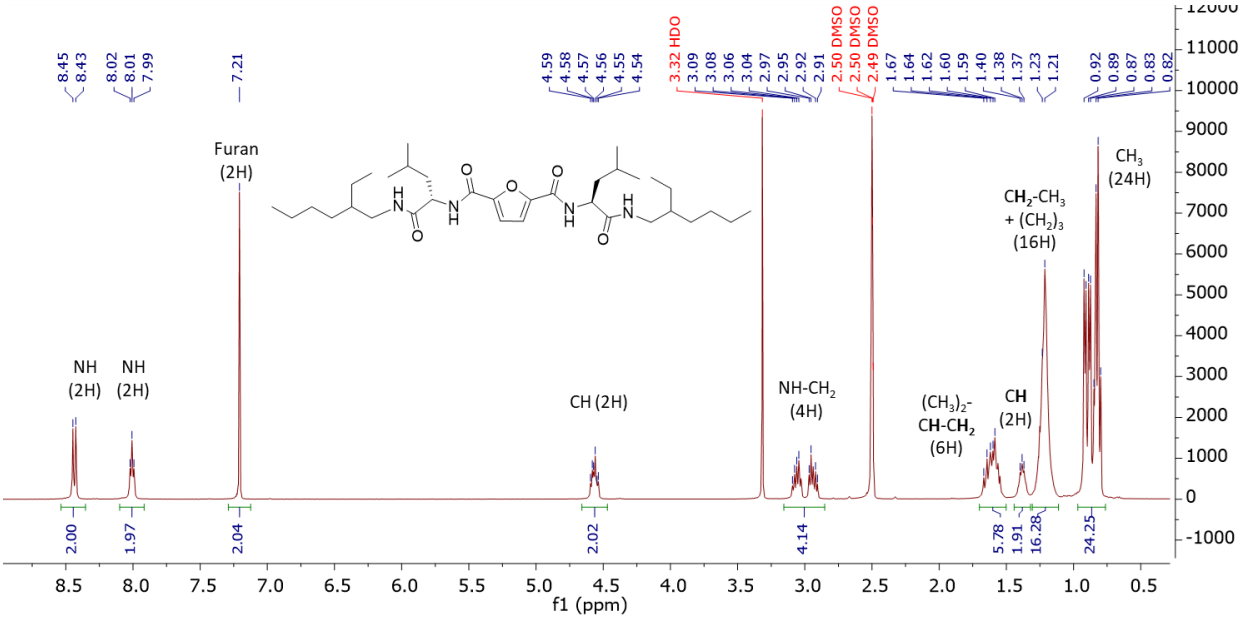

Figure III.28. ^{1}H NMR spectrum of compound **18b** in DMSO-D$_6$

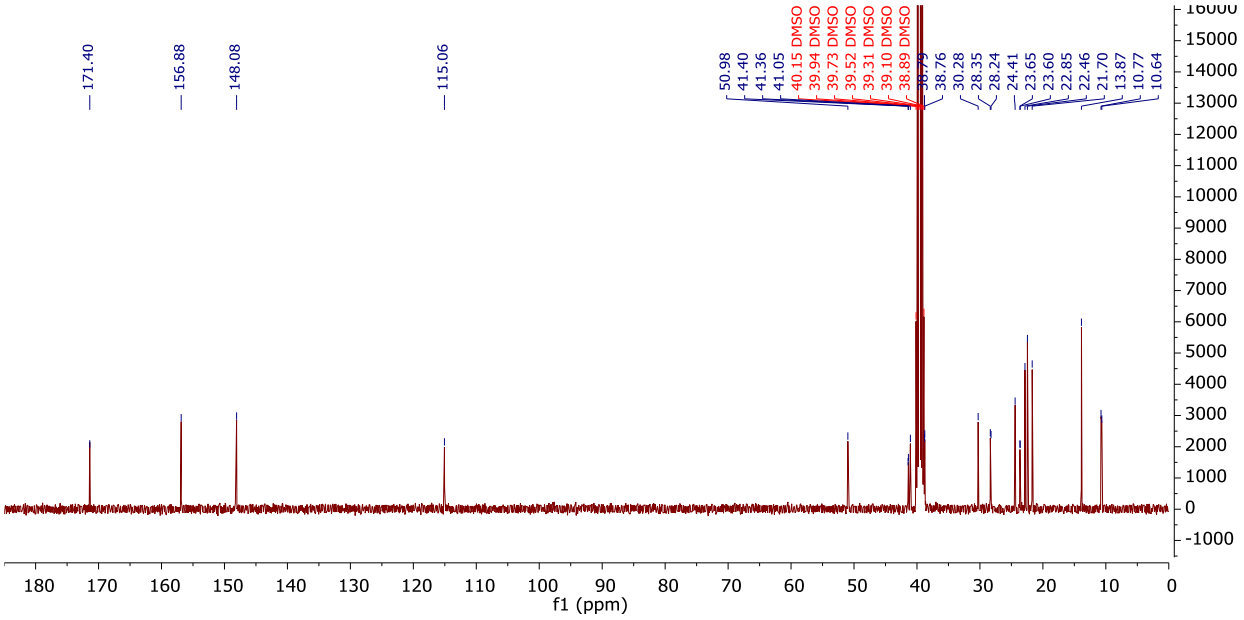

Figure III.29. ^{13}C NMR spectrum of compound **18b** in DMSO-D$_6$

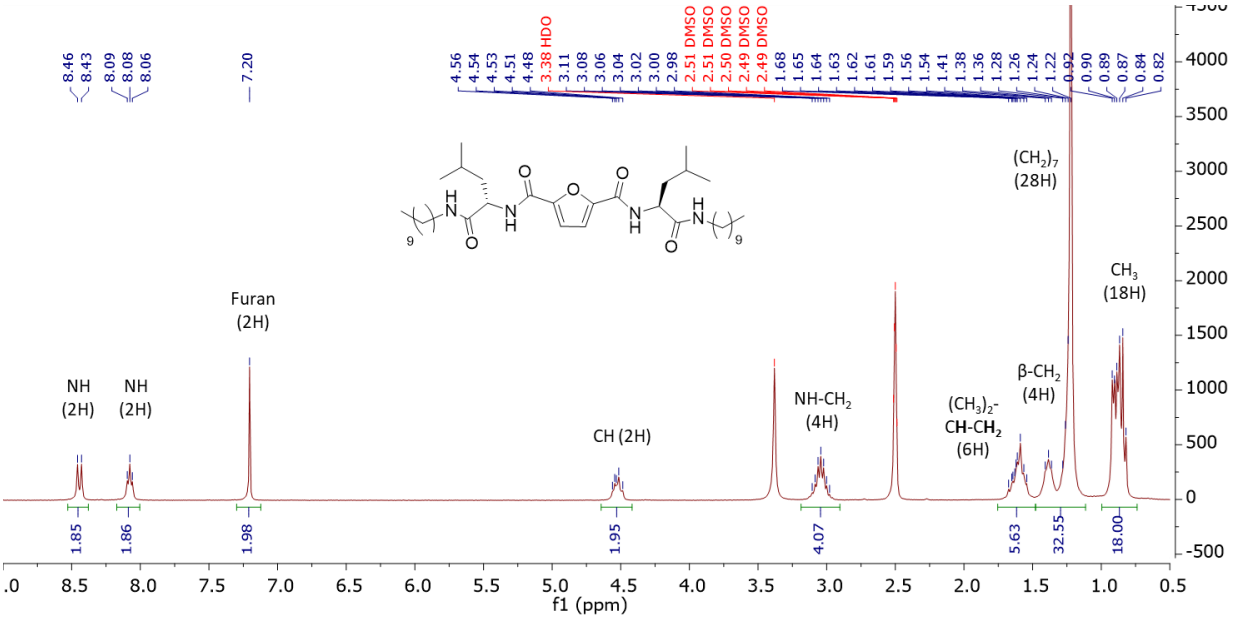

Figure III.30. ^{1}H NMR spectrum of compound **18c** in DMSO-D_6

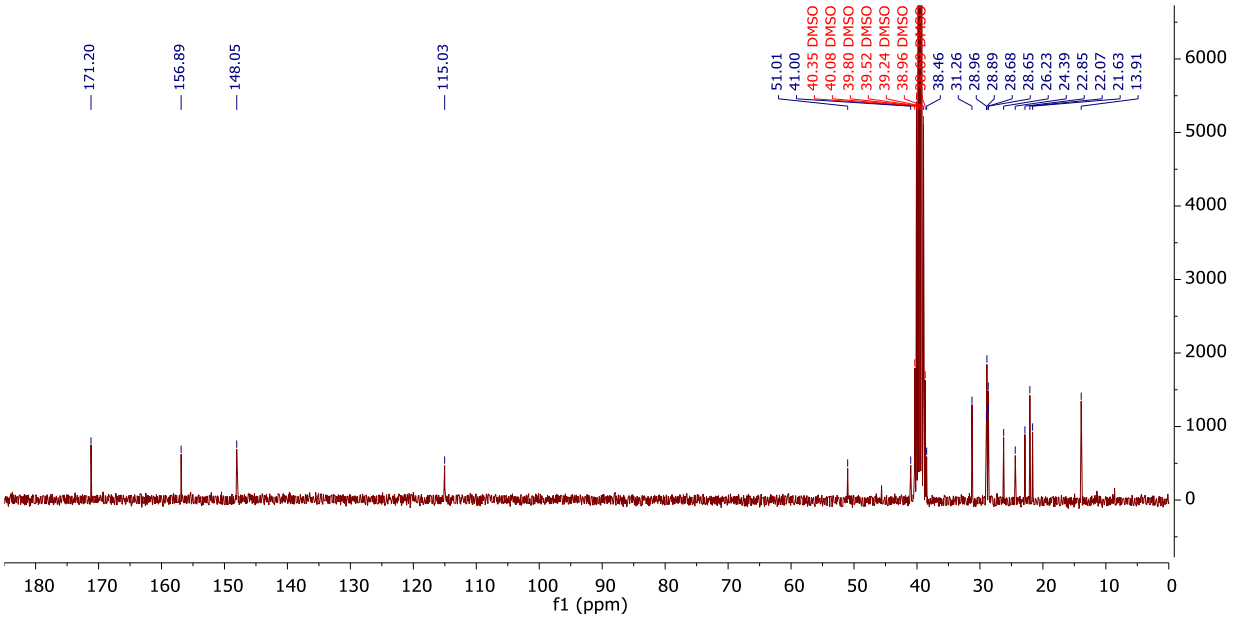

Figure III.31. ^{13}C NMR spectrum of compound **18c** in DMSO-D_6

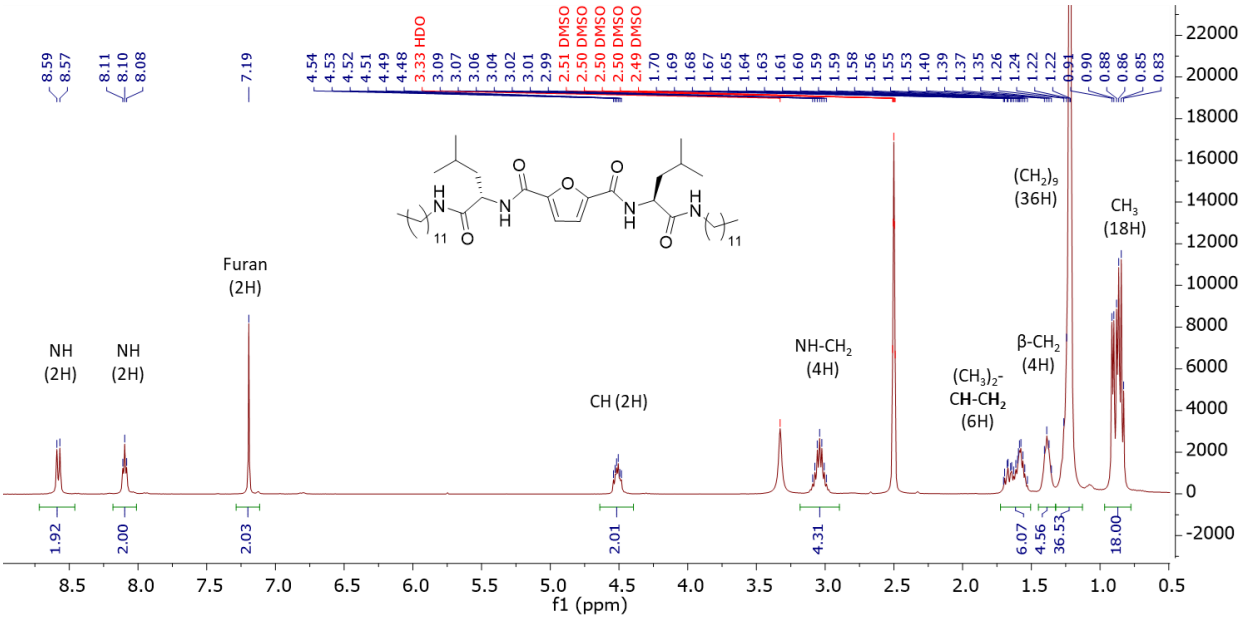

Figure III.32. ^{1}H NMR spectrum of compound **18d** in DMSO-D$_6$

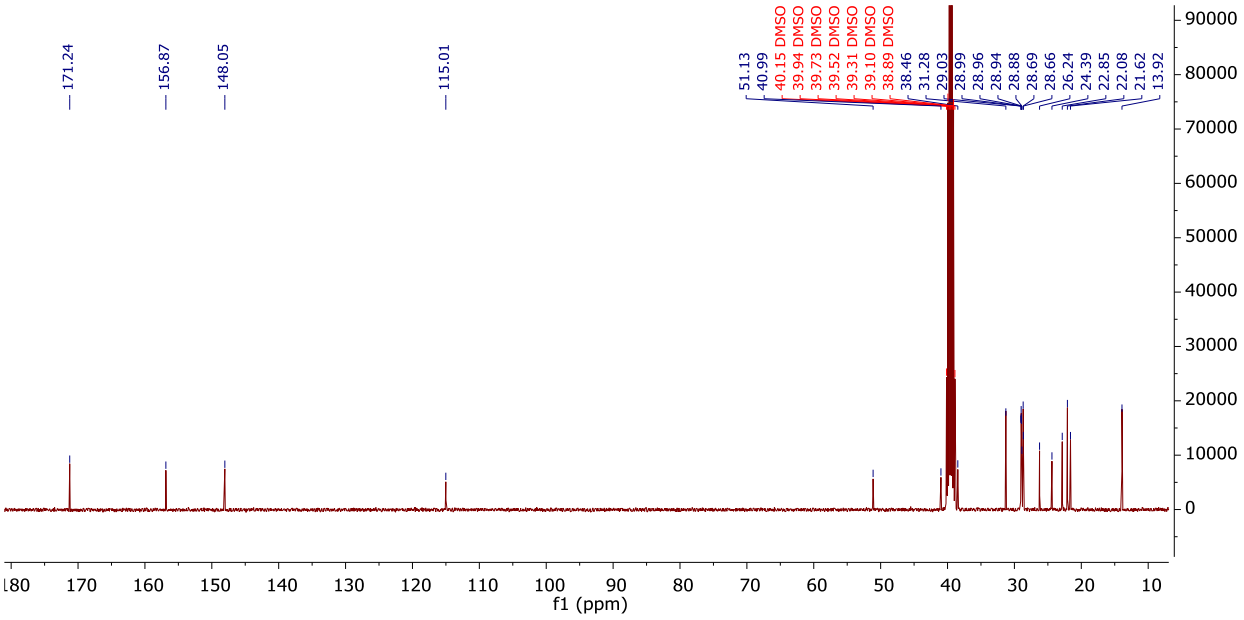

Figure III.33. ^{13}C NMR spectrum of compound **18d** in DMSO-D$_6$

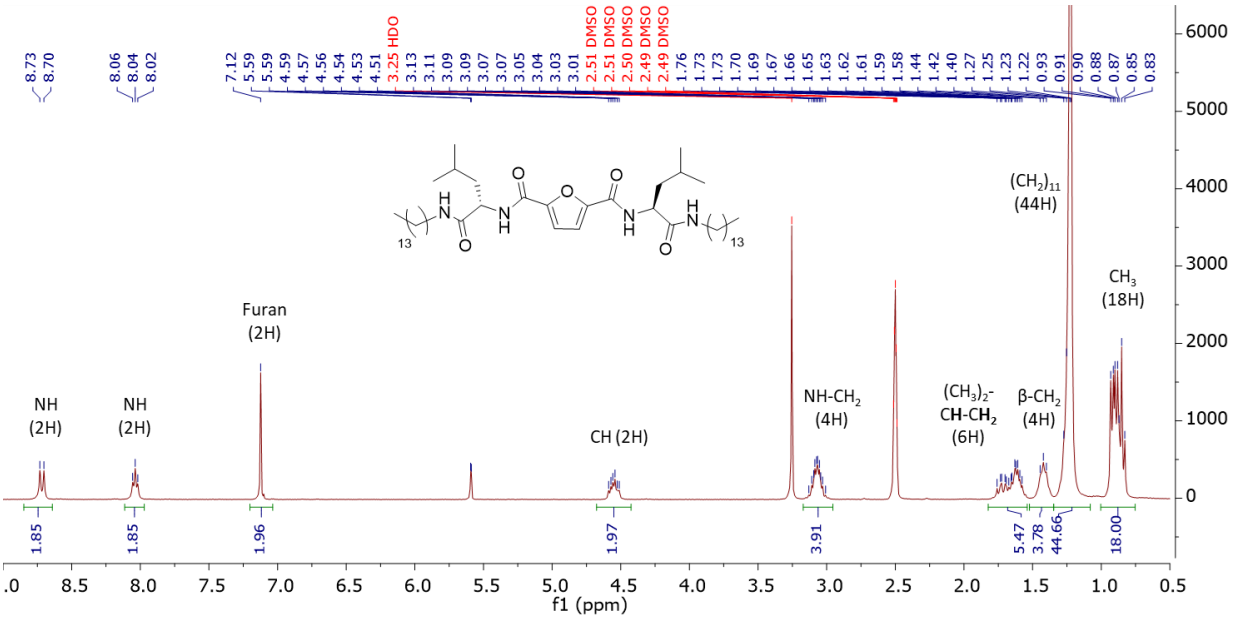

Figure III.34. ^{1}H NMR spectrum of compound **18e** in CD_2Cl_2/DMSO-D_6

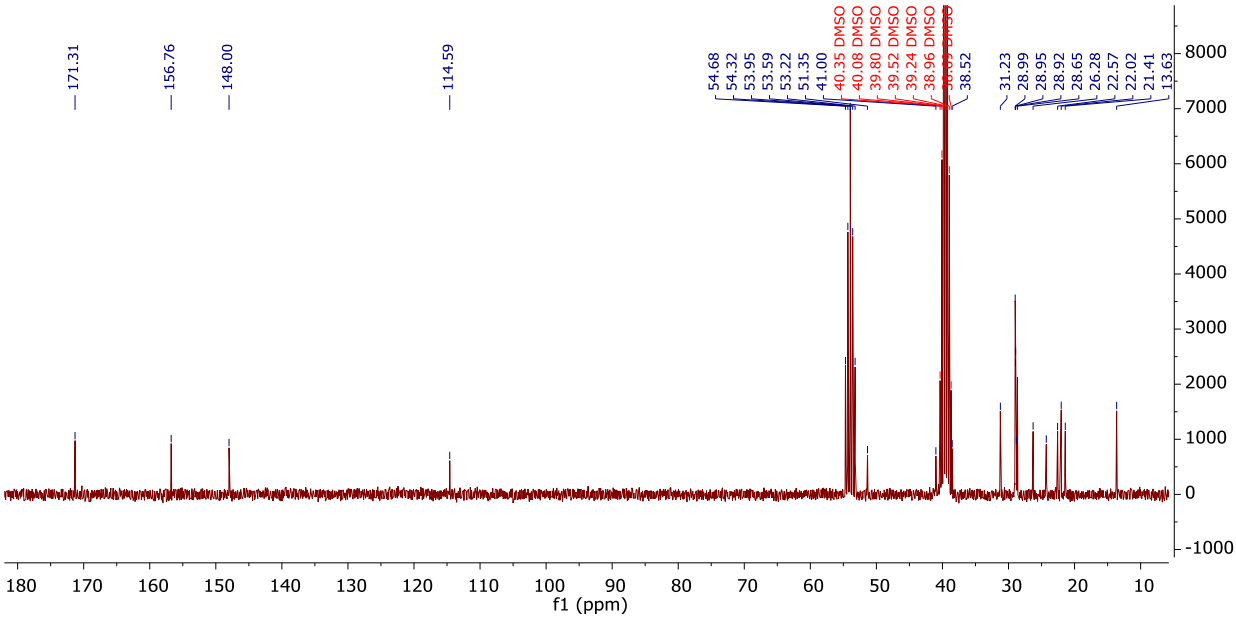

Figure III.35. ^{13}C NMR spectrum of compound **18e** in CD_2Cl_2/DMSO-D_6

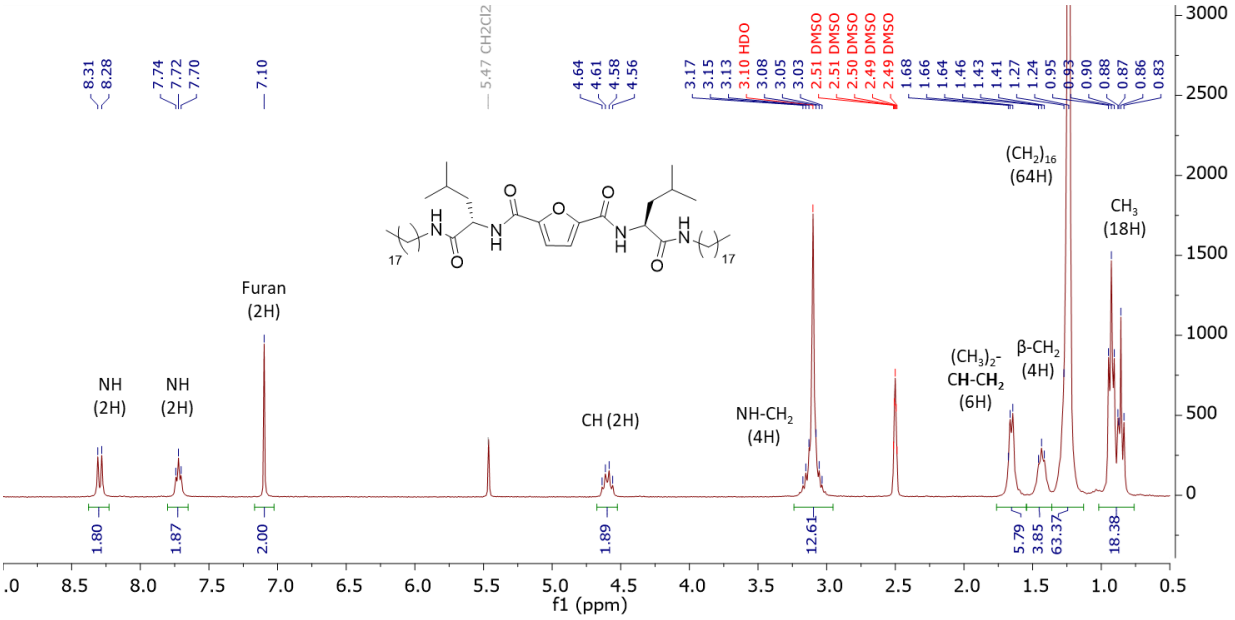

Figure III.36. ^{1}H NMR spectrum of compound **18f** in CD_2Cl_2/DMSO-D_6

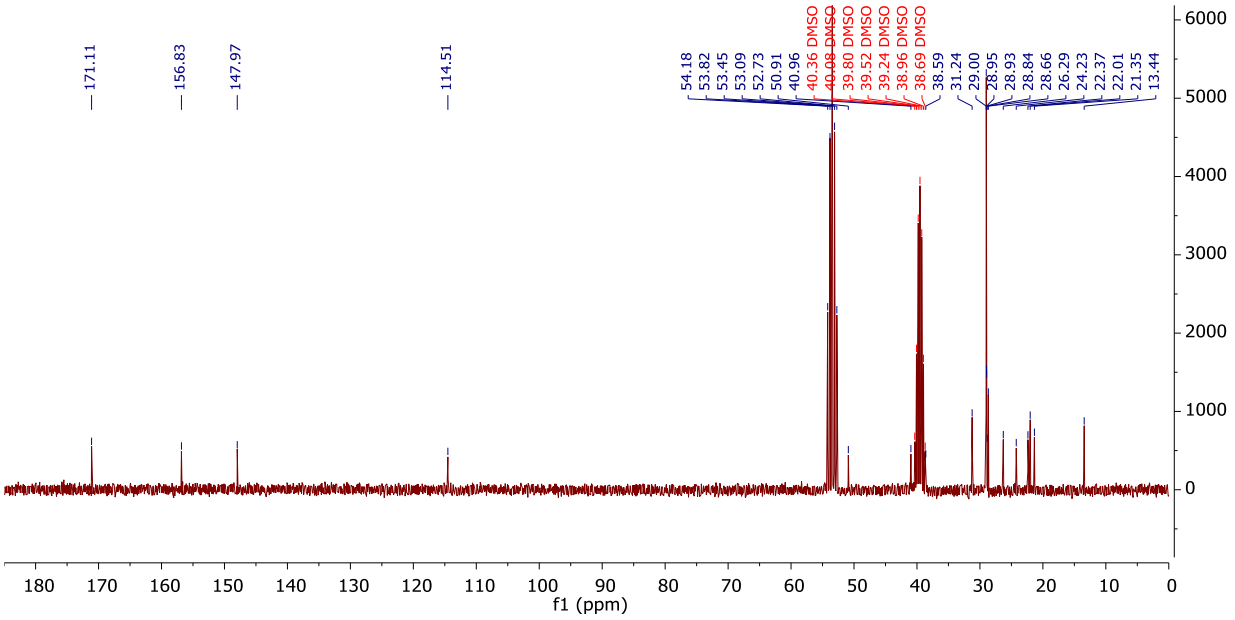

Figure III.37. ^{13}C NMR spectrum of compound **18f** in CD_2Cl_2/DMSO-D_6

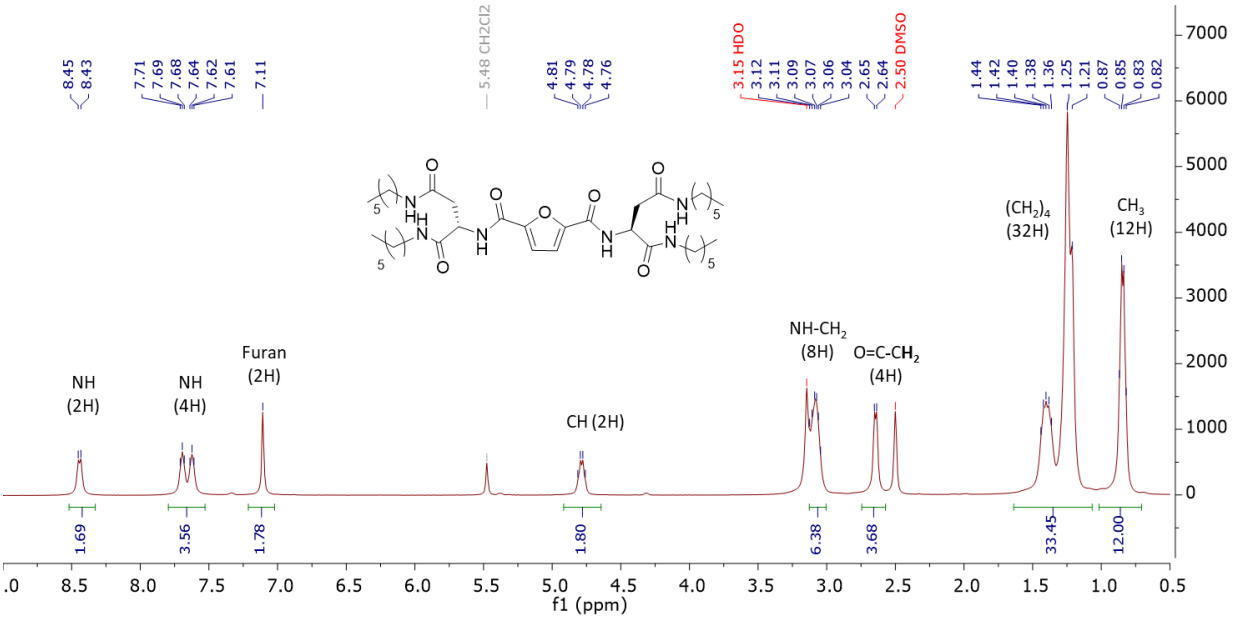

Figure III.38. ^{1}H NMR spectrum of compound **19a** in CD_2Cl_2/DMSO-D_6

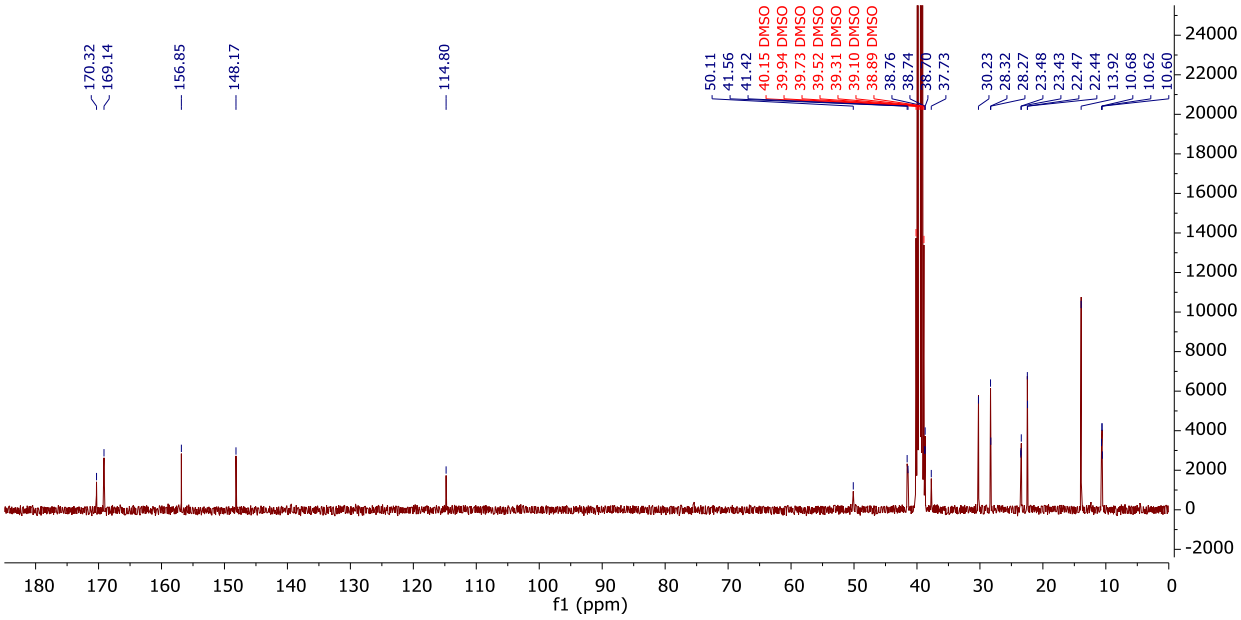

Figure III.39. ^{13}C NMR spectrum of compound **19a** in CD_2Cl_2/DMSO-D_6

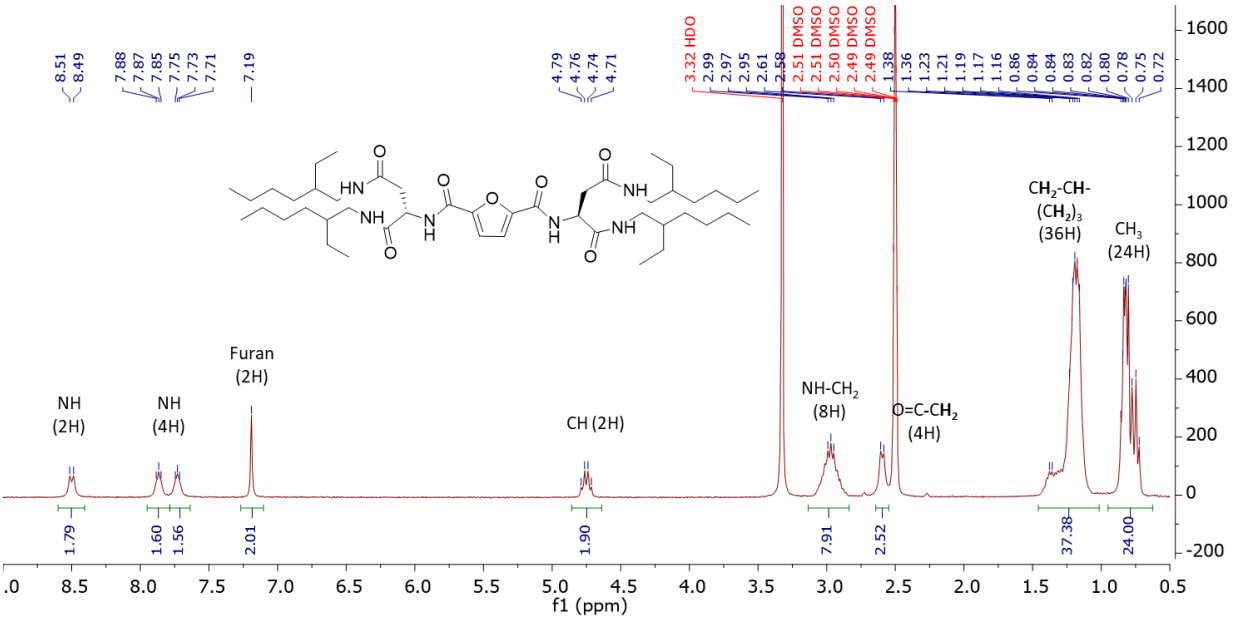

Figure III.40. ^{1}H NMR spectrum of compound **19b** in DMSO-D_6

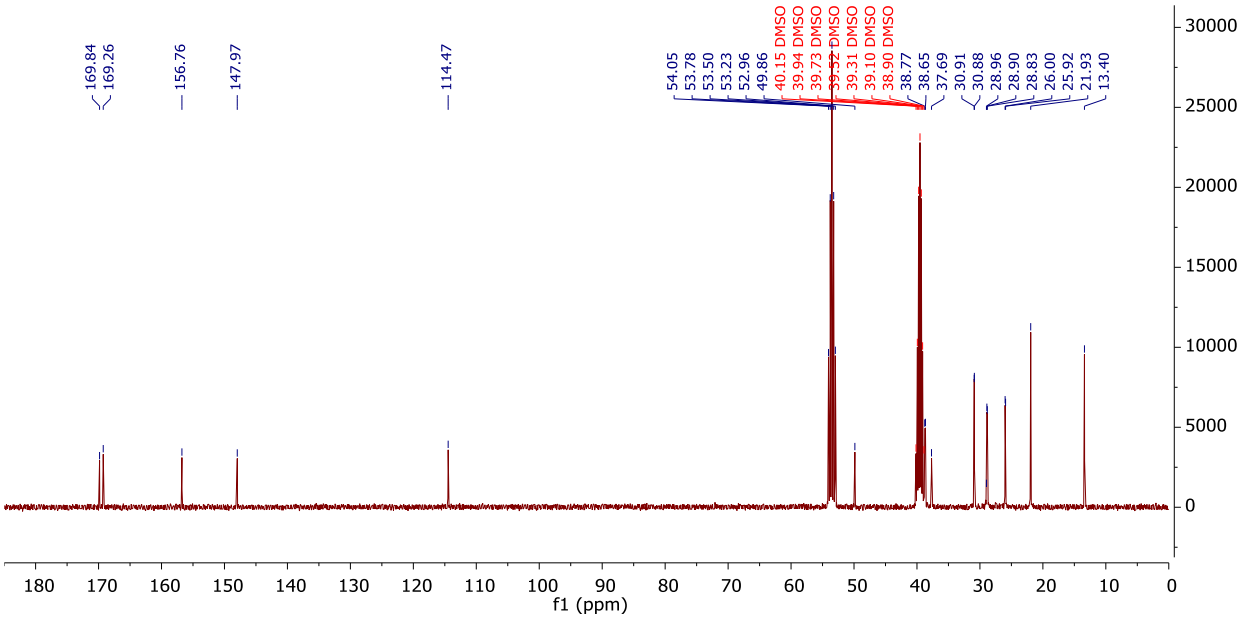

Figure III.41. ^{13}C NMR spectrum of compound **19b** in DMSO-D_6

VII.2. FTIR spectroscopy

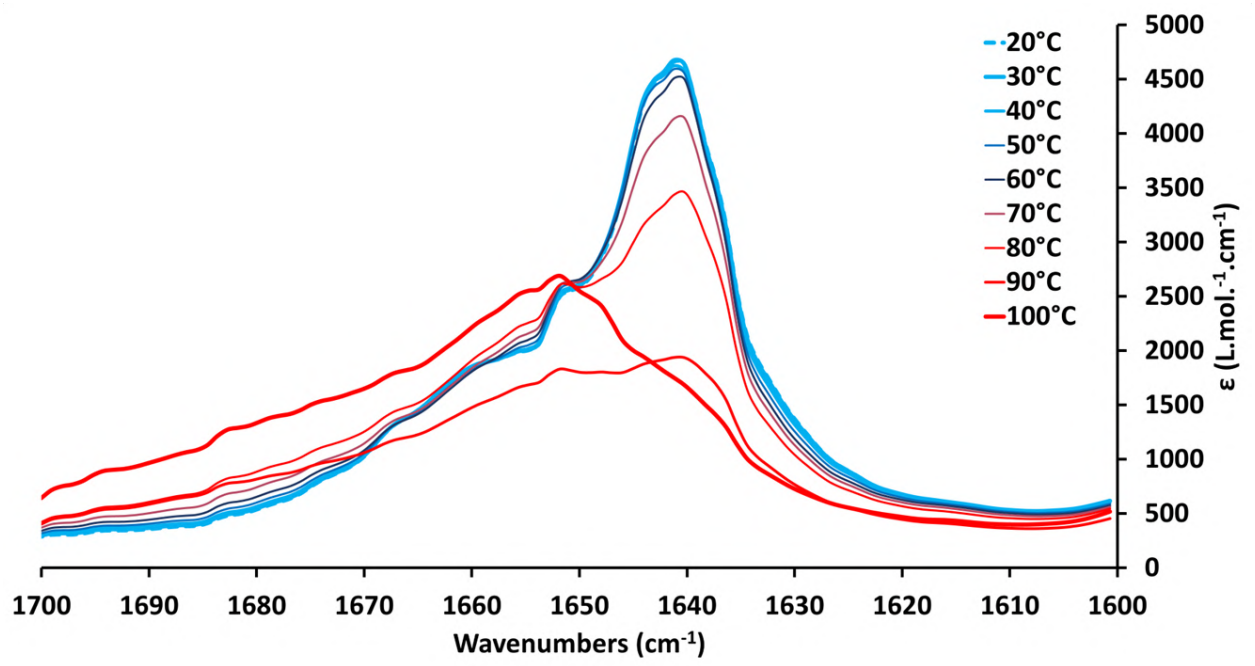

Figure III.42. VT-FTIR spectra of gelator **18d** in methylcyclohexane; 1wt%, heating process, 1°C/min ramp; C=O bands.

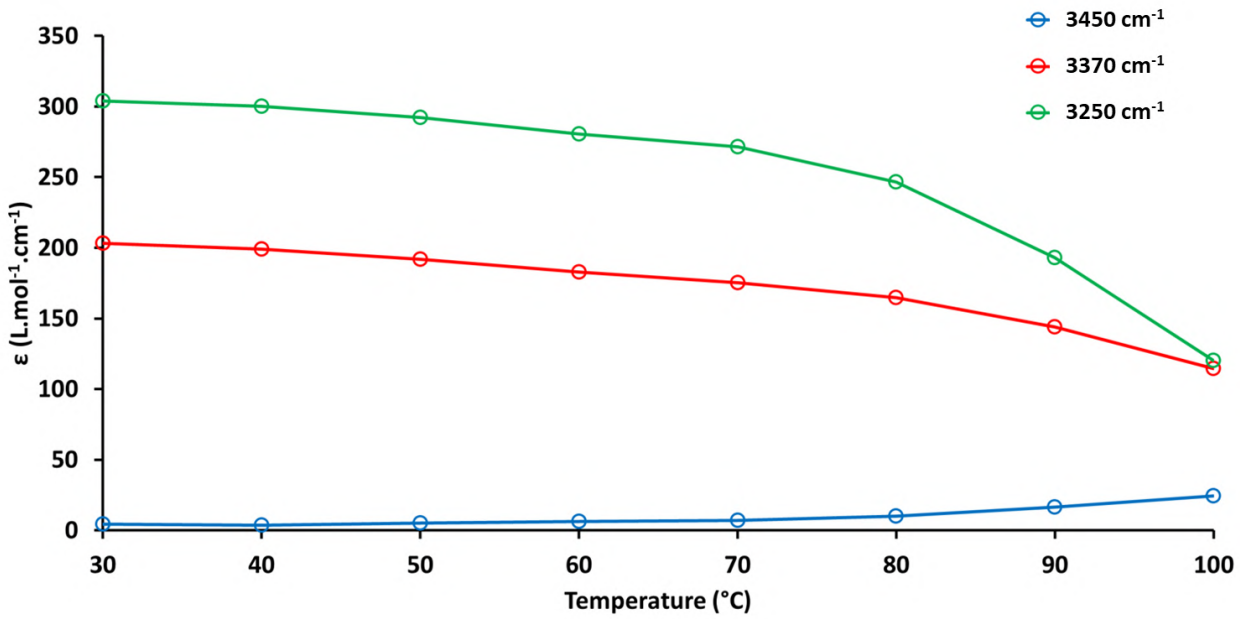

Figure III.43. Intensity of the NH bands depending on the temperature of gelator **18d** in methylcyclohexane; 1wt%, heating process, 1°C/min ramp; free NH 3450 cm^{-1} (blue line), bonded NH 3370 cm^{-1} (red line) and 3250 cm^{-1} (green line).

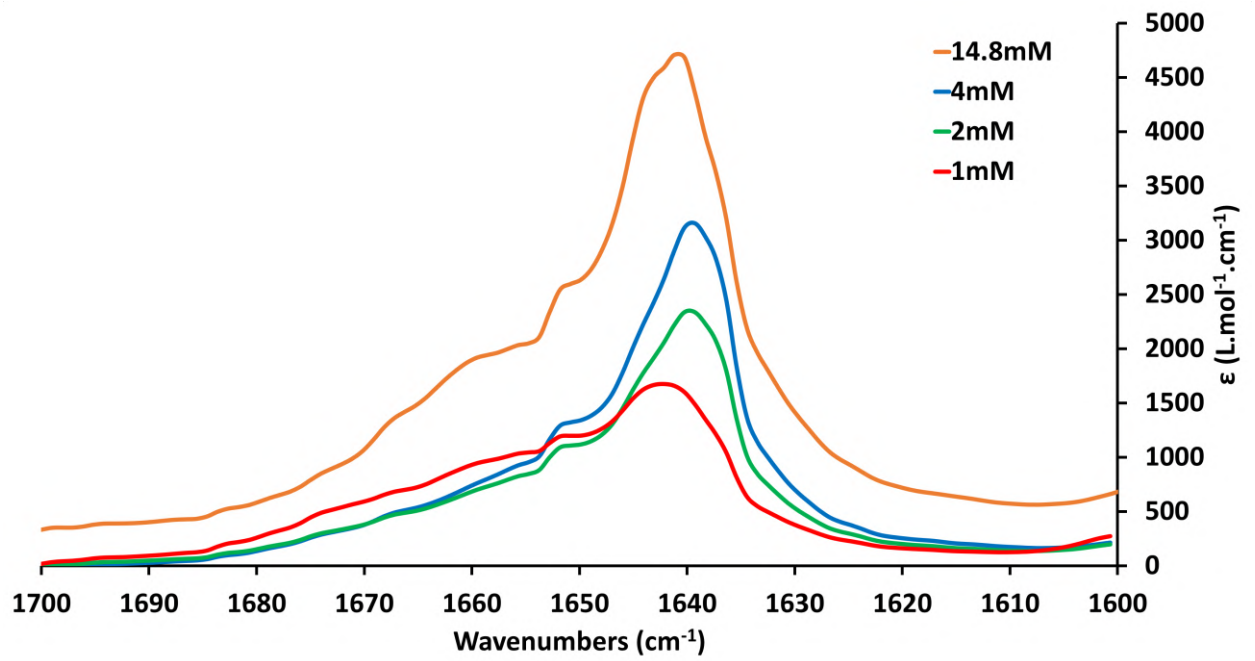

Figure III.44. FTIR spectra of gelator **18d** solutions at 20°C in methylcyclohexane at various concentrations: 14.8mM (orange line), 4mM (blue line), 2mM (red line) and 1mM (green line); C=O bands.

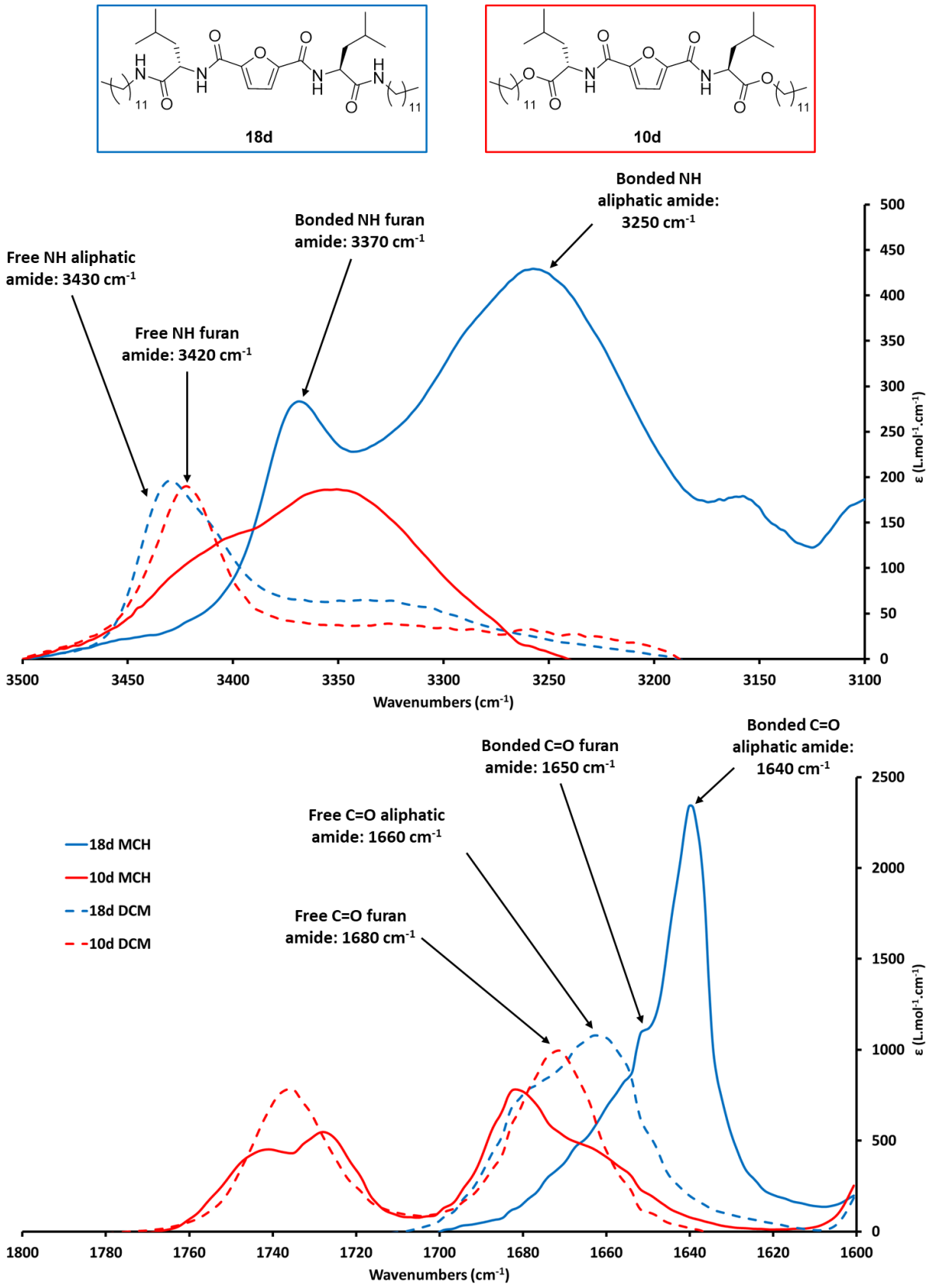

Figure III.45. FTIR analyses of compounds **18d** (red) and **10d** (blue) in MCH (bold lines) and DCM (dotted lines), absorbance mode. Top) NH region (3500-3100 cm^{-1}); Bottom) C=O region (1800-1600 cm^{-1})

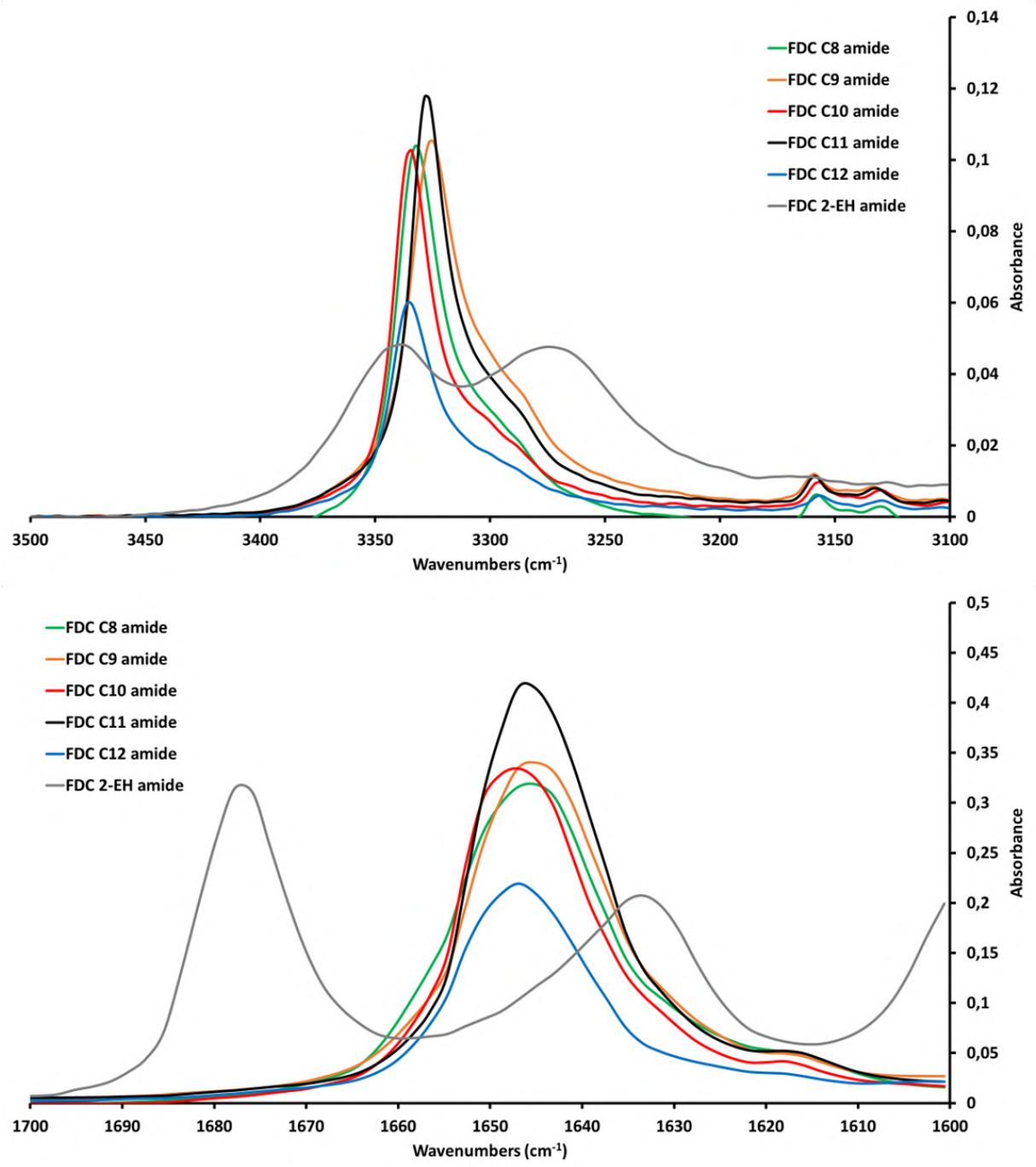

Figure III.46. FTIR analyses of FDC-alkyl diamides compounds, ATR, absorbance mode. Top) NH region (3500-3100 cm^{-1}); Bottom) C=O region (1800-1600 cm^{-1}).

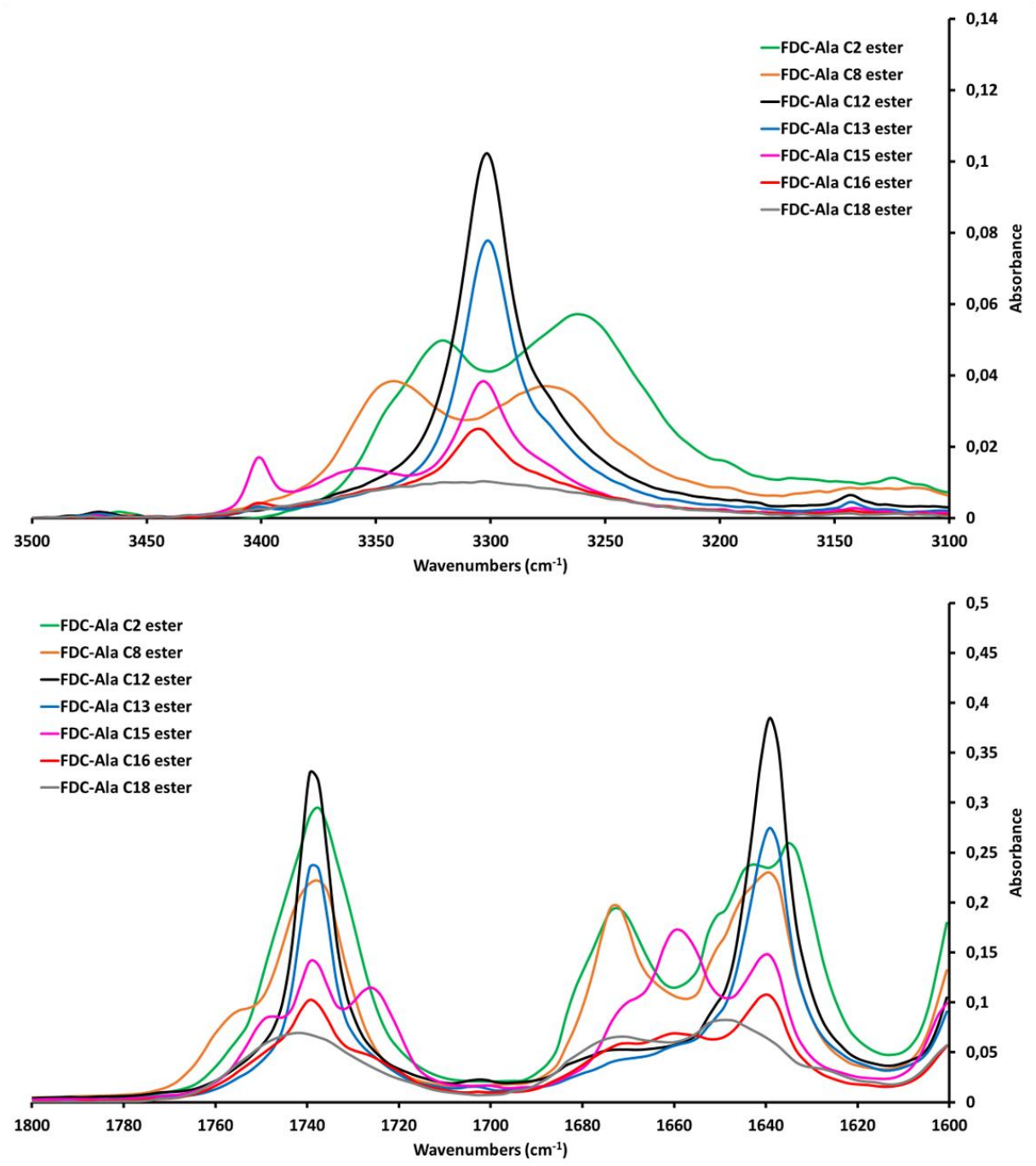

Figure III.47. FTIR analyses of FDC-Ala ester compounds, ATR, absorbance mode. Top) NH region (3500-3100 cm^{-1}); Bottom) C=O region (1800-1600 cm^{-1}).

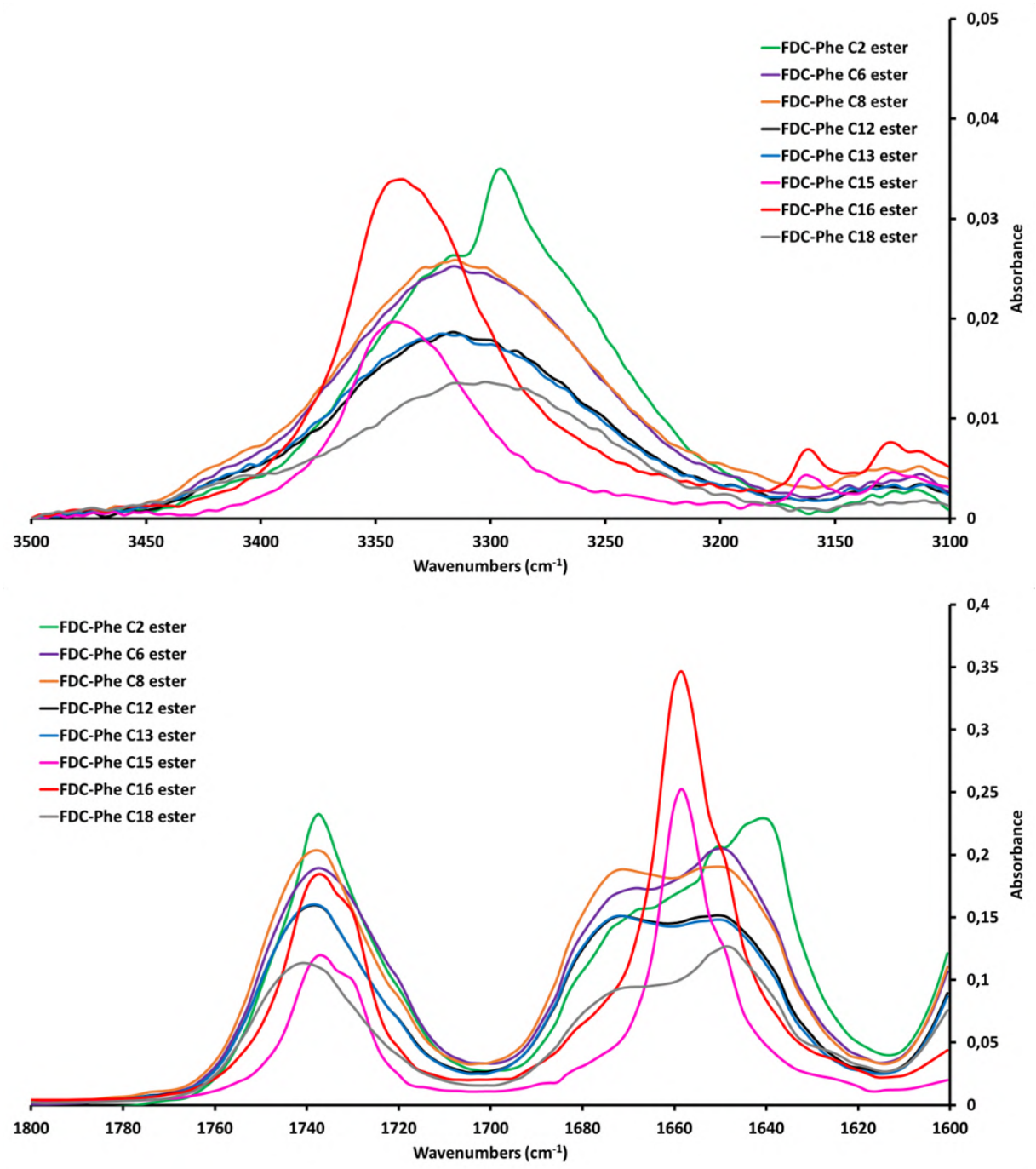

Figure III.48. FTIR analyses of FDC-Phe ester compounds, ATR, absorbance mode. Top) NH region (3500-3100 cm^{-1}); Bottom) C=O region (1800-1600 cm^{-1}).

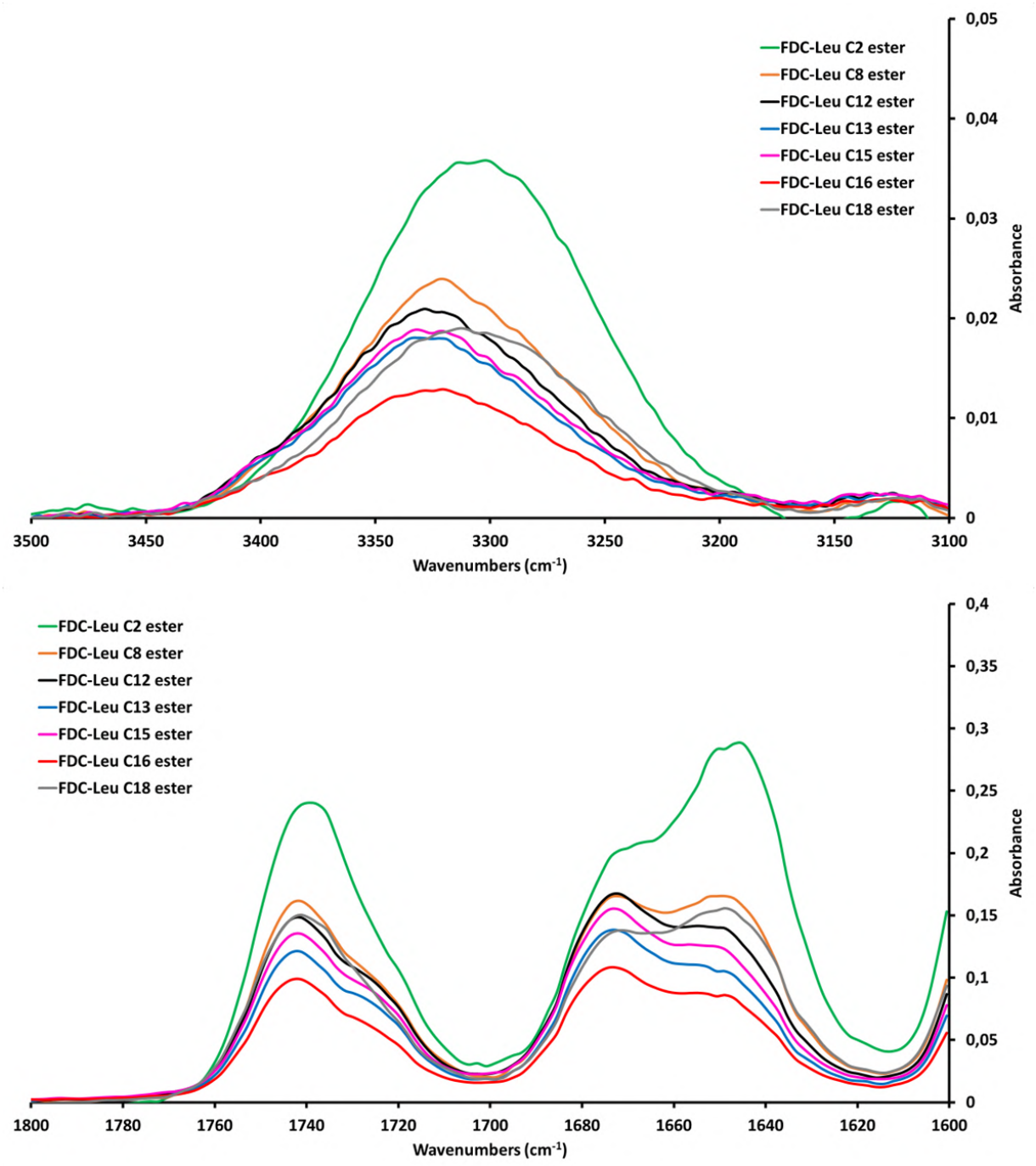

Figure III.49. FTIR analyses of FDC-Leu ester compounds, ATR, absorbance mode. Top) NH region (3500-3100 cm^{-1}); Bottom) C=O region (1800-1600 cm^{-1}).

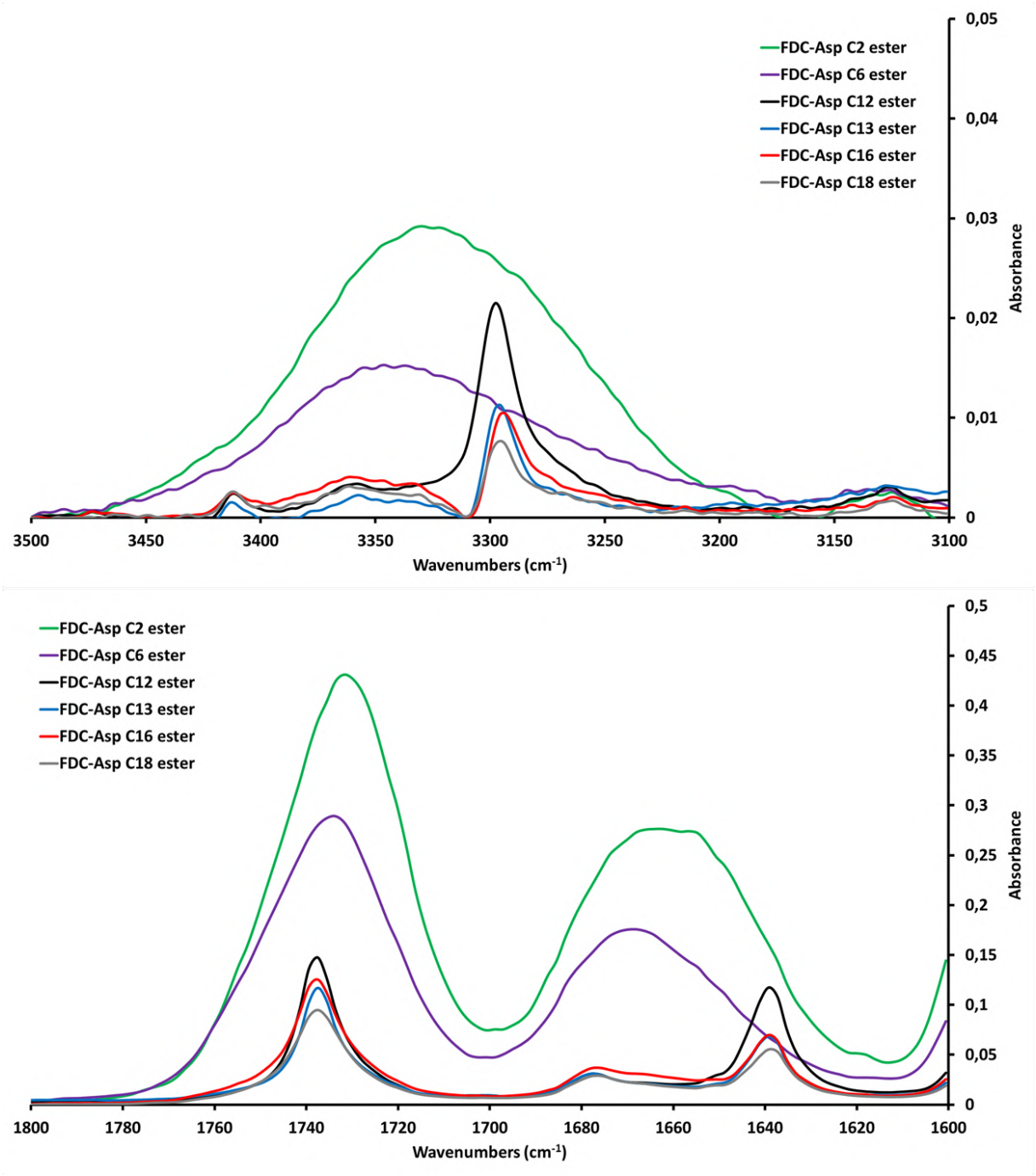

Figure III.50. FTIR analyses of FDC-Asp ester compounds, ATR, absorbance mode. Top) NH region (3500-3100 cm^{-1}); Bottom) C=O region (1800-1600 cm^{-1}).

VII.3. Rheology

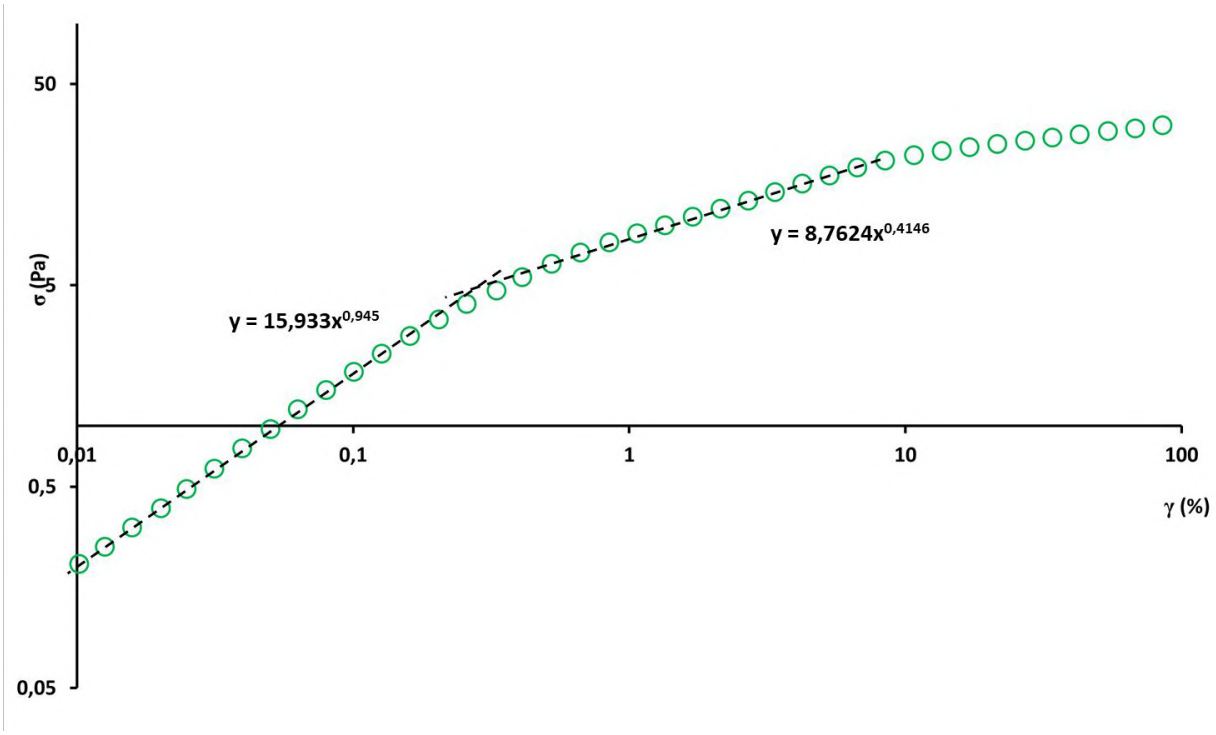

Figure III.51. Evolution of the stress (σ) as a function of strain (γ) for the 2wt% gel in rapeseed oil. The dotted lines correspond to the linear regression lines used to determine the yield stress

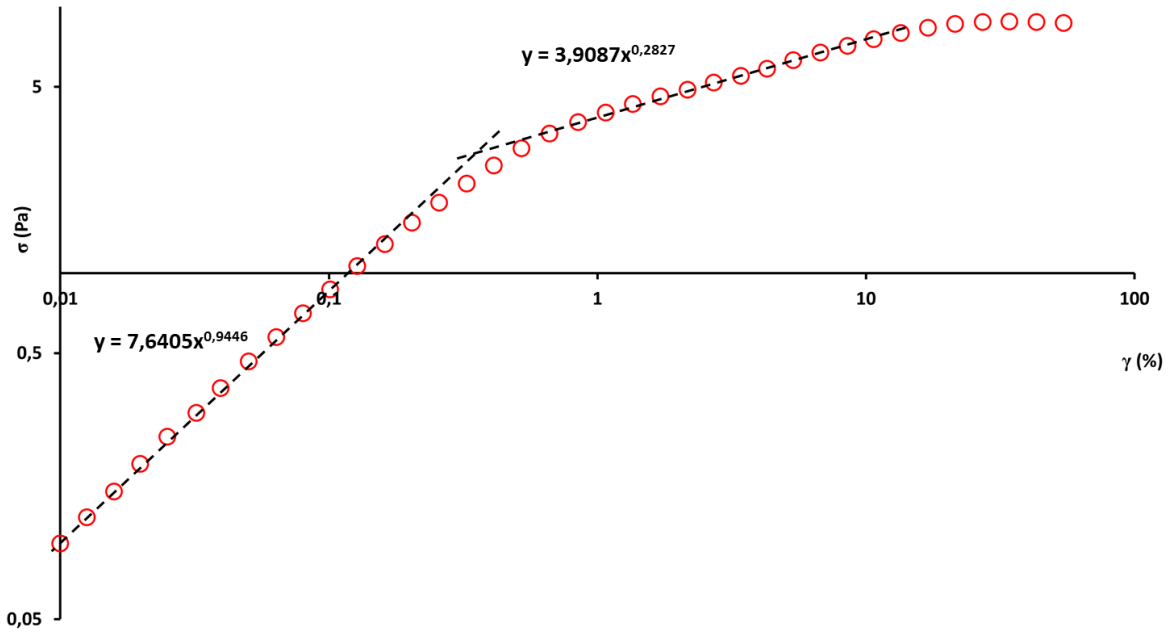

Figure III.52. Evolution of the stress (σ) as a function of strain (γ) for the 1.5wt% gel in rapeseed oil. The dotted lines correspond to the linear regression lines used to determine the yield stress

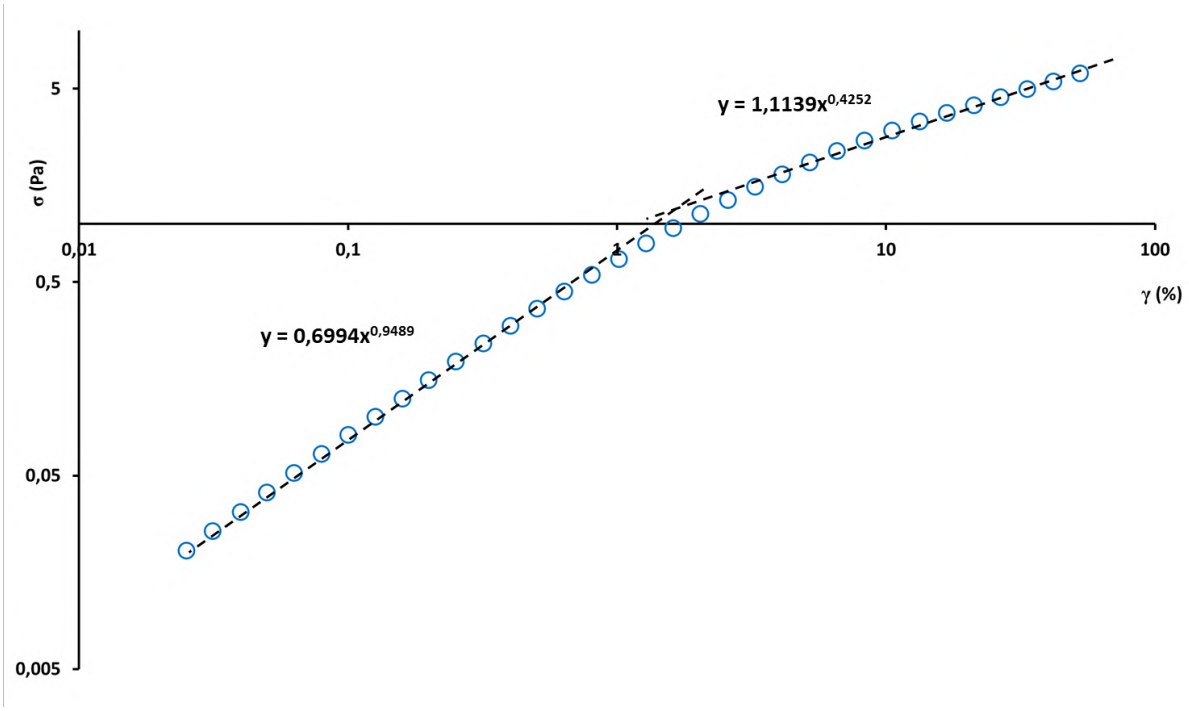

Figure III.53. Evolution of the stress (σ) as a function of strain (γ) for the 1wt% gel in rapeseed oil. The dotted lines correspond to the linear regression lines used to determine the yield stress

VII.4. Circular dichroism

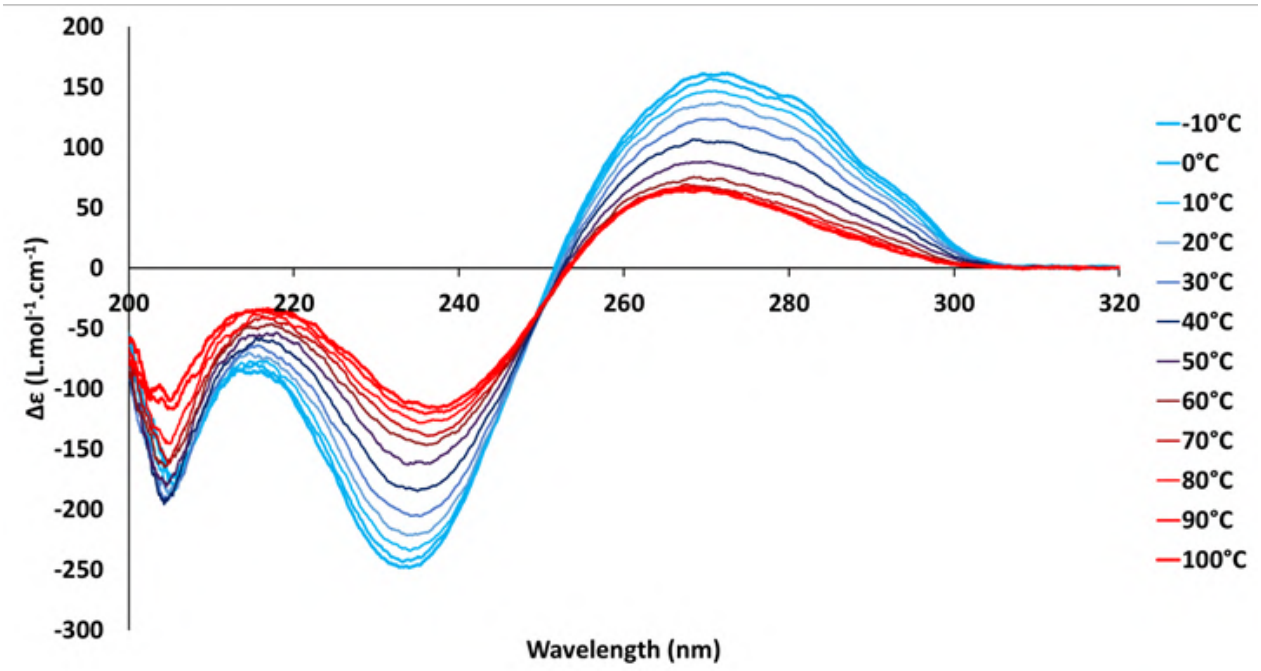

Figure III.54. CD spectra of gelator **18d** in methylcyclohexane at 1mM (heating process, 1°C/min ramp)

VII.5. TGA analyses

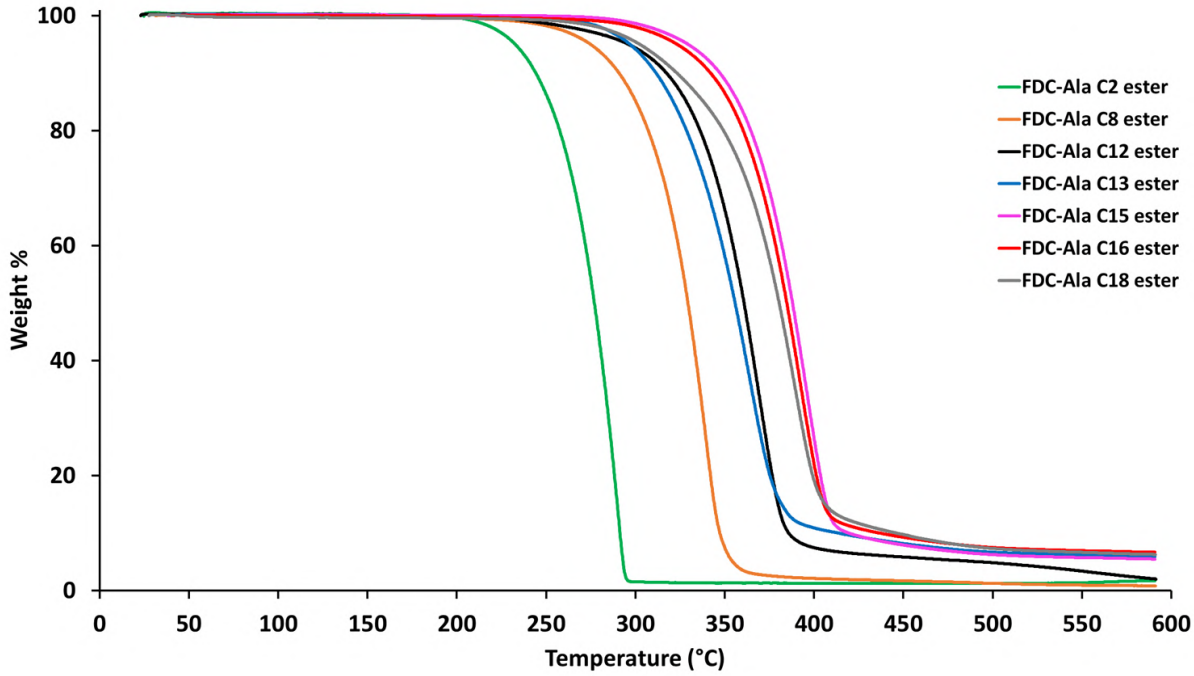

Figure III.55. TGA thermograms of FDC-Ala ester compounds (under argon, 20°C/min ramp)

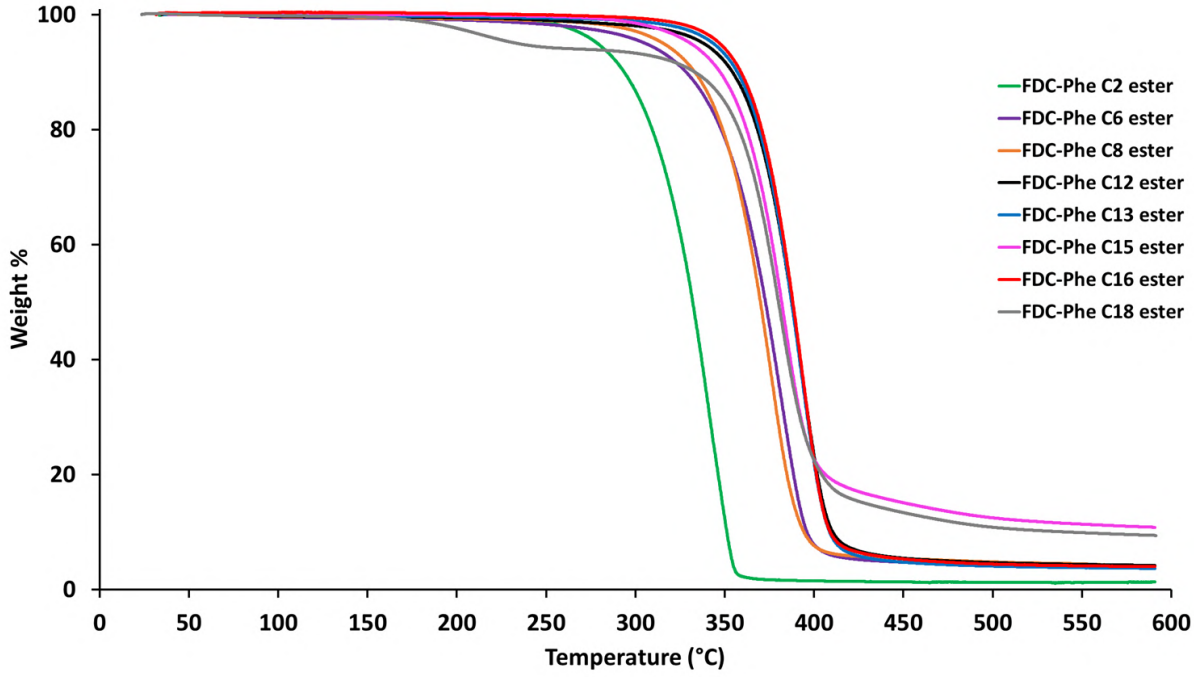

Figure III.56. TGA thermograms of FDC-Phe ester compounds (under argon, 20°C/min ramp)

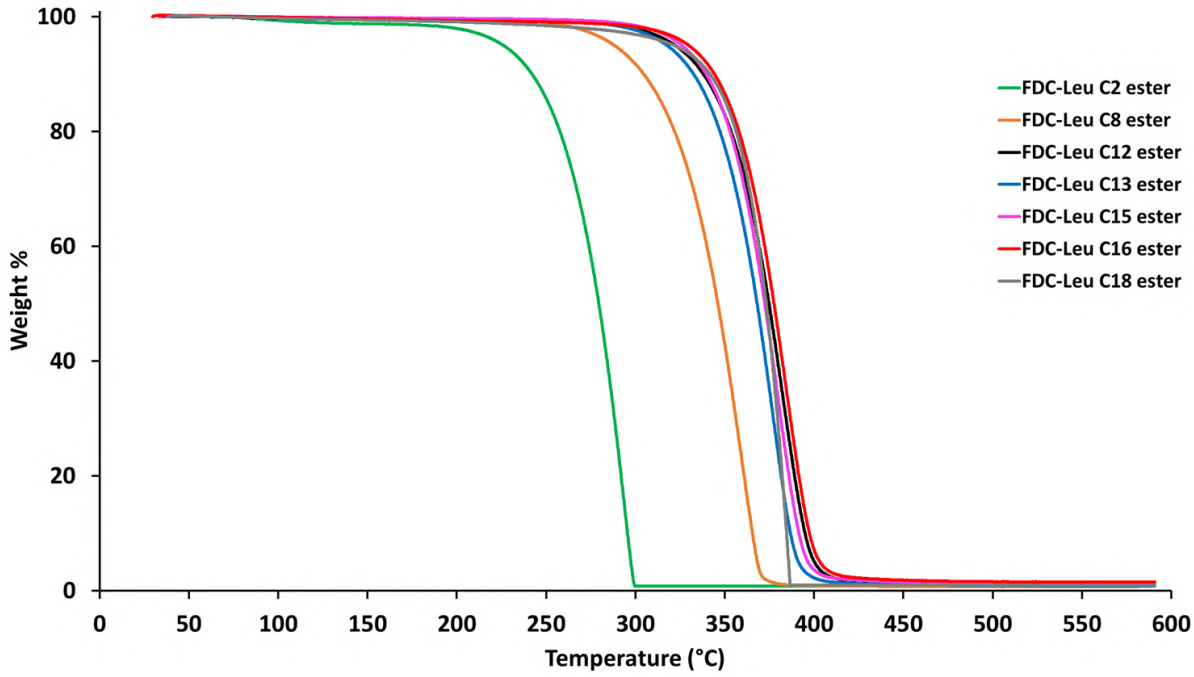

Figure III.57. TGA thermograms of FDC-Leu ester compounds (under argon, 20°C/min ramp)

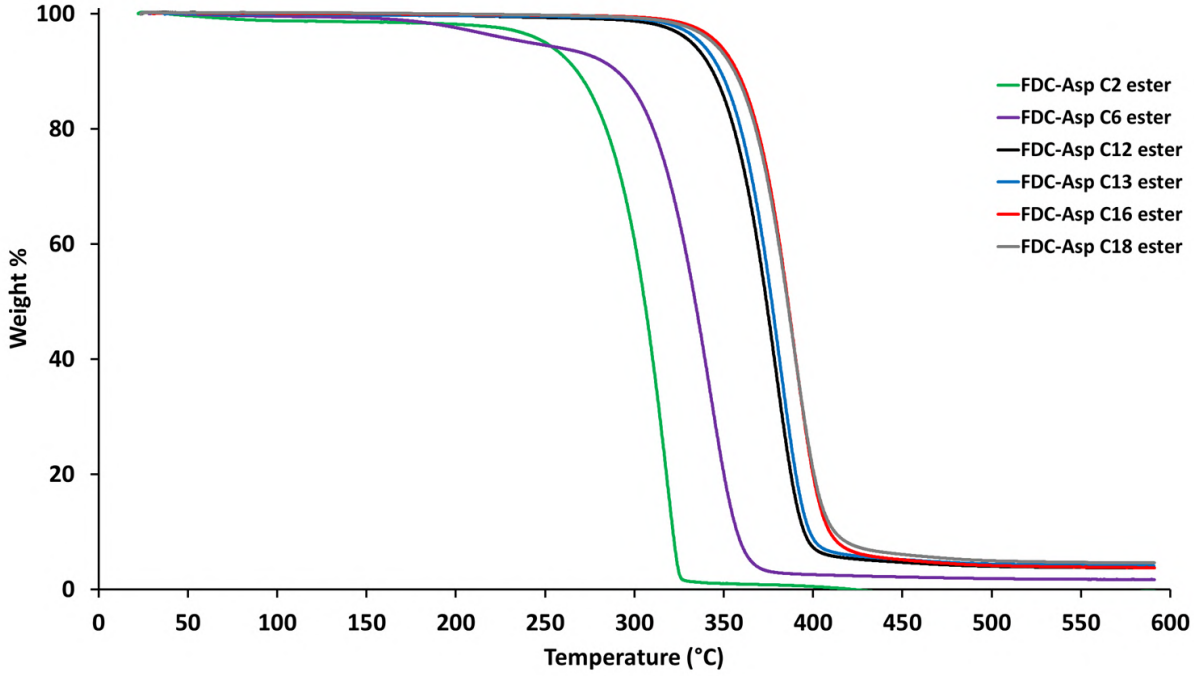

Figure III.58. TGA thermograms of FDC-Asp ester compounds (under argon, 20°C/min ramp)

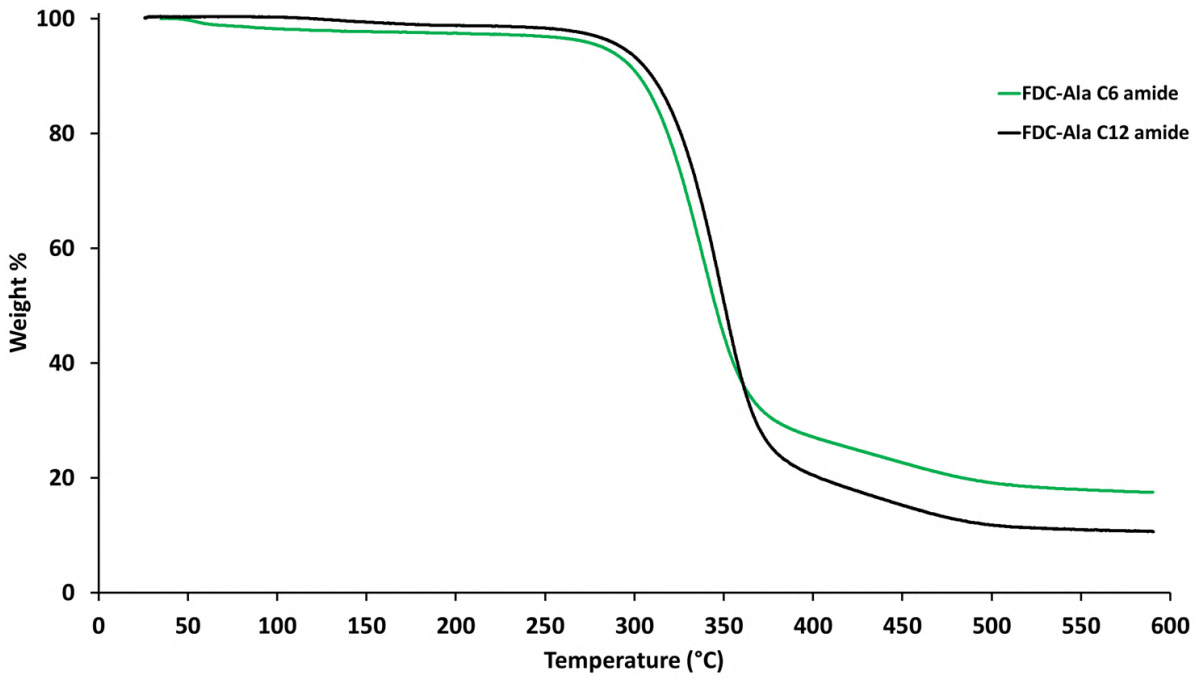

Figure III.59. TGA thermograms of FDC-Ala amide compounds (under argon, 20°C/min ramp)

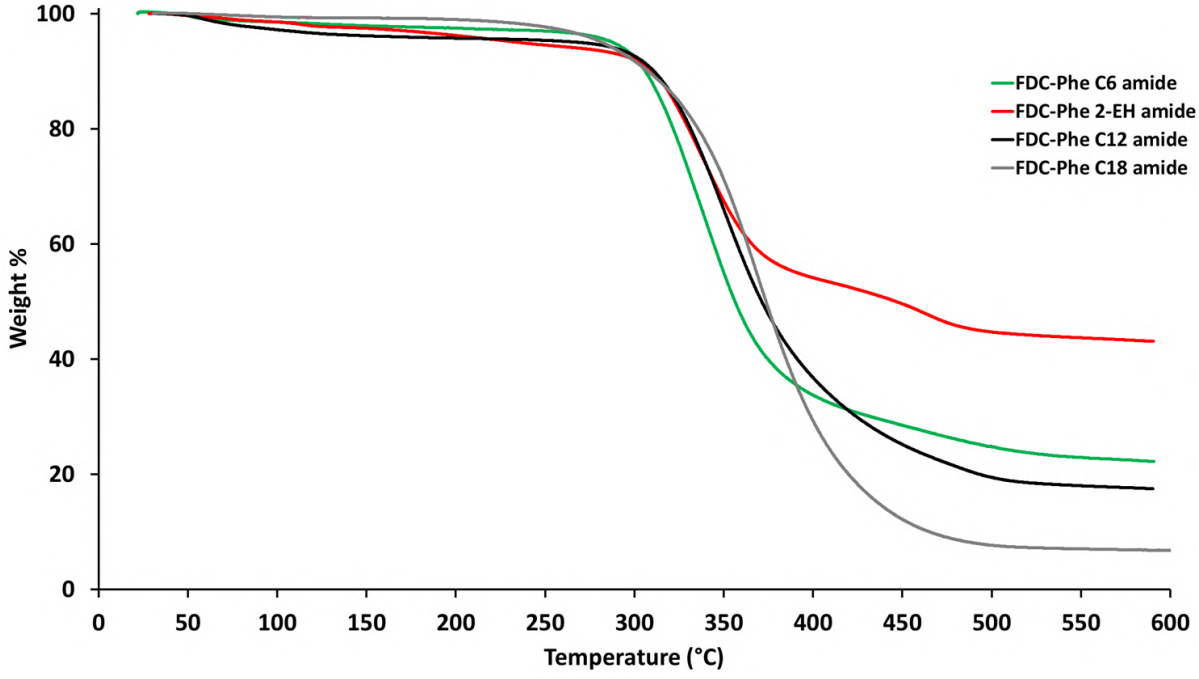

Figure III.60. TGA thermograms of FDC-Phe amide compounds (under argon, 20°C/min ramp)

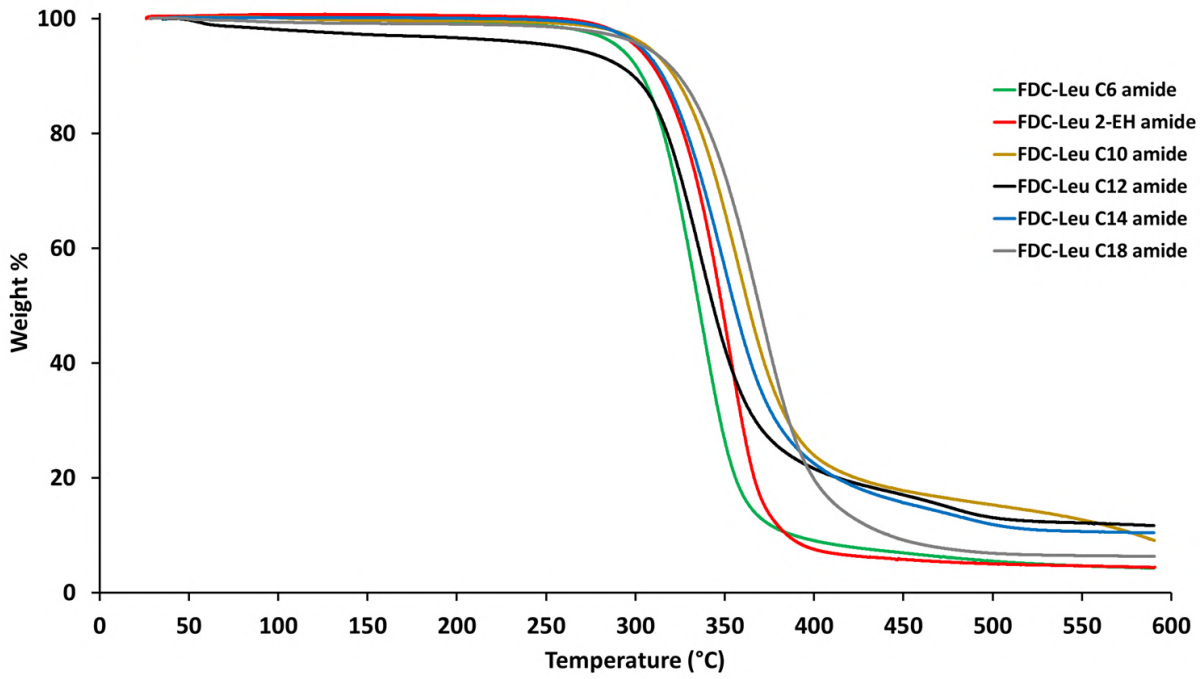

Figure III.61. TGA thermograms of FDC-Leu amide compounds (under argon, 20°C/min ramp)

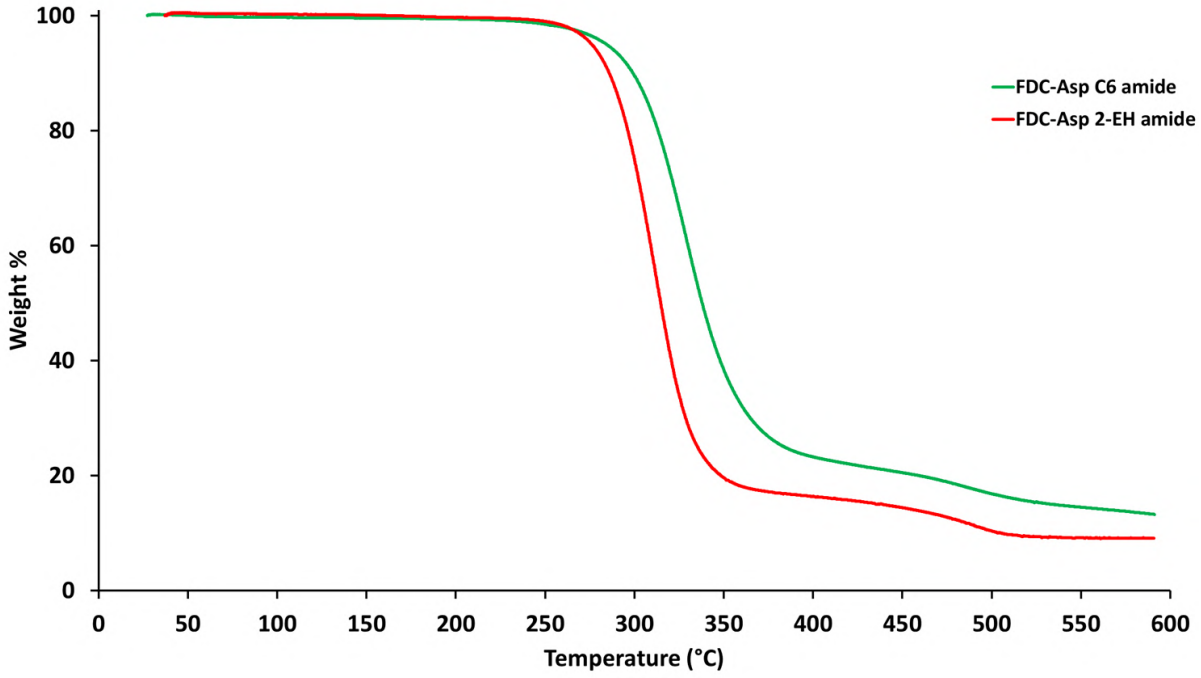

Figure III.62. TGA thermograms of FDC-Asp amide compounds (under argon, 20°C/min ramp)

VII.6. DSC analyses

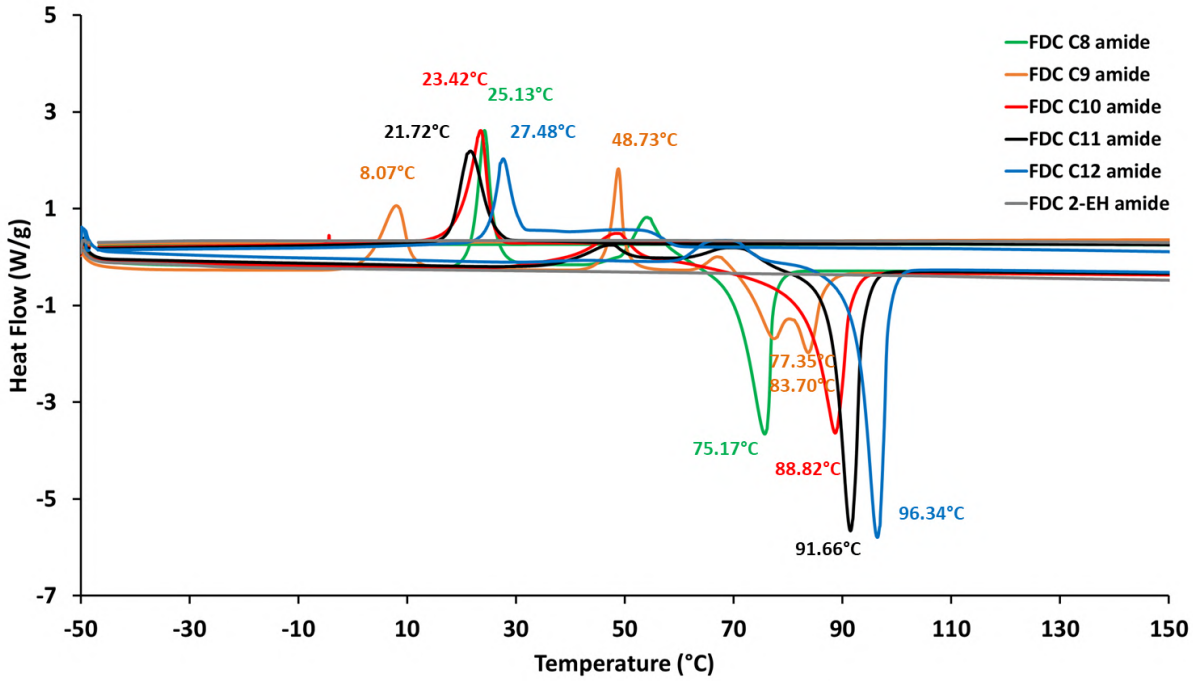

Figure III.63. DSC thermograms of FDC-alkyl diamides (under argon, 10°C/min ramp)

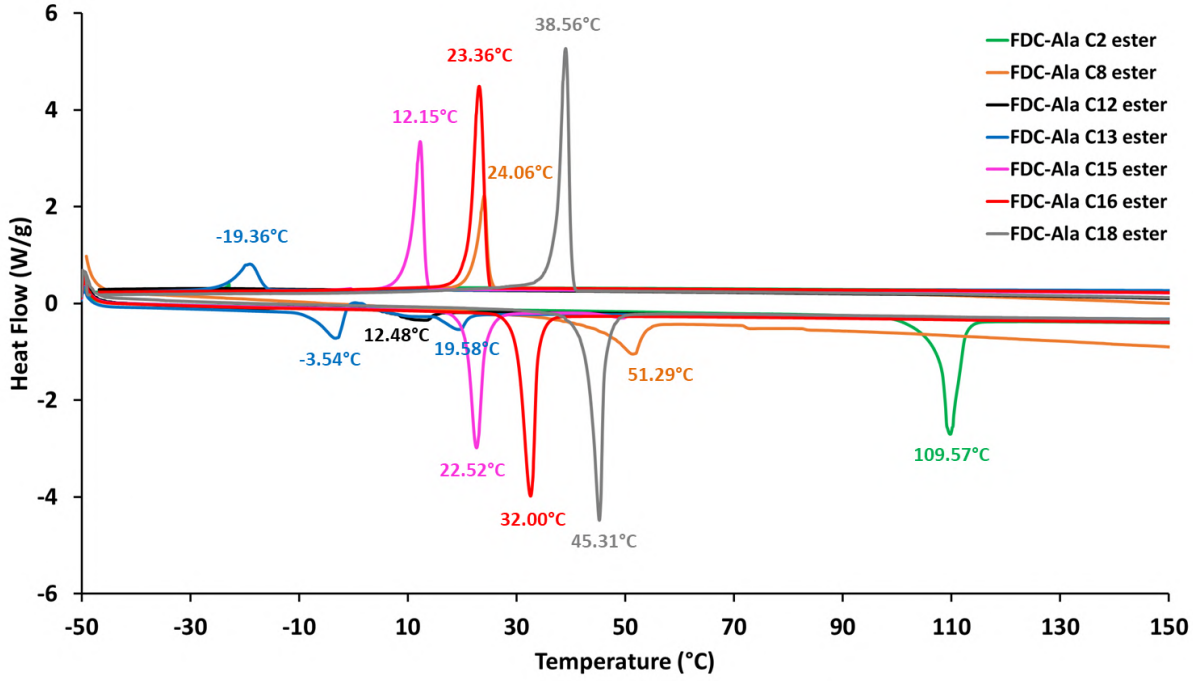

Figure III.64. DSC thermograms of FDC-Ala ester compounds (under argon, 10°C/min ramp)

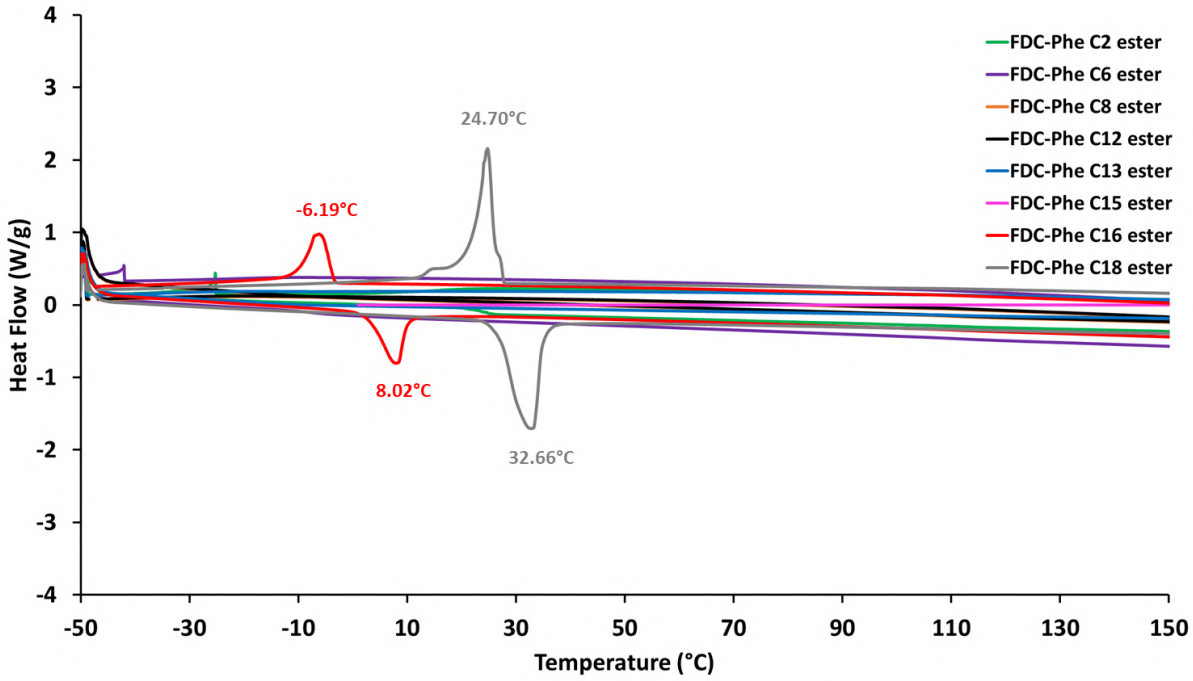

Figure III.65. DSC thermograms of FDC-Phe ester compounds (under argon, 10°C/min ramp)

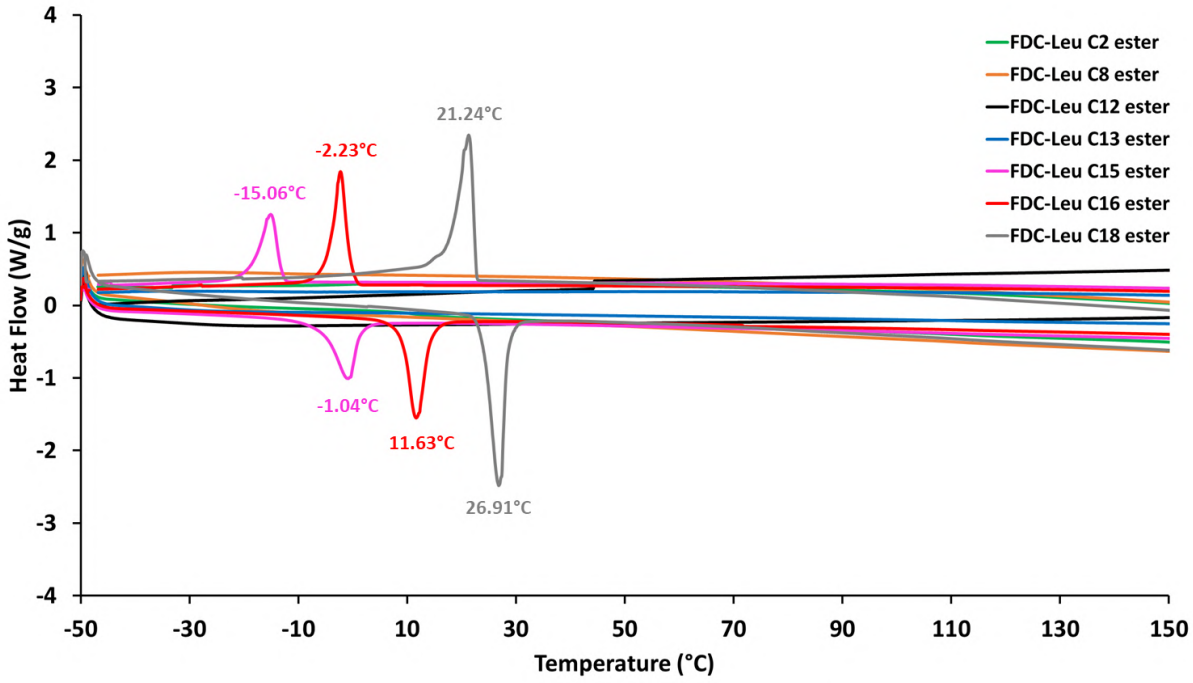

Figure III.66. DSC thermograms of FDC-Leu ester compounds (under argon, 10°C/min ramp)

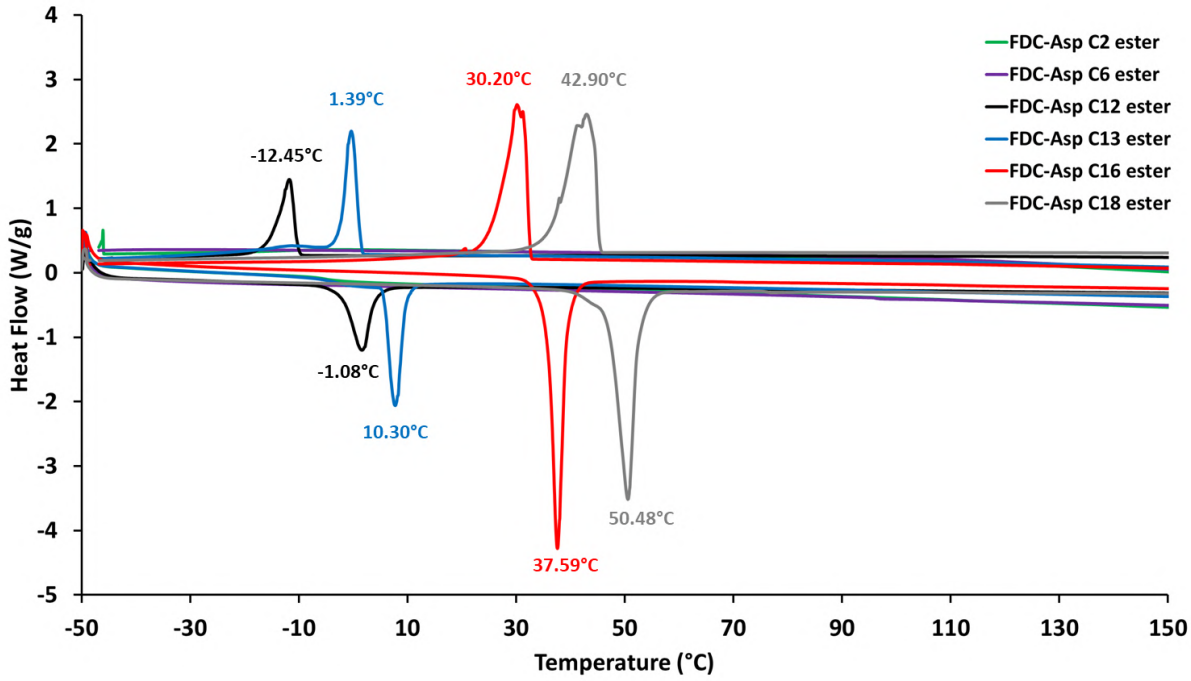

Figure III.67. DSC thermograms of FDC-Asp ester compounds (under argon, 10°C/min ramp)

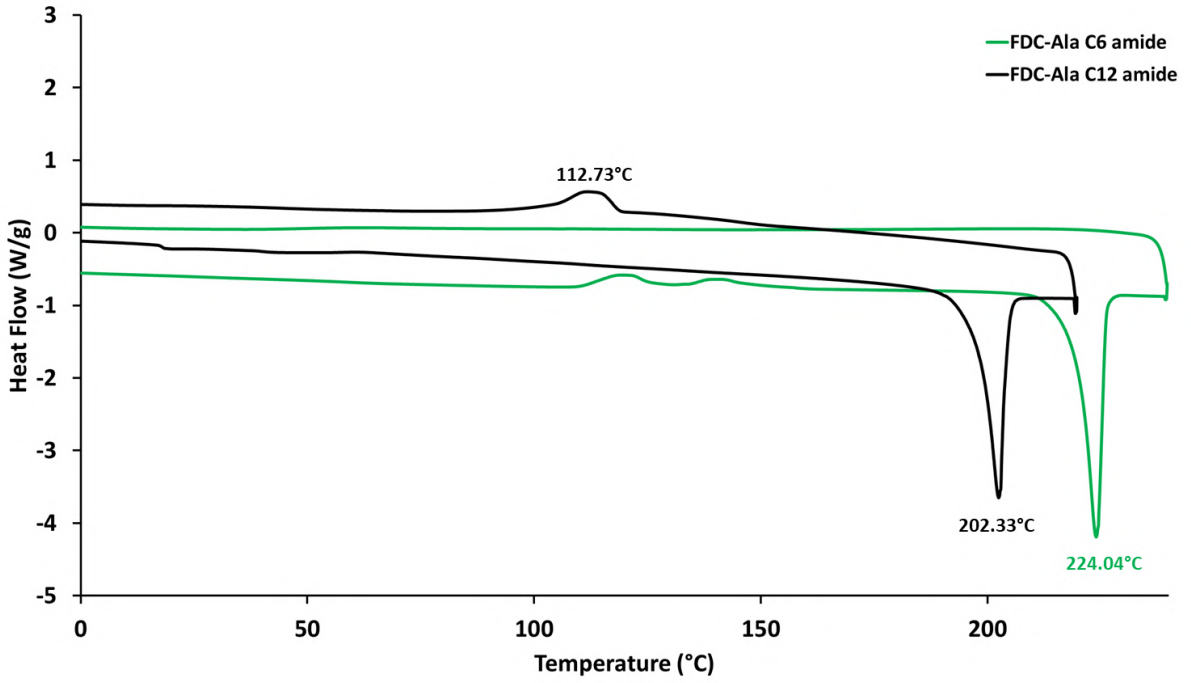

Figure III.68. DSC thermograms of FDC-Ala amide compounds (under argon, 10°C/min ramp)

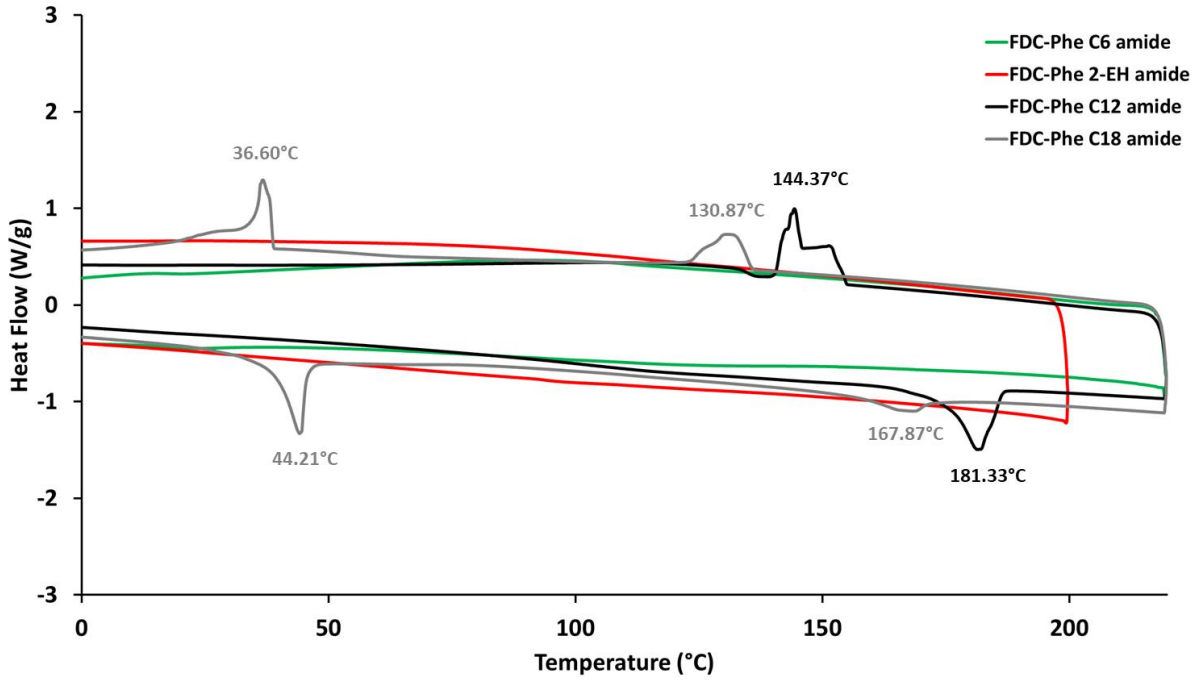

Figure III.69. DSC thermograms of FDC-Phe amide compounds (10°C/min ramp)

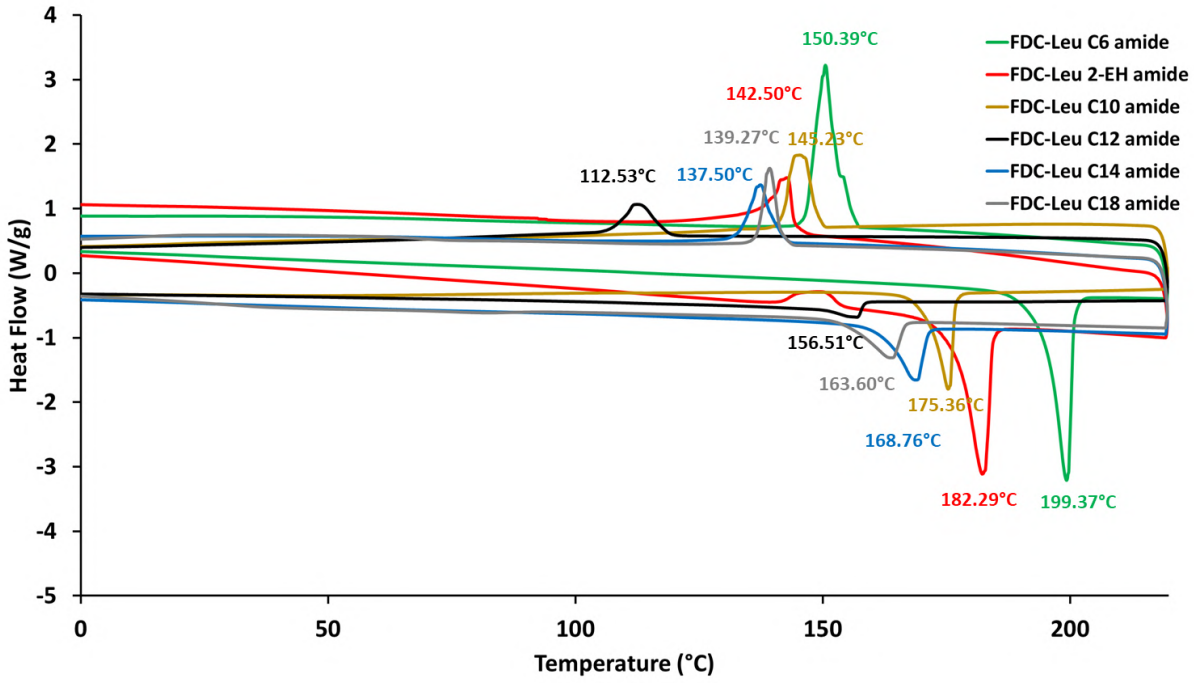

Figure III.70. DSC thermograms of FDC-Leu amide compounds (10°C/min ramp)

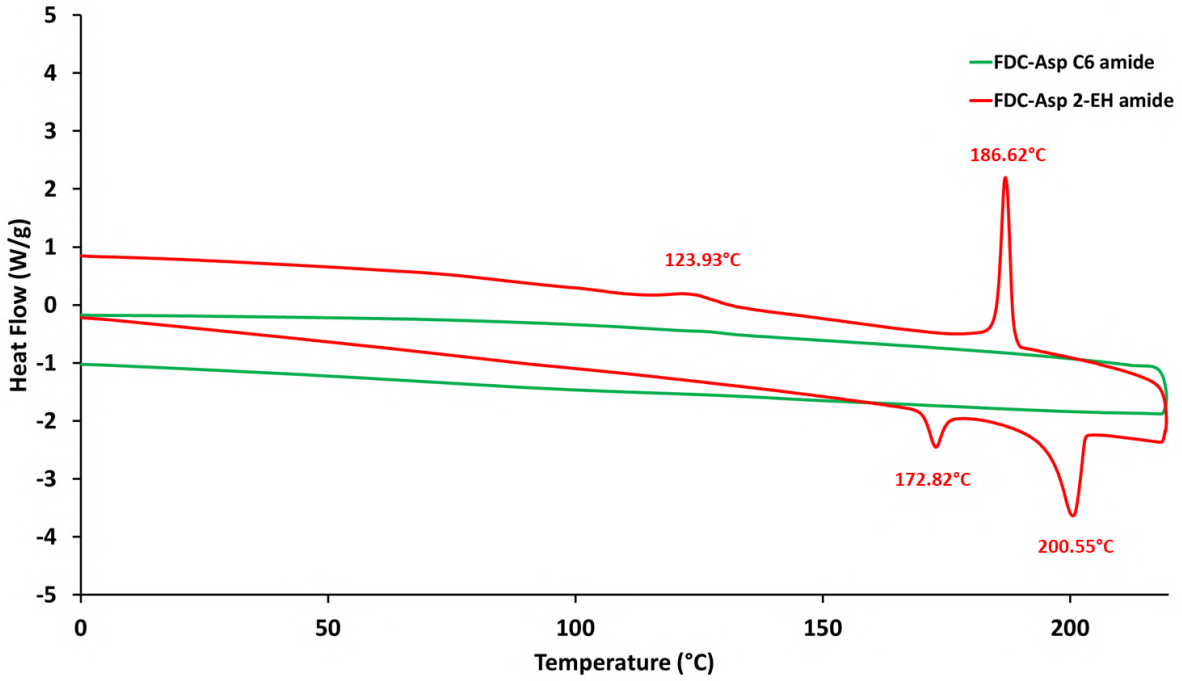

Figure III.71. DSC thermograms of FDC-Asp amide compounds (10°C/min ramp)

General conclusion

The main objective of this thesis was to develop new bio-sourced Low Molecular Weight Organogelators starting with bio-sourced building blocks. Prior to this work, no LMOGs have been referenced starting from our starting materials: tannic acid or furan-2,5-dicarboxylic acid.

From these bio-sourced hydrophilic building blocks, the methodology was to increase the hydrophobicity of these molecules in order to obtain a good balance in term of the solubility for these products. In order to achieve self-assembly, chemical functions capable of creating weak interactions such as hydrogen bonds or π- π stacking as well as hydrophobic chains are required. The self-assembly of these two molecules is of course expected to be totally different as their structures are very different.

In **Chapter II**, the syntheses of many tannic acid derivatives have been displayed. The methodology was to functionalize the phenol groups of tannic acid, totally or partially using three different groups: acetyl, long chain ester, and ether. The supramolecular self-assembly of these molecules could occur by π- π stacking for the fully functionalized derivatives and by hydrogen bonding also for the partially functionalized derivatives.

These newly designed molecules have been thoroughly characterized, as determination of the functionalization rate was challenging. Indeed, analyses of the acetyl derivatives such as ^{1}H and ^{31}P NMR, for example, allowed the rate of functionalization to be determined accurately. However, for the ester and ether derivatives, the analyses did not allow us to determine this rate precisely. Moreover, the purification of these molecules could not be complete since some of the starting reagent remained. This may be due to the conformation of tannic acid and its possible folding on itself.

Gelation tests at 1wt% on selected molecules have been carried out. In general, tannic acid derivatives showed a very high solubility in the large majority of the solvents tested. Despite different functions (esters and ethers), different chain lengths providing more or less hydrophobicity as well as different degree of functionalization, these derivatives did not show any gelation behavior.

In **Chapter III**, the bio-sourced platform has been changed by using furan-2,5-dicarboxylic acid (FDCA) for the design of organogelators. In the first part, diamides and mono-amides from alkyl and aromatic amines have been synthesized. Subsequent gelation tests have shown that the majority of the synthesized molecules remain poorly or not soluble in the list of solvents

used. The functionalization of FDCA was performed with amino acids to improve the solubility. In a first step, the carboxylic acid of the amino acids was esterified, which increases the solubility of the resulting molecules. The gelation tests showed that the solubility increased, but none of the solvent were gelated. Indeed, almost the entire set of molecules is soluble in the solvents used. The esters bring too much hydrophobicity compared to the number of hydrogen bond donor/acceptor groups. In order to balance the hydrophilicity/hydrophobicity of the molecules, the ester functions were replaced by amide functions. The same amino acids and similar chain lengths were used and gelation tests were performed. Gelation tests at 1wt% have revealed several molecules with interesting gelation properties in organic solvents.

Subsequently, we studied and characterized the most promising molecule, based on FDCA, leucine and dodecylamine, to get an insight into the supramolecular assembly. We studied the macroscopic behavior of these organogels by rheology. This study demonstrated the viscoelastic character of these gels, as well as a shear-thinning behavior. As expected, the strength of the gel increases as the wt% increases. FTIR and CD spectroscopies have also been performed in order to study the microscopic behavior, and to monitor the temperature stability. This study allowed us to determine the lowest concentration at which self-assembly occurs, i.e., 1mM or 0.07wt%.

In conclusion, this exploratory work has made it possible to highlight a whole new family of bio-based organogelators based on FDCA, being even the first ones in the literature. This discovery allowed us to file a patent on these organogelators. For the future, the synthesis should be improved by using less toxic reagents and by reducing the number of steps.

Currently, studies of the toxicity of the molecule and of gelation of commercial oils are underway, with the help of SATT Lutech.

Résumé

Un gel peut être défini comme un état intermédiaire entre des comportements rhéologiques de type liquide et solide. Il est constitué d'une phase dispersée (polymères ou colloïdes) et d'un milieu dispersant (eau ou autres liquides). Ce sont des matériaux considérés comme semi-solides. Les propriétés de type liquide sont dues au fait que le principal constituant est l'eau ou d'autres solvants. Les comportements de type solide sont dus au réseau qui empêche le système de s'écouler, et caractérisés par un module d'élasticité fini. Comme le gel est composé de liquide et de solide, ses propriétés mécaniques se situent entre l'élasticité idéale (Hookéen) et la viscosité idéale (Newtonien).

Les gels supramoléculaires peuvent être divisés en deux catégories selon le milieu gélifié : les hydrogels dans l'eau et les organogels dans les milieux organiques. Ces gels supramoléculaires sont formés à l'aide de gélateurs de faible poids moléculaire (LMWG), qui s'auto-assemblent selon une direction préférentielle. Cela conduit à la formation de structures allongées, principalement des fibres, qui forment un réseau enchevêtré appelé réseau fibrillaire auto-assemblé (SAFiN). Ce mécanisme d'auto-assemblage est dirigé par des interactions non covalentes comme les liaisons hydrogène, π-π stacking, ou les forces de van der Waals (**Figure 1**).

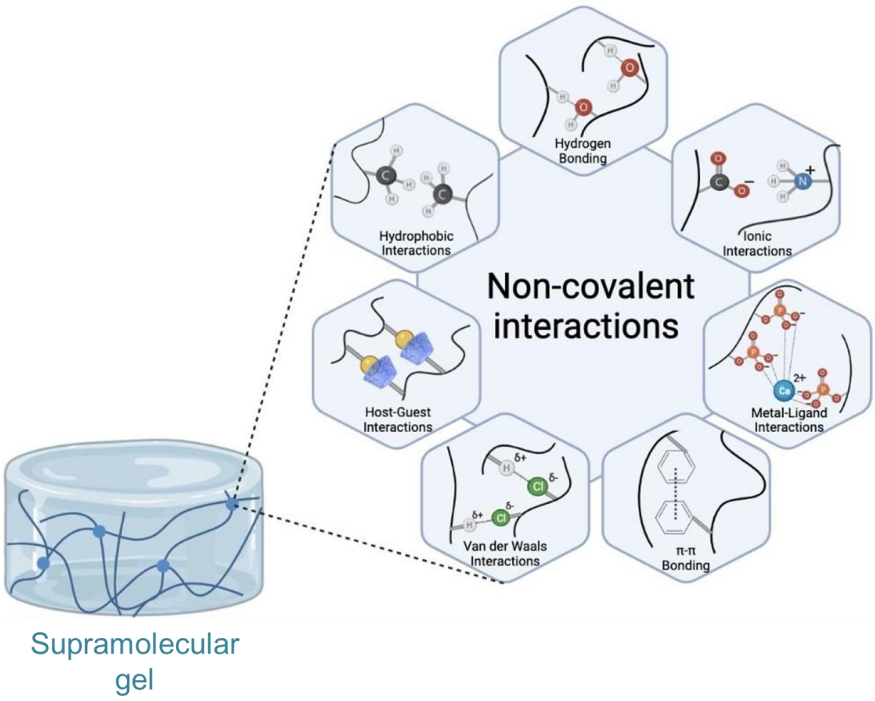

Figure 1. Interactions non covalentes utilisées pour former des gels supramoléculaires [1]

Les gélateurs de faible poids moléculaire (LMWG) sont de petites molécules organiques, généralement inférieures à 3000 Da qui, à de faibles concentrations (≤ 2wt%) en solution, forment un gel.

Les organogels diffèrent des gels classiques formés par liaison covalente. En effet, la réticulation est réversible dans le cas d'un organogel, ce qui signifie que le processus peut être inversé si une certaine quantité d'énergie est appliquée au système.

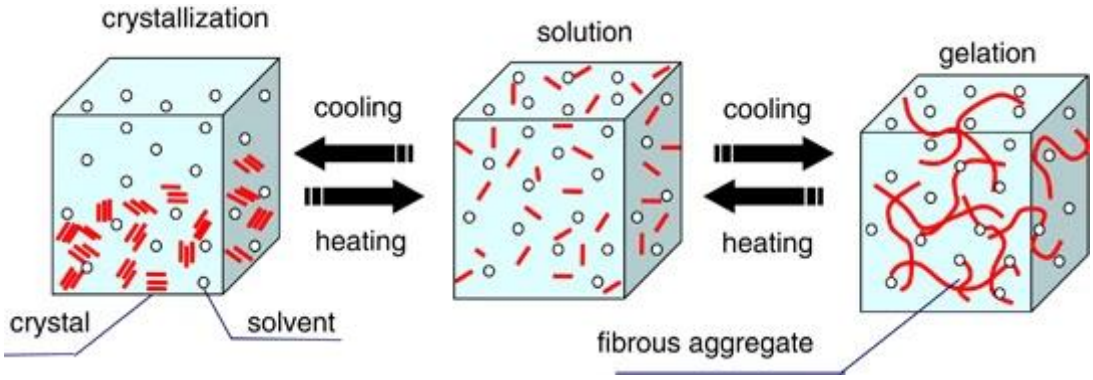

Figure 2. Cristallisation et gélification des composés de faible poids moléculaire [2]

Plusieurs phénomènes peuvent déclencher la gélification du solvant, comme la variation de température, la sonication, la variation du pH ou l'ajout d'une molécule permettant l'allongement et la percolation des fibres. Sur la **Figure 2**, la cristallisation et la gélification d'un gélifiant de faible poids moléculaire sont comparées. Lorsque les cristaux sont chauffés dans un solvant approprié, une solution homogène est formée. Lorsque celle-ci est refroidie, la cristallisation se produit en réponse à la différence de solubilité. Cependant, dans de rares cas, une gélification se produit plutôt qu'une cristallisation. Lorsque ce gel est chauffé, il se transforme à nouveau en une solution homogène. La cristallisation se produit lorsque les molécules peuvent se condenser et se disposer selon un modèle tridimensionnel ordonné. En revanche, la gélification se produit lorsque les molécules s'assemblent en fibres, qui s'enchevêtrent les unes dans les autres, retiennent le solvant et forment ainsi un gel.

Au cours de la dernière décennie, le remplacement des produits de l'industrie pétrochimique par des molécules issues de la biomasse est l'un des sujets les plus importants de l'industrie chimique. L'objectif de cette thèse est de développer de nouveaux organogélateurs à partir de briques biosourcées, afin de pouvoir utiliser ces organogels dans des domaines tels que la cosmétique ou l'industrie alimentaire.

Dans le **Chapitre I**, nous avons présenté les différentes familles d'organogélateurs biosourcés ainsi que les domaines d'application des organogels. Ceux-ci ont des domaines d'application variés, bien qu'ils ne soient pas encore très utilisés à l'échelle industrielle.

Dans le **Chapitre II**, nous nous sommes concentrés sur la synthèse d'organogélateurs à partir de l'acide tannique. Cette molécule est un polyphénol de la famille des tannins, plus précisément de la classe des tannins hydrolysables. Les tannins sont des composés phénoliques présents naturellement dans les plantes. La structure de l'acide tannique consiste en des unités galliques liées à un glucose. En fait, il s'agit d'un mélange de polygalloyl glucose avec un nombre d'unités galliques pouvant aller de deux à douze. Il faut également noter qu'au sein même de la structure de l'acide tannique, il existe plusieurs isomères de position. En effet, les unités galliques sont liées par une fonction ester appelée liaison depside qui peut être en position méta ou para avec une proportion différente de l'une ou l'autre selon les échantillons d'acide tannique (**Figure 3**). La chimie de l'acide tannique est complexe en raison de son origine naturelle et consiste en un mélange de molécules. De plus, il existe peu d'études sur la modification chimique des tannins hydrolysables. La raison principale est la fragilité de la liaison depside qui peut conduire à une dégradation de la molécule.

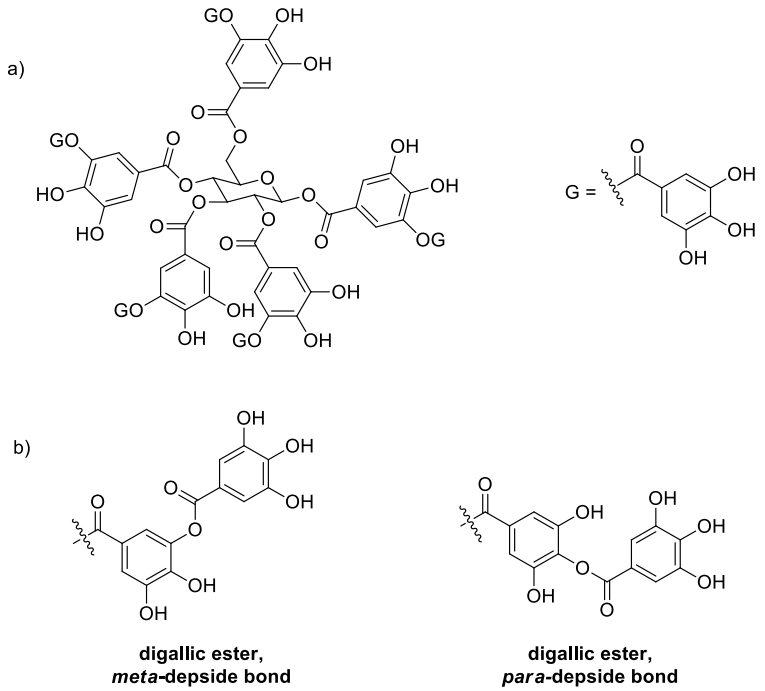

Figure 3. a) Structure nominale de l'acide tannique, b) isomérie structurelle de la liaison depside (*méta* ou *para*)

Dans ce chapitre, nous avons tout d'abord caractérisé notre acide tannique par diverses techniques (RMN, FTIR, spectrométrie de masse). La RMN ^{31}P a montré que nous avions un produit contenant 30% de liaison *para*-depside et 70% de liaison *méta*-depside. La spectrométrie de masse a montré que notre produit est un mélange de plusieurs isomères possédant plus ou moins d'unités galliques., allant au-delà de onze unités. Par la suite, nous avons fonctionnalisé totalement ou partiellement les phénols de cet acide tannique avec trois groupes différents permettant la solubilisation des molécules synthétisées dans des milieux organiques (**Figure 4**).

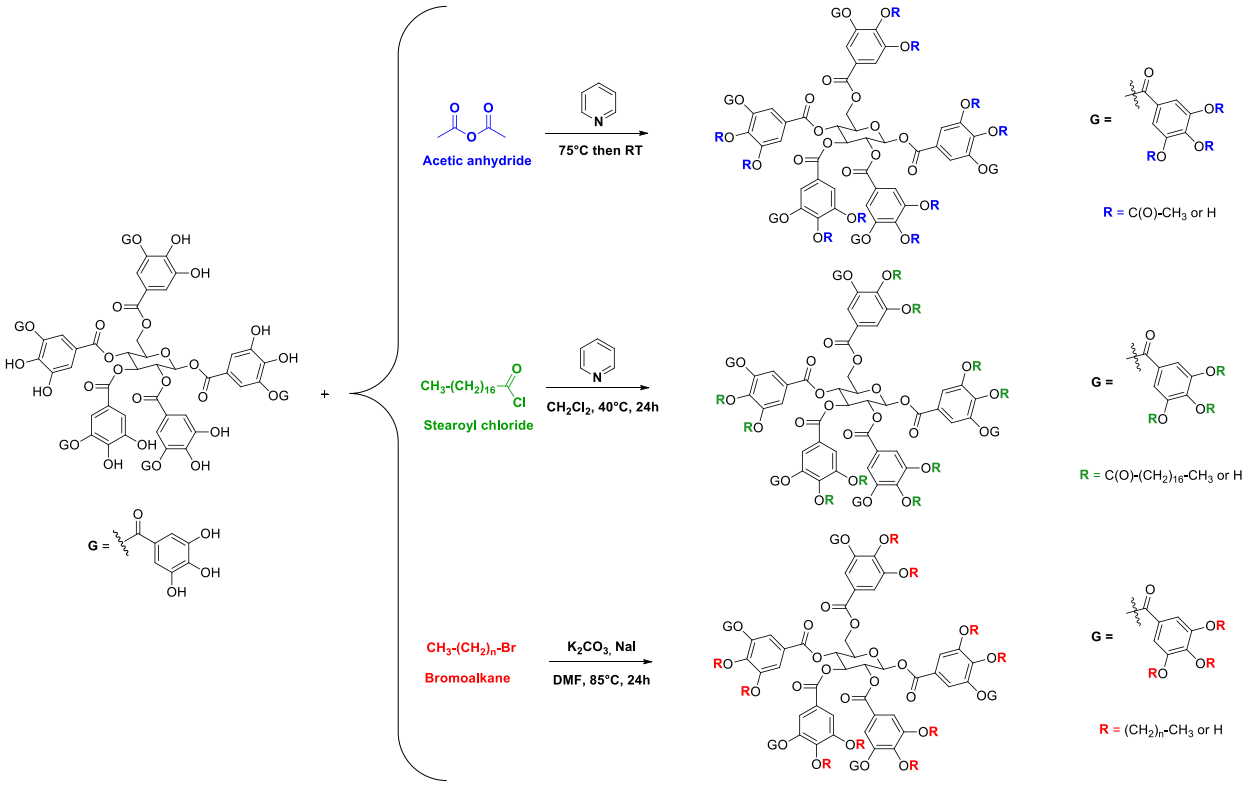

Figure 4. Synthèse des dérivés d'acide tannique

La difficulté principale rencontrée avec ces molécules a été la détermination du taux de fonctionnalisation de chaque molécule. Nous avons ainsi caractérisé ces molécules par de nombreuses méthodes analytiques. Nous avons montré que les dérivés acétylés de l'acide tannique étaient caractérisés plus facilement que les dérivés éthérifiés et estérifiés. Ceci implique que la fonctionnalisation par une chaîne trop longue, comme un acide gras, peut empêcher la caractérisation du cœur des dérivés de l'acide tannique. En effet, la détermination du taux de fonctionnalisation est plus précise pour les molécules acétylées que pour les autres. Par RMN ^{1}H, nous avons pu déterminer avec précision le nombre de phénols acétylés. Nous avons également observé que ces molécules sont difficiles à purifier, en effet, le solvant des

molécules acétylées est encore visible en RMN ^{1}H ainsi que des traces de bromoalcane pour certaines molécules éthérifiées et d'acide stéarique pour les molécules estérifiées.

Les nombreuses analyses ne nous ont pas permis de déterminer précisément le taux de fonctionnalisation des différents dérivés d'acide tannique. Cependant, les résultats nous ont permis de déterminer que plus le nombre d'équivalents utilisé est élevé, plus le nombre de phénols non réagis diminue. Les tests de gélification effectuées ont montré que ces molécules ne possédaient de propriétés gélifiantes puisque nous n'avons formé aucuns gels.

Dans le **Chapitre III**, nous nous sommes concentrés sur la synthèse d'organogélateurs à partir du FDCA. L'acide furan-2,5-dicarboxylique a été identifié comme une plateforme biosourcée clé en raison de son potentiel comme source d'une grande variété de produits chimiques et de matériaux. Le FDCA est composé d'un cycle furane et de deux fonctions acide carboxylique. Dans ce chapitre, nous avons fonctionnalisé les acides carboxyliques par des amines ou acides aminés afin de former des fonctions amides (**Figure 5**).

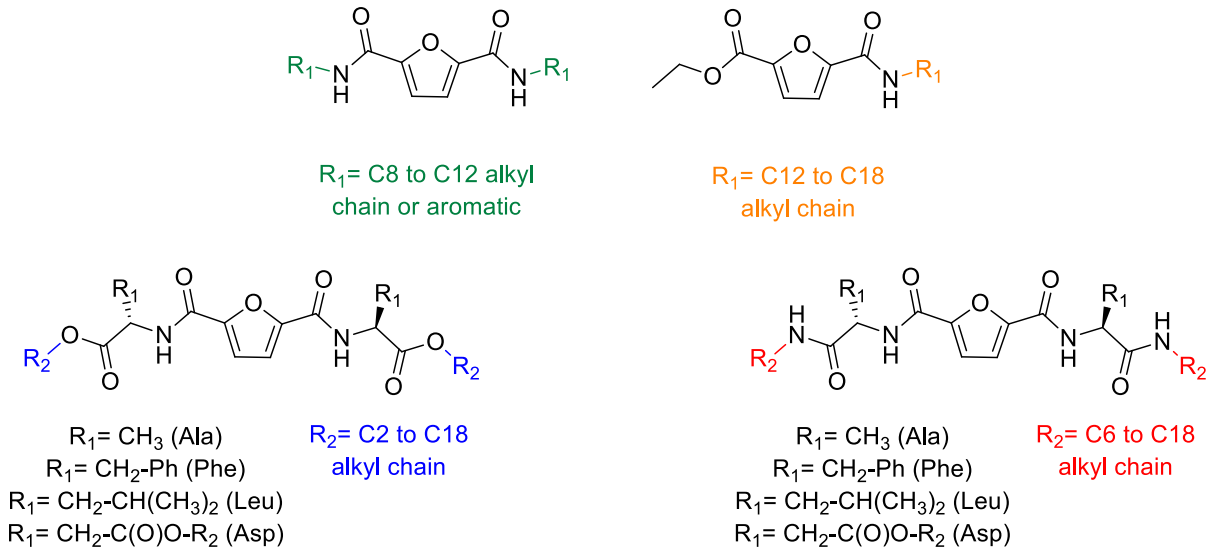

Figure 5. Dérivés du FDCA synthétisés

Dans un premier temps, des diamides et des mono-amides à partir d'amines aliphatiques ou aromatiques ont été synthétisées. Par la suite, les tests de gélification ont montré que la majorité des molécules synthétisées restent peu ou pas solubles dans la liste des solvants utilisés. Afin de remédier à cela, la fonctionnalisation du FDCA a été réalisée avec des acides aminés. Tout d'abord, l'acide carboxylique des acides aminés a été estérifié afin d'augmenter la solubilité des molécules obtenues. Les tests de gélification ont montré que la solubilité avait augmentée mais qu'elle devenait trop élevée. En effet, la quasi-totalité de l'ensemble des molécules est soluble

dans les solvants utilisés. Afin d'équilibrer le rapport polaire/apolaire des molécules, les fonctions esters ont été remplacées par des fonctions amides. Les mêmes acides aminés et des longueurs de chaîne similaires ont été utilisés et des tests de gélification ont été effectués. Les tests de gélification à 1% en poids ont révélé que plusieurs molécules possédaient des propriétés de gélification des milieux organiques.

Nous avons ensuite étudié et caractérisé l'assemblage supramoléculaire des solutions et organogels faits à partir de FDC-Leu C12 amide, la molécule la plus prometteuse. Nous avons étudié le comportement macroscopique de ces organogels par rhéologie. Cette étude a démontré le caractère viscoélastique de ces gels, ainsi qu'un comportement rhéofluidifiant. Comme prévu, la résistance du gel augmente avec l'augmentation du % massique. Des analyses spectroscopiques FTIR et CD ont également été réalisées afin d'étudier le comportement microscopique, et d'observer la stabilité en température de l'assemblage. Ces études ont montré que de l'assemblage subsistait à 100°C mais dans un état désordonné. Cela nous a également permis de déterminer la concentration la plus faible à laquelle l'auto-assemblage se produit, c'est-à-dire 1mM.

En conclusion, ce travail exploratoire a permis de mettre en évidence une toute nouvelle famille d'organogélateurs biosourcés à base de FDCA. Pour le développement de ces matériaux, la synthèse devrait être améliorée en utilisant des réactifs moins toxiques et en réduisant le nombre d'étapes.

Actuellement, des études de toxicité sont effectuées sur la molécule ainsi que des essais sur des huiles commerciales, en collaboration avec la SATT Lutech.

[1] J. Omar, D. Ponsford, C. A. Dreiss, T.-C. Lee, X. J. Loh, *Chemistry – An Asian Journal* **2022**, *17*, e202200081.

[2] K. Hanabusa, M. Suzuki, *Polym J* **2014**, *46*, 776–782.

Synthèse et développement de nouveaux organogélateurs biosourcés

Les organogels sont des gels supramoléculaires ou gels physiques formés à partir d'organogélateurs dans des solvants organiques. Ces organogélateurs ou gélateurs de faible poids moléculaire (LMOGs) sont de petites molécules organiques (< 2000 Da) capables de s'auto-assembler. Cela conduit à la formation de structures anisotropes, principalement des fibres, qui forment un réseau fibrillaire auto-assemblé enchevêtré (SAFiN), dont le mécanisme d'assemblage est dirigé par des interactions non covalentes. L'objectif de cette thèse est de développer de nouveaux organogélateurs à partir de briques biosourcées. Dans un premier temps, nous avons synthétisé des molécules à base d'acide tannique. En faisant varier la nature des groupements et les longueurs de chaine, nous avons ainsi adapté la solubilité des molécules et cartographié une famille de molécules qui n'a pas démontré de propriétés intéressantes. Par la suite, nous avons synthétisé des molécules à base de FDCA contenant des fonctions amides. En variant la nature de l'amine et les longueurs de chaine, nous avons ainsi découvert une nouvelle famille d'organogélateurs.

Mots clés : organogélateur ; biosourcé, interactions supramoléculaires ; liaisons hydrogène ; auto-assemblage ; gel ; acide tannique ; FDCA ; acide aminé

Synthesis and development of new bio-sourced LMOGs

Organogels are supramolecular gels or physical gels formed from organogelators in organic solvents. These organogelators or low molecular weight organogelators (LMOGs) are small organic molecules (< 2000 Da) capable of self-assembly. This leads to the formation of elongated structures, mainly fibers, which form an entangled self-assembled fibrillar network (SAFiN), whose assembly mechanism is driven by non-covalent interactions. The objective of this thesis is to develop new organogelators from biobased building blocks. In a first step, we synthesized molecules based on tannic acid. By varying the nature of the groups and the chain lengths, we adapted the solubility of the molecules and mapped a family of molecules that, however, did not show interesting properties. Subsequently, we synthesized FDCA-based molecules containing amide functions. By varying the nature of the amine and the chain lengths, we discovered a new family of organogelators.

Keywords : organogelator ; LMWG ; bio-sourced, supramolecular interactions ; hydrogen bonds ; self-assembly ; gel ; tannic acid ; FDCA ; amino acid